Investigation of the anti-proliferative and anti-invasive properties of Conjugated Linoleic Acid and novel 5-Fluorouracil derivatives including enzyme-activated prodrugs

A dissertation submitted for the degree of Ph.D

by

Aisling M. Redmond B.A. (Mod) Natural Sciences
(Genetics)

Under the supervision of Dr. Susan McDonnell and Dr. Rosaleen Devery

May 2007

School of Biotechnology and National Institute for Cellular Biotechnology,
Dublin City University, Dublin 9, Ireland

UCD School of Chemical and Bioprocess Engineering

Declaration

'I hereby certify that this material, which I now submit for the assessment on the programme of study leading to the award of Doctor of Philosophy is entirely my own work and has not been taken from the work of others save and to the extent that such work has been cited and acknowledged within the text of my work'.

Signed: _____ I.D. Number: 52164705

Date: _____ Wednesday 30th May 2007

Table of Contents

Acknowledgements

There are many people I wish to thank for their help during my Ph.D. Firstly, I am very grateful to Dr Susan McDonnell for taking me on in the first place and for her constant guidance and supervision over the past number of years. Dave, thanks for the help in the early years in the lab. Lynda, it was great to start with you and learn from you. Thank you for your friendship, help and generosity during the last few years. Kate and Jess, it was a pleasure sharing the lab with you both during my Ph.D. Kate, thanks for your ever-thoughtfulness but especially over the last number of months and for being there after the viva! Jess, thanks for the yoga sessions, the many dinners and shelter after nights out!

This thesis could not have come about without the help of a number of people. Rosaleen, thanks for providing the CLA and for your constructive criticism of each chapter. Ian Gray and Kieran Nolan, thanks for synthesising the 5-FU derivatives and entrusting them to me to test. I'm very grateful to Professor Al-Rubeai and his group for allowing me to use their Guava so often! Thanks to Judy Harmey for the hypoxia facilities. Thank you to Robert O'Connor and Rachel Wall for their time and effort with the mass spectrometry experiments. Barry Ryan, Ciarán Fagan and Pam O'Brien, I appreciate your help with the enzyme kinetics which was badly needed! Many thanks to the National Institute for Cellular Biotechnology at DCU for funding my work for four years.

In the Biotechnology department in DCU I had the pleasure of meeting a number of wonderful people, had really enjoyable times, including some very educational trips with the BRS to Barcelona, Kilkenny and Galway! It's hard to single out people but thanks especially to Pam, Isobel, Conor and Nora for your friendship over the years. Moving to UCD also allowed me to meet another great bunch of people - the Chem Eng postgrads. I miss the many entertaining lunchtime conversations, games of frisbee in the sun and attempts at yoga/pyramid conformations after a few beers. Your collective energy and enthusiasm is a welcome and inspiring addition to my life. Roll on the skiing!

I have to thank my very close friends, Caitriona, Fiona, Louise and Neasa. You four are my second family and have always been there for me. Thanks for supporting me over the last four and a half years without question and never tiring of

the ‘PhD excuse’ which ruled my life for a while! A special mention must go to Dr. Tom Bannon for your constant encouragement and inspiring chats during this PhD. You should become a full-time motivational speaker!

Finally, I must dedicate this thesis to my family, Dad, Mam, Fiona, Niamh and Barry. Thank you all for your love and support through the last three decades (ouch). I am very grateful to my parents for always encouraging me throughout my education, and especially for their help over the last year and a half when I moved back home. Fiona thanks for the encouragement and advice over the years. Niamh, best of luck finishing up, thanks for the proof-reading and for your constant energy. Bar, thanks for helping keep me sane during the writing months at home!

Abstract

Over 20,000 people are diagnosed with cancer every year in Ireland, with colorectal and breast cancers contributing significantly to that figure. Approximately 8,000 deaths occur annually from cancer and the majority of these patients die because their tumour has metastasised to secondary sites in the body. Current treatments of surgery, radiotherapy and chemotherapy are still limited in their effectiveness, and have various side-effects and disadvantages. New anti-cancer and anti-metastatic agents are urgently required to decrease the number of deaths occurring and more targeted therapies would allow increased doses to be tolerated without the corresponding side-effects. In this study, conjugated linoleic acid (CLA) and novel 5-Fluorouracil (5-FU) derivatives were analysed with regards to regulating cytotoxicity, cell cycle kinetics, apoptosis, migration, invasion, adhesion, colony formation in soft agar and MMP/TIMP levels.

CLA is a polyunsaturated fatty acid found in the meat and dairy products of ruminant animals. Numerous isomers exist and have previously been shown to exhibit anti-cancer activity. A mix of CLA isomers proved more toxic than the individual *c*9,*t*11-CLA and *t*10,*c*12-CLA isomers to the 4T1 murine mammary and Hs578T human breast cancer cell lines. Treatment with CLA and the isomers resulted in a predominant G1 phase arrest in the 4T1 cells. Migration and invasion of the 4T1 cell line was increased after treatment with *c*9,*t*11-CLA and decreased after treatment with *t*10,*c*12-CLA ($p<0.05$). The *t*10,*c*12-CLA isomer had a significant effect on colony formation of the 4T1 cells in soft agar, with a 25-fold increase in colonies formed in comparison to the control ($P<0.00005$). The *c*9,*t*11-CLA isomer and CLA also increased the number of colonies formed ($p<0.01$). MMP-9 mRNA and protein levels were increased following treatment with CLA and *t*10,*c*12-CLA, which correlated with decreased TIMP-1 mRNA levels.

5-FU is an antimetabolite agent commonly used in chemotherapy. Despite its widespread use in cancer patients, it has many side-effects and low response rates, and is generally used in combination with a number of other agents. Novel 5-FU derivatives were synthesised and their anti-proliferative and anti-invasive activity analysed using a murine mammary and a human colon cancer cell line. Cytotoxicity analysis revealed a derivative, compound 10, considerably more toxic than the parent

5-FU. This compound also exhibited toxicity towards a 5-FU resistant cell line and caused a dramatic S phase arrest during cell cycle analysis, indicating a different mode of action to the parent 5-FU. A number of these derivatives were synthesized as prodrugs, non-toxic agents requiring enzyme activation to release 5-FU. Activation of these prodrugs was initially investigated using hypoxic conditions and then an *E.coli* nitroreductase enzyme. Activation of two prodrugs, compounds 13 and 14 was confirmed in a cell line expressing this enzyme. Compound 14 had an IC_{50} value that was greater than 73.5-fold lower in the nitroreductase-expressing cell line in comparison to the control cell line after treatment for 3 days. Mass spectrometry analysis confirmed production of 5-FU from compound 13 in this cell line.

This work has looked at two potential new approaches to cancer treatment. CLA is part of the growing industry of dietary supplements or functional foods that may aid chemoprevention or supplementary chemotherapy. 5-FU has been used for decades in chemotherapy regimes. However, derivatives with increased toxicity or specificity will certainly be beneficial to numerous patients. In the coming years, these two approaches promise to signal a major change in the impact of cancer on people's lives and will significantly decrease the rate of fatalities.

Abbreviations and Acronyms

5-DFCR	5-Deoxy-5-Fluorocytidine
5-DFUR	5-Deoxy-5-Fluorouridine
5-FC	5-Fluorocytosine
5-FdUDP	5-Fluorodeoxyuridine Diphosphate
5-FdUMP	5-Fluorodeoxyuridine Monophosphate
5-FdUrd	5-Fluorodeoxyuridine
5-FdUTP	5-Fluorodeoxyuridine Triphosphate
5-FU	5-Fluorouracil
5-FUDP	5-Fluorouridine Diphosphate
5-FUMP	5-Fluorouridine Monophosphate
5-FUrd	5-Fluorouridine
5-FUTP	5-Fluorouridine Triphosphate
7-AAD	7-Amino Actinomycin D
AA	Arachadonic Acid
Abs	Absorbance
ADEPT	Antibody-Directed Enzyme Prodrug Therapy
AIF	Apoptosis Inducing Factor
ALA	α-Linolenic Acid
APC	Adenomatous Polyposis Coli
ATCC	American Type Culture Collection
BCSC	Breast Cancer Stem Cell
BD	Becton Dickinson
BHK	Baby Hamster Kidney
BP	Base Pair
BSA	Bovine Serum Albumin
c	*Cis*
CCC	Cytoplasmic Cell-Adhesion Complex
CD	Cytosine Deaminase
CDHP	5-Chloro-2,4-dihydroxypyrimidine
CDK	Cyclin-Dependent Kinase
cDNA	Complementary Deoxyribonucleic Acid

CH_2THF	5,10-methylenetetrahydrofolate
CI	Continuous Infusion
CIN	Chromosomal Instability
CLA	Conjugated Linoleic Acid
CMV	Cytomegalovirus
CRC	Colorectal Cancer
DCIS	Ductal Carcinoma *in situ*
DEPC	Diethyl Pyrocarbonate
DGLA	Dihomo-γ-Linolenic Acid
DHFU	Dihydrofluorouracil
DLT	Dose-Limiting Toxicity
DMBA	Dimethyl-benz(*a*)anthracene
DMEM	Dublecco's Modified Eagle's Medium
DMSO	Dimethyl Sulfoxide
DNA	Deoxyribonucleic Acid
DNase	Deoxyribonuclease
dNTP	Deoxyribonucleotide Triphosphate
DPD	Dihydropyrimidine Dehydrogenase
dTMP	Deoxythymidine Monophosphate
dTTP	Deoxythymidine Triphosphate
dUMP	Deoxyuridine Monophosphate
dUTP	Deoxyuridine Triphosphate
ECL	Enhanced Chemiluminescence
ECM	Extracellular Matrix
EDTA	Ethylenediamine Tetraacetic Acid
EF-1α	Elongation Factor 1α
EFA	Essential Fatty Acid
EGFR	Epidermal Growth Factor Receptor
EPA	Eicosapentanoic Acid
EPT	Enzyme Prodrug Therapy
ER	Estrogen Receptor
ERBB2	Erythroblastic Leukemia Viral Oncogene Homolog 2
ERE	Estrogen Response Element

EU	Eniluracil
FADD	Fas-Associated Death Domain
FAP	Familial Adenomatous Polyposis
FBS	Fetal Bovine Serum
FMN	Flavin Mononucleotide
FT	Ftorafur
GDEPT	Gene-Directed Enzyme Prodrug Therapy
GI	Gastrointestinal
HER	Human Epidermal Growth Factor Receptor
HNPCC	Hereditary Non-Polyposis Colon Cancer
IDC	Invasive Ductal Carcinoma
Ig	Immunoglobulin
IGF-BP	Insulin Growth Factor Binding Proteins
i.v.	Intravenously
k_{cat}	Catalytic Constant
K_m	Michaelis Constant
LA	Linoleic Acid
LB	Luria-Bertrani
LCIS	Lobular Carcinoma *In Situ*
LC-MS	Liquid Chromatography-Mass Spectrometry
LDS	Lithium Dodecyl Sulphate
LV	Leucovorin
MAPK	Mitogen Activated Protein Kinase
MES	2-(N-Morpholino) Ethane Sulfonic acid
MIN	Microsatellite Instability
MMLVRT	Moloney Murine Leukemia Virus Reverse Transcriptase
MMP	Matrix Metalloproteinase
MMR	Mutation Mismatch Repair
MNU	Methylnitrosourea
mRNA	Messenger RNA
MT-MMP	Membrane-Type MMP
MTS	[3-(4,5-dimethylthiazol-2-yl)-5-(3-carboxymethoxyphenyl)-2-(4-sulfonyl)-2H-tetrazolium]
MTX	Methothrexate

NADH	Nicotinamide Adenine Dinucleotide
NCRI	National Cancer Registry Ireland
ND	Not Determined
NICB	National Institute for Cellular Biotechnology
NMR	Nuclear Magnetic Resonance
NRH	Dihydronicotinamide Riboside
NTR	Nitroreductase
OPRT	Orotate Phosphoribosyltransferase
OXO	Potassium Oxonate
PAGE	Polyacrylamide Gel Electrophoresis
PBS	Phosphate Buffered Saline
PCA	Personal Cell Analysis
PCR	Polymerase Chain Reaction
PDK	Pyrimidine Diphosphate Kinase
PDT	Photodynamic Therapy
PE	Phycoerythrin
PET	Polyethylene Terephthalate
PI	Propidium Iodide
PMA	Phorbol 12-Myristate 13-Acetate
PMK	Pyrimidine Monophosphate Kinase
*p*NPP	*p*-Nitrophenyl Phosphate
PPRE	Peroxisome Proliferator Response Element
PUFA	Polyunsaturated Fatty Acid
RNA	Ribonucleic Acid
RNase	Ribonuclease
RP	RNA Polymerase
RR	Ribonucleotide Reductase
rRNA	Ribosomal RNA
RT-PCR	Reverse Transcription PCR
S_0	Serum-free media
S_{20}	Media containing 20% FBS
SAR	Structure-Activity Relationship
SDS	Sodium Dodecyl Sulphate
Sec	Second

snRNA	Small nuclear RNA
Strep	Streptomycin
t	*Trans*
Taq	Thermus Aquaticus
TAP	Tumour Activated Prodrug
TBE	Tris Borate EDTA
TBST	Tris Buffered Saline plus Tween
TE	Tris EDTA
TEB	Terminal End Bud
TEMED	NNN'N'-Tetramethylethyldiamine
TGF-β	Transforming Growth Factor β
TIMP	Tissue Inhibitor of Metalloproteinases
TK	Thymidine Kinase
TNF	Tumour Necrosis Factor
TP	Thymidine phosphorylase
TPZ	Tirapazamine
TRAIL	TNF-Related Apoptosis Inducing Ligand
Triton X100	t-Octylphenoxypolyethoxyethanol
tRNA	Transfer RNA
TS	Thymidylate Synthase
UFT	Uracil/Ftorafur
UK	Uridine Kinase
UP	Uridine Phosphorylase
UTP	Uridine-5-Triphosphate
UVP	Ultraviolet Products
VDEPT	Virus-Directed Enzyme Prodrug Therapy
VEGF	Vascular Endothelial Growth Factor
V_{max}	Maximum Velocity

Units

Å	Angstrom
bp	Base Pair
g	Gram or gravities
kDa	Kilodalton
L	Litre
M	Molar
mA	Milliamp
mg	Milligram
ml	Millilitre
mM	Millimolar
nm	Nanometre
°C	Degrees Celsius
U	Units of enzymatic activity
V	Volt
v/v	Volume per volume
W	Watt
w/v	Weight per volume
µg	Microgram
µl	Microlitre
µM	Micromolar

Publications

Gray, I., **Redmond, A.**, McDonnell, S. and Nolan, K. The preparation of a new third generation photosensitiser and the development of new acetonide cleavage reaction (submitted to *Tetrahedron Letters*).

McDonnell, S., Murray, D., Hughes, L. and **Redmond, A.** (2006) Molecular aspects of cancer invasion. Chapter 3 pp73-96. The Molecular and Cellular Pathology of Cancer Progression and Prognosis. Edited by G.V. Sherbet. Research Signpost.

Redmond, A., Gray, I., Nolan, K. and McDonnell, S. (2004). Cytotoxicity of bioreductive drugs derived from 5-Fluorouracil. *Anticancer Research* **24**: 3610.

Redmond, A., Murray, D., Devery, R., Stanton, C. and McDonnell, S. (2003). Inhibition of invasion and migration by CLA in breast cancer cell lines. *Anticancer Research* **24**: 517.

Oral Presentations

Conjugated linoleic acid and 5-Fluorouracil derivatives: Potential new anti-cancer treatments. UCD School of Chemical and Bioprocess Engineering Seminar Series, 6th April 2006.

Effect of novel 5-Fluorouracil pro-drugs on proliferation and invasion of cancer cell lines. National Institute for Cellular Biotechnology Cancer Day, Dublin City University, 8th April 2005.

Poster Presentations

Redmond, A., Gray, I., Nolan, K. and McDonnell, S. Novel 5-Fluorouracil pro-drug derivatives. EMBO Molecular Medicine Conference: Common Molecular

Mechanisms of Mammary Gland Development and Breast Cancer Progression, Dublin, June 2006.

Redmond, A., Gray, I., Nolan, K. and McDonnell, S. Investigation of novel 5-Fluorouracil derivatives for gene-directed enzyme pro-drug therapy using the nitroreductase enzyme. Irish Association for Cancer Research, Annual Meeting, Galway, March 2006.

Redmond, A. and McDonnell, S. Effect of conjugated linoleic acid on proliferation, invasion and migration in 4T1 murine mammary cell line. Irish Association for Cancer Research, Annual Meeting, Kilkenny, March 2005.

Redmond, A., Gray, I., Nolan, K. and McDonnell, S. Cytotoxicity of bioreductive drugs derived from 5-Fluorouracil. Seventh International Conference of Anticancer Research, Greece, October 2004.

Redmond, A., Murray, D. and McDonnell, S. Molecular mechanisms involved in tumour invasion and metastasis. National Institute for Cellular Biotechnology Open Day, Dublin, June 2004.

Redmond, A., Gray, I., Nolan, K. and McDonnell, S. Cytotoxicity of novel 5-Fluorouracil derivatives in colon and breast cancer cell lines. Irish Association for Cancer Research, Annual Meeting, Belfast, April 2004.

Redmond, A., Murray, D., Devery, R., Stanton, C. and McDonnell, S. Inhibition of invasion and migration by CLA in breast cancer cell lines. Biotechnology, Cancer and Drug Resistance, Dublin, July 2003.

Awards

Cancer Research Ireland, Oncology Scholars Travel Award 2005. To attend ECCO European Cancer Conference, Paris, November 2005.

Chapter 1

Introduction

1.1 Cancer

1.1.1 Cancer statistics

Statistics from the National Cancer Registry Ireland (NCRI) for the years 1998 to 2000 state that on average there were 22,019 new cases of cancer and 7,661 deaths from cancer *per annum* (Campo *et al*., 2004). Of the total annual number of new cases, 1,927 patients presented with breast cancer and on average 642 deaths occurred as a result. 1,861 patients were diagnosed annually with colorectal cancer (CRC), with 915 deaths. A report produced by the NCRI in June 2006 predicted that by the year 2020 there will be 4,734 cases of breast cancer and 3,193 cases of colorectal cancer *per annum* (National Cancer Registry, 2006). Thus new and improved avenues of treatment and care are urgently required. The focus for a better cancer strategy must include chemoprevention through exercise and diet, screening for earlier detection, prediction of patient response to different treatments by using genomic and proteomic analysis, and more effective anticancer drugs with reduced side-effects and resistance.

1.1.2 Breast cancer

The human breast consists of 15 to 20 sections called lobes, which are sub-divided into lobules. At the end of the lobules are dozens of glands that can produce milk. Thin tubes called ducts connect the lobes, lobules and glands. Cancer in the cells of the ducts (ductal carcinoma) is the most common type of breast cancer. Lobular carcinoma, which begins in the lobes or lobules, accounts for approximately 10% of breast cancers (www.cancer.gov and Cocquyt and van Belle, 2005). The ducts contain a central lumen, which is surrounded by a single layer of luminal epithelial cells, outside which is a layer of myoepithelial cells resting on the extracellular matrix (ECM) (Figure 1.1). The myoepithelial cells are seen as having a tumour suppression effect, by depositing ECM components and producing proteinase inhibitors, with loss of the myoepithelial cell layer observed in invasive tumours (Lacroix *et al*., 2004). During development, the ducts are formed as the terminal end

buds (TEBs) move through the mammary fat pad. The TEBs are bulbous structures, which consist of a mass of body cells surrounded by a layer of cap cells (Figure 1.1). The cap cells have a high proliferation rate and eventually give rise to the myoepithelial cells of the duct. The body cells give rise to the luminal epithelial cells. Once the TEBs have completed their development, they regress to form terminal ducts. Upon puberty, lateral and alveolar buds develop in the mammary gland and during pregnancy considerable proliferation occurs, giving rise to side branches and alveoli (Smalley and Ashworth, 2003). Upon lactation, the luminal cells produce the milk and contraction of the myoepithelial cells squeezes the milk out of the alveoli and down the ducts to the nipple (Richert *et al*., 2000 and Smalley and Ashworth, 2003).

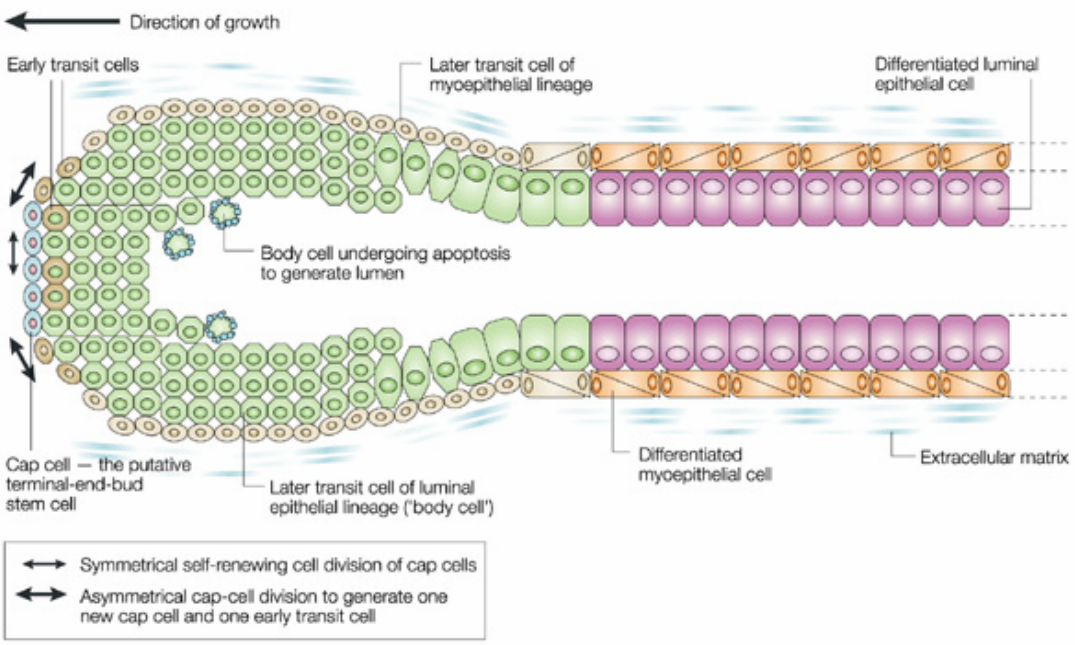

Figure 1.1 Structure of the ducts and terminal end buds in mammary gland development. From Smalley and Ashworth, 2003.

There are many risk factors involved in breast cancer including older age; beginning menstruation at an early age; having no children or having the first child at an older age; taking estrogen or progesterone hormones; alcohol intake and being of

Caucasian race (www.cancer.gov). Stages of breast cancer range from Stage 0 to IV. Stage 0 refers to carcinoma *in situ* where abnormal cells are found in the lobules of the breast (lobular carcinoma *in situ* – LCIS) or in the lining of the duct (ductal carcinoma *in situ* – DCIS). At this stage, precancerous cells are confined and have not spread to other tissues. In Stage IV, the cancer has metastasised to other organs of the body, most often the lungs, bones, liver or brain. The intervening stages are differentiated by the increasing size of the primary tumour and the presence or absence of cancer cells in the lymph nodes (www.cancer.gov).

The development of breast cancer begins with atypical epithelial hyperplasia, followed by *in situ* carcinoma, invasive carcinoma and finally metastatic disease (Figure 1.2) (LaCroix *et al*., 2004 and Polyak, 2001). Nuclear grade, which represents the size and shape of the nucleus in tumour cells and the percentage of tumour cells that are in the process of dividing or growing, correlates with outcome in cases of DCIS. High grade DCIS has a 25-30% rate of local recurrence while low grade has 0-5% recurrence rate after 12 years follow-up (Polyak, 2001). Also, high-grade tumours tend to recur within a shorter time period than low grade (Lacroix *et al*., 2004). High grade DCIS and high grade invasive ductal carcinoma (IDC) are more likely to be estrogen receptor (ER) and progesterone receptor negative, to exhibit amplification of erythroblastic leukaemia viral oncogene homolog 2/human epidermal growth factor receptor 2 (ERBB2/HER2), p53 mutations, decreased bcl-2 levels and have higher proliferation and apoptosis rates in comparison to low grade DCIS/IDC (Polyak, 2001 and Lacroix *et al.*, 2004).

Figure 1.2 Progression of breast cancer from normal epithelium to metastasis. Adapted from Polyak, 2001.

Microarray studies of breast tumours have identified a number of major phenotypes including a 'luminal epithelial/ER-positive' subtype, a 'normal breast-like' subtype, 'basal/myoepithelial' subtype and 'ERBB2+' subtype. The luminal epithelial/ER-positive subtype accounts for 60-65% of tumours, which are generally low-grade. The basal/myoepithelial and ERBB2+ subtypes are associated with poor clinical outcome. These microarray studies have identified expression signatures, which can predict the occurrence of metastasis or 10-year survival rates, giving the possibility of aiding selection of treatment for these patients (Lacroix *et al.*, 2004).

More than 90% of breast cancers are sporadic or non-hereditary, with the remaining 10% of cases being inherited forms (Polyak, 2001). Breast cancers caused by germ-line mutations in the *BRCA1* and *BRCA2* tumour suppressor genes contribute significantly to this 10% figure (Polyak, 2001). Also, mutations in *PTEN*, *TP53*, *ATM* and *MCH2/MLH1* genes are associated with hereditary breast cancer (Polyak, 2001).

TP53 is a tumour suppressor gene encoding a transcription factor, p53, which is mutated in 15-34% of sporadic breast tumours (Ingvarsson, 1999). The p53 protein is involved in the G1 checkpoint of the cell cycle. The protein accumulates in the cell following DNA damage and, via activation of p21, halts the cell in the G1 phase until the damage is repaired (Ingvarsson, 1999). Mutations in the gene encoding E-cadherin are found in a majority of lobular breast tumours but not in ductal carcinomas. However, reduced expression of the E-cadherin protein is seen in both lobular and ductal breast cancer. This protein is involved in cell-cell interactions and therefore loss of function appears to affect adhesion and consequently facilitates invasion (Ingvarsson, 1999).

Recently, a hypothesis regarding the origin of breast cancer from stem cells has been postulated and is now being researched considerably. It states that only a small distinct subset of cells, the breast cancer stem cells (BCSCs), have the ability to form new tumours but are extremely efficient at doing so (Al-Hajj *et al.*, 2003). This theory is supported by the fact that stem cells are believed to have a long life in the body, therefore allowing a number of mutations to accumulate, and have a large replicative potential that could give rise to a mass of tumour cells (Smalley and Ashworth, 2003). Al-Hajj *et al*. (2003) identified a population of breast tumour cells, which had a 10 to 50-fold increase in the ability to form tumours in xenografts when compared with the remaining tumour cells. Ponti *et al*. (2005) confirmed these

results by successfully propagating BCSCs as floating spheres from three patients and induced tumours in mice by injecting as few as 10^3 cells.

This hypothesis may explain why only a portion of patients with evident micrometastasis subsequently develops secondary tumours. However, stem cells are thought to have a slow rate of division, and this theory has a major impact on the treatment of breast cancer with the possibility that current treatments may kill off the main tumour mass but leave behind the BCSCs (Kalirai and Clarke, 2006). This would allow regeneration of the tumour and recurrence of the disease. Normal stem cells are known to be more resistant to chemotherapy than their mature cell counterparts due to increased levels of anti-apoptotic proteins and membrane transporter proteins (Al-Hajj *et al*., 2003 and Reya *et al*., 2001). Hence, new therapies targeting specific markers of BCSCs are required in conjunction with current treatments to ensure complete elimination of all tumour cells, including the BCSCs.

1.1.3 Colorectal Cancer

Colorectal cancer refers to cancer of the colon or large intestine and the rectum. Using the Dukes' staging to describe the progression of colorectal cancer, stages A and B describe cancers confined to the bowel wall, in stage C the cancer has spread to the lymph nodes and finally, stage D refers to cases where distant metastases are evident (Hendon and DiPalma, 2005 and McLeod *et al*., 2000). Dukes' staging A-D represents progression of the disease and subsequently survival rates after 5 years decrease from >80% for stage A to 5% for stage D (Hendon and DiPalma, 2005 and de la Chapelle, 2004). Due to non-specific or non-existent symptoms at early stages, only 10% of patients present with Dukes' stage A and the majority of patients have disease at stage C or D before presentation (McLeod *et al*., 2000). 60% of patients will develop metastases, with liver being the most common site probably due to the portal drainage of blood from the intestine (McLeod *et al*., 2000).

Risk factors for colorectal cancer include age, family history, diet, smoking and conditions such as Crohn's disease and ulcerative colitis (www.cancer.gov). Most colon cancers occur in individuals over the age of 50, with 64 being the mean

age of diagnosis for sporadic cancers (Grady, 2006). Diets high in fat and red meat and low in calcium and fibre may increase the risk of colorectal cancer (www.cancer.gov and Hendon and DiPalma, 2005). Crohn's disease and ulcerative colitis cause inflammation of the colon and therefore may contribute to the development of CRC (www.cancer.gov).

Colorectal cancer development begins with aberrant crypt proliferation, which leads to benign adenomas, followed by carcinoma *in situ* and metastatic carcinoma (de la Chapelle, 2004). The progression of colorectal cancer is stepwise and generally occurs over a number of years. The somatic mutations which result in colorectal cancer occur in the *adenomatous polyposis coli* (*APC*) gene, followed by mutations in the *Ras* family of genes and then subsequent changes in the *p53* gene (Figure 1.3) (de la Chapelle, 2004 and Michor *et al*., 2005). The APC and p53 pathways are altered in 95% of patients with colorectal cancer, while mutations in the Ras pathway are found in 70% of patients (Michor *et al*., 2005). Mutations causing inactivation of the tumour suppressor APC lead to increased transcription of growth-promoting genes (Michor *et al*., 2005 and Hendon and DiPalma, 2005). H, N and K human *Ras* genes encode four proteins, which play a role in signal transduction via the mitogen activated protein kinase (MAPK) pathway (McWilliams and Erlichman, 2005). Mutations in the K-*ras* gene, which lead to over-expression of the protein, result in increased cell proliferation and production of matrix-degrading proteases (McWilliams and Erlichman, 2005). Constitutive expression of this gene, as a result of missense mutations, occurs in 50% of CRCs (McWilliams and Erlichman, 2005).

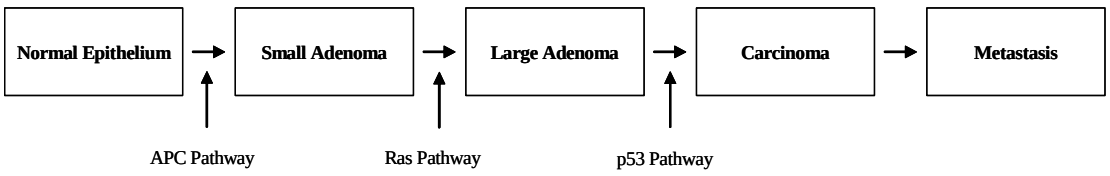

Figure 1.3 Genetic changes in colorectal tumourigenesis. Adapted from Michor *et al*., 2005.

Changes in expression of numerous other proteins also play a role in the development of CRC, including epidermal growth factor receptor (EGFR), cyclins, members of the bcl-2 family and vascular endothelial growth factor (VEGF) (McWilliams and Erlichman, 2005). EGFR belongs to the human epidermal growth factor receptor (HER) family of tyrosine kinases (McWilliams and Erlichman, 2005). Activation of the receptor leads to proliferation and production of angiogenic factors and matrix metalloproteinases (MMPs). Up to 77% of colorectal cancers over-express EGFR and its over-expression inversely correlates with survival (McWilliams and Erlichman, 2005). Cyclin D1, which is involved in the movement of the cell through the G1 phase of the cell cycle, is over-expressed in one third of CRCs and is associated with poorer prognosis for the patient (McWilliams and Erlichman, 2005). Over-expression of cyclin D1 may tie-in with mutations in the *APC* gene, through loss of inhibition of the Wnt-catenin pathway (McWilliams and Erlichman, 2005). The complex formed between cyclin dependent kinase 2 (cdk2) and cyclin E is involved in initiating progression to the S-phase of the cell cycle. Activity of this complex is increased in 90-100% of colorectal adenomas and carcinomas, promoting movement through the cell cycle (McWilliams and Erlichman, 2005). VEGF plays an important role in angiogenesis which is required for tumour growth and subsequent metastasis. Expression of VEGF in primary tumours is inversely correlated to survival (McWilliams and Erlichman, 2005).

Approximately 20-25% of colorectal cancers are familial or hereditary (de la Chapelle, 2004). Hereditary non-polyposis colon cancer (HNPCC), also known as Lynch Syndrome, and familial adenomatous polyposis (FAP) are two well-understood familial syndromes. HNPCC is the most common type of inherited colorectal cancer and accounts for approximately 2% of all cases of colorectal cancer (www.cancer.gov). Mutations linked to HNPCC confer an 80% chance of developing the disease (de la Chapelle, 2004 and http://coloncancer.about.com/cs/types/a/TypesOfCRC.htm). The syndrome also confers predisposition to developing a number of other cancers including stomach, ovarian, endometrial and brain (de la Chapelle, 2004). HNPCC is an autosomal dominant condition, caused by aberrations in the mutation mismatch repair (MMR) genes *MLH1*, *MSH2*, *MSH6*, *PMS2*, *MLH3* and *PMS1* (de la Chapelle, 2004, Grady 2006 and Hendon and DiPalma, 2005). Dysplasia of the mucous membrane of the colon and rectum leads to development of adenocarcinomas, in contrast to the standard progression from adenomas to

adenocarcinomas (http://coloncancer.about.com/cs/types/a/TypesOfCRC.htm). FAP is also an autosomal dominant syndrome and is caused by mutations in the *APC* tumour suppressor gene (www.cancer.gov and Hendon and DiPalma, 2005). The majority of mutations are insertions or deletions, causing a change in the reading frame. Individuals with germ-line mutations in this gene have almost a 100% chance of developing FAP. Patients with FAP develop hundreds to thousands of adenomas in the colon and rectum (www.cancer.gov and de la Chapelle, 2004). The adenomas develop into adenocarcinomas unless treatment is sought.

1.2 Invasion and Metastasis

The spread of cancer cells to other sites in the body and the subsequent formation of secondary tumours is the main cause of death in cancer patients. In approximately 50% of patients, metastatic disease has already been established at diagnosis (Ahmad and Hart, 1997). Metastasis is a complex process involving numerous adhesion factors, motility factors, proteases and angiogenic factors. Cells from the primary tumour must invade through the ECM, intravasate into the lymph or blood system, survive in the circulation, arrest and extravasate in a distant organ and proliferate successfully to form metastases (Figure 1.4) (Bogenrieder and Herlyn, 2003). The limiting factor in this process is growth of the tumour cells at the secondary site (Chambers *et al*., 2002) and less than 0.05% of tumour cells in the circulation are capable of forming metastases (Geho *et al*., 2005).

Cell adhesion molecules include integrins, the immunoglobulin (Ig) superfamily and the cadherins. The integrin family of membrane proteins consists of at least 18α and 8β subunits which heterodimerise and mediate communication between the cell and the ECM (Bogenrieder and Herlyn, 2003). Signals relayed by the integrins activate pathways involved in migration and survival (Bogenrieder and Herlyn, 2003). The Ig superfamily comprises transmembrane proteins containing one or more Ig-like repeats in their extracellular domain. They mediate cell-cell interactions by binding to similar sequences on adjacent cells (King, 2000) and thereby direct the flow of information between cells through various kinases and growth factor receptors (Bogenrieder and Herlyn, 2003). The cadherin subfamily has

numerous members involved in calcium-dependent cell-cell adhesion at adherens junctions and tight junctions (Cross and Bury, 2003). The extracellular domain of the E-cadherin molecule mediates adhesion to homophilic cells by binding with another E-cadherin molecule on an adjacent cell. The intracellular domain affiliates with various catenin proteins, forming the cytoplasmic cell-adhesion complex (CCC) that mediates the link to the actin cytoskeleton, strengthening the bond between adjacent cells (Bissell and Radisky, 2001 and Cavallaro and Christofori, 2004). Adhesion molecules play a complex role in metastasis; with changes in adhesive preferences occurring during the processes of migration, invasion, arrest and extravasation.

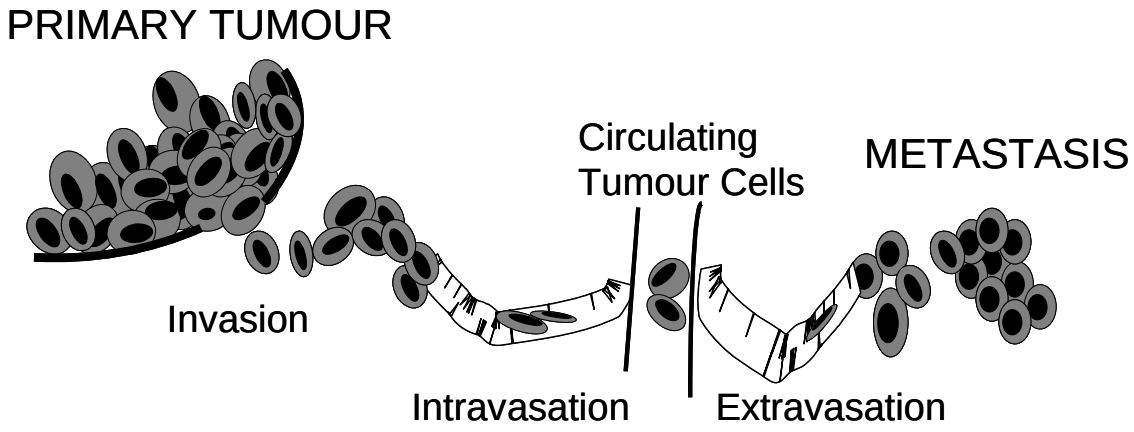

Figure 1.4 The process of metastasis of cancer cells involves invasion, intravasation, survival in the circulatory system, extravasation and formation of a secondary tumour. Adapted from McDonnell *et al*., 2006.

Another family of molecules that play a critical role in this process are the MMPs. There are over 24 members of this family of protease enzymes, each highly conserved, and collectively able to degrade the entire ECM (Lynch and Matrisian, 2002 and Curran and Murray, 2000). The ECM is a physical boundary around tissues which consists of numerous proteins, proteoglycans and glycoproteins such as collagens, gelatin, entactin, fibronectin and laminin (Lynch and Matrisian, 2002). The MMPs also degrade non-matrix substrates such as insulin growth factor binding

proteins (IGF-BPs), transforming growth factor-β (TGF-β) and E-cadherin (Lynch and Matrisian, 2002).

The MMPs contain a highly conserved three histidine-motif at the catalytic site which binds zinc and is essential for activity (Sternlicht and Werb, 2001). They consist of an N-terminal propeptide or pre-domain, a pro-domain and a catalytic domain (Lynch and Matrisian, 2002). The pre-domain is removed once the protein has been directed to the endoplasmic reticulum (Sternlicht and Werb, 2001). The majority of MMPs are then secreted as proenzymes or latent zymogens from the cell with activation occurring extracellularly by removal of the N-terminal pro-domain. The enzymes are thus found in the conditioned medium of cultured cells. Some MMPs contain a transmembrane domain and are known as membrane type-MMPs (MT-MMPs). The majority of MMPs have a hemopexin domain which contains a three repeat unit and plays a role in cleavage of substrates and binding of inhibitors (Murphy, 1998 and Sternlicht and Werb, 2001). The tissue inhibitors of metalloproteinases (TIMPs) act as inhibitors of the MMPs, by binding to the active site of the enzyme in a 1:1 molar ratio. There are four TIMPs identified to date, they are secreted proteins of 20 – 29 kDa in size (Lynch and Matrisian, 2002 and Sternlicht and Werb, 2001).

MMP-2 and MMP-9 are the two gelatinase enzymes, termed due to their ability to degrade gelatin. They have three cysteine-rich repeats within their catalytic domain (Sternlicht and Werb, 2001). Activation of MMP-2 occurs at the cell surface involving interactions with TIMP-2 and MT1-MMP. TIMP-2 binds to the membrane-bound MT1-MMP by its N-terminal domain (Egeblad and Werb, 2002). The C-terminal domain of TIMP-2 then sequesters the latent MMP-2 to the complex while a second MT1-MMP molecule cleaves part of the pro-domain of MMP-2. Another MMP-2 molecule is required to cleave the remaining section of the pro-domain before activation is complete (Sternlicht and Werb, 2001). Following activation, the activity of MMP-2 is partially regulated by interaction with the N-terminal domain of TIMP-2. MMP-9 binds to the cell surface hyaluronan receptor CD44, which appears to promote tumour cell invasion (Sternlicht and Werb, 2001). MMP activity is also controlled by the plasma protein α-macroglobulin, which binds MMPs and recruits them to a scavenger receptor. Endocytosis of the complex occurs,

eliminating the MMP protein. Thrombospondin-1 and -2 also play roles in regulating the activity of MMP-2 and MMP-9.

MMP expression is generally high in the tumour region, due to secretion from the cancer cells but also from the surrounding stromal cells. Expression of MMPs generally correlates with the aggressiveness of the tumour and subsequent prognosis (Lynch and Matrisian, 2002 and Sternlicht and Werb, 2001). This has been confirmed by animal studies, with over-expression of MMPs contributing to tumourigenesis and metastasis while deficiencies of MMPs have shown decreased tumour formation (Lynch and Matrisian, 2002). Increased expression of TIMP-1 has also been shown to cause a decrease in tumour formation (Sternlicht and Werb, 2001).

1.3 Treatments

When a patient presents with cancer, there are a number of treatment options available depending on the type of tumour and the stage of the disease. Surgery to remove a solid tumour is common, with radiation therapy, chemotherapy and hormonal therapy all playing roles in reduction of the size of the tumour prior to excision or in the fight against recurrence of the disease. Chemotherapy given before surgery is called neoadjuvant therapy, while adjuvant therapy refers to chemotherapy given after surgery. There are numerous types of chemotherapeutic drugs used in the clinical setting. Alkylating agents, antimetabolites, cytotoxic antibiotics, mitotic inhibitors and monoclonal antibodies are the main forms of treatment (Saeb-Parsy *et al*., 1999 and Lazo and Larner *et al*., 1998).

Alkylating agents include cyclophosphamide and cisplatin. They form covalent bonds between the bases of DNA, either inter-strand or intra-strand, blocking cells from moving from the S phase into the G2 phase and leading to apoptosis (Lazo and Larner *et al*., 1998). Antimetabolites interfere with the metabolic pathways involved in DNA synthesis and include 5-fluorouracil (5-FU) and methotrexate (MTX). 5-FU inhibits thymidylate synthesis while MTX inhibits dihydrofolate reductase, blocking synthesis of both pyrimidines and purines (Lazo and Larner *et al*., 1998). Cytotoxic antibiotics are of microbial origin and act to

prevent cell division. The anthracycline doxorubicin is a cytotoxic antibiotic which binds DNA, inhibits topoisomerase II activity and thus disrupts DNA and RNA synthesis (Minotti *et al*., 2004). Epirubicin, bleomycin and mitomycin are other cytotoxic antibiotics. Mitotic inhibitors prevent spindle formation causing cell cycle arrest in the mitosis (M) phase and include the plant derivatives vincristine and paclitaxel.

The main monoclonal antibody currently in use is trastuzumab, which blocks ERBB2/HER2 signalling. This receptor is over-expressed in 25-30% of breast cancers, due to amplification of the gene. Over-expression of ERBB2/HER2 has been associated with more aggressive disease, higher mortality rates and resistance to treatment (Buzder *et al*., 2005). Hormonal therapy includes the antagonist Tamoxifen which binds ERβ and blocks estrogen-dependent transcription and cell proliferation (Lazo and Larner *et al*., 1998). Anti-metastatic agents have been given a lot of attention as the majority of cancer patients die because their tumour has metastasised (Bogenrieder and Herlyn, 2003). MMP inhibitors have been investigated for several decades. Collagen-based peptidomimetic MMP inhibitors Batimastat and Marimastat showed promising results in tumour cell and animal models. However, clinical results were disappointing, with dose-limiting muscular and skeletal pain, partially due to the broad-spectrum of MMPs that these drugs inhibit (Hidalgo and Eckhardt, 2001 and Fisher and Mobashery, 2006).

While most of the chemotherapies aim to cause apoptosis of the cancer cells, there are limitations to this effect due to the nature of solid tumours. Only a fraction of tumour cells are actively dividing at any one time, with the remainder of the cells in G0 phase of the cell cycle. The majority of cancer treatments kill the actively dividing cells of the tumour, thus eliminating only a fraction of the cancer cells. Combination therapies of the above-mentioned drugs tackle this problem to some extent, by using different modes of toxicity. Side-effects of chemotherapy can include hair loss, nausea, vomiting, diarrhoea and immunosuppression. These are due to the nature of most of the drugs which attack rapidly dividing cells of the body. Besides the tumour cells, this also includes cells of the hair follicles, bone marrow and gastrointestinal tract. These side-effects can be somewhat reduced by the method of administration of the drug to maximise exposure of the tumour cells with minimum exposure to non-neoplastic cells. Resistance to chemotherapeutic agents also causes

limitations with regards to the treatment of patients. Tumours may be intrinsically resistant to the therapy or may acquire resistance following repeated doses (Lazo and Larner *et al*., 1998 and Liang *et al*., 2002). This can be due to a decrease in uptake of the drug or increased production of transmembrane pumps which rid the cell of the drug. Up-regulation or mutation of target proteins may also play a role in resistance, or changes in DNA repair mechanisms and anti-apoptotic proteins (Lazo and Larner *et al*., 1998).

1.4 Objectives of thesis

- The main objective of this thesis was to explore two possible new avenues for the treatment of cancer: CLA and novel 5-FU derivatives. These represent two different approaches to anticancer therapy.
- CLA is a component of dairy products and meat from ruminant animals and could be supplemented in the diet as a component of a functional food. The aim of chapter 3 was to look at the effect of a mixture of CLA isomers and two individual isomers on cell proliferation, cell cycle kinetics and apoptosis in murine mammary and human breast cancer cell lines.
- Investigation of *in vitro* cell invasion, migration, adhesion and colony formation in soft agar following CLA treatment was conducted to determine effects on these processes. MMP and TIMP expression at the mRNA and protein levels was quantified to examine changes at the molecular level.
- 5-FU has been used extensively in chemotherapy regimens for a number of decades, but with dose-limiting toxicities and low response rates. 5-FU derivatives, including prodrugs, may provide a more targeted therapy to tumour cells, thus reducing side-effects and offering more efficacious treatments.
- Chapter 4 focused on a number of novel 5-FU and 5-Fluorouridine (5-FUrd) derivatives with nitro-benzyl, ester and acid side-chains. Cytotoxicity of these compounds was examined in a murine mammary cancer cell line, a human colorectal cancer cell line and a 5-FU resistant human colorectal cancer cell line. The effect of these derivatives on cell cycle kinetics, apoptosis, migration, invasion and soft agar colony formation was investigated.
- A sub-set of these compounds was designed as prodrugs and this aspect was the focus for chapter 5. Activation of the prodrugs was assessed under hypoxic conditions and by enzymatic cleavage with the *E. coli* nitroreductase enzyme. Cytotoxicity in a cell line transfected with the cDNA for this enzyme was examined along with mass spectrometry analysis to confirm activation. Analysis of the 5-FU prodrugs as substrates for the enzyme was conducted using enzyme kinetics studies. A human colorectal cancer cell line was transfected with the cDNA for nitroreductase and cytotoxicity examined.

Chapter 2

Materials & Methods

2.1 Materials

All general-purpose reagents and chemicals used in the experimental work were of analytical grade and, unless otherwise stated, were obtained from Sigma-Aldrich Inc., Dublin, Ireland.

1 kb DNA ladder was supplied by Sigma-Aldrich Inc., Dublin, Ireland.

5-Fluorouracil and 5-Fluorouridine derivatives were provided by Dr. Ian Gray and Dr. Kieran Nolan, School of Chemical Sciences, Dublin City University, Ireland.

Acetonitrile was supplied by Labscan, Stillorgan, Co. Dublin, Ireland.

Acid phosphatase assay was kindly donated by Dr. Robert O'Connor, National Institute for Cellular Biotechnology, Dublin City University, Ireland.

Agar noble was supplied by Difco, distributed by Unitech, Dublin, Ireland.

AMP-D1 kit containing Deoxyribonuclease I, was supplied by Sigma-Aldrich Inc., Dublin, Ireland.

Amicon® Ultra-4 Centrifugal Filter Devices with Ultracel-10 membrane were supplied by Amicon Ltd., Limerick, Ireland.

Anti-MMP-2 antibody (GL8) was obtained from Dr. Andrew Docherty, Celltech, Slough, England.

Anti-MMP-9 antibody (Ab2) was supplied by Calbiochem, distributed by Merck Biosciences, Nottingham, England.

Baby Hamster Kidney (BHK) cells transfected with the human MMP-9 cDNA (BHK92) were obtained from Professor Dylan Edwards, University of East Anglia, Norwich, England.

Bacto-tryptone was supplied by Oxoid Ltd., Basingstoke, Hampshire, England, distributed by Fannin Healthcare, Ireland.

Bacto-yeast extract was supplied by Oxoid Ltd., Basingstoke, Hampshire, England, distributed by Fannin Healthcare, Ireland.

Bacto-yeast agar was supplied by Oxoid Ltd., Basingstoke, Hampshire, England, distributed by Fannin Healthcare, Ireland.

BD Biocoat™ Matrigel™ Invasion Chambers were supplied by Becton Dickinson Labware, Bedford, MA, USA.

BD Falcon™ TC Companion Plates were supplied by Unitech, Dublin, Ireland.

Blue/Orange Loading Dye was supplied by Promega, distributed by the Medical Supply Company, Dublin, Ireland.

Bradford reagent for protein quantification was supplied by Sigma-Aldrich Inc., Dublin, Ireland.

Bovine serum albumin was supplied by Sigma-Aldrich Inc., Dublin, Ireland.

CB1954 was supplied by Sigma-Aldrich Inc., Dublin, Ireland.

Cell culture medium (Dublecco's Modified Eagle's Medium [DMEM] and McCoys 5A medium) and the supplements L-glutamine, sodium pyruvate, insulin, fetal bovine serum (FBS), 5-Fluorouracil and penicillin/streptomycin, all supplied by Sigma-Aldrich Inc., Dublin, Ireland.

Cell freezing medium was supplied by Sigma-Aldrich Inc., Dublin, Ireland.

CellTiter 96® AQ_{ueous} One Solution Cell Proliferation Assay was supplied by Promega, distributed by Medical Supply Company, Dublin, Ireland.

Chemichrome™ Western Control was supplied by Sigma-Aldrich Inc., Dublin, Ireland.

Chloroform was supplied by Sigma-Aldrich Inc., Dublin, Ireland.

Conjugated linoleic acid was supplied by Nu-Chek-Prep Inc., Minnesota, USA.

Crystal violet was supplied by Lancaster Synthesis, Eastgate White Land, Morecambe, England.

Diethyl pyrocarbonate (DEPC) was supplied by Sigma-Aldrich Inc., Dublin, Ireland.

Dimethyl sulfoxide (DMSO) was supplied by Sigma-Aldrich Inc., Dublin, Ireland.

dNTP Mix was supplied by Merck Biosciences, UK.

F179 and F184 plasmids were kindly provided by Dr. Steve Hobbs, CRUK Centre for Cancer Therapeutics, Institute of Cancer Research, Surrey, UK.

Falcon™ cell culture inserts were supplied by Becton Dickinson Labware, Bedford, MA, USA.

GeneJuice® Transfection Reagent was supplied by Novagen, Merck KGaA, Darmstadt, Germany.

Glycogen was supplied by Ambion Inc., Cambridgeshire, England.

Guava® Nexin™ Kit was supplied by Guava® Technologies Inc., Hayward, California, USA.

Guava® Cell Cycle Reagent was supplied by Guava® Technologies Inc., Hayward, California, USA.

HCT116 parental and HCT116 5-FU-resistant cell lines were kindly provided by Professor Patrick G. Johnston, Department of Oncology, Cancer Research Centre, Queen's University Belfast, Belfast, Northern Ireland.

Hyperfilm was supplied by Amersham Biosciences, Buckinghamshire, UK.

IGEPAL was supplied by Sigma-Aldrich Inc., Dublin, Ireland.

Max Efficiency DH5α competent cells were supplied by Invitrogen, distributed by Bio-sciences, Dublin, Ireland.

MemCode™ Reversible Protein Stain Kit was supplied by Pierce Chemicals, distributed by Medical Supply Company, Dublin, Ireland.

MMLV-RT was supplied by Promega, distributed by Medical Supply Company, Dublin, Ireland.

Nicotinamide adenine dinucleotide (NADH) was supplied by Sigma-Aldrich Inc., Dublin, Ireland.

Nitrocellulose membranes, supported, 0.45 µm pore size supplied by Sigma-Aldrich Inc., Dublin, Ireland.

Nitroreductase was supplied by Sigma-Aldrich Inc., Dublin, Ireland.

Novagen SpinPrep™ Plasmid Kit was supplied by Merck Biosciences, UK.

Novex® development buffer 10X, pre-cast 10% Zymogram (Gelatin) Gel, Tris-Glyine SDS running buffer and Zymogram renaturing buffer supplied by Invitrogen, distributed by Bio-sciences, Dublin, Ireland.

NuPAGE™ 4-12% Bis-Tris gels, LDS sample buffer, antioxidant, sample reducing agent and transfer buffer were supplied by Invitrogen, distributed by Bio-sciences, Dublin, Ireland.

Oligo $(dT)_{15}$ Primers supplied by Promega, distributed by the Medical Supply Company, Dublin, Ireland.

Polymerase chain reaction (PCR) 100 bp low ladder supplied by Sigma-Aldrich Inc., Dublin, Ireland.

PCR primers were supplied by MWG Biotech, Ebersberg, Germany.

P-Iodonitrotetrazolium Chloride was supplied by Sigma-Aldrich Inc., Dublin, Ireland.

Phosphate buffered saline (PBS) tablets supplied by Oxoid Ltd., Basingstoke, Hampshire, England.

Phosphoric acid (HPLC grade) was supplied by Sigma-Aldrich Inc., Dublin, Ireland.

Plastic consumables for cell culture were supplied by Sarstedt, Sinnottstown Lane, Drinagh, Co. Wexford, Ireland.

Protease Inhibitor Cocktail was supplied by Sigma-Aldrich Inc., Dublin, Ireland.

Proteinase K was supplied by Roche Diagnostics GmBH, Mannheim, Germany, distributed by Fannin Healthcare, Ireland.

Puromycin dihydrochloride was supplied by Sigma-Aldrich Inc., Dublin, Ireland.

Qiagen Maxi-prep plasmid kit was supplied by QIAGEN Ltd., Crawley, West Sussex, England.

Restriction enzymes were supplied by Promega, distributed by Medical Supply Company, Dublin, Ireland.

RNA Sample Loading Buffer was supplied by Sigma-Aldrich Inc., Dublin, Ireland.

SigmaMarker™ Wide Molecular Weight Range was supplied by Sigma-Aldrich Inc., Dublin, Ireland.

Super Signal West ECL detection kit obtained from Pierce Chemicals, Rockford, Il., USA.

SYBR Safe™ DNA gel stain was supplied by Molecular Probes/Invitrogen, distributed by Bio-sciences, Dublin, Ireland.

Taq polymerase and Magnesium Chloride were obtained from Sigma-Aldrich Inc., Dublin, Ireland.

TIMP recombinant proteins were supplied by Chemicon International, Temecula, California, USA.

Tissue culture plates 96, 24 and 6 well obtained from Sarstedt, Sinnottstown Lane, Drinagh, Co. Wexford, Ireland.

TRI REAGENT™ was supplied by Sigma-Aldrich Inc., Dublin, Ireland.

Trypsin-EDTA was supplied by Sigma-Aldrich Inc., Dublin, Ireland.

Trypan blue was supplied by Sigma-Aldrich Inc., Dublin, Ireland.

V79-C and V79-NTR cell lines were supplied by Morvus Technology Ltd., Salisbury, UK.

2.2 Methodology

2.2.1 Cell culture methods

All cell culture techniques were performed in a sterile environment using a Holten HB2448 laminar airflow cabinet. Cells were visualised with an Olympus CK2 inverted phase contrast microscope.

2.2.1.1 Cell lines

The following cell lines were used in this study: 4T1, Hs578T, SW480, HCT116 parental, HCT116 5-FU-resistant, V79-NTR and V79-C. 4T1 (ATCC No CRL-2539), Hs578T (ATCC No HTB-126) and SW480 (ATCC No CCL-228) were obtained from the American Type Culture Collection (ATCC). 4T1 is a murine mammary cancer cell line. Hs578T is a human breast carcinoma cell line. SW480 is derived from a human colorectal adenocarcinoma. HCT116 parental and 5-FU-resistant cell lines were kindly provided by Professor Patrick G. Johnston, Department of Oncology, Cancer Research Centre, Queen's University Belfast, Belfast, Northern Ireland. HCT116 parental (HCT(P)) is a human colorectal carcinoma cell line. The HCT116 5-FU-resistant (HCT(R)) cell line was established from the HCT(P) cell line by repeated exposure to stepwise increasing concentrations of 5-FU (Boyer *et al*., 2004). The V79-NTR and V79-C cell lines were obtained from Morvus Technology Ltd., Salisbury, UK. V79-NTR and V79-C are Chinese hamster lung fibroblast cell lines. V79-NTR had been transfected with the cDNA for the *Escherichia coli* nitroreductase (NTR) enzyme, while V79-C was transfected with the control vector. Cell lines were routinely tested for mycoplasma contamination in the Conway Institute, University College Dublin.

2.2.1.2 Sub-culturing of cells

The cell lines under study were maintained in medium as outlined in Table 2.1. Cells were cultured in 25 cm^2 or 75 cm^2 tissue culture flasks and incubated in a humid, 5% (v/v) CO_2 atmosphere in a 37°C Thermo Electron Corporation cell culture

incubator. All cell lines were adherent and required trypsinisation for harvesting of cells prior to sub-culturing. For trypsinisation, the growth medium was aspirated and the flask rinsed with 1.5 ml trypsin ethylenediamine tetraacetic acid (EDTA) (0.025% (w/v) trypsin with 0.02% (w/v) EDTA in 0.15 M Phosphate Buffered Saline (PBS), pH 7.4). 2.5 ml of fresh trypsin was then placed in each flask and the flask incubated at 37°C for 10-15 minutes or until all the cells had detached from the surface. The cell suspension was pipetted up and down gently to aid detachment of the cells from each other. 3 ml medium was added to the flask and the total volume was removed to a sterile universal container and centrifuged at 720 g for 5 minutes in an Eppendorf Centrifuge 5804. The supernatant was poured off and the cells were resuspended in culture medium and seeded at relevant cell density, with 13 ml of medium in total in a 75 cm^2 flask and 5 ml in a 25 cm^2 flask. Cells were typically passaged 2-3 times per week.

Table 2.1 Medium supplements for individual cell lines.

Cell Line	Description	Medium	FBS	L-Glutamine	Penicillin-Streptomycin	Other
4T1	Murine mammary cancer	DMEM	5% (v/v)	2 mM	50 U/ml Penicillin 50 μg/ml Streptomycin	
SW480	Human colorectal adenocarcinoma	DMEM	10% (v/v)	2 mM	50 U/ml Penicillin 50 μg/ml Streptomycin	
Hs578T	Human breast carcinoma	DMEM	10% (v/v)	4 mM	50 U/ml Penicillin 50 μg/ml Streptomycin	10μg/ml Insulin
V79-NTR	Chinese hamster lung fibroblast transfected with cDNA for NTR	DMEM	10% (v/v)	4 mM		10μg/ml Puromycin
V79-C	Chinese hamster lung fibroblast transfected with empty vector	DMEM	10% (v/v)	4 mM		10μg/ml Puromycin
HCT(P)	Human colorectal carcinoma	McCoys 5A	10% (v/v)	2 mM	50 U/ml Penicillin 50 μg/ml Streptomycin	1mM Sodium Pyruvate
HCT(R)	Human colorectal carcinoma resistant to 5-Fluorouracil	McCoys 5A	10% (v/v)	2 mM	50 U/ml Penicillin 50 μg/ml Streptomycin	1mM Sodium Pyruvate 2μM 5-FU

2.2.1.3 Cell counts

Cells were counted following a 5 minute incubation with trypan blue. Typically, a 500 μl aliquot of cell suspension was mixed with 100 μl of trypan blue.

Following incubation, 10 µl of this mixture was added to a Neubauer haemocytometer slide and cells counted in the four corner quadrants. Viable cells excluded the dye and remained clear while dead cells stained blue. Calculation of the number of cells per millilitre was as follows:

[(Average no. viable cells per quadrant) x 1.2 (dilution factor) x 10^4 (area under the coverslip) = viable cells/ml of cell suspension

The required volume of the cell suspension was then calculated using the following equation:

[(Cell density required)/(Cell density have)] x [Volume required] = Volume of cell suspension to add (with remaining volume made up with medium)

2.2.1.4 Storage and recovery of cells

For long term storage cells were trypsinised and centrifuged as per section 2.2.1.2 then resuspended in cell freezing medium and 1 ml was aliquoted into cryotubes. Generally one confluent 75 cm^2 flask was frozen down into one cryotube. The cells were incubated at -20°C for 30 minutes then transferred to a Sanyo Ultra Low -80°C freezer overnight and placed in a Taylor Wharton VHC35 liquid nitrogen vessel. For recovery of cells, a vial was removed from the liquid nitrogen and defrosted in a 37°C water-bath. Cells were removed to 5 ml culture medium in a universal tube, centrifuged at 720 g for 5 minutes. The pellet was resuspended in fresh culture medium and added to a 25 cm^2 cell culture flask which was incubated at 37°C, 5% CO_2.

2.2.1.5 Preparation and storage of stocks of conjugated linoleic acid

Conjugated linoleic acid (CLA) was obtained from Nu-Chek-Prep. The CLA mixture of isomers had the following composition: *cis*9,*trans*11/*trans*9,*cis*11 (~41%), *trans*10,*cis*12 (~44%), *cis*10,*cis*12 (~10%), others (~5%). CLA stocks were made to 10 mg/ml using filter-sterilised ethanol and stored at -20°C. Further dilutions were

made up fresh in cell culture medium before use in assays. The top concentration of 30 μg/ml (107 μM) therefore contained 0.3% ethanol. Controls were treated with this amount of ethanol in medium.

2.2.1.6 Preparation and storage of stocks of 5-FU derivatives

5-FU derivatives were supplied in powder form from Dr. Ian Gray and Dr. Kieran Nolan, School of Chemical Sciences, Dublin City University. The powder was dissolved in dimethyl sulfoxide (DMSO) to 100 mg/ml and stored at -20°C. Further dilutions made up fresh in cell culture medium before use in assays. Therefore, the top concentration of 100 μg/ml contained 0.1% DMSO. Controls were treated with this amount of DMSO in medium.

2.2.2 Cytotoxicity assays

Cells were seeded at a specific density, dependent on the cell line and the duration of the assay, in 100 μl in 96-well plates and allowed to attach overnight at 37°C, 5% CO_2. 100 μl of a 2X solution of relevant treatment was added to triplicate wells and incubated at 37°C, 5% CO_2 for the relevant time period. Standard curves were set up for each experiment to ensure cells were in the exponential phase of growth. Cells for treatment were seeded at the second highest point on the standard curve. The CellTiter 96® AQ_{ueous} One Solution Cell Proliferation Assay (MTS), crystal violet assay and acid phosphatase assay were used to quantify cytotoxicity. For the MTS assay, 40 μl of the MTS was added to each well, allowed to develop in a 37°C incubator for 1-4 hours, after which time the absorbance was read at 492 nm on the Tecan Sunrise multiwell plate reader. The crystal violet assay involved aspiration of medium, cells were washed twice with sterile PBS, fixed with 100 μl 10% formalin for 10 minutes and stained with 100 μl 0.25% aqueous crystal violet for 10 minutes. The 96-well plate was allowed to dry and cells could be visualised using a microscope and photographed. The stain was then eluted with 100 μl 33% glacial acetic acid and absorbance read at 570 nm. The acid phosphatase assay involved aspiration of medium then cells were washed twice with sterile PBS. The *p*-

nitrophenyl phosphate was dissolved in sodium acetate buffer (0.1 M, pH 5.5, containing 0.1% Triton X-100) to a concentration of 10 mM. 100 µl of this solution was added to each well. The plate was covered loosely with tin-foil and incubated at 37°C for 2 hours. To stop the reaction, 50 µl 1 M NaOH was added to each well and the absorbance read at 405 nm.
Percentage cell death was calculated in relation to control cells as follows:

$$[100-\{(Abs_{Sample} - Abs_{Blank} / Abs_{Control} - Abs_{Blank})*100\}] = \% \text{ Cell Death}$$

Results shown are mean cell death values with error bars for standard deviations.

2.2.3 Hypoxic experiments

The hypoxic experiments were carried out in collaboration with Dr. Judith Harmey, Royal College of Surgeons in Ireland, Education and Research Centre, Beaumont Hospital, Dublin. Cytotoxicity assays were set up as described in section 2.2.2 and plates were incubated at 37°C, 5% CO_2, 2% O_2 in a Thermo Electron Corporation cell culture incubator for the relevant time period. The MTS assay was used to calculate cell death as outlined above.

2.2.4 Flow cytometric analysis

The Guava® Personal Cell Analysis (PCA) system was used for flow cytometric analysis of cells, including cell cycle analysis and apoptosis assays.

2.2.4.1 Cell cycle analysis

Cells were seeded in 6-well plates and allowed to attach overnight. Treatment was added at the specified concentrations and cells were incubated for 3 days. Medium was removed from the cells and retained in a universal tube. Cells were washed with 500 µl trypsin which was removed to the same universal tube. 750 µl

trypsin was added to each well and the plate incubated for 10-15 minutes to detach the cells. 1 ml medium was added to the wells to stop the action of the trypsin. The cell suspension was removed from the well to the universal tube and was centrifuged at 720 g for 5 minutes. The supernatant was decanted, the cell pellet resuspended in PBS and a cell count performed as per section 2.2.1.3. 2 x 10^6 cells were removed to a universal tube and centrifuged at 450 g for 8 minutes with the brake on low. The pellet was resuspended in 1 ml PBS before repeating centrifugation under the same conditions. Half the supernatant was removed and the cell pellet was resuspended in the remaining PBS. Drop-wise, the cell suspension was added to 3 ml ice-cold 70% ethanol with vortexing between drops. The sample was stored at 4°C for a minimum overnight incubation. 2 x 10^5 cells were centrifuged at 450 g for 8 minutes with the brake on low, resuspended in PBS, vortexed and allowed to stand for 1 minute. The cells were centrifuged again at 450 g for 8 minutes with the brake on low and resuspended in 200 µl Guava® Cell Cycle Reagent. The suspension was incubated at room temperature for 30 minutes, protected from light. Cells were analysed on the Guava® PCA. Data was analysed using the Multicycle software (Phoenix Flow Systems, CA) to determine the cell cycle stages.

2.2.4.2 Apoptosis analysis

Cells were seeded in 6-well plates and allowed to attach overnight. Treatment was added at the specified concentrations and cells were incubated for 3 days. Medium was removed from the cells and retained in a universal tube. Cells were washed with 500 µl trypsin, which was removed to the same universal tube. 750 µl trypsin was added to each well and the plate incubated for 10-15 minutes to detach the cells. 1 ml medium was added to the wells to stop the action of the trypsin. The cell suspension was removed from the well to the universal tube and centrifuged at 720 g for 5 minutes. The pellet was resuspended in 1 ml Guava® Nexin Buffer. The cell suspension was centrifuged at 400 g for 10 minutes at 4°C and the pellet resuspended in 1 ml Guava® Nexin Buffer. A cell count was performed as per section 2.2.1.3. 2 x 10^6 cells were centrifuged at 400 g for 10 minutes at 4°C and resuspended in 1 ml Guava® Nexin Buffer. 40 µl was removed to an eppendorf tube and 5 µl Annexin V-Phycoerythrin (PE) and 5 µl Nexin 7-Amino Actinomycin D (7-

AAD) added. This suspension was vortexed briefly and incubated on ice for 20 minutes, protected from light. 450 µl cold Guava® Nexin Buffer was added to the suspension and the sample was analysed on the Guava® PCA.

2.2.5 Migration and invasion assays

Falcon™ cell culture inserts used for migration assays and BD BioCoat™ Matrigel™ Invasion Chambers were used for invasion assays. Both these chambers contained 8 µm pores in a polyethylene terephthalate (PET) membrane. The cells may migrate through the pores from the upper side of the membrane to the lower side. Invasion chambers contained an extra coating of Matrigel™ basement membrane matrix which the cells must degrade before they can move through the pores. Both assays were carried out in 24-well format. Figure 2.1 illustrates the arrangement of these chambers. The invasion chambers were stored at -20°C and were brought to room temperature for 30 minutes before use. 500 µl serum-free (S_0) medium was added to each well and the inside of each chamber to re-hydrate the membrane, and incubated at 37°C, 5% CO_2 for 2 hours. Cells were treated for 48 hours with a sub-lethal dose of relevant treatment, trypsinised and counted as described in section 2.2.1. 750 µl medium containing 20% fetal bovine serum (S_{20}) was added to the wells of a BD Falcon™ TC Companion Plates (24-well) to act as a chemo-attractant. The re-hydration medium was removed from the chamber which was then positioned in the companion plate. 5×10^4 cells in 500 µl S_0 medium were added to the chamber for migration assays and 1×10^5 cells in 500 µl S_0 medium were added to the chamber for invasion assays. Relevant treatment was added to the medium in the well and in the chamber. A blank chamber was also used containing medium but no cells. The chambers were incubated at 37°C, 5% CO_2 for 24 hours. Each chamber was removed from the 24-well plate, the medium aspirated from within and the cells remaining on the top of the membrane removed with a cotton swab dipped in sterile PBS. The cells on the bottom of the membrane were fixed by placing the chamber in 10% formalin for 10 minutes followed by staining with 0.25% aqueous crystal violet for 10 minutes. The chambers were washed in three consecutive beakers of PBS to remove any excess stain and then allowed to dry for 30 minutes in a 37°C oven. The

stain was eluted by soaking in 200 µl 33% glacial acetic acid on a rocking platform for 30 minutes. 100 µl was transferred to a 96-well plate and the absorbance read at 595 nm in a multiwell plate-reader. 100% control chambers were set up using the same procedure as above but the cells from the top of the membrane were not removed before staining. The percentage cells migrated/invaded was calculated as follows:

$$\% \text{ Migrated/invaded cells} = [(OD_{Sample} - OD_{Blank}) / (OD_{100\% \text{ Control}} - OD_{Blank})] \times 100$$

Following elution of the stain, the membranes were re-stained, removed from the chambers, mounted on a glass slide and visualised under the microscope. Photographs were taken using an Olympus BX51 microscope with an Olympus DP70 camera attached.

2.2.6 Adhesion assays

Cells were pre-treated for 3 days, trypsinised and counted as per section 2.2.1. A cell suspension was made up to 10^5 cells per ml and 100 µl aliquoted in triplicate into duplicate 96-well plates. The plates were incubated at 37°C, 5% CO_2 for 100 minutes. The medium and any non-adhered cells were removed from one plate by inverting the plate and removing any remaining medium with a pipette. 100 µl medium was then added to each well. 20 µl MTS was added to the wells of both plates, allowed to develop at 37°C in incubator for 1-4 hours, and the absorbance read at 492 nm on the Tecan Sunrise multiwell plate reader. Results were expressed in relation to the 100% control plate – the plate that was not inverted.

2.2.7 Colony formation in soft agar assays

Figure 2.2 illustrates the arrangement of the soft agar assays. A solution of 3% noble agar was made up and autoclaved. 467 µl of the 3% sterile noble agar was mixed with 1.533 ml S_{20} medium (yielding a final concentration of 0.7% noble agar),

poured quickly into the well of a 6-well plate and incubated overnight at 4°C. The following day, the plates were brought to room temperature. 1.633 ml S_{20} medium was mixed with 267 µl 3% sterile noble agar and vortexed. Cells were pre-treated for 3 days, then trypsinised and counted as per section 2.2.1. 100 µl of cell suspension (2 x 10^5 cells/ml) was added to the S_{20}/noble agar mix (giving a final concentration of 0.4% noble agar) and quickly poured on top of the layer plated the previous day. The plate was incubated at 4°C for 5 minutes to set and then placed at 37°C, 5% CO_2 overnight. 2 ml S_{20} medium was added to each well the following day. After incubation for 10 days, colonies were stained with 1 ml *p*-iodonitrotetrazolium chloride solution (1 mg/ml) and incubated overnight at 37°C, 5% CO_2. Stained colonies with a diameter of greater than 100 µm were counted using a graticule inserted into the eyepiece of the microscope.

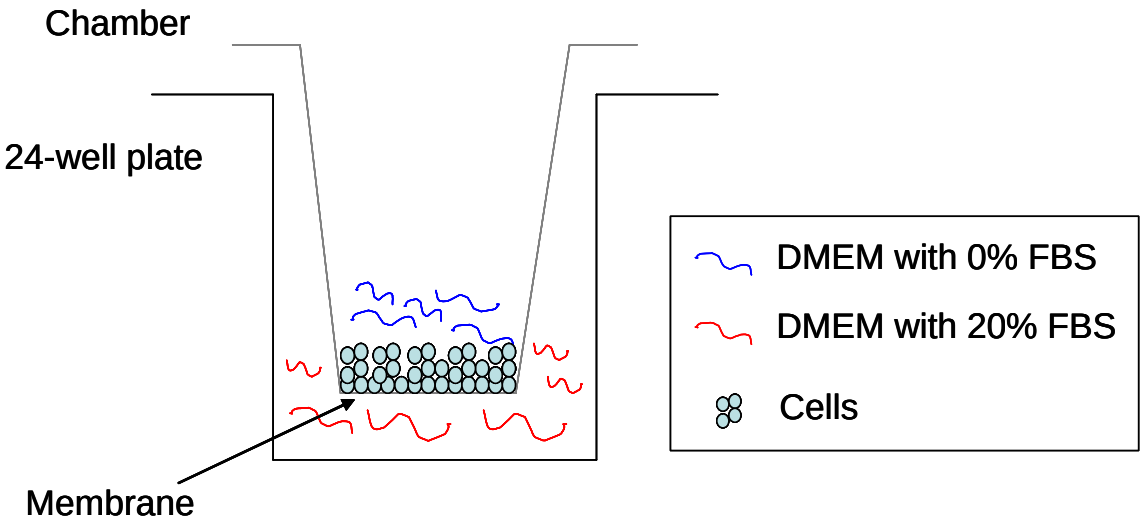

Figure 2.1 Representation of the *in vitro* migration and invasion assays. DMEM with 20% FBS was placed in the well and the pre-treated cells, in DMEM with 0% FBS were added to the chamber.

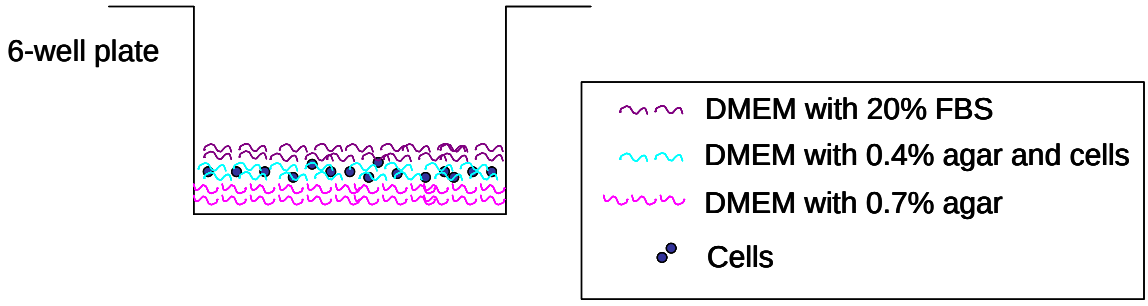

Figure 2.2 Representation of the colony formation in soft agar assays. A base layer of DMEM with 0.7% noble agar was plated and allowed to solidify overnight. Cells in DMEM with 0.4% agar were plated and incubated overnight. DMEM with 20% FBS was added and the plate was incubated for 10 days.

2.2.8 Collection of conditioned medium and RNA from cells

Cells were seeded into 25 cm^2 or 75 cm^2 flasks and allowed to attach overnight at 37°C, 5% CO_2. Cells were treated for 3 days, medium removed and replaced with S_0 medium – 3 ml for 25 cm^2 flask or 5 ml for 75 cm^2 flask – and incubated for 3-4 hours, 37°C, 5% CO_2. The medium was removed and replaced with fresh S_0 medium and incubated for 24 hours, 37°C, 5% CO_2, then transferred to a sterile universal tube and centrifuged at 720 g for 5 minutes. The supernatant was retained and stored at 4°C until analysis as per section 2.2.10. 1ml TRI REAGENT™ was added to the cells in the flasks, incubated for 5-10 minutes at room temperature, and removed to a sterile eppendorf tube. This was stored at -80°C for up to a month until processing as per section 2.2.9.1.

2.2.9 RNA analysis

2.2.9.1 RNA extraction

Samples were removed from the -80°C freezer and allowed to defrost, then stored on ice during all subsequent manipulations. 200 µl chloroform was added to each tube, shaken for 30 seconds and allowed to stand at room temperature for 15 minutes. Samples were centrifuged for 15 minutes at 10,625 g, which resulted in 3 layers forming. The top layer contained the RNA and was removed to a fresh sterile eppendorf tube, which left the middle layer of DNA and the bottom organic layer containing the protein. 500 µl sterile ice-cold isopropanol and 2 µl 5mg/ml glycogen was added to the removed RNA layer, allowed to sit at room temperature for 5-10 minutes, vortexed and incubated overnight at -20°C. The following day, samples were centrifuged for 10 minutes at 10,625 g and the supernatant removed. The pellet was washed with 1 ml 75% ethanol and centrifuged for 5 minutes at 4,150 g. The ethanol was removed and the pellet allowed to air dry at room temperature for 5-10 minutes. The pellet was resuspended in 50 µl diethyl pyrocarbonate (DEPC) treated water and stored at -80°C.

2.2.9.2 Quantification and electrophoresis of RNA

5 μl RNA was added to 495 μl DEPC treated water. The absorbance was read at 260 nm and 280 nm on an Agilent 8453 UV/vis spectrophotometer, using DEPC treated water as blank. The absorbance at 260 nm was used to calculate the concentration of RNA in the sample because 40 μg/ml RNA had an absorbance of 1. The ratio of 260 nm/280 nm reflected the purity of the sample. A ratio of 1.8 was recommended, a higher ratio indicated protein contamination and a lower ratio indicated organic solvent contamination. The quality of RNA was examined by running 1 μg on a 1.2% agarose gel. 1 μg RNA was made up to 5 μl with DEPC treated water. 2 μl RNA Sample Loading Dye (containing ethidium bromide) was added to each sample, heated to 65°C for 10 minutes to denature the RNA and then ran on the gel. The gel was then visualised using an Ultraviolet Products (UVP) High Performance Ultraviolet transilluminator and photographed using Olympus C400 Zoom digital camera. Two bands for 28S and 18S subunits should be seen on the gel. The 28S band should be approximately twice the intensity of the 18S band if the RNA is intact.

2.2.9.3 Reverse transcription

RNA prepared in section 2.2.9.1 was subjected to Deoxyribonuclease (DNase) treatment followed by reverse transcription (RT) to yield cDNA. 2 μg RNA was made up to 8 μl with DEPC treated water. 1 μl 10X reaction buffer and 1 μl DNase I (1 unit) was added to the RNA and incubated at room temperature for 15 minutes, to eliminate any DNA remaining in the sample. 1 μl of stop solution (50 mM EDTA) was added and the samples were heated to 70°C for 10 minutes in an Eppendorf Mastercycler Personal PCR machine. 1 μl Oligo $(dT)_{15}$ primer (0.5 μg) was added to each sample and heated to 70°C for 10 minutes to melt the secondary structures in the RNA. Samples were placed on ice and the following reagents added, giving a total volume of 20 μl:

- 4 μl 5X MMLV-RT Buffer
- 1 μl dNTP Mix (giving final concentration of 0.5 mM)

- 2 µl DEPC treated water
- 1 µl MMLV-RT (200 units)

The samples were incubated at 37°C for 1 hour for cDNA synthesis followed by 2 minutes at 95°C in Eppendorf Mastercycler Personal PCR machine. Samples were stored at 4°C until required for PCR analysis.

2.2.9.4 Polymerase chain reaction

For polymerase chain reaction (PCR) amplification, 5 µl RT product was added to the following reagents:

- 34.5 µl sterile water
- 5 µl 10X reaction buffer
- 2 µl $MgCl_2$ (giving final concentration of 1 mM)
- 1 µl dNTP Mix (giving final concentration of 0.2 mM)
- 1 µl Forward Primer (100 pmol)
- 1 µl Reverse Primer (100 pmol)
- 0.5 µl Taq Polymerase (2.5 units)

Samples were amplified using the following cycle in the PCR machine:

1) 95°C	3 minutes	Initial Denaturation
2) 95°C	1 minutes	Denaturation
3) Annealing Temp	3 minutes	Primer Annealing
4) 72°C	3 minutes	Extension
5) 72°C	10 minutes	Final Elongation

- Steps 2-4 were repeated for 30 cycles before proceeding to step 5

Annealing temperatures varied for different primers and are listed in Table 2.2 along with the primer sequences and product sizes. PCR products were run on

agarose gels (1-1.5% depending on size of product). The agarose gels were made up using Molecular Probes SYBR Safe™ DNA gel stain. 15 µl PCR products were mixed with 3 µl 6X blue/orange loading dye and ran on the gel along with the PCR 100 bp low ladder. The gels were visualised using the UVP High Performance Ultraviolet transilluminator, photographed using an Olympus C400 Zoom digital camera and densitometry analysis performed using the AlphaEaseFC™ Software from Alpha Innotech.

Table 2.2 Details of primers used for PCR.

Gene	Primers	Product Size	Annealing Temperature
Actin	Forward: TCA GGA GGA GCA ATG ATC TTG A Reverse: GAA ATC GTG CGT GAC ATT AAG GAG AAG CT	554 bp	56°C
MMP-2	Forward: CCG CCC TGC AGG TCC ACG ACG GCA T Reverse: CTG AGA TCT GCA AAC AGG ACA TTG T	475 bp	60°C
MMP-9	Forward: GTA TGG TCG TGG CTC TAA GC Reverse: AAA ACC CTC TTG GTC TGC GG	467 bp	61°C
TIMP-1	Forward: CTG TGC CCC ACC CCA CCC AC Reverse: AAG GCT TCA GGT CAT CGG GC	584 bp	62°C
TIMP-2	Forward: TGC AGC TGC TCC CCG GTG CAC Reverse: TTA TGG GTC CTC GAT GTC GAG	341 bp	64°C
Ampicillin	Forward: TTT GCC TTC CTG TTT TTG CT Reverse: ATA ATA CCG CGC CAC ATA GC	189 bp	58.5°C
NTR	Forward: TGC CGG TAA TTA CGT GTT CA Reverse: ACC TGT TTT GCC ATC CAC TC	237 bp	58.5°C

2.2.10 Analysis of protein levels

2.2.10.1 Concentration and quantification of protein in conditioned medium

Conditioned medium collected in section 2.2.8 was concentrated using Amicon® Ultra-4 Centrifugal Filter Device with Ultracel-10 membrane. The conditioned medium was added to the top of the filter unit and centrifuged at 7,500 g using a fixed angle rotor for 10-12 minutes until the desired final volume was reached. The concentrated conditioned medium was removed to a fresh eppendorf

tube and quantified using the Bradford assay. Bovine serum albumin (BSA) standards ranging from 0.2 to 1.4 mg/ml were prepared in water for the standard curve. 5 µl of standards and samples was aliquoted in triplicate into a 96-well plate along with S_0 medium as a blank for the samples. 250 µl Bradford reagent was added to each well, the plate covered in tin-foil and incubated at room temperature for 10-40 minutes. Absorbance was read at 595 nm and concentration of samples calculated by extrapolation from the BSA standard curve.

2.2.10.2 Gelatin zymography

10% 1 mm Novex® pre-cast zymogram gels were used. Conditioned medium samples containing equal amounts of protein were made up to 12.5 µl with sterile water and mixed with 12.5 µl 2X Novex® tris-glycine SDS sample buffer and loaded on the gel. Novex® tris-glycine SDS running buffer was used to fill the Scie-Plas vertical gel rig and the gel was run at 125 V until the dye front reached the end of the gel. After electrophoresis, the gel was washed with Novex® zymogram renaturing buffer for 30 minutes, then Novex® zymogram developing buffer for 30 minutes and finally incubated with fresh Novex® zymogram developing buffer for 24 hour and stained with Coomassie blue stain [0.5% (w/v) Coomassie Brilliant Blue in acetic acid:isopropanol:H_2O (1:3:6, v/v/v)]. After de-staining with acetic acid:isopropanol:H_2O (1:3:6, v/v/v), clear bands appeared against the blue gel, corresponding to degradation of gelatin in the position of a gelatinase enzyme. Gels were photographed using an Olympus C400 Zoom digital camera and a light box. Densitometry analysis was performed using the AlphaEaseFC™ Software from Alpha Innotech. Baby Hamster Kidney (BHK) conditioned medium was used as control. This cell line constitutively expressed MMP-2 and was transfected with the cDNA for human MMP-9.

2.2.10.3 Reverse zymography

Reverse zymography was used to investigate the levels of TIMP proteins in conditioned medium samples. The gels were made as follows:

Resolving gel:

- 2.5 ml buffer A (1.5 M Tris-HCl, pH 8.8; 0.4% (w/v) SDS)
- 2.5 ml 3 mg/ml gelatin stock
- 5 ml 30% acrylamide stock
- 1 ml BHK medium
- 100 μl 10% ammonium persulphate
- 20 μl TEMED

Stacking gel:

- 0.8 ml buffer B (0.5 M Tris-HCl, pH 6.8; 0.4% SDS)
- 0.5 ml 30% acrylamide stock
- 2 ml distilled water
- 50 μl 10% ammonium persulphate
- 20 μl TEMED

The resolving gel ingredients were mixed and poured. Once this had set, the stacking gel was added, the comb inserted and allowed to set. Conditioned medium samples containing equal amounts of protein were made up to 12.5 μl with sterile water and mixed with 12.5 μl 2X Novex® tris-glycine SDS sample buffer and loaded on the gel. Novex® tris-glycine SDS running buffer was used to fill the Scie-Plas vertical gel rig and the gel was run at 125 V until the dye front reached the end of the gel. After electrophoresis, the gel was washed with Novex® zymogram renaturing buffer for 30 minutes, then Novex® zymogram developing buffer for 30 minutes and finally incubated with fresh Novex® zymogram developing buffer for 48 hours and stained with Coomassie blue stain. After de-staining with acetic acid:isopropanol:H_2O (1:3:6, v/v/v), blue bands appeared against the clear gel, corresponding to bands of TIMPs where the gelatin had not been degraded by the MMPs in the BHK medium. TIMP recombinant proteins were used as positive controls. Gels were photographed using an Olympus C400 Zoom digital camera and a light box. Densitometry analysis was performed using the AlphaEaseFC™ Software from Alpha Innotech.

2.2.10.4 Western blotting

NuPAGE™ Novex 4-12% Bis-Tris gels were used for western blotting. Conditioned medium samples containing equal amounts of protein were made up to 16.25 µl with sterile water and mixed with 6.25 µl NuPAGE™ 4X Lithium Dodecyl Sulphate (LDS) sample buffer and 2.5 µl NuPAGE™ Reducing Agent, heated to 65°C for 10 minutes and loaded on the gel. Sigma Chemichrome™ western control was used as a ladder and positive control for transfer and detection. Following vertical electrophoresis, the proteins on the gel were transferred to a nitrocellulose membrane using horizontal electrophoresis. This involved putting the gel into a gel cassette sandwich as follows: sponge - 2 x filter paper – gel - nitrocellulose - 2 x filter paper - sponge. The proteins were transferred for 1 hour in a Bio-Rad Mini PROTEAN 3 cell wet transfer apparatus with an ice block to maintain a low temperature and with a magnetic stirrer to keep the temperature constant throughout the apparatus. The membrane was stained with MemCode™ reversible protein stain kit and photographed. This involved rinsing the membrane with ultrapure water, then incubating with the stain for 30 seconds. The membrane was rinsed three times with De-stain solution and incubated for 5 minutes in the De-stain solution. The membrane was rinsed four times with ultrapure water and agitated for 5 minutes in ultrapure water, then photographed using an Olympus C400 Zoom digital camera and a light box. The Eraser solution was added to the membrane and agitated for 2 minutes until the stain was removed. The membrane was rinsed four times and agitated for 5 minutes in ultrapure water. The nitrocellulose membrane was then washed with blocking solution (5% dried milk in Tris Buffered Saline with Tween – TBST [1 mM Tris pH 8.0, 150 mM NaCl, 0.05% Tween]) for 2 hours at room temperature on a rocking platform. The primary antibody was added in 5 ml TBST and incubated overnight at 4°C on a rocking platform. The membrane was washed three times for 10 minutes with TBST and incubated with the secondary antibody in 5 ml TBST for 2 hours at room temperature on a rocking platform. This was followed by three 10 minute washes with TBST and development with Pierce Supersignal Enhanced Chemiluminescence (ECL) Kit. 500 µl of Pierce Supersignal® west pico luminol/enhancer solution was mixed with 500 µl Pierce Supersignal® west pico stable peroxide solution and added to the membrane. A piece of Amersham

Biosciences hyperfilm was applied to the nitrocellulose membrane in a dark room. The film was exposed for a certain length of time and then developed using the Hyper Processor (Amersham Pharmacia Biotech). The Chemichrome^{TM} Western Control contains Colourburst^{TM} markers and a band of mouse IgG, which binds the primary and secondary antibodies and thus reacts with the ECL reagents and appears as a band on the film when exposed. The films were photographed using an Olympus C400 Zoom digital camera and a light box. Densitometry analysis performed using the AlphaEaseFC^{TM} Software from Alpha Innotech.

2.2.11 Nitroreductase enzyme assays

2.2.11.1 Enzyme assays

The substrates, CB1954 and the 5-FU derivatives, were dissolved in 50 mM sodium phosphate buffer (pH 7.0) and stored at -20°C. The co-factor, nicotinamide adenine dinucleotide (NADH), was dissolved in 0.01 M Tris buffer (pH 8.5) to 10 mg/ml (13.5 mM), aliquoted and stored at -80°C. The nitroreductase (NTR) enzyme was dissolved in sterile water to 1 mg/ml, aliquoted and stored at -20°C. The enzyme reactions were carried out in 96-well plates in 50 mM sodium phosphate buffer with the following components: 500 μM NADH, 3 μg/ml NTR and varying concentrations of substrate (CB1954 or 5-FU derivatives). After addition of the enzyme, the absorbance was read at 340 nm using the Tecan Sunrise multiwell plate reader and the plate was incubated at 37°C. Absorbance at 340 nm was read every 5 minutes for 1 hour.

2.2.11.1.1 Enzyme kinetics studies

Enzyme kinetics of the compounds was analysed using the Lineweaver-Burk, Hanes-Woolf and Eadie-Hofstee plots, as well as the non-linear regression software Enzfitter (Elsevier Biosoft) to calculate the Michaelis constant (K_m) and maximum velocity (V_{max}). Determination of k_{cat} was then calculated from the equation:

$$k_{cat} = V_{max} / E_t$$

where E_t was the total enzyme, and was calculated as follows:

Concentration used in reaction ($g.ml^{-1}$) / Molecular weight ($g.mole^{-1}$) = E_t ($mole.ml^{-1}$)

For these experiments, 3 μg/ml enzyme was used, with molecular weight of 24,000 $g.mole^{-1}$. Thus:

$$E_t\ (mole.ml^{-1}) = 3 \times 10^{-6}\ g.ml^{-1} / 24{,}000\ g.mole^{-1} = 1.25 \times 10^{-10}\ mole.ml^{-1}$$

2.2.11.2 Enzyme assays using cell lysates

Cells were trypsinised and centrifuged as per section 2.2.1.2 and frozen. 500 μl lysis buffer (PBS containing 1% IGEPAL, 1% protease inhibitor cocktail) was added to frozen cell pellets, thawed at 37°C, pipetted up and down, incubated for 5 minutes at -80°C and thawed at 37°C, pipetted up and down. Samples were centrifuged at 12,500 g for 3 minutes and supernatant retained for assay. Total protein in the samples was quantified using the Bradford assay as outlined in section 2.2.10.1. The supernatant was concentrated when required using the Amicon® Ultra-4 Centrifugal Filter Device with Ultracel-10 membrane. An aliquot of the supernatant was added to a 96-well plate containing 200 μM substrate (CB1954 or 5-FU derivatives) and 500 μM co-factor, NADH, in 50 mM sodium phosphate buffer, pH 7.0. Absorbance at 340 nm was read upon addition of supernatant and every 5 minutes after incubation for 2 hours.

2.2.11.2.1 Specific activity

Specific activity (Units/mg) of the sample was calculated using the equations:

$$1)\ A_{340nm} = \varepsilon.c.l \qquad \text{Beer Lambert Law}$$

A = Absorbance

ε: Molar absorption co-efficient of NADH, 6.3×10^3 $mole^{-1}$ cm^{-1}

c: Concentration moles/L

l: path length

2)

$$\text{Specific Activity} = \frac{\text{Change in concentration over time} \times \text{Volume of solution in well}}{\text{Volume of original sample} \times \text{Concentration total protein}}$$

Specific activity is expressed as Units/mg, with 1 Unit equivalent to 1 μmol.min^{-1}.

2.2.12 Liquid chromatography-mass spectrometry (LC-MS)

2.2.12.1 Sample preparation for LC-MS

Compound 13 was diluted in fresh medium to a concentration of 75 μM. An aliquot was frozen immediately and another aliquot incubated for 5 days at 37°C and then frozen. Compound 13 in medium was added to the V79-C and V79-NTR cells and incubated for 5 days before removal to a universal and storage at -20°C for analysis.

2.2.12.2 Sample analysis by LC-MS

Solvents for extraction were HPLC grade; LC-MS solvents and water were LC-MS grade. The following solutions were added to 50 μl of sample in order: 20 μl of 1% phosphoric acid, 250 μl of acetonitrile followed by mixing on a vortex for several seconds and finally 1 ml of ethyl acetate with further vortex mixing. The tube was then centrifuged at 12,500 g in a microfuge to pellet non-dissolved components and clarify the liquid layers. 1.2 ml of the solvent mixture was evaporated by vacuum drying on a Heto Holten Maxi-prep system. The sample was reconstituted in 40 μl of LC mobile phase and 20 μl was injected automatically using the instrument

autosampler. Analysis of levels of compound 13 and 5-FU was performed by LC-MS using a GE Healthcare MDLC system coupled to Thermo Scientific LTQ hybrid Mass Spec detector. Chromatographic conditions: A Thermo Scientific Hypercarb LC column was employed with a 5 μm particle size and 100x 2.1 mm dimensions. The LC mobile phase consisted of two components, 0.1% formic acid and 100% acetonitrile. A gradient elution methodology with a 300 μl/minute flow-rate was employed. Each chromatographic run began with 89% formic acid, 11% acetonitrile. This rose to 100% acetonitrile in a linear gradient over 6 minutes. At 11 minutes the gradient switched back to 11% acetonitrile over 1 minute and flow continued for a further 3 minutes to give a total run time of 15 minutes. Mass spectral conditions: Analysis was performed in negative ion mode. The detector was tuned individually to 5-FU and to compound 13 using direct infusion. With the resulting tune methods, tune method 1 (5-FU) was used for the first 7.5 minutes of analysis and switched to the tune method 2 (compound 13) for the remainder of the analysis. Data on the ions from 100 to 350 Da was collected.

2.2.13 Plasmid DNA preparation

All bacterial work was carried out using aseptic technique in a Gelman Sciences Australia Laminar Flow hood.

2.2.13.1 Transformation

F179 and F184 DNA plasmids were supplied on sterile discs of filter paper. See Appendix A for plasmid maps. Each disc was transferred to a sterile eppendorf tube, 10 μl sterile Tris-EDTA (TE) buffer added and incubated overnight at 4°C. The tube was centrifuged and the TE removed to a fresh sterile eppendorf tube.

Luria-Bertrani (LB) broth was prepared by adding the following to 1 L of water:

- 10 g Bacto-tryptone
- 5 g Bacto-yeast extract

- 10 g NaCl

The pH was adjusted to 7.5 with NaOH and the solution autoclaved. After allowing the LB broth to cool to 55°C, ampicillin was added to a final concentration of 100 μg/ml. LB agar plates were made using LB broth, as above, with 15 g yeast agar added before autoclaving. Ampicillin was added, to a final concentration of 100 μg/ml, after cooling to 55°C and approximately 20 ml was poured into 100 mm petri dishes, allowed to set and stored inverted at 4°C for up to a month.

An aliquot of MAX Efficiency® DH5α™ competent cells was thawed on ice and 2 μl (1 μg) plasmid DNA added. The tube was mixed by tapping gently, placed on ice for 30 minutes and transferred to a water bath at 42°C for 45 seconds to heat-shock the cells. The tube was placed back on ice for 2 minutes. 900 μl room temperature SOC medium (supplied with the competent cells) was added to the cells and incubated in HT Orbital Shaker incubator at 37°C for 1 hour with gentle agitation (200 rpm). 5 μl, 10 μl, 100 μl and 300 μl were spread onto LB agar plates, containing 100 μg/ml ampicillin, and incubated overnight at 37°C in an inverted position. Three control plates were also set up, one with nothing added, one with just SOC medium and one with SOC medium and bacteria which had not been transformed with the plasmid DNA. These were used to confirm the sterility of the plates, of the SOC medium and the cytotoxicity of the ampicillin, respectively.

2.2.13.2 Plasmid DNA mini-prep

Upon formation of colonies, a sterile pipette tip was used to transfer bacteria from an individual colony to a 25 ml universal tube containing 5 ml LB broth culture with 100 μg/ml ampicillin and incubated overnight at 37°C and 200 rpm. A control was set up with LB broth but no cells added. These cultures were used to prepare the plasmid DNA using the Novagen SpinPrep™ Plasmid Kit. 1.5 ml culture was transferred to a sterile eppendorf tube and centrifuged at 7,500 g for 1 minute. The pellet was resuspended fully in 100 μl resuspension buffer and vortexed gently. 200 μl lysis buffer was added, mixed by gentle inversion and the sample incubated for 5 minutes at room temperature. 400 μl neutralisation buffer was added, the tubes inverted gently and centrifuged for 10 minutes at 14,500 g. 650 μl supernatant was

added to the filter unit, positioned in a receiver tube, and centrifuged at 14,500 g for 30 seconds. The flow-through was discarded, 650 µl wash buffer added and centrifuged for 30 seconds at 14,500 g. The flow-through was again discarded, the filter and tube centrifuged for 2 minutes at 14,500 g and the filter transferred to an eluate receiver tube. 30 µl pre-warmed elute buffer was added to the filter, incubated for 3 minutes at 50°C and centrifuged for 1 minute at 14,500 g. This step was repeated for maximum yield. The elution was stored at 4°C until digestion.

2.2.13.3 Plasmid DNA digestion

To confirm the presence of the plasmid, enzymatic digestion was performed by making the following mixture:

- 5 µl Elution
- 2 µl 10X Reaction buffer
- 1 µl Restriction enzyme
- 12 µl Sterile water

If a double digest was performed i.e. two restriction enzymes, 1 µl of each was added and the amount of water reduced accordingly. This mixture was incubated in a 37°C water bath for 3 hours. 5 µl of digested sample was mixed with 1 µl 6X blue/orange loading buffer and ran on a 1% agarose gel made with Molecular Probes SYBR Safe™ DNA gel stain, along with 2.5 µl of the undigested plasmid and 10 µl 1 kb DNA ladder. The gels were visualised using the UVP High Performance Ultraviolet transilluminator, photographed using Olympus C400 Zoom digital camera. Eco RI restriction enzyme was used to digest F179 plasmid and Bam HI and Xho I restriction enzymes were used to digest F184.

2.2.13.4 Plasmid DNA maxi-prep

Following confirmation of the presence of the plasmid by restriction enzyme digest, the culture volume was increased to obtain higher yields of plasmid DNA. 400 µl of culture from the mini-prep was added to 100 ml LB broth and incubated

overnight at 37°C, 200 rpm. The Qiagen Maxi-prep kit was used to purify the plasmid DNA. Bacterial cells were harvested by centrifugation at 6,000 g for 15 minutes at 4°C in Beckman Coulter™ Allegra™ 64R Centrifuge. The supernatant was drained from the tubes and the pellets resuspended in 10 ml resuspension buffer containing RNase A. 10 ml lysis buffer was added, mixed by inversion and incubated at room temperature for 5 minutes. 10 ml chilled neutralisation buffer was added, mixed by inversion and incubated on ice for 20 minutes, followed by centrifugation at 10,000 g for 45 minutes at 4°C. The supernatant was removed to a fresh tube and again centrifuged at 10,000 g for 30 minutes at 4°C. The supernatant was added to the Qiagen-tip 500, which had been equilibrated and washed with proprietary buffers. The DNA was eluted into a fresh universal tube with 15 ml elute buffer. 10.5 ml isopropanol was added to precipitate the DNA and centrifuged at 10,000 g for 45 minutes. The pellet was washed with 5 ml 70% ethanol and centrifuged at 10,000 g for 45 minutes at 4°C. The supernatant was carefully removed and the pellet allowed to air dry for 5-10 minutes. 50 µl TE buffer, pH 8.0, was used to dissolve the DNA. Plasmid digests were carried out as described in section 2.2.13.3.

2.2.13.5 Quantification of plasmid DNA

5 µl plasmid DNA suspension was added to 495 µl sterile water. The absorbance was read at 260 nm and 280 nm on an Agilent 8453 UV/vis spectrophotometer, using sterile water as blank. The absorbance at 260 nm is used to calculate the concentration of DNA in the sample as 50 µg/ml DNA has an absorbance of 1. The ratio of 260 nm/280 nm reflects the purity of the sample. A ratio of 2 is recommended.

2.2.13.6 Glycerol stocks of transformed bacteria

800 µl of freshly grown culture was added to 200 µl sterile 50% glycerol stock and 200 µl aliquots added to sterile eppendorf tubes which were stored at -80°C.

2.2.14 Transfection

2.2.14.1 β-galactosidase transfection

Transfection of the HCT116 cell line with the plasmid pCH110, containing the *lac Z* gene, was performed to determine transfection efficiency. See Appendix A for plasmid map of pCH110. 1.3 x 10^6 cells were seeded in a 25 cm^2 flask and allowed to attach overnight. 20 µl GeneJuice® Transfection Reagent was added drop-wise to 300 µl DMEM (with no supplements), vortexed and incubated at room temperature for 5 minutes. 10 µg pCH110 was added to this solution and mixed by gentle pipetting, giving a DNA (µg):GeneJuice® (µl) ratio of 1:2. This mix was incubated for 15 minutes at room temperature. Medium was removed from the flask and cells washed with 3 ml sterile PBS. 3 ml medium (with additives) was added to the flask and the DNA/GeneJuice® mix was added drop-wise and incubated at 37°C, 5% CO_2 for 4 hours. 3 ml fresh medium was added and incubated for 48 hours at 37°C, 5% CO_2. The medium was aspirated and the cells rinsed twice with 3 ml sterile PBS. 3 ml fix solution (0.2% glutaraldehyde, 0.1 M phosphate buffer pH 7.3, 5 mM EGTA pH 8, 2 mM sterile $MgCl_2$) was added and incubated for 10 minutes at room temperature, this step was repeated twice. 3 ml rinse solution (0.1 M phosphate buffer pH 7.3, 2 mM sterile $MgCl_2$, 0.24 mM sodium deoxycholate, 40 µl IGEPAL) was added and incubated for 10 minutes at room temperature, this step was repeated twice. 1.5 ml stain solution (1 mg/ml X-gal, 1.65 mg/ml potassium ferricyanide and 1.65 mg/ml potassium ferrocyanide in 10 ml rinse solution) was added and incubated overnight at 37°C. In cells containing the plasmid, production of the β-galactosidase protein from the *lac Z* gene caused the cells to turn blue in the presence of the substrate, 5-bromo-4-chloro-3-indolyl-β-D-galactopyranoside (X-gal). Stain solution was aspirated and the cells were rinsed twice with 3 ml rinse solution. 3 ml sterile PBS was added. Blue and clear cells were counted in 10 fields using the microscope and transfection efficiency calculated as follows:

(No. blue cells/Total no cells (blue and white))*100

Photographs were taken using an Olympus BX51 microscope with an Olympus DP70 camera attached. The flask was stored at 4°C after replacing the PBS with 3 ml 10% glycerol.

2.2.14.2 Nitroreductase transfection

HCT116 cells were transfected with F179, the control plasmid, and F184, the plasmid containing the cDNA for *E.coli* nitroreductase enzyme. 1.3 x 10^6 cells were seeded in a 25 cm^2 flask and allowed to attach overnight. 20 μl or 50 μl GeneJuice® Transfection Reagent was added drop-wise to 300 μl DMEM (with no supplements), vortexed and incubated at room temperature for 5 minutes. 10 μg plasmid DNA was added to this solution and mixed by gentle pipetting, giving a DNA (μg):GeneJuice® (μl) ratio of 1:2 and 1:5. This mix was incubated for 15 minutes at room temperature. Medium was removed from the flask and cells washed with 3 ml sterile PBS. 3 ml medium (with additives) was added to the flask and the DNA/GeneJuice® mix was added drop-wise and incubated at 37°C, 5% CO_2 for 4 hours. A control flask which was not transfected was also set up. In the 1:2 ratio flasks, 3 ml fresh medium was added, while in the 1:5 flasks, the medium was removed and replaced with 5 ml fresh medium. The flasks were incubated for 48 hours at 37°C, 5% CO_2. The medium was aspirated, replaced with fresh medium containing 2 μg/ml puromycin dihydrochloride and incubated at 37°C, 5% CO_2. The medium was replenished every 2-3 days until a stably transfected cell line was established. All cells in the control flask died after 1-2 weeks treatment with puromycin dihydrochloride.

2.2.14.3 DNA extraction using proteinase K

To confirm the presence of the plasmid in the transfectants, DNA was extracted and PCR performed. Medium was removed from a confluent flask of cells and rinsed twice with 5 ml sterile PBS. 1 ml sterile PBS was added and a sterile cell scraper used to detach the cells from the bottom of the flask. The cell suspension was transferred to a sterile eppendorf tube and centrifuged at 665 g for 5 minutes. The pellet was resuspended in 100 μl PCR lysis buffer (100 μl 10X PCR buffer, 891 μl sterile water, 4.5 μl IGEPAL, 4.5 μl Tween 20). 1 μl proteinase K was added to the

resuspended cells and incubated at 65°C for 10 minutes. The solution was pipetted up and down, 1 μl proteinase K added and incubated at 65°C for 50 minutes, followed by incubation at 95°C for 10 minutes to inactivate the proteinase K. The solution was centrifuged at 10,625 g for 5 minutes and the supernatant removed to a fresh tube and stored at 4°C. The DNA was quantified and 1 μg used for amplification in PCR as described in section 2.2.9.4.

2.2.15 SDS gel electrophoresis of cell extracts

A NuPAGE™ Novex 4-12% Bis-Tris gel was used for the SDS gel electrophoresis. Protein samples from cell pellets were made up to 16.25 μl with sterile water and mixed with 6.25 μl NuPAGE™ 4X LDS sample buffer and 2.5 μl NuPAGE™ Reducing Agent, heated to 65°C for 10 minutes and loaded on the gel. NuPAGE™ 2-(N-morpholino) ethane sulfonic acid (MES) SDS buffer was used to fill the Scie-Plas vertical gel rig and the gel was run at 125 V until the dye front reached the end of the gel. Recombinant NTR protein was used as a positive control. The gel was stained with Coomassie blue stain and de-stained in water. Blue protein bands were visible against a white background. Gels were photographed using an Olympus C400 Zoom digital camera and a light-box.

Chapter 3

Evaluation of the biological effects of conjugated linoleic acid on murine mammary and human breast cancer cell lines

3.1 Introduction

3.1.1 Fatty acids and cancer

Fatty acids are the simplest form of lipids. Polyunsaturated fatty acids (PUFAs) are fatty acids with two or more carbon-carbon double bonds, of which there are four families: n-3, n-6, n-7 and n-9. The nomenclature refers to the position of the first double bond from the methyl end of the molecule (Jiang *et al*., 1998). The metabolism of n-3, n-6 and n-9 PUFA families is shown in Figure 3.1. Desaturases, referred to as Δ4/5/6, introduce double bonds into the molecules while elongation of the carbon chain is carried out by elongases (Jiang *et al*., 1998). The Δ4/5/6 nomenclature refers to the position at which the double bond is introduced – for example Δ4 desaturase will introduce a double bond between carbon atoms 4 and 5 from the carboxyl end (Rose and Connolly, 1999). There is competition between the desaturases that act on the n-3, n-6 and n-9 fatty acids. The n-3 fatty acids have the greatest affinity for these enzymes followed by the n-6 family, and so the ratio of n-3:n-6 fatty acids in the diet will determine metabolism along these pathways (Rose and Connolly, 1999 and Das, 2006).

The essential fatty acids (EFAs) linoleic acid (LA) and α-linolenic acid (ALA) cannot be synthesised within the human body and so they must be consumed in the diet (Jiang *et al*., 1998). LA is the most abundant PUFA in the western diet and is found mainly in cereals, eggs, poultry, vegetable oils, whole-grain breads, margarines and baked goods (Whelan and McEntee, 2004 and Das, 2006). ALA is found in canola, flaxseed, linseed and rapeseed oils; walnuts and leafy green vegetables. The average daily intake of EFAs in Europe and the US is 7-15 g/day (Das, 2006). LA and ALA play a role in providing energy to the body, form part of cellular membranes and can also be converted to eicosanoids. Eicosanoids are derived from dihomo-γ-linolenic acid (DGLA), arachadonic acid (AA) and eicosapentanoic acid (EPA). They include prostaglandins, thromboxanes and leukotrienes, which are chemical transmitters for a variety of intercellular and intracellular signals (Rose and Connolly, 1999).

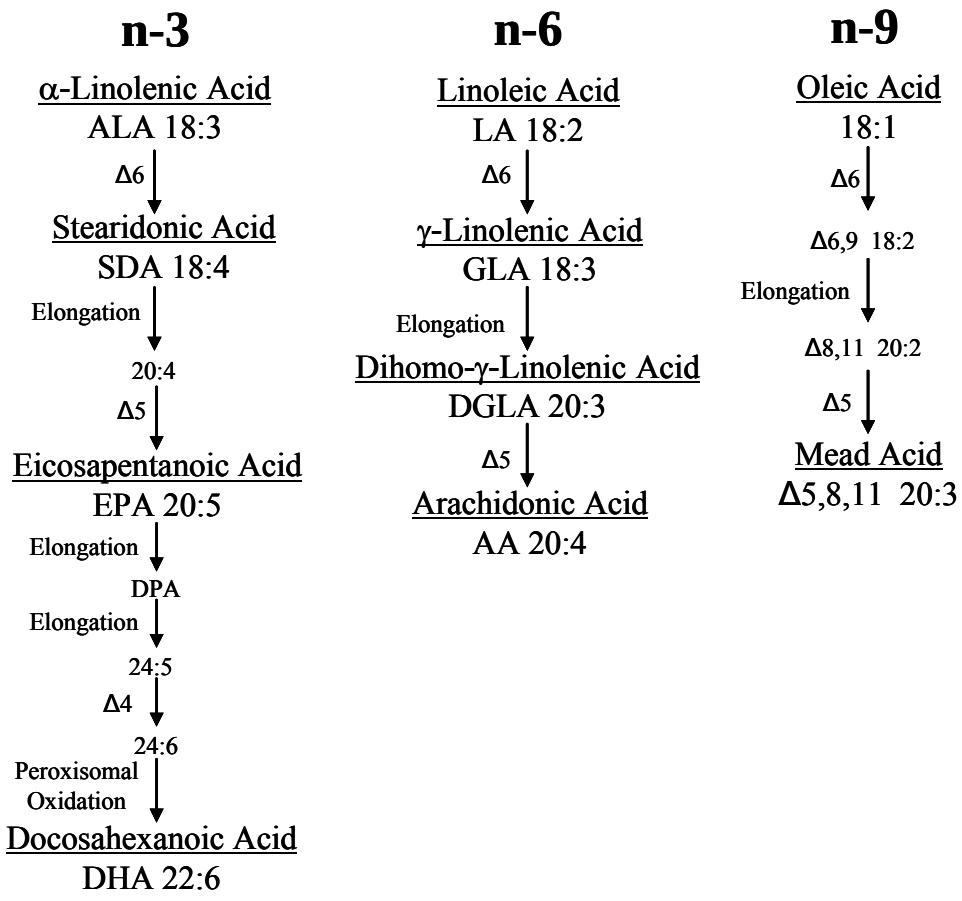

Figure 3.1 PUFA metabolism of n-3, n-6 and n-9 families.

The relationship between fatty acids and cancer has been the subject of intensive research and debate over several decades. Studies involving women who migrated from Japan to the United States reported an increase in breast cancer risk after just one generation in the United States. This was thought to be the result of the dietary fat differential between these societies (Rose and Connolly, 1999). Western society tends to have a higher intake of n-6 fatty acids, particularly LA (Stoll, 1998). Hubbard *et al*. (1998) used fish oil and safflower oil – rich in n-3 and n-6 fatty acids respectively – to investigate the effects on murine mammary tumourigenesis. The fish oil diet resulted in longer latency and slower growth of tumours, as well as decreased primary nodules and total metastatic load in spontaneous metastasis models, indicating a significant effect of the n-3 fatty acids in fish oil on primary breast cancer growth and metastasis (Hubbard *et al*., 1998). There is also some argument that it is not the total consumption of fats but the balance between types of fats that is important, with a diet richer in n-3 fats having more beneficial effects

(Greenwald, 1999). Maillard *et al*. (2002) examined the levels of fatty acids in breast adipose tissue of 241 patients with invasive, nonmetastatic breast carcinoma and 88 patients with benign disease. They found an inverse correlation between the ratio of n-3/n-6 fatty acids and breast cancer risk, with a p-value of 0.00002. Fatty acids have been reported to have similar effects in colorectal cancer (Whelan and McEntee, 2004).

3.1.2 Conjugated Linoleic Acid

Conjugated Linoleic Acid (CLA) is a term used to describe a group of positional and geometric isomers of LA (Figure 3.2) (Pariza *et al*., 2000). The double bonds in CLA are conjugated or contiguous i.e. they are not separated by a methyl group as in LA. The double bonds are found at positions 7 and 9, 8 and 10, 9 and 11, 10 and 12, 11 and 13 or 12 and 14, and each double bond can be in either the *cis* (*c*) or *trans* (*t*) configuration (Lee *et al*., 2005). The variation between the position and configuration of the double bonds gives rise to numerous different isomers (Lee *et al*., 2005). It has been suggested that only a few of these isomers are biologically active (Hubbard *et al*., 2003).

The major naturally occurring dietary isomer is *cis*-9, *trans*-11 (*c*9,*t*11-CLA), also called rumenic acid (Pariza *et al*., 2000 and Belury, 2002a). After *c*9,*t*11-CLA, the major isomers found in food rank as follows: *t*7,*c*9-CLA > 11,13-CLA (*c*/*t*) > 8,10-CLA (*c*/*t*) > *trans*10,*cis*12-CLA (*t*10,*c*12-CLA) > other isomers (Belury, 2002a). Commercial preparations of CLA contain mainly the *c*9,*t*11-CLA and the *t*10,*c*12-CLA isomers in equal amounts and thus they have been the most extensively studied isomers (Wahle *et al*., 2004). In this thesis, the term 'CLA' refers to a mixture of isomers, while properties relating to the individual isomers will be specified.

CLA is found in meat and dairy products from ruminant animals, which includes sheep and cows. The *c*9,*t*11-CLA isomer is produced by microbial biohydrogenation of LA and ALA by rumen bacteria (Miglietta *et al*., 2006a and Roche *et al*., 2001). Linoleate isomerase converts LA into *c*9,*t*11-CLA, which is then absorbed (Figure 3.3). *c*9,*t*11-CLA can also be converted to vaccenic acid in the rumen and then reverted back to CLA by desaturase enzymes in mammalian cells (Pariza *et al*., 2000 and Bauman *et al*., 1999).

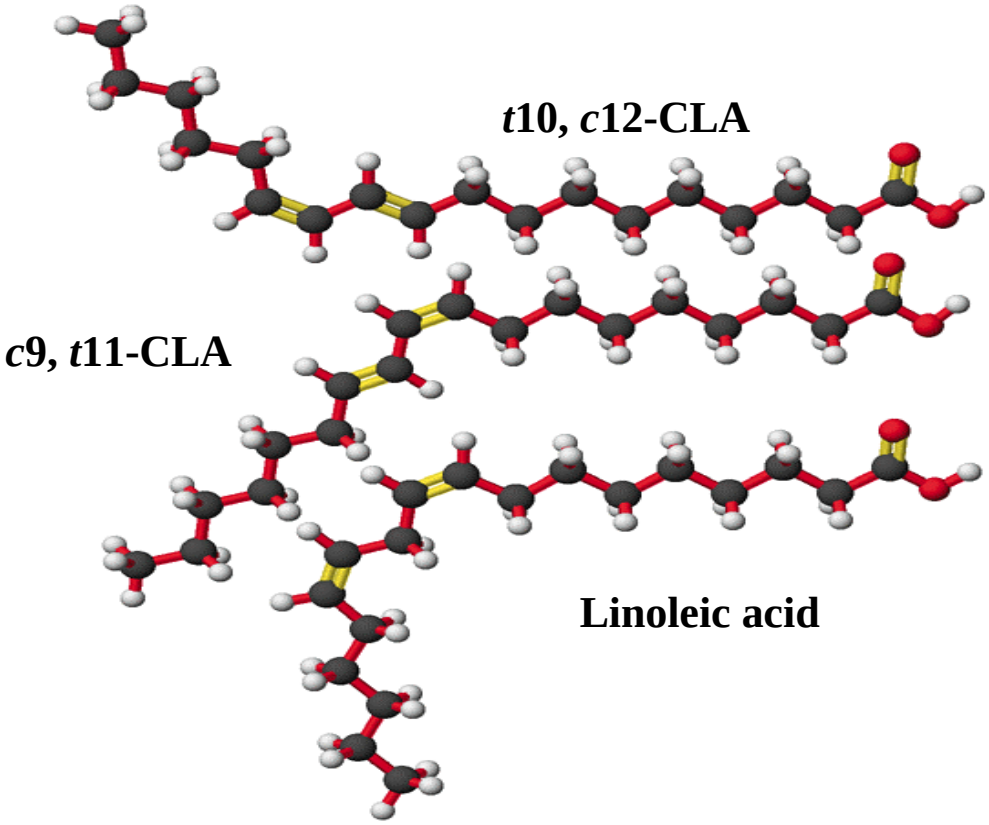

Figure 3.2 Structure of *t*10,*c*12-CLA, *c*9,*t*11-CLA and LA. From Pariza *et al*., 2001.

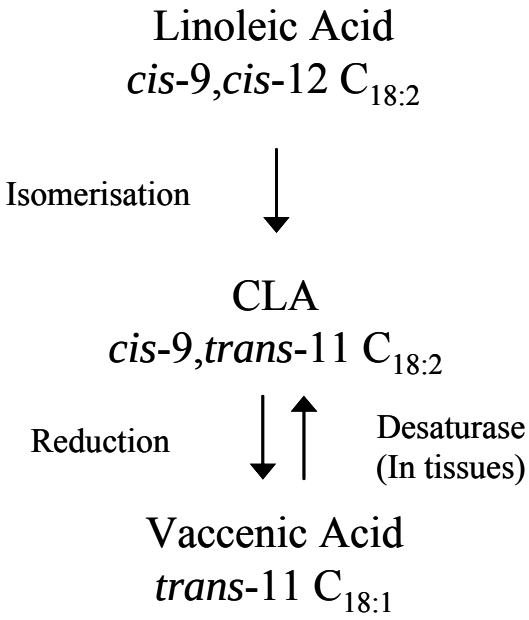

Figure 3.3 Production of *c*9,*t*11-CLA from LA and vaccenic acid. Adapted from Bauman *et al*., 1999.

The *c*9,*t*11-CLA isomer accounts for approximately 90% of the total CLA content in dairy products (O'Shea *et al*., 1998). CLA content in food varies from 0.2 mg/g in corn and peanut oils, 17 mg/g in beef and 30 mg/g in milk-fat (O'Shea *et al*., 1998). CLA levels in milk can vary depending on the type of feed given to the cows, with forage and grain reducing CLA levels in comparison to milk from pasture-grazing animals. Seasonal variation also occurs with lower levels in spring than in summer (Roche *et al*., 2001).

CLA was first identified as an anticarcinogen in fried ground beef (Ha *et al*., 1987). Since then, CLA has also been shown to exert beneficial effects against atherosclerosis, diabetes and obesity (Wahle *et al*., 2004 and Belury, 2002b). For this reason, there has been widespread interest in CLA as a functional food, defined as a food ingredient that provides beneficial effects beyond the traditional nutrients it contains (Bauman *et al*., 1999). While early research analysed the effect of a mixture of CLA isomers, recent studies have also included the individual isomers and have shown that they can work through different cell signalling pathways and have different effects on cell functions and metabolism (Wahle *et al*., 2004).

3.1.3 Effect of CLA on mammary tumourigenesis *in vivo*

Numerous studies have been conducted using rats to determine the effect of CLA on mammary tumourigenesis. Details of the experiments discussed in this section are outlined in Table 3.1. The anti-cancer properties of CLA in mammary cancer were first investigated by Ip *et al*. (1991). This was also the first report to look at cancer prevention using a dietary form of CLA. The CLA used was a mixture of isomers but contained predominantly *c*9,*t*11-CLA/*t*9,*c*11-CLA (~42.5%) and *t*10,*c*12-CLA (43%). Rats were fed CLA, in the form of free fatty acids, starting two weeks prior to induction of mammary cancer by treatment with a single dose of dimethyl-benz(*a*)anthracene (DMBA). The rats were maintained on diets supplemented with 0.5%, 1% or 1.5% CLA until the end of the experiment, thus they were exposed to the CLA prior to, during, and after DMBA treatment at 10 mg. The 1% and 1.5% diets produced a statistically significant ($p<0.05$) reduction in tumour incidence (Ip *et al*., 1991). Investigation of the incorporation of CLA into the mammary tumours showed a 20-fold increase of CLA levels in rats fed the 1.5% diet in comparison to the

control. The *c*9,*t*11-CLA isomer alone was found to be incorporated into phospholipids. The authors also found that CLA acted as an effective antioxidant in the mammary tissues, possibly accounting for the antitumourigenic effect (Ip *et al*., 1991).

In a further study, Ip *et al*. (1994) decreased the levels of dietary CLA to 0.05-0.5% and decreased the DMBA dose to 5 mg. The number of tumours in rats fed a diet supplemented with just 0.1% CLA was significantly reduced compared to the control ($p<0.05$). An experiment was also undertaken to analyse the effect of short-term CLA exposure on mammary carcinogenesis. Rats were fed 1% CLA from weaning until 1 week after treatment with 10 mg DMBA – a total of 5 weeks. This period covered rat mammary gland maturation to the adult stage, with differentiation of the terminal end buds into alveolar buds and lobules. Feeding with CLA during this time period significantly reduced the number of mammary tumours that developed, indicating a lasting protection against subsequent cancer risk (Ip *et al*., 1994).

When administering a single carcinogen dose to rats at 56 days of age, Ip *et al*. (1995) narrowed down the requirement of exposure to CLA to 21 – 42 days of age in order to reduce tumourigenesis. Feeding of CLA after treatment with the carcinogen only exhibited an anti-cancer effect if the intake was continuous, for both carcinogens methylnitrosourea (MNU) and DMBA (Ip *et al*., 1995 and Ip *et al*., 1997). In order to determine the influence of the amount and composition of total dietary fat on the anti-carcinogenic effects of CLA, Ip *et al*. (1996) looked at varying fat sources in rats. The diets contained either high corn oil (unsaturated fats) or high lard (saturated fats) content. The authors found a reduction in tumour incidence following CLA feeding independent of the level of fat in the diet (Ip *et al*., 1996).

Thompson *et al*. (1997) investigated further the timing of CLA exposure, comparing a 6-month continuous feeding treatment and a 1-month CLA feeding protocol during the period of mammary morphogenesis. Animals fed 1% CLA from weaning (21 days) to 50 days of age (group B), as well as animals fed 1% CLA from 55 days of age to the termination of the experiment (group C), both showed a reduction of approximately 50% in the total number of tumours, when compared to the control. A group of rats exposed to the same level of CLA for the total time period i.e. from weaning to termination of the experiment (group D), only showed a reduction of approximately 57%. Thus the effect of the CLA feeding was not

additive, suggesting that there may be different mechanisms of inhibition depending on the timing of CLA exposure i.e. during mammary gland morphogenesis or during tumour progression. The authors suggested that the small difference observed between the effect of CLA on groups B and D may be due to modification, during mammary gland maturation, of the development of a subset of target cells. The CLA-resistant cells were therefore available for carcinogen targeting. CLA feeding after carcinogen administration, was only effective against the transformed cells that originated from the CLA-sensitive progenitors, thus a similar reduction in tumour incidence was observed (Thompson *et al*., 1997).

In an experiment feeding rats with high CLA butter fat, it was confirmed for the first time that CLA in a food form had anti-cancer properties (Ip *et al*., 1999). CLA feeding during pubescent mammary gland development down-regulated mammary epithelial growth, decreased the population and proliferative activity of the target TEB cells, and therefore reduced mammary cancer risk when the rats were challenged with a carcinogen (Ip *et al*., 1999).

While I have concentrated here on the effects of CLA on mammary tumourigenesis, there have also been extensive studies on the effects in other types of cancer. The earliest work investigating the anti-cancer effects of CLA looked at skin carcinogenesis (Ha *et al*., 1987) and forestomach tumourigenesis (Ha *et al*., 1990) in mice. Since then, CLA has been shown to inhibit the growth of the HepG2 hepatoma cell line (Igarashi *et al*., 2001), the PC-3 prostate cancer cell line (Palombo *et al*., 2002) the colorectal cancer cell lines Caco-2 (Kim *et al*., 2002), HT-29 and MIP-101 (Palombo *et al*., 2002), among others.

Table 3.1 Animal studies investigating the effect of CLA on mammary tumourigenesis

Reference	Carcinogen	CLA Diet	Time/Duration of Exposure
Ip *et al*., 1991	DMBA, 10 mg, 51 days old	0.5%/1%/1.5%	From 2 wks before DMBA administration to end of experiment (total 50 wks)
Ip *et al*., 1994	DMBA 5 mg, 50 days old	a) 0.05%/0.1%/ 0.25% /0.5% b) 1%	a) From 2 wks before DMBA administration to end of experiment (total 36 wks) b) From 4 wks before DMBA administration to 1 wk after (total 5 wks)
Ip *et al*., 1995	MNU, 56 days old	1%	21 to 42 days of age
Ip *et al*., 1996	DMBA 7.5 mg, 50 days old	1% CLA, in a background of 10%/13.3%/16.7%/ 20% total fat	From 1 wk before DMBA administration to end of experiment (total 24 wks)
Ip *et al*., 1997	DMBA 10 mg, 50 days old	1% CLA in a background of 20% corn oil	From 4 days after DMBA administration, for a total of 4 wks/8 wks or 20 wks
Thompson *et al*., 1997	DMBA 10 mg, 50 days old	A: Control, 0% CLA B: 1% CLA C: 1% CLA D: 1% CLA	 B: From weaning (21 days) to 50 days old C: From 55 days to end of experiment (total 21 wks) D: From weaning to end of experiment (total 26 wks)
Ip *et al*., 1999	MNU (50 mg/kg), 55 days old	Control butter fat (0.1% CLA in diet) High CLA butter fat (0.8% CLA in diet)	23 – 55 days old

3.1.4 Mechanisms of anti-cancer activity of CLA

The experiments outlined above focused predominantly on the effects of CLA on mammary carcinogenesis *in vivo* without looking at the changes at the molecular level. Having confirmed the anti-cancer properties of CLA in numerous animal studies from various sources of CLA, attention turned to the mechanisms behind this activity. CLA has been reported to decrease the expression of cell cycle proteins cyclin D1 and cyclin A in TEBs and alveolar clusters of the mammary epithelium (Ip *et al*., 2001). In the MCF-7 breast cancer cell line, CLA increased mRNA and protein levels of pro-apoptotic p53 and p21WAF1/CIP1 and decreased anti-apoptotic bcl-2 (Majumder *et al*., 2002). In the MDA-MB-231 breast cancer cell line, which expressed mutant p53, mRNA levels of p53 were not affected by CLA but protein levels were completely suppressed. p21WAF1/CIP1 and bcl-2 mRNA and protein levels were increased. Bax and bcl-Xs levels were also increased, giving an overall ratio of Bax/bcl-Xs to bcl-2 that would promote apoptosis (Majumder *et al*., 2002). These authors did not investigate the effect on growth of these two cell lines (Majumder *et al*., 2002).

Tanmahasamut *et al*. (2004) reported growth inhibition by CLA in the ER positive cell line, MCF-7, but not in the ER negative cell line, MDA-MB-231, indicating a role of ER in this inhibition. The authors determined that CLA treatment downregulated levels of ERα mRNA and protein, and also interfered with binding to the estrogen response elements (EREs). Results also demonstrated that CLA activated a peroxisome proliferator response element (PPRE). The effect of CLA on peroxisome proliferators activated receptors (PPARs) was also examined by Maggiora *et al*. (2004). An increase in PPARα was noted in a number of cell lines following CLA treatment, in conjunction with a decrease in PPARβ/δ.

CLA has also been reported to modulate AA distribution in MCF-7 and SW480 cells (Miller *et al*., 2001). AA uptake into monoglyceride fractions in MCF-7 cells was increased after treatment with CLA and the *c*9,*t*11-CLA isomer, while uptake into triglyceride fractions was increased in the SW480 cell line. The *c*9,*t*11-CLA isomer caused a decrease in AA incorporation into phosphatidylcholine and an increase into phosphatidylethanolamine in both cell lines. Treatment with CLA and *t*10,*c*12-CLA isomer resulted in increased AA uptake into the phosphatidylserine

fraction in the SW480 cell line. AA conversion to PGE_2 was inhibited by CLA and *c*9,*t*11-CLA isomer in both cell lines. Thus CLA and its isomers resulted in changes in AA distribution in cellular lipids and also modulated the prostaglandin production within cells.

One possibility regarding the mechanism of action is that CLA derivatives act as a distinct set of PUFAs (Figure 3.4) (Banni *et al*., 2004). Δ6 desaturase, elongase and Δ5 desaturase enzymes are involved in the metabolism of CLA to new metabolites, 18:3, 20:3 and 20:4. The *c*9,*t*11-CLA isomer is metabolized easily to the 20:4 molecule but *t*10,*c*12-CLA appears to be resistant to the elongation and desaturation to the 20:3 and 20:4 molecules respectively. CLA would thus compete with LA for the desaturase and elongase enzymes of the PUFA pathways, and the CLA metabolites could also compete with LA metabolites for lipid incorporation (Banni *et al*., 2004).

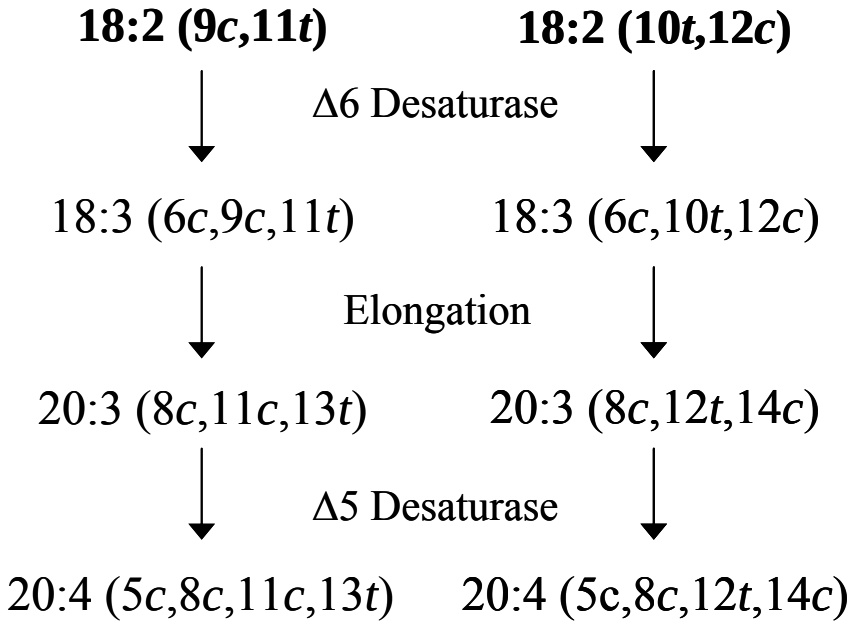

Figure 3.4 Distinct conjugated PUFAs derived from *c*9,*t*11-CLA and *t*10,*c*12-CLA. Adapted from Banni *et al*., 2004.

3.1.5 Invasion and metastasis and CLA

Hubbard *et al*. (2000) were the first group to describe the anti-metastatic effects of CLA by using experimental and spontaneous metastasis models in mice. Latency was calculated as the time from injection to when tumours reached a volume of 8 mm^3. Exposure to 0.5% and 1% CLA for the duration of the experiment increased latency significantly. However the growth of the tumour, as calculated by tumour volume, was not altered by the CLA diets (0.1/0.5/1%). Spontaneous metastasis experiments involved implantation of cells from the 4526 mouse mammary tumour into the mammary fat pad followed by removal of the primary tumour upon reaching a certain volume. This mimics the clinical course of breast cancer progression. Mice fed 0.1%, 0.5% and 1% CLA had significantly fewer pulmonary nodules in comparison to the control. In experimental metastasis studies, tumour cells were injected into the tail vein of the mice but did not result in any significant difference in the number of pulmonary nodules. Tumour burden (the total volume of lung nodules per mouse) in these mice was however, significantly decreased. Thus, the authors concluded that CLA not only affected tumour initiation and promotion but metastasis as well.

This group went on to look at the effect of two of the individual CLA isomers, *c*9,*t*11-CLA and *t*10,*c*12-CLA, on murine mammary tumourigenesis (Hubbard *et al*., 2003). Mice were fed diets of 0.1% or 0.25% *c*9,*t*11-CLA or *t*10,*c*12-CLA or a mixed diet containing 0.125% of each isomer. All diets were found to have no significant effect on latency or growth of primary tumours, when compared with the control. For metastasis, there was no significant difference among the different CLA diets in the number of pulmonary nodules in the lungs of the mice. However, compared to the control diet, there was a significant difference in the average size of nodules in the lungs of mice fed the CLA diets. The higher concentration of the individual isomers had a greater effect on the metastatic nodule size and total tumour burden than the lower concentrations. The mixed CLA diet had a similar effect on total tumour burden to the diets containing the lower concentration of the individual isomers, thus the anti-cancer effects did not appear to be additive.

This study (Hubbard *et al*., 2003) looked more specifically at where along the metastasis pathway the CLA effects were exerted – lodgement, survival or growth. When compared to the control group, the CLA diets significantly decreased the

number of cells, which survived and grew as pulmonary nodules. In all the CLA-fed groups, the metastatic tumour burden was significantly decreased compared to the control group. The reasoning for using spontaneous and experimental metastasis was to try to determine if the effects of CLA were on early events in the metastatic cascade (tumour cell release, entry into bloodstream) or later events (lodgement, extravasation and survival). CLA treatments were consistent in reducing total pulmonary tumour burden in both experiments. This would suggest an effect on growth of metastases once they have lodged and survived.

Harris *et al*. (2001) looked at the effect of CLA on MMP levels in serum from pregnant rats. The levels of MMP-2 and MMP-9 proteins were shown to be decreased in the CLA-fed rats. Chen *et al*. (2003) examined the effect of the *c*9,*t*11-CLA isomer on invasion, migration and MMP levels in a human gastric carcinoma cell line, SGC-7901. They reported inhibition of both invasion and migration of cells and a corresponding reduction in expression of MMP-9 with an increase in TIMP1 and TIMP2 mRNA levels. Kunayasi *et al*. (2006) found CLA to decrease invasion rates of a human gastric cancer cell line, MKN28, and a human colon cancer cell line, Colo320. CLA injections into mice also significantly reduced metastatic foci of both cell lines in the peritoneal cavity. Masso-Welch *et al*. (2002) investigated the effect of CLA on angiogenesis. Mice fed 1% or 2% CLA for 6 weeks prior to angiogenic challenge by Matrigel pellet assay showed significantly decreased functional angiogenesis. The levels of angiogenic inhibition peaked at 1% dietary CLA, with no increase observed at 2%. Levels of vascular endothelial growth factor (VEGF) and its receptor, foetal liver kinase-1 (Flk-1/VEGFR-2), were decreased after feeding with CLA diets, giving some explanation for the decrease in angiogenesis. No studies have been published to date looking at the effect of CLA or individual isomers on MMP levels in breast cancer cell lines. The effects on invasion, migration and angiogenesis illustrate the great potential of using CLA as a multipotent anti-cancer agent.

3.1.6 Epidemiological studies and CLA

Despite the significant number of investigations into the effect of CLA on carcinogenesis and mechanisms of action, few epidemiological studies have been

conducted to confirm these effects in humans. Aro *et al*. (2000) found an inverse association between dietary or serum CLA levels and breast cancer risk in postmenopausal women. This correlation did not however extend to premenopausal women. In contrast, the Netherlands Cohort Study found a weak positive association between CLA intake and breast cancer risk in postmenopausal women (Voorrips *et al*., 2002). Chajes *et al*. (2002) investigated the levels of CLA in breast adipose tissue in relation to breast cancer risk. No significant association was found between these two factors. In a study looking at the relationship of CLA levels in breast adipose tissue and the occurrence of metastatic breast cancer, no significant association was found (Chajes *et al*., 2003). McCann *et al*. (2004) examined the correlation between breast cancer and the intake of CLA and the *c*9,*t*11-CLA isomer. No association between intake and the overall risk of breast cancer was observed in premenopausal or postmenopausal women. In non-breast cancer, the only epidemiology study published to date was by Larsson *et al*. (2005). They found an inverse correlation between CLA intake and colorectal cancer risk in a Swedish Mammography cohort of 60,708 women.

3.1.7 Objectives of Chapter 3

CLA has been reported to have significant effects on tumourigenesis in both *in vitro* and *in vivo* models. The aim of this present study was to look at the effects of a CLA mix, and the individual isomers, *c*9,*t*11-CLA and *t*10,*c*12-CLA, on cell proliferation of the 4T1 murine mammary cancer cell line and the Hs578T human breast cancer cell line. Apoptosis and cell cycle kinetics were analysed following treatment of the 4T1 cell line with LA, CLA, *c*9,*t*11-CLA and *t*10,*c*12-CLA. Modulation of invasion, migration, adhesion and colony formation in soft agar by CLA was also examined for the first time in a mammary cancer cell line. The effects of CLA on expression of MMP and TIMP levels in breast or mammary cancer have not been analysed previously. Thus protein and mRNA levels of MMP-2, MMP-9, TIMP-1 and TIMP-2 following treatment with CLA was investigated to determine the effect on the cells at the molecular level.

3.2 Results

The 4T1 murine mammary cancer cell line was chosen for the CLA experiments because it can form highly metastatic tumours in BALB/c mice. Following mammary fat pad injection, spontaneous metastases develop in the lung, liver, lymph nodes and the brain (ATCC and Heppner *et al*., 2000). This occurs without surgical removal of the primary tumour and is an animal model for stage IV human breast cancer. The 4T1 cell line is also one of very few cell lines, of any origin, to form bone metastasis (Heppner *et al*., 2000). Using this cell line would allow animal studies on the effects of CLA to be conducted in BALB/c mice, eliminating the need for nude mice. In order to analyse the effects of CLA on human breast cancer cells, the Hs578T human breast carcinoma cell line was used. This cell line was derived from a 74-year old female and while it formed colonies in semisolid medium, it was not tumourigenic in mice (ATCC).

3.2.1 Cytotoxicity assay system

Cytotoxicity can be quantified using a number of different assay systems. We assessed three assays for this work – the MTS assay, the crystal violet assay and the acid phosphatase assay, as outlined in section 2.2.2. The MTS assay contained a novel tetrazolium compound [3-(4,5-dimethylthiazol-2yl)-5-(3-carboxymethoxyphenyl)-2-(4-solfophenyl)-2H-tetrazolium], which was bioreduced by cells into a coloured formazan product (Figure 3.5) (Promega Technical Bulletin 245). This reaction occurs in the presence of metabolically active cells. The absorbance at 492 nm reflected the level of the coloured product in the well and thus the number of metabolically active cells.

The crystal violet assay involved removal of the medium, washing and fixing of the cells before staining with a solution of 0.25% crystal violet. The crystal violet stains chromatin and nucleoli. The cells can be visualized under the microscope and photographed. The stain was eluted with glacial acetic acid and absorbance read at 570 nm. Acid phosphatase is an acid hydrolase found in the lysosome of the cell. The acid phosphatase assay is based on the hydrolysis of *p*-nitrophenyl phosphate (*p*NPP) by acid phosphatases in viable cells to produce *p*-nitrophenol (Figure 3.6)

(Yang *et al*., 1996). The production of *p*-nitrophenol is relative to the number of viable cells in the well. Addition of sodium hydroxide to the well produced a colour change due to the conversion of *p*-nitrophenol to *p*-nitrophenolate and absorbance was read at 405 nm.

Sample standard curves using each assay to quantify cell numbers are shown in Figure 3.7 (A-C). After comparison of these three assays, it was decided to use the MTS assay for the cytotoxicity experiments. The R^2 values for the MTS assay were consistently higher than the other two assays. Another important advantage with this assay was the absence of the necessity to remove the medium and wash the cells before addition of the substrates or stains. It was felt that this would introduce additional error into the results. With the MTS assay, the substrate was added direct to the medium after the treatment period and the coloured product was soluble in the medium. After incubation the plate was simply read using a plate-reader.

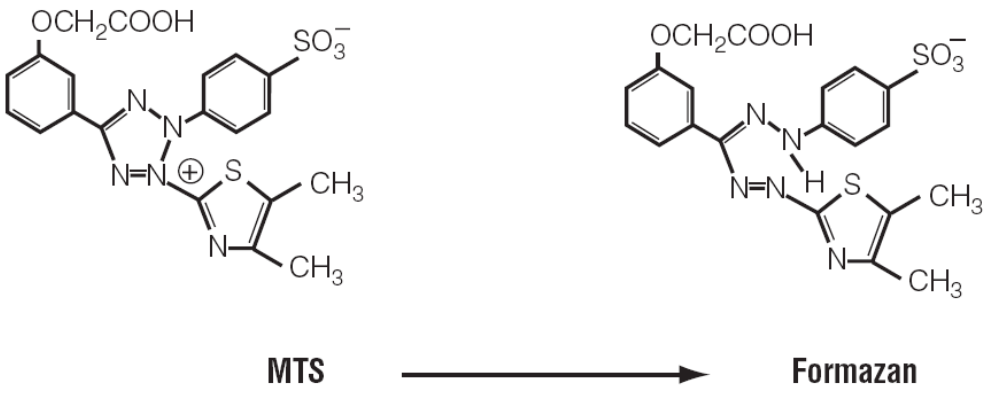

Figure 3.5 Conversion of MTS into a formazan product by metabolically active cells. From Promega Technical Bulletin 245.

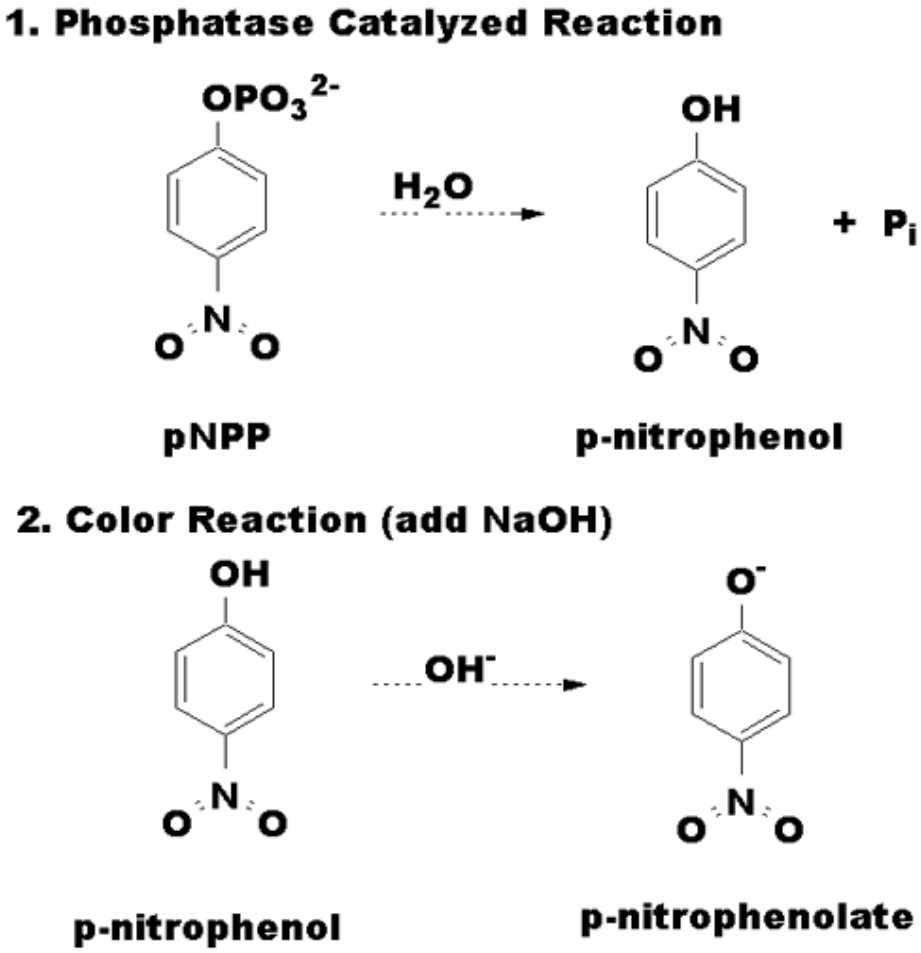

Figure 3.6 Reaction of *p*NPP with acid phosphatases and sodium hydroxide to produce *p*-nitrophenolate in the acid phosphatase assay. From http://www.bio.mtu.edu/campbell.

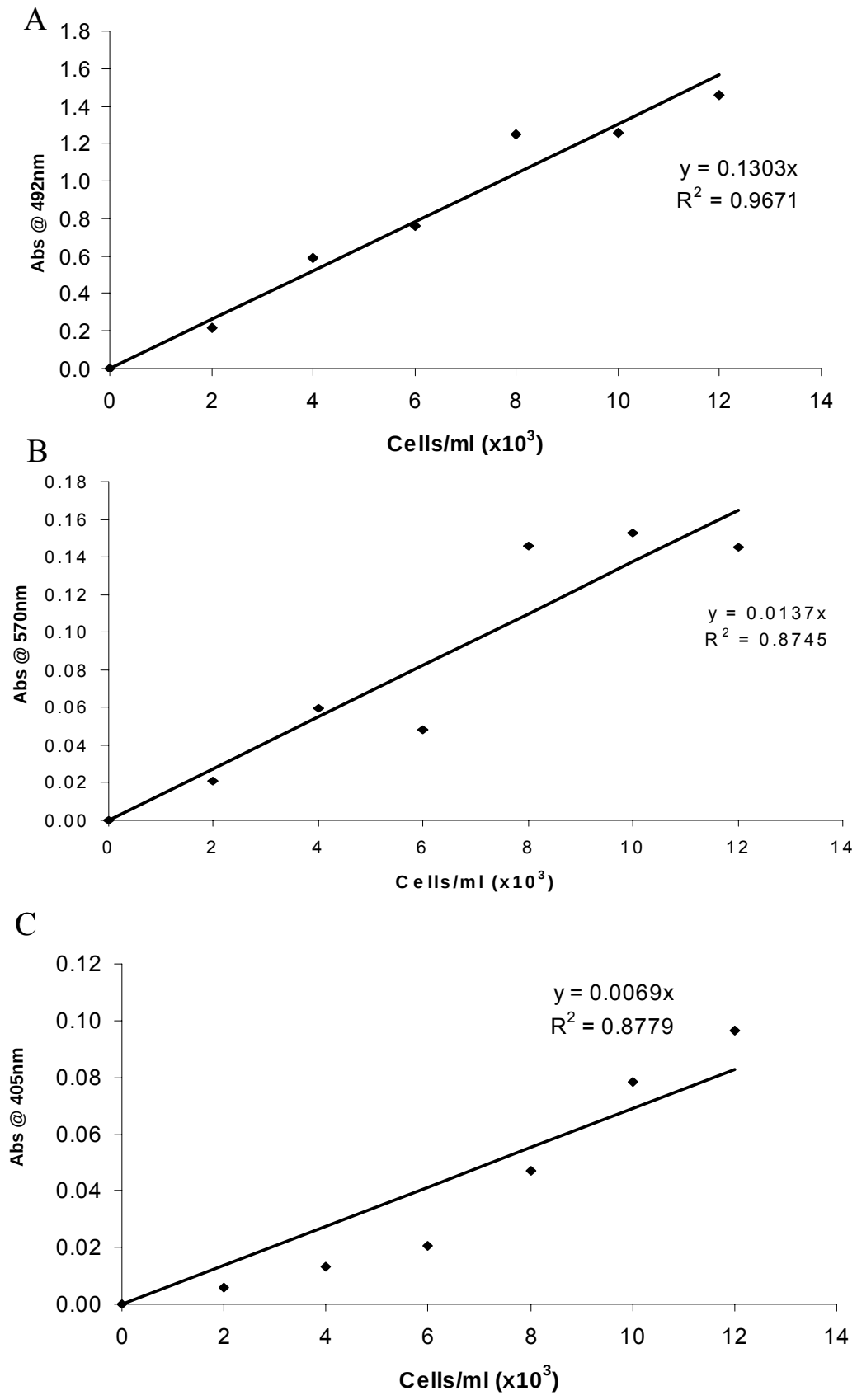

Figure 3.7 Standard curves comparing the MTS (A), crystal violet (B) and acid phosphatase (C) assays using the 4T1 cell line after incubation for 3 days.

3.2.1.1 Optimisation of cell numbers for cytotoxicity assays

Cytotoxicity assays were optimised with regards to cell numbers. The cell numbers chosen to seed into 96-well plates had to allow the cells to proliferate over the specified time period without imposing a limitation on space or medium supplements. Cells were required to be in the logarithmic phase of growth in order to confirm that the cell death noted upon treatment was in fact due to the treatment and not due to insufficient space or lack of essential medium components. The cytotoxicity was examined after treatment for 1, 3 and 5 days, so a range of different cell numbers was examined and optimised over these three time points (Figures 3.8 and 3.9). The 4T1 cell line was an extremely fast growing cell line and thus cell numbers used were lower than for the Hs578T cell line. Cell numbers used are outlined in Table 3.2. Cells for treatment were seeded at the second highest point on the standard curve. Having determined the optimum cell numbers and the most efficient assay, the cytotoxicity of CLA was examined.

Table 3.2 Cell numbers seeded into 96-well plates for 1, 3 and 5 day assays for the 4T1 and Hs578T cell lines.

Cytotoxicity Assays Cells/ml (x10^3)			
	1 Day	**3 Days**	**5 Days**
4T1	30	12	6
Hs578T	60	30	18

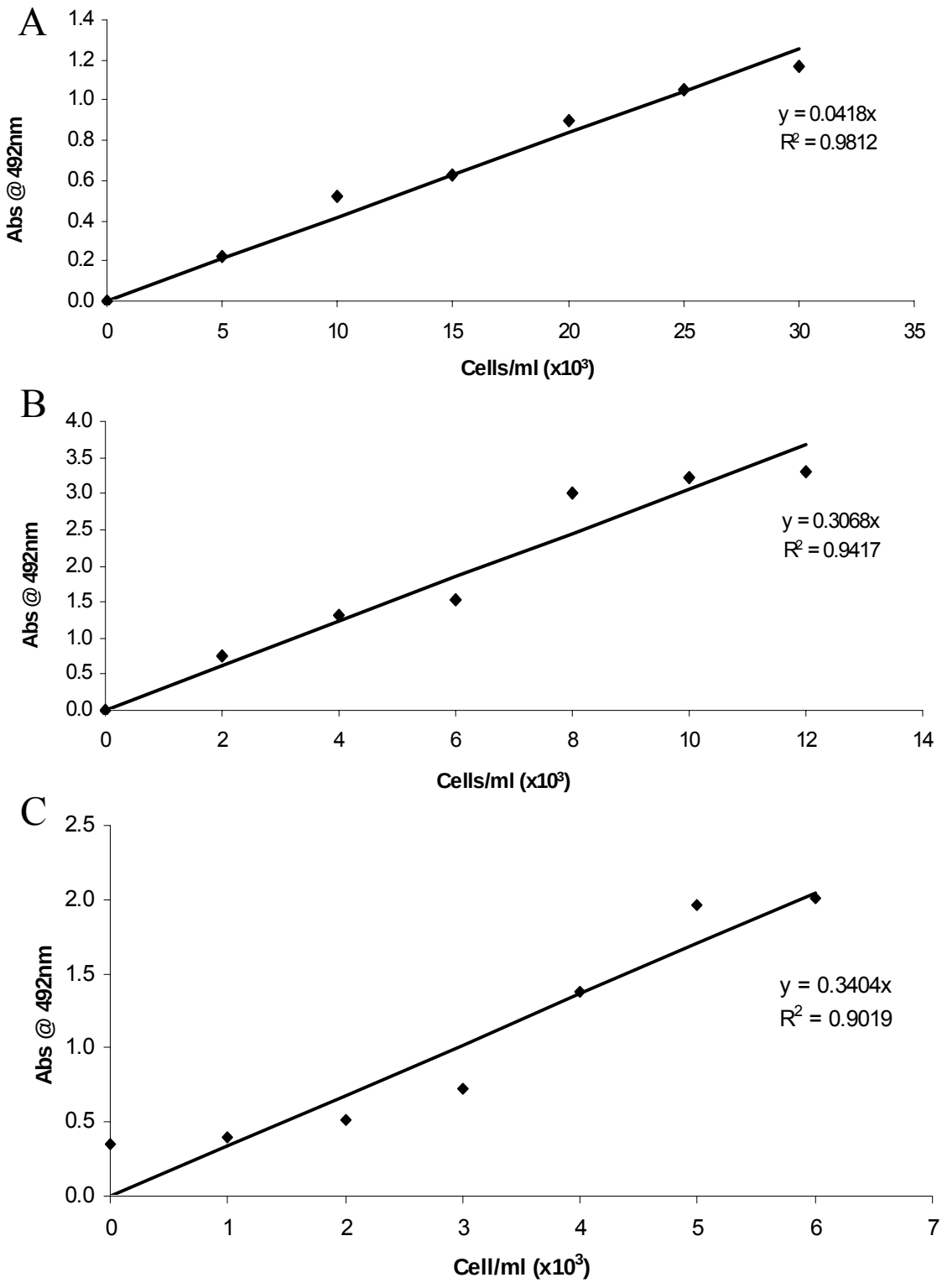

Figure 3.8 Standard curves for the 4T1 cell line for 1 day (A), 3 days (B) and 5 days (C). Cell numbers were optimised for each time point.

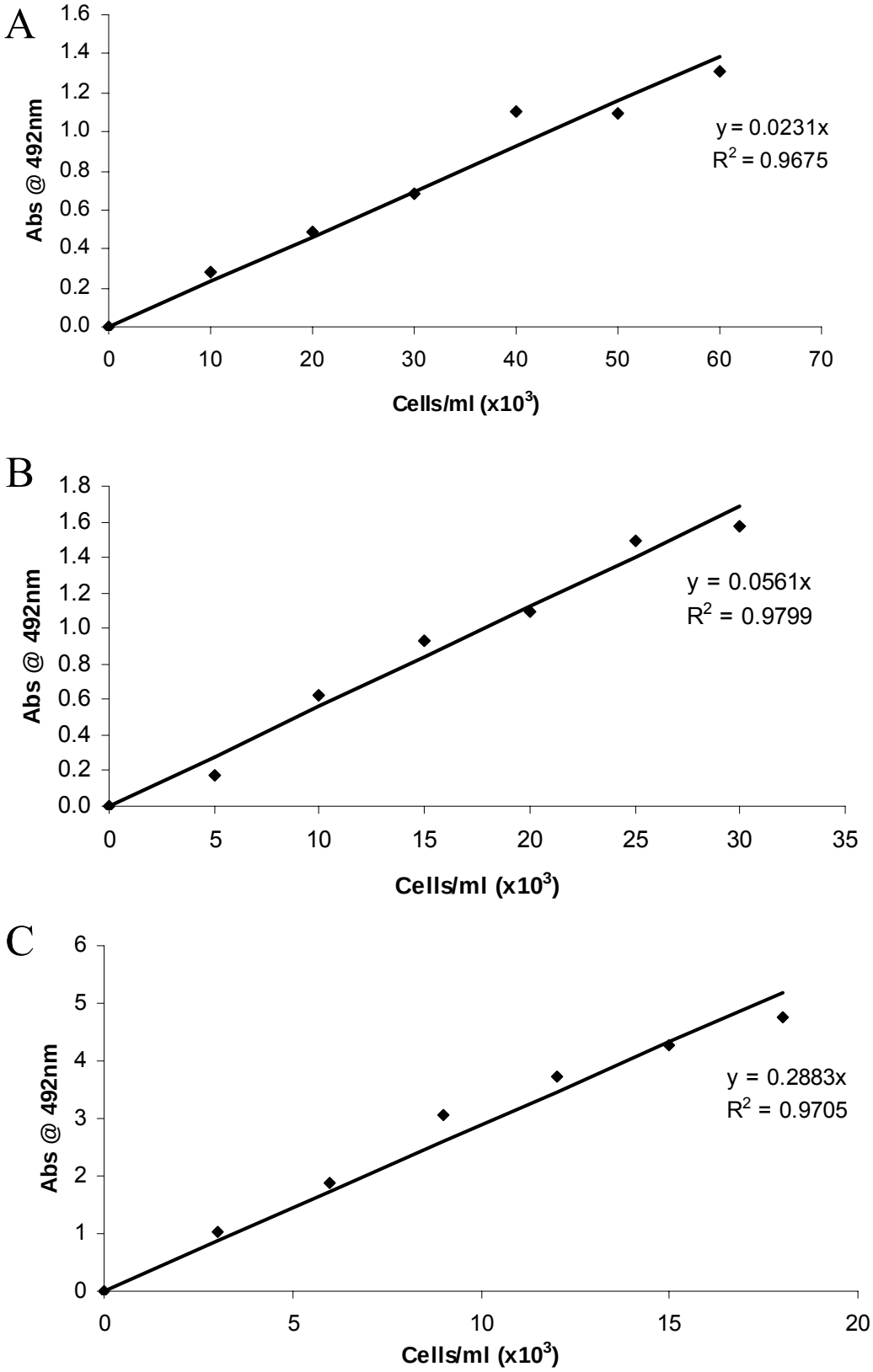

Figure 3.9 Standard curves for the Hs578T cell line for 1 day (A), 3 days (B) and 5 days (C). Cell numbers were optimised for each time point.

3.2.2 Cytotoxicity of CLA and individual isomers in the 4T1 murine mammary cancer cell line

Cytotoxicity assays were conducted as outlined in section 2.2.2. Cytotoxicity of LA, a mix of CLA isomers (designated 'CLA'), and two individual isomers, *c*9,*t*11-CLA and *t*10,*c*12-CLA, were tested in the 4T1 cell line over 1, 3 and 5 days. The CLA mixed isomers contained *c*9,*t*11-CLA/*t*9,*c*11-CLA (~41%), *t*10,*c*12-CLA (~44%), *c*10,*c*12-CLA (~10%) and others (~5%). The range of concentrations tested was 18 μM (5 μg/ml) to 107 μM (30 μg/ml), levels found in human serum (Tanmahasamut *et al*., 2004). LA was also used in these experiments as it has previously been shown to have a stimulatory effect on mammary and breast cancer cell growth and metastasis (Reyes *et al*., 2004 and Connolly *et al*., 1999). The cytotoxicity results are from a minimum of duplicate experiments, completed in triplicate.

Cytotoxicity of LA, *c*9,*t*11-CLA and *t*10,*c*12-CLA was low over the range of concentrations tested after treatment for 1 day (Figure 3.10). IC_{50} values were not established for LA, *c*9,*t*11-CLA or *t*10,*c*12-CLA over the range of concentrations tested (Table 3.3). For CLA, toxicity was only observed at the highest concentration of 107 μM, with 100% cell death noted (Figure 3.10). An IC_{50} value was established for CLA at 98 μM (Table 3.3). After treatment for 3 days, CLA caused the highest toxicity, with an IC_{50} value of 44 μM (Figure 3.11 and Table 3.3). Treatment with the *c*9,*t*11-CLA isomer resulted in toxicity at the two highest concentrations tested, with 100% cell death at 107 μM (Figure 3.11). The IC_{50} value for *c*9,*t*11-CLA was 82 μM after 3 days treatment (Table 3.3). The *t*10,*c*12-CLA isomer caused 80% cell death at the top concentration of 107 μM after treatment for 3 days, with an IC_{50} value of 98 μM (Figure 3.11 and Table 3.3). LA caused low toxicity at the majority of the concentrations, with cell death reaching 30% at 107 μM, thus an IC_{50} value was not established (Figure 3.11 and Table 3.3).

Cytotoxicity over 5 days is illustrated in Figure 3.12. CLA was the most toxic over the range of concentrations tested, with an IC_{50} value of 58 μM established (Figure 3.12 and Table 3.3). Treatment with the *t*10,*c*12-CLA isomer resulted in similar toxicity to CLA, with an IC_{50} value of 62 μM established (Figure 3.12 and Table 3.3). The *c*9,*t*11-CLA isomer was less toxic with an IC_{50} value of 78 μM

(Figure 3.12 and Table 3.3). LA caused low toxicity at the lower concentrations, with the cell death rising to 87% at the highest concentration, 107 μM (Figure 3.12). An IC_{50} value of 100 μM was established for LA over 5 days (Table 3.3).

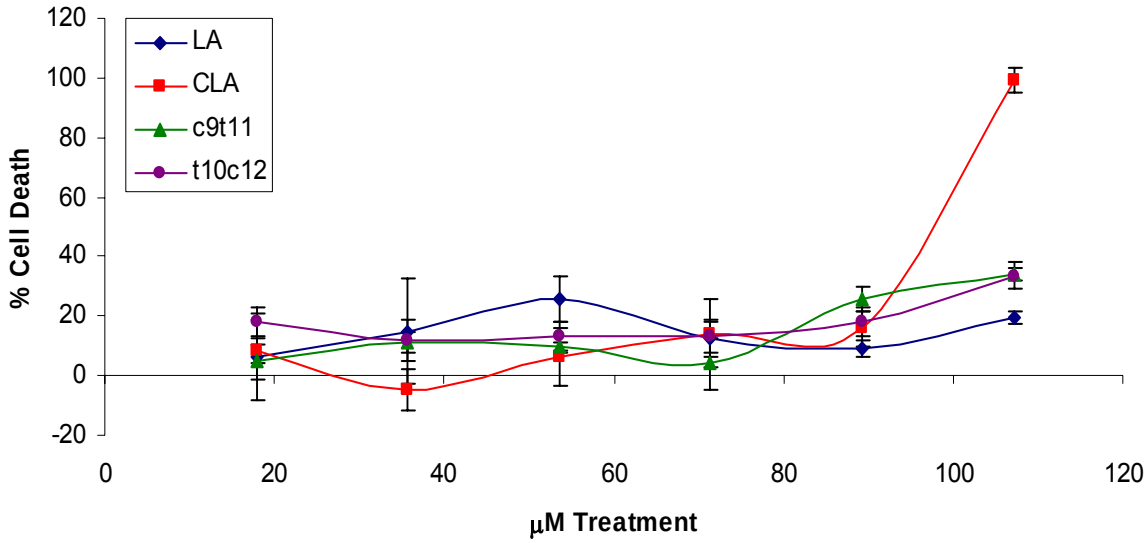

Figure 3.10 Cytotoxicity of LA, CLA, *c*9,*t*11-CLA and *t*10,*c*12-CLA in the 4T1 cell line after treatment for 1 day. Cell death was low in all instances except following CLA treatment at the top concentration of 107 μM.

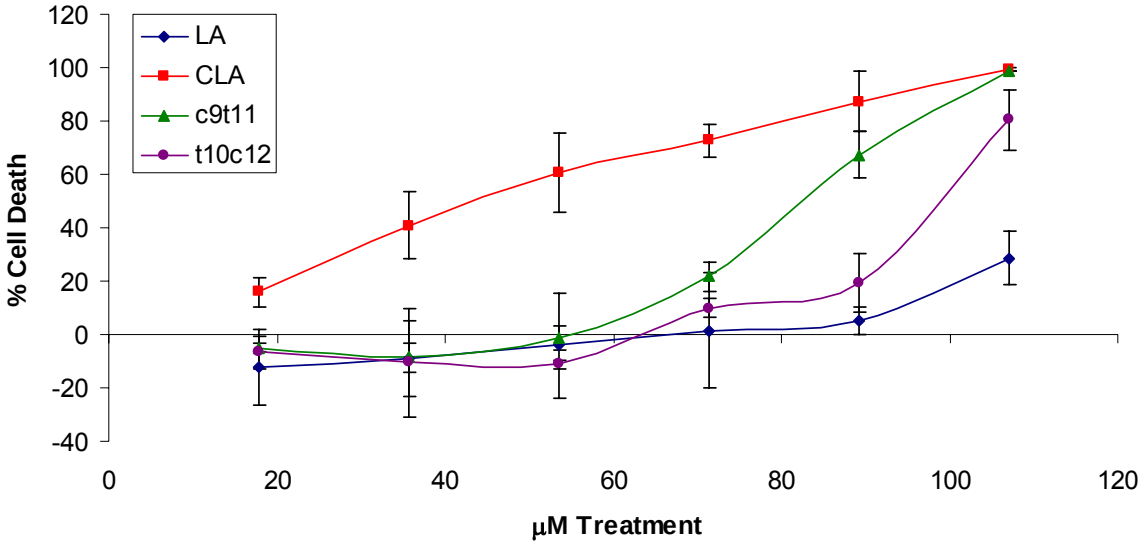

Figure 3.11 Cytotoxicity of LA, CLA, *c*9,*t*11-CLA and *t*10,*c*12-CLA in the 4T1 cell line after treatment for 3 days. CLA exhibited the highest toxicity towards the cell line, followed by the *c*9,*t*11-CLA isomer.

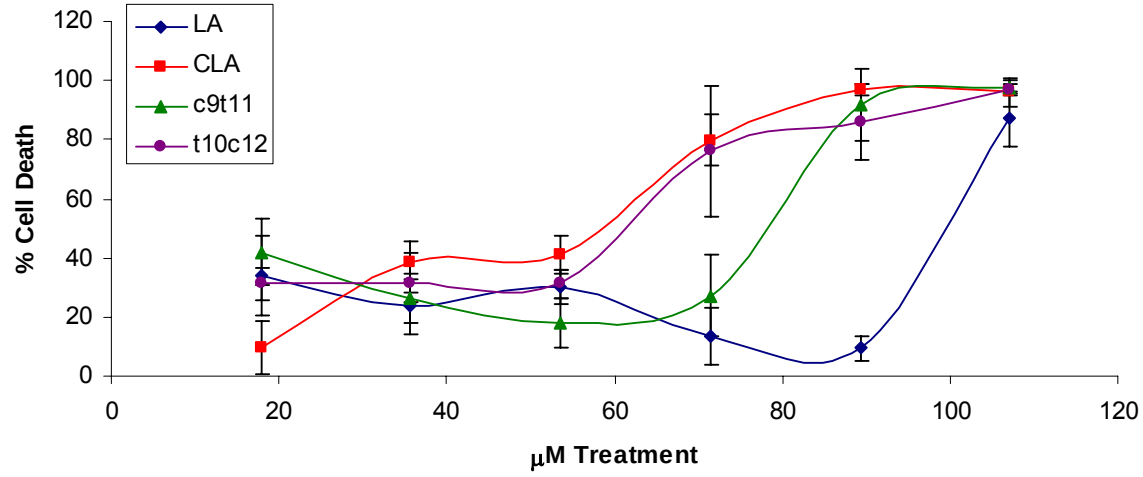

Figure 3.12 Cytotoxicity of LA, CLA, *c*9,*t*11-CLA and *t*10,*c*12-CLA in the 4T1 cell line after treatment for 5 days. CLA was the most toxic to the cells, closely followed by the *t*10,*c*12-CLA isomer and the *c*9,*t*11-CLA isomer.

Table 3.3 IC_{50} values for LA, CLA, *c*9,*t*11-CLA and *t*10,*c*12-CLA in the 4T1 cell line after treatment for 1, 3 and 5 days.

IC_{50} Values 4T1 Cell Line (μM)			
	1 Day	**3 Days**	**5 Days**
LA	>107[a]	>107[a]	100±2
CLA	98±2	44±8	58±3
***c*9*t*11**	>107[a]	82±2	78±4
***t*10*c*12**	>107[a]	98±3	62±3

Mean±SD
(a) IC_{50} value not reached up to highest concentration tested

3.2.3 Cytotoxicity of CLA and individual isomers in the Hs578T human breast cancer cell line

The Hs578T human breast carcinoma cell line was chosen to test the cytotoxicity of LA, CLA and the isomers, *t*10,*c*12-CLA and *c*9,*t*11-CLA. After treatment for 1 day relatively low toxicity was observed for all concentrations of fatty acids used (Figure 3.13). An increase in cell growth was noted at the lower concentrations for the *t*10,*c*12-CLA isomer and the *c*9,*t*11-CLA isomer. IC_{50} values were not reached over the range of concentrations tested (Table 3.4).

After treatment for 3 days, cytotoxicity for all fatty acids was low and IC_{50} values were not reached over the range of concentrations tested (Figure 3.14 and Table 3.4). CLA proved the most toxic to the Hs578T cells over 5 days, with an IC_{50} value of 58 μM (Figure 3.15 and Table 3.14). The *c*9,*t*11-CLA and *t*10,*c*12-CLA isomers caused toxicity at the highest concentration, 107 μM (Figure 3.15). IC_{50} values for these isomers were 104 μM and 98 μM respectively (Table 3.4). LA showed low toxicity over the range of concentrations tested with no IC_{50} value reached (Figure 3.15 and Table 3.14).

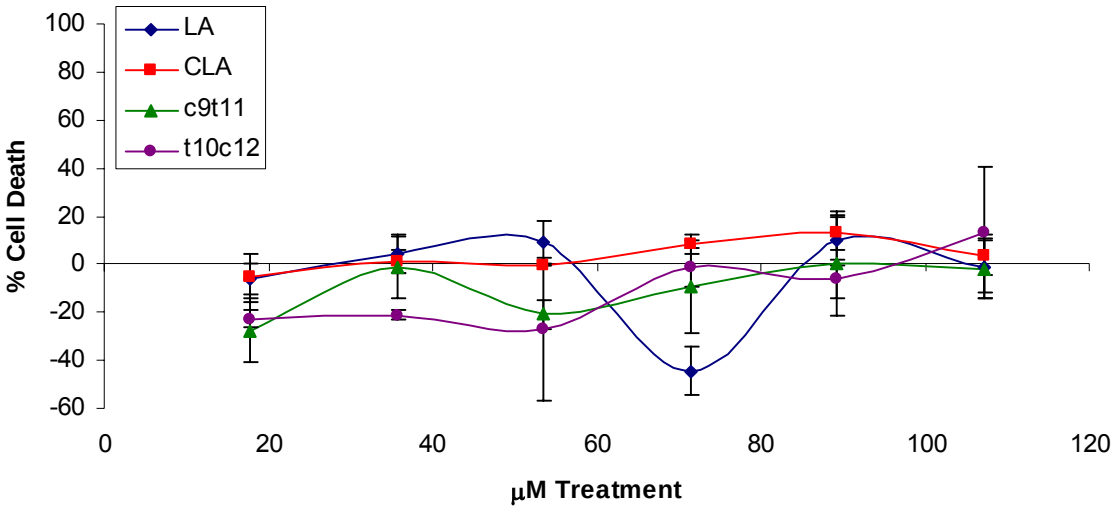

Figure 3.13 Cytotoxicity of LA, CLA, *c*9,*t*11-CLA and *t*10,*c*12-CLA in the Hs578T cell line after treatment for 1 day. Low toxicity was observed over the range of concentrations tested.

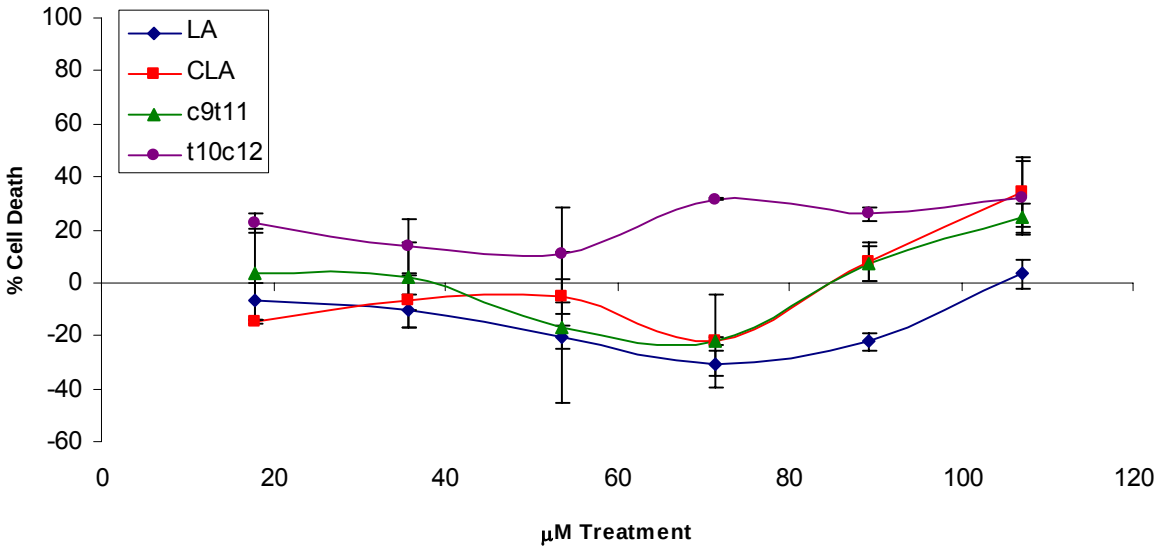

Figure 3.14 Cytotoxicity of LA, CLA, *c*9,*t*11-CLA and *t*10,*c*12-CLA in the Hs578T cell line after treatment for 3 days. Low toxicity was observed over the range of concentrations tested.

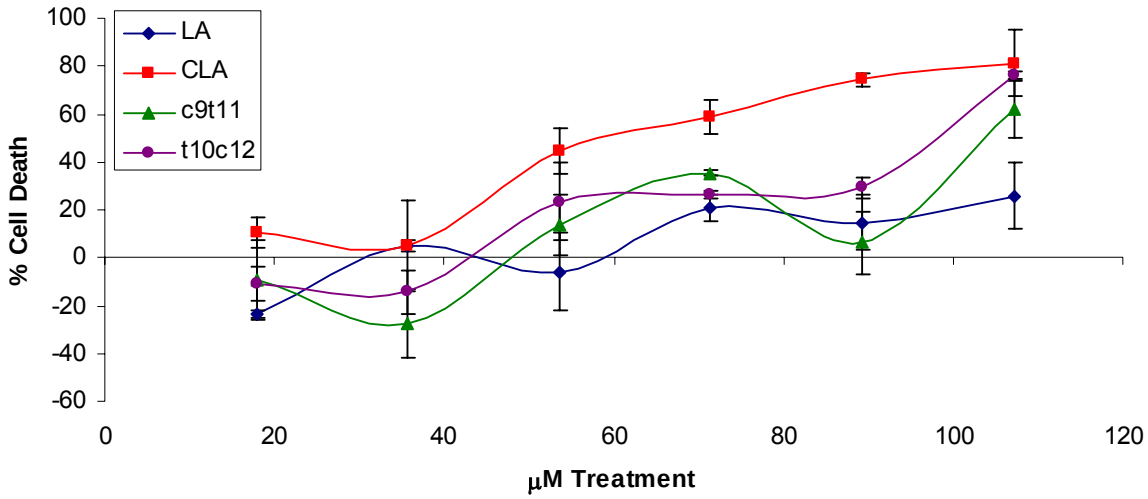

Figure 3.15 Cytotoxicity of LA, CLA, *c*9,*t*11-CLA and *t*10,*c*12-CLA in the Hs578T cell line after treatment for 5 days. CLA showed the most toxicity, followed by the *t*10,*c*12-CLA isomer and the *c*9,*t*11-CLA isomer.

Table 3.4 IC_{50} values for LA, CLA, *c*9,*t*11-CLA and *t*10,*c*12-CLA in the Hs578T cell line after treatment for 1, 3 and 5 days.

IC_{50} Values Hs578T Cell Line (µM)			
	1 Day	**3 Days**	**5 Days**
LA	>107[a]	>107[a]	>107[a]
CLA	>107[a]	>107[a]	58±3
***c*9*t*11**	>107[a]	>107[a]	104±2
***t*10*c*12**	>107[a]	>107[a]	98±1

Mean±SD
(a) IC_{50} value not reached up to highest concentration tested

3.2.4 Guava® cell cycle analysis of 4T1 cells following treatment with CLA and individual isomers

Flow cytometry has become a very useful tool to analyse numerous aspects of individual cells. The Guava® PCA is a bench-top cell analyser with extremely user-friendly interfaces and applications. This machine was used to analyse the effect of the fatty acids on cell cycle kinetics and apoptosis in the 4T1 cell line. Cell cycle stages were analysed using propidium iodide (PI), which intercalates with DNA. In normal cycling cells in culture, the G0/G1 contains quiescent cells and cells preparing for DNA replication. During S phase, replication of the genome occurs with a subsequent increase in the amount of PI bound to the genomic DNA (Figure 3.16). In the G2/M phase, the cell has double the amount of DNA as in the G0/G1 phase. Cell division occurs in the M phase, with the individual cells reverting back to the amount of DNA of cells in G0/G1. In this analysis, cells in G0/G1 are referred to as G1 and cells in G2/M are referred to as G2.

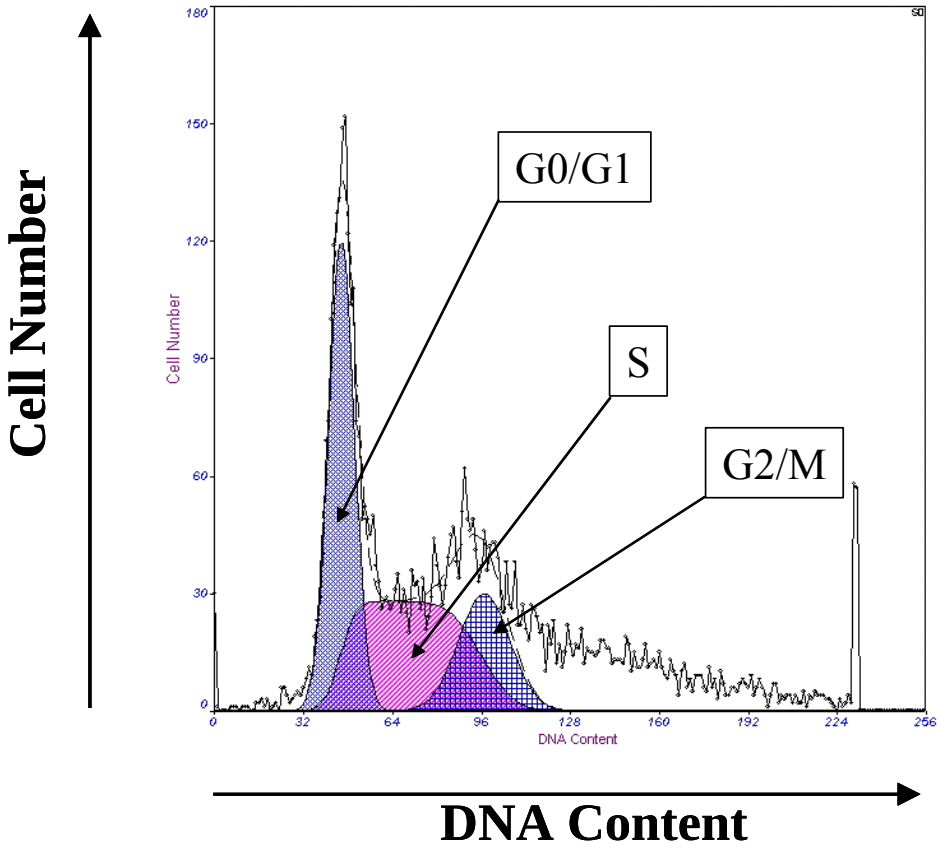

Figure 3.16 Cell cycle analysis from Multicycle software, indicating individual populations.

4T1 cells were treated with 54 μM and 89 μM of fatty acids for 3 days then assessed on the Guava® PCA. These concentrations were chosen as they covered a range of toxicities and would therefore give a good indication of the effect on the cell cycle as toxicity increased. Cells were harvested and prepared as described in section 2.2.4.1. Results are representative of three independent experiments. Data was analysed using Multicycle software (Phoenix Flow Systems, CA) which uses a more accurate method for deciphering the populations in the different stages. This software uses an algorithm which makes two assumptions – firstly, that the G2/M population will have double the DNA content than the G1/G0 and secondly, that the G1/G0 and G2/M phases have normal distribution. The S phase population is then calculated accordingly.

Figure 3.17 and Figure 3.18 show results following treatment with 54 μM of fatty acids for 3 days and the results are summarised in Table 3.5. In comparison to the control, all treatments caused a distinct arrest in the G1 population and a decrease in the S and the G2 phase populations. CLA and *t*10,*c*12-CLA increased the G1 phase population to 67.5% and 65.3% respectively while the G1 population for the control was 37%. LA and *c*9,*t*11-CLA caused a greater increase in the G1 population, to 74.4% and 71.7% respectively. The S phase population for the control was 39.7% and following treatment with *c*9,*t*11-CLA this population was reduced to 8.2%, with LA and CLA treatments reducing the populations to 12.5% and 15.4% respectively. LA, CLA, *c*9,*t*11-CLA and *t*10,*c*12-CLA caused a decrease in the G2 phase population to 13.2%, 17.1%, 20.1% and 10.2% respectively, in comparison to the control (23.2%).

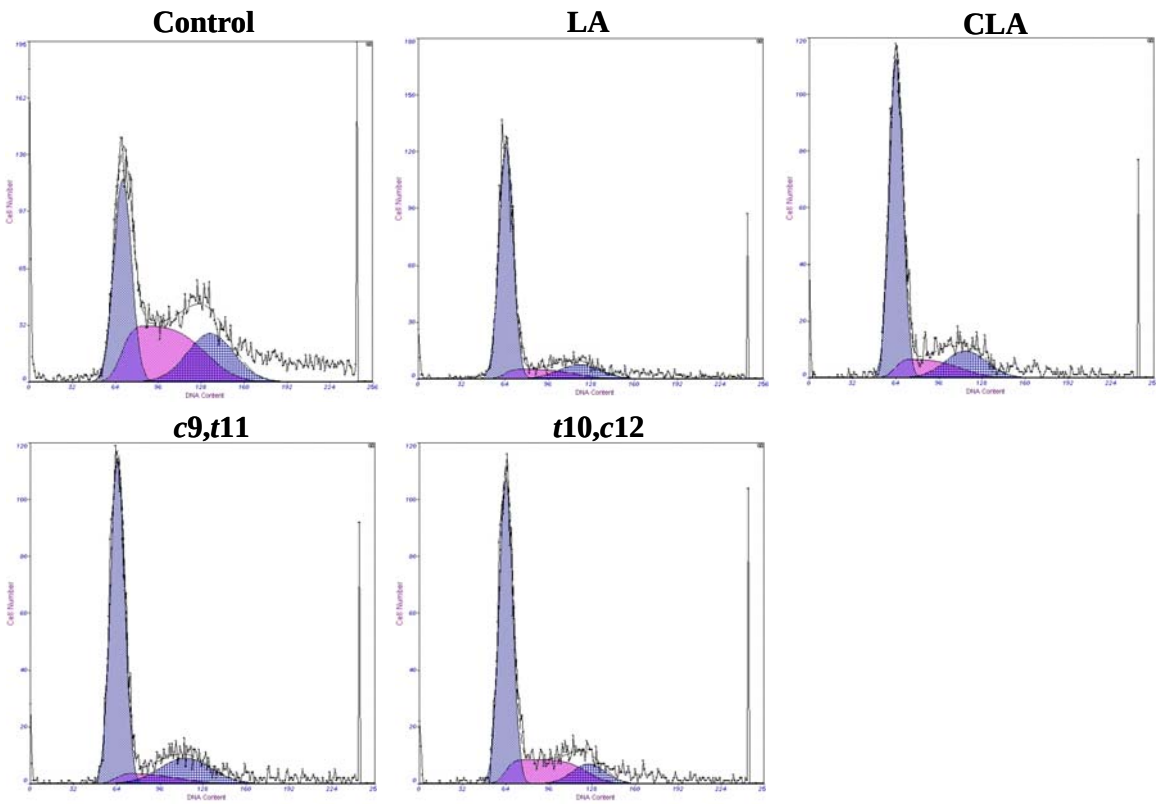

Figure 3.17 Cell cycle analysis of 4T1 cells following treatment for 3 days with 54 μM LA, CLA, *c*9,*t*11-CLA and *t*10,*c*12-CLA. X-axis shows DNA content, y-axis represents counts of cells. G1 phase is in light blue, S phase in pink and G2 phase in dark blue.

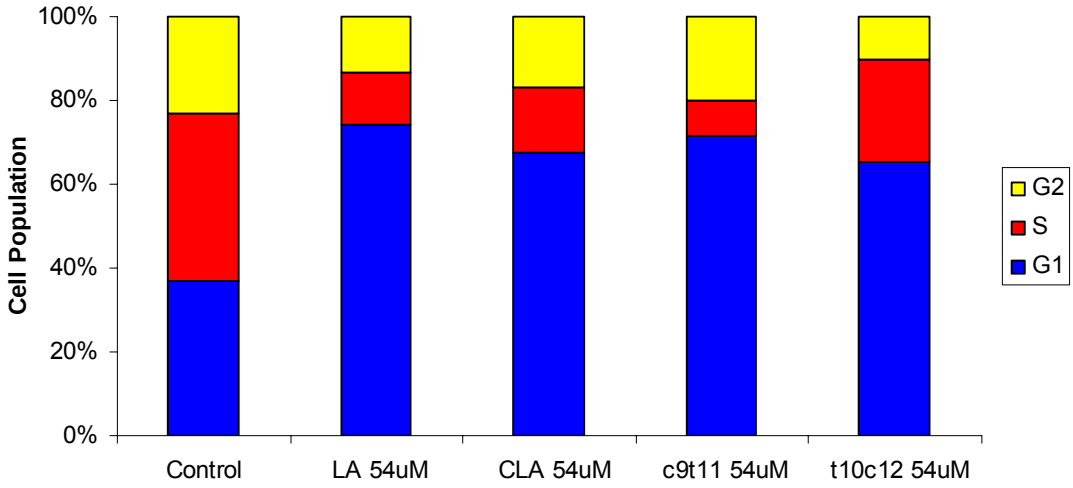

Figure 3.18 Cell cycle analysis of 4T1 cells following treatment for 3 days with 54 μM LA, CLA, *c*9,*t*11-CLA and *t*10,*c*12-CLA.

Table 3.5 Percentages of cell cycle populations following treatment for 3 days with 54 μM LA, CLA, *c*9,*t*11-CLA and *t*10,*c*12-CLA.

Cell Cycle Analysis: 54μM			
	G1 (%)	S (%)	G2 (%)
Control	37	39.7	23.2
LA	74.4	12.5	13.2
CLA	67.5	15.4	17.1
*c*9*t*11	71.7	8.2	20.1
*t*10*c*12	65.3	24.5	10.2

Treatment with 89 μM of fatty acids also caused an increase in G1 phase population and a decrease in S and G2 phase populations (Figures 3.19 and 3.20, Table 3.6). LA again caused the greatest increase in G1 phase population, at 69%, followed by the *c*9,*t*11-CLA isomer (65.3%), the *t*10,*c*12-CLA isomer (64%) and CLA (57.8%). The effect on the S phase populations varied, the control population was 45.4%, with LA causing a decrease to 13.5% while treatment with CLA caused a decrease to 29.5%. Treatment with the *c*9,*t*11-CLA isomer and the *t*10,*c*12-CLA isomer resulted in S phase populations of 22.8% and 20.7% respectively. Treatment with LA only caused a slight decrease in the G2 phase population, from 19.3% for the control to 17.5% for LA. The *t*10,*c*12-CLA isomer decreased the G2 phase population to 15.3% while CLA and the *c*9,*t*11-CLA isomer caused decreases to 12.7% and 11.9% respectively. In general there was a decrease in the G1 phase population from the lower to the higher concentration of treatment. The S phase population increased following treatment with the higher concentration of LA, CLA and the *c*9,*t*11-CLA isomer, in comparison to the lower concentration. There was an increase in the G2 phase populations following treatment with the higher concentrations of LA, the *c*9,*t*11-CLA isomer and the *t*10,*c*12-CLA isomer.

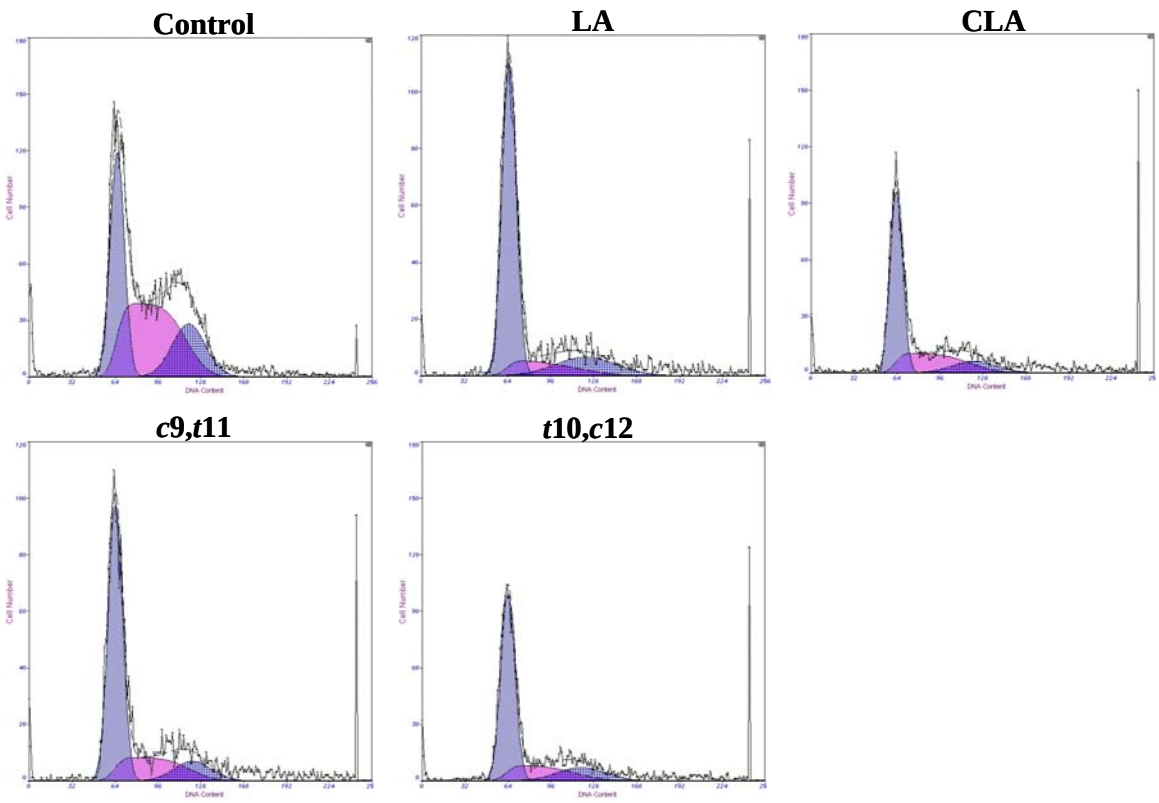

Figure 3.19 Cell cycle analysis of 4T1 cells following treatment for 3 days with 89 µM LA, CLA, *c*9,*t*11-CLA and *t*10,*c*12-CLA. X-axis shows DNA content, y-axis represents counts of cells. G1 phase is in light blue, S phase in pink and G2 phase in dark blue.

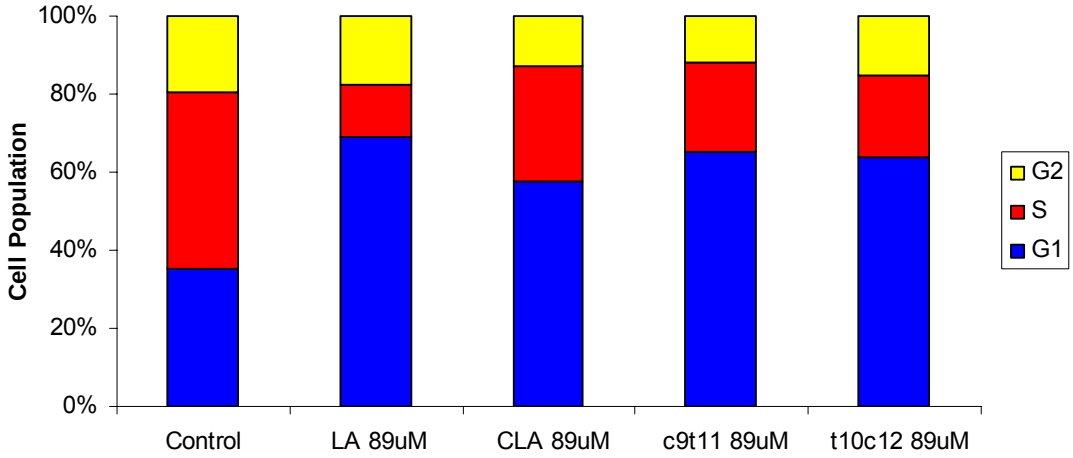

Figure 3.20 Cell cycle analysis of 4T1 cells following treatment for 3 days with 89 µM LA, CLA, *c*9,*t*11-CLA and *t*10,*c*12-CLA.

Table 3.6 Percentages of cell cycle populations following treatment for 3 days with 89 μM LA, CLA, *c*9,*t*11-CLA and *t*10,*c*12-CLA.

Cell Cycle Analysis: 89μM			
	G1 (%)	S (%)	G2 (%)
Control	35.3	45.4	19.3
LA	69	13.5	17.5
CLA	57.8	29.5	12.7
*c*9,*t*11	65.3	22.8	11.9
*t*10,*c*12	64	20.7	15.3

3.2.5 Guava® apoptosis analysis of 4T1 cells following treatment with CLA and individual isomers

Apoptosis of cells was analysed using two dyes, annexin V and 7-aminoactinomycin D (7-AAD). Annexin V binds to phosphatidylserine molecules which move to the outer surface of the cell membrane during early apoptosis. 7-AAD is a cell impermeable dye and only enters cells late in the apoptotic process once the membrane integrity has been compromised. Hence, healthy viable cells will not have staining with either of the dyes. Cells in the early apoptotic stages will be positive for annexin V and negative for 7-AAD and cells going through necrosis or the later stages of apoptosis will be positive for both annexin V and 7-AAD. In Figures 3.21-3.23, the individual cells are represented by dot-plots, with the x-axis and y-axis representing annexin V and 7-AAD staining of the cells respectively. Healthy cells without any dye are present in the lower left quadrant of the dot-plot, while cells undergoing apoptosis move firstly into the lower right quadrant (following translocation of phosphatidylserine molecule from inner to outer surface to cell membrane) then move to the upper right quadrant (following breach of the integrity of the membrane).

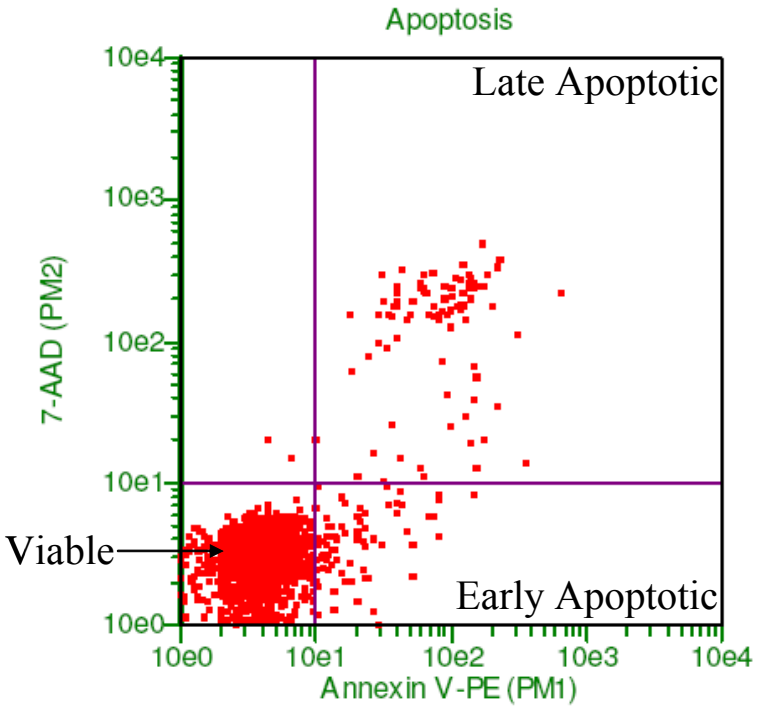

Figure 3.21 Guava® apoptosis analysis of cells, showing quadrants containing viable, early apoptotic and late apoptotic cells.

Cells were harvested and prepared as described in section 2.2.4.2. Apoptosis analysis was conducted using 4T1 cells treated for 3 days with 54 μM (Figure 3.22) and 89 μM (Figure 3.23) of fatty acids. Results are representative of three independent experiments. Figure 3.24 summarises the data, illustrating the percentage of annexin V positive cells, which includes both early and late apoptotic cells. The control cells had approximately 20% apoptotic cells. Treatment with 54 μM of *t*10,*c*12-CLA caused an increase in apoptotic cells to approximately 40% in comparison to the control ($p<0.05$) (Figures 3.22 and 3.24). The early apoptotic cells can be observed in the lower right quadrant and the cells in late apoptosis or undergoing necrosis can be seen in the upper right quadrant. Treatment with LA, CLA and *c*9,*t*11-CLA did not cause any significant change in the level of apoptotic cells.

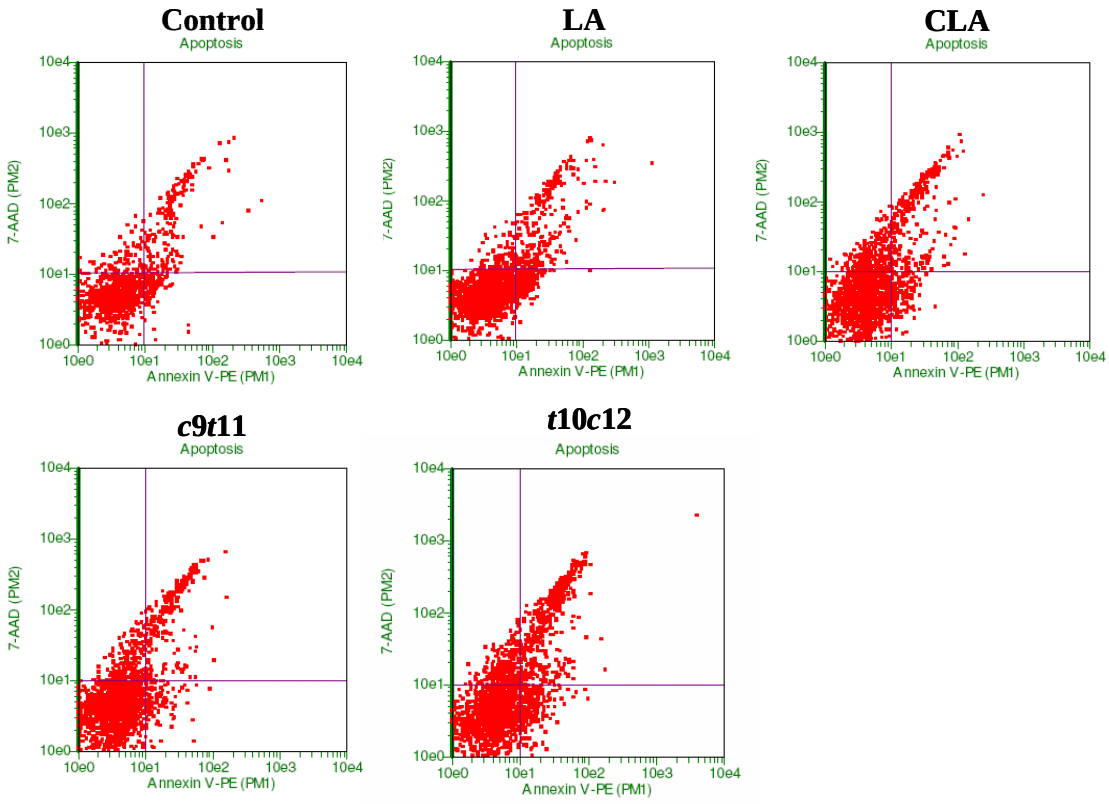

Figure 3.22 Apoptosis analysis of cells following treatment for 3 days with 54 µM fatty acids.

After 89 µM treatment, CLA and *c*9,*t*11-CLA caused a significant increase in the level of apoptotic cells to 75% and 59% respectively ($p<0.05$) (Figures 3.23 and 3.24). The increase in apoptotic cells can be mainly observed in the upper right quadrant, indicating an increase of cells either in late apoptosis or undergoing necrosis (Figure 3.23). These results correlate with the cytotoxicity noted following treatment with these fatty acids (Figure 3.11). Treatment with 89 µM LA did not cause any increase in apoptotic cells, while treatment with the *t*10,*c*12-CLA isomer caused an increase in apoptotic cells in comparison to the control, but this result was not significant (Figures 3.23 and 3.24).

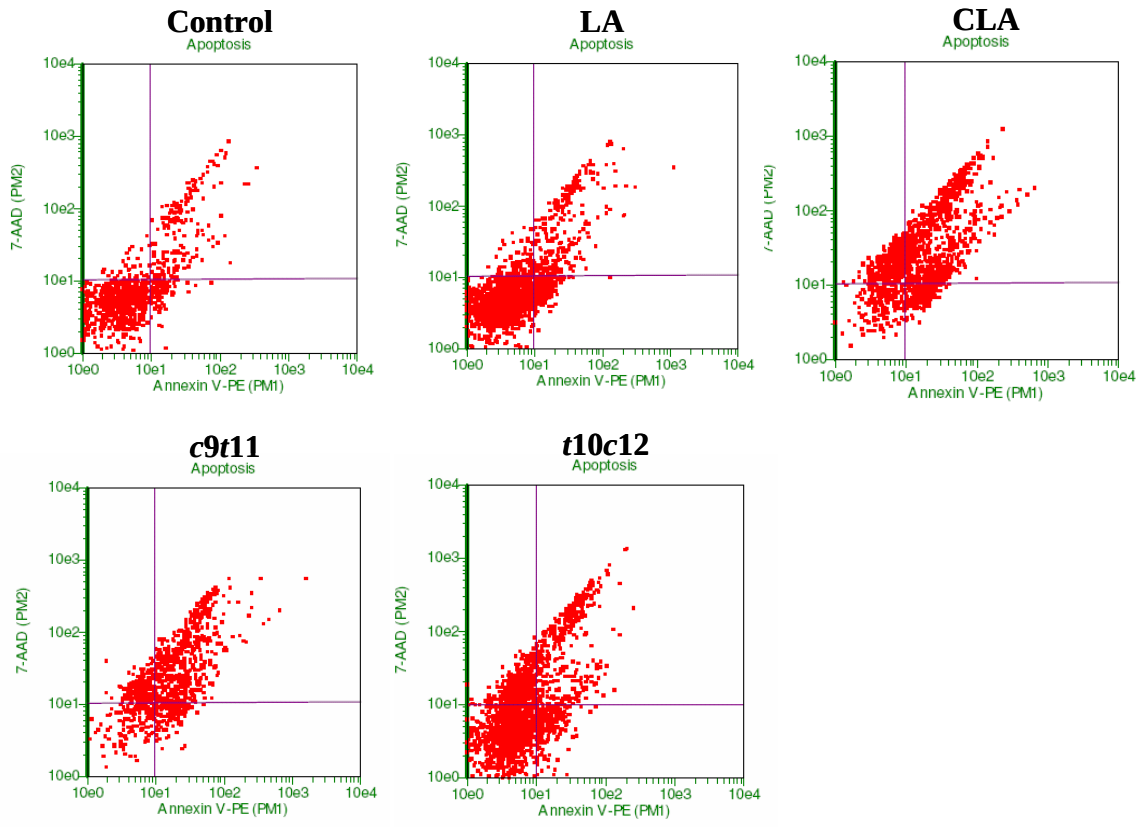

Figure 3.23 Apoptosis analysis of cells following treatment for 3 days with 89 µM fatty acids.

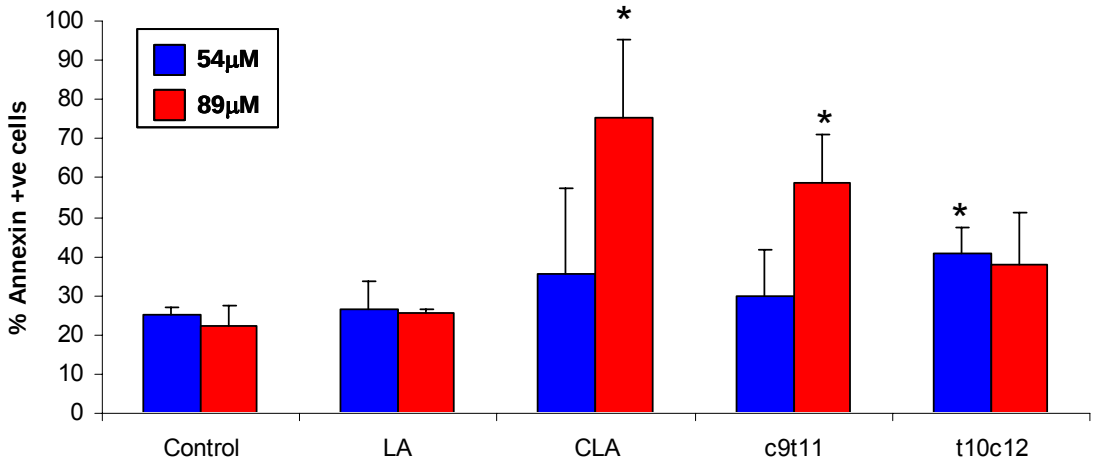

Figure 3.24 Apoptosis analysis of 4T1 cells following treatment for 3 days with 54 µM and 89 µM fatty acids. Graph indicates percentage of annexin positive cells, including both early and late apoptotic cells. Treatment with 54 µM *t*10,*c*12-CLA, 89 µM CLA and 89 µM *c*9,*t*11-CLA caused significant increases in annexin positive cells. *$p<0.05$, Student's t-test.

3.2.6 Effect of CLA and individual isomers on migration of the 4T1 cell line

To determine the effect of LA, CLA, *c*9,*t*11-CLA and *t*10,*c*12-CLA on the migratory capabilities of 4T1 cells, *in vitro* migration assays were conducted and analysed as per section 2.2.5. Results are from duplicate experiments, completed in triplicate. Cells were initially pre-treated in 25 cm^2 cell culture flasks with 18 μM of the fatty acids for 48 hours. The cells were then trypsinised and seeded into Falcon™ cell culture inserts, with treatment added, incubated for 24 hours and the level of migration quantified. This concentration of fatty acid was chosen to ensure minimal toxicity for all fatty acids (≤ 10% cell death) in order to determine effects that were due to changes in migratory or invasive ability rather than being due to cell death.

The results for migration assays are outlined in Figure 3.25. Whole stained membranes are presented in Figure 3.26 and magnified at 200X under the microscope in Figure 3.27. Treatment with LA and CLA had little effect on the level of migration of the 4T1 cell line in comparison to the control. The *c*9,*t*11-CLA and the *t*10,*c*12-CLA isomers caused an increase and decrease in migration of the 4T1 cells respectively. The result following treatment with *t*10,*c*12-CLA was statistically significant in comparison to the control ($p<0.05$).

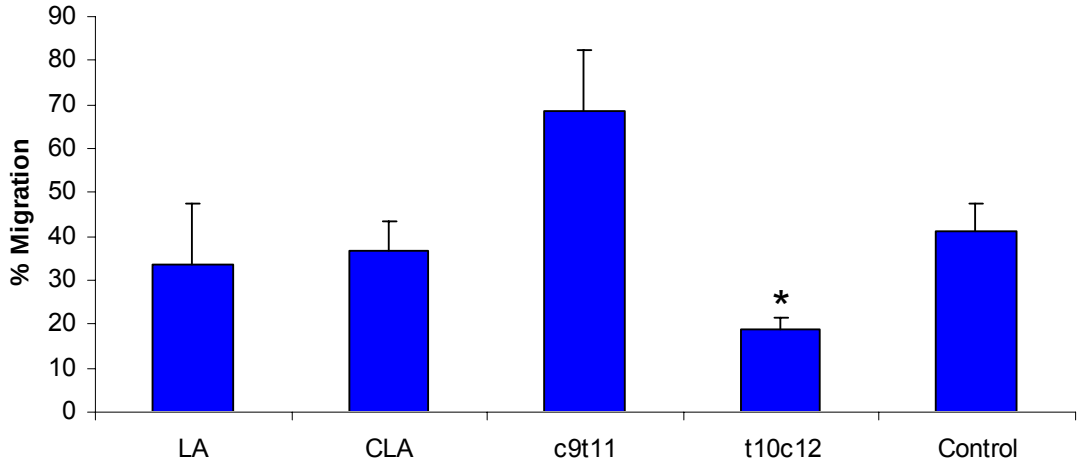

Figure 3.25 Effect of treatment with 18 μM LA, CLA, *c*9,*t*11-CLA and *t*10,*c*12-CLA for 3 days on migration of the 4T1 cell line. The *t*10,*c*12-CLA isomer caused a significant decrease in the migration of the 4T1 cells. *$p<0.05$, Student's t-test.

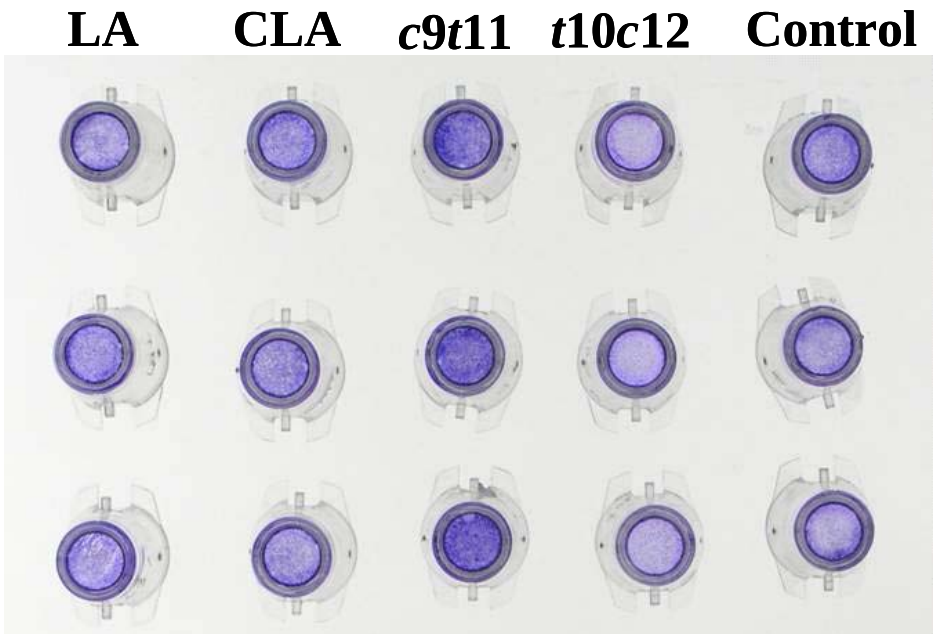

Figure 3.26 Falcon™ cell culture inserts following fixing and staining of the membrane with crystal violet. Chambers containing the *t*10,*c*12-CLA-treated cells had less stain.

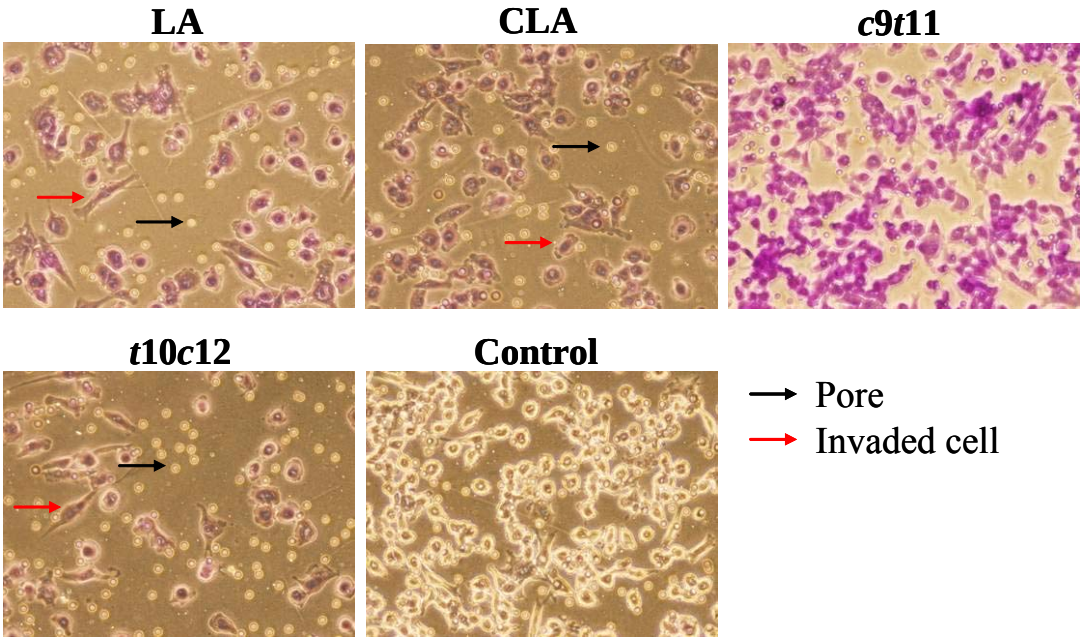

Figure 3.27 Falcon™ cell culture inserts following fixing and staining of the membrane with crystal violet. A decrease in the number of migrated cells following treatment with *t*10,*c*12-CLA was clearly seen. 200X magnification of membranes.

3.2.7 Effect of CLA and individual isomers on invasion of the 4T1 cell line

Invasion assays were set up in the same manner as migration assays. Unlike the Falcon™ cell culture inserts, the BD BioCoat™ Matrigel™ Invasion Chambers contained a layer of Matrigel on the top of the membrane, which must be degraded by the cells before they can move through the pores. Results are from duplicate experiments, completed in triplicate. The results for invasion assays are outlined in Figure 3.28. Whole stained membranes are presented in Figure 3.29 and magnified at 200X under the microscope in Figure 3.30. Treatment with LA and *t*10,*c*12-CLA caused a decrease in invasion of the 4T1 cells, while CLA and *c*9,*t*11-CLA treatment resulted in an increase in the invasion of the cells. However, these results were not statistically significant due to large standard deviations.

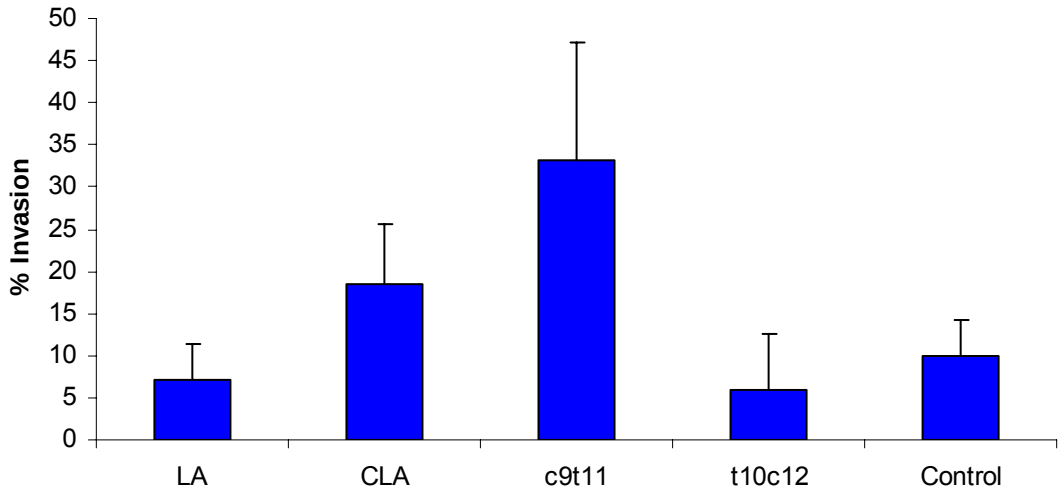

Figure 3.28 Effect of treatment with 18 μM LA, CLA, *c*9,*t*11-CLA and *t*10,*c*12-CLA for 3 days on invasion of the 4T1 cell line. The *c*9,*t*11-CLA isomer caused an increase in the invasion of the 4T1 cells.

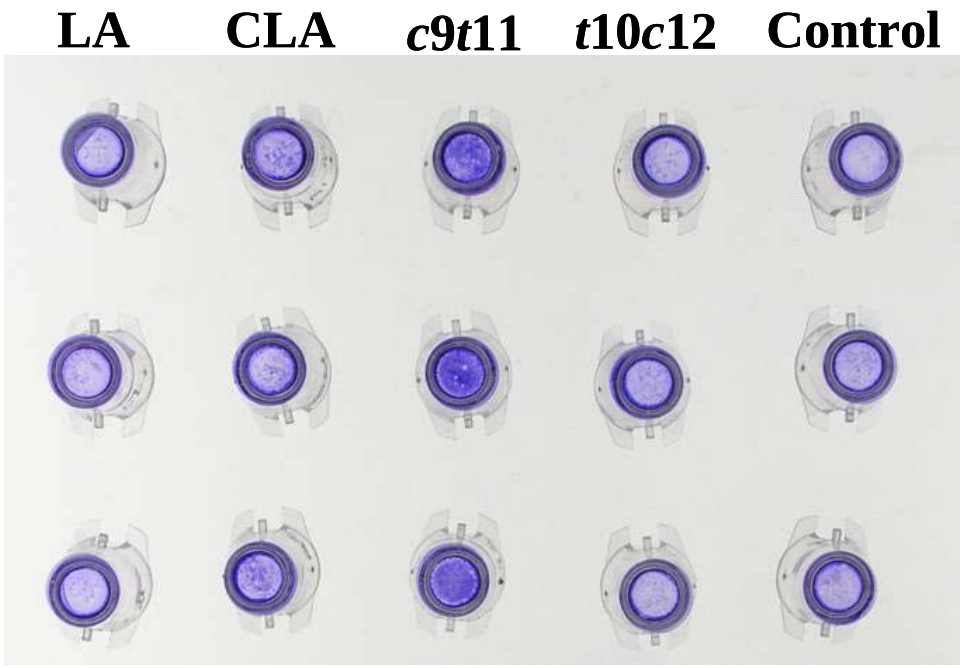

Figure 3.29 BD BioCoat™ Matrigel™ Invasion Chambers following fixing and staining of the membrane with crystal violet. Darker staining of the chambers containing *c*9,*t*11-CLA treated cells were evident.

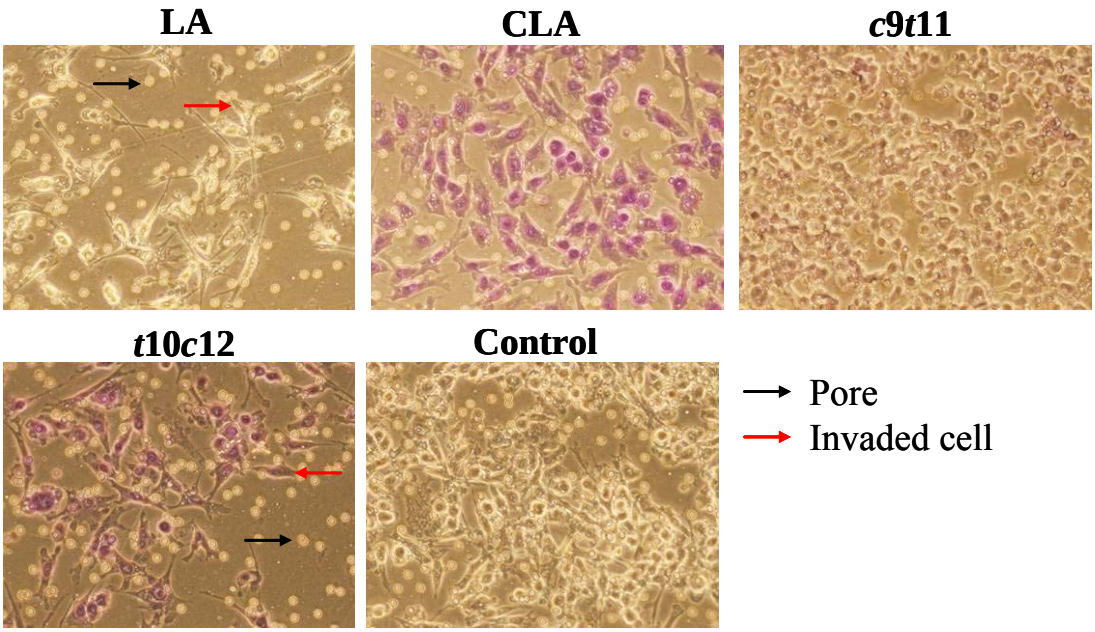

Figure 3.30 BD BioCoat™ Matrigel™ Invasion Chambers following fixing and staining of the membrane with crystal violet. An increase in the number of invasive cells treated with *c*9,*t*11-CLA was clearly seen. 200X magnification of membranes.

3.2.8 Effect of CLA and individual isomers on adhesion of the 4T1 cell line

Cell adhesion involving numerous cell adhesion molecules play an important role in invasion and metastasis (Hanahan and Weinberg, 2000). Cells must be able to attach to and move through the ECM for intravasation and extravasation. Loss of cell adhesion molecules like the cadherins and integrins can contribute to movement of the cells in this crucial step in metastasis (Cavallaro and Christofori, 2004). Cell adhesion was examined following treatment with the fatty acids as outlined in section 2.2.6. Cells were pre-treated with 18 μM fatty acid for 3 days before being seeded into a 96-well plate and incubated at 37°C, 5% CO_2 for 100 minutes. Non-adhered cells were then removed from the plate and the adhered cells quantified using the MTS assay. Figure 3.31 shows the results from the adhesion assay. CLA treatment caused a decrease in adhesion of the 4T1 cells. Treatment with the *c*9,*t*11-CLA and the *t*10,*c*12-CLA isomers resulted in an increase in adhesive cells in comparison to the control. However, these results were not statistically significant.

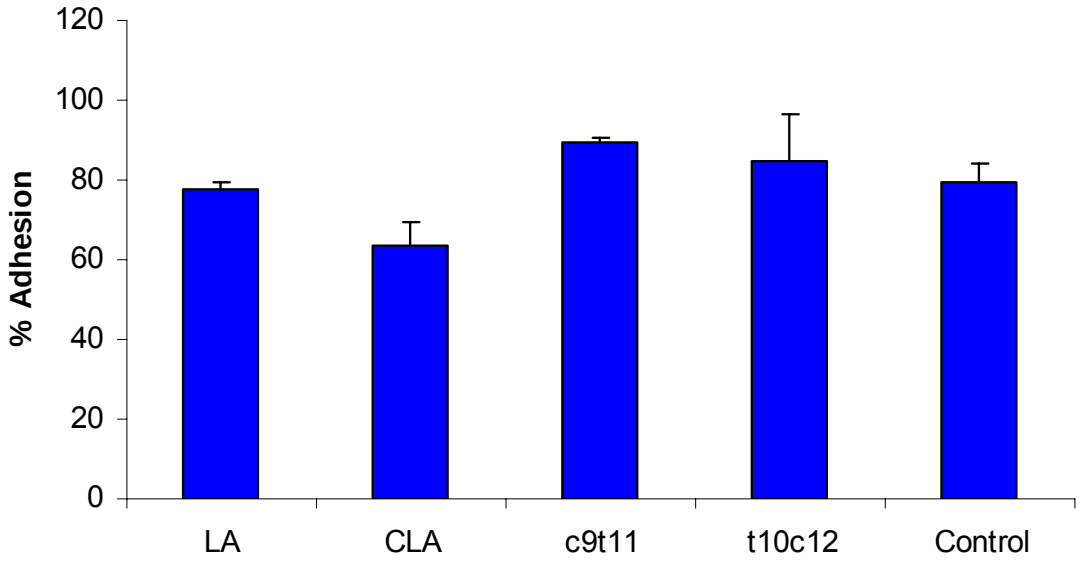

Figure 3.31 Effect of treatment with 18 μM LA, CLA, *c*9,*t*11-CLA and *t*10,*c*12-CLA for 3 days on adhesion of 4T1 cells. Percentage adhesion is in relation to the control plate, in which non-adhered cells were not removed from the wells. No significant effect on adhesion of the cells was observed after incubation for 100 minutes.

3.2.9 Effect of CLA and individual isomers on colony formation of the 4T1 cell line in soft agar

The anchorage-independent growth of cells in soft agar is generally regarded as an indication of tumourigenicity and can be used to assess the efficacy of anticancer compounds. A compound is considered efficacious if treatment results in a reduction in the number of colonies to below 30% of that in the control sample (Fiebig *et al*., 2004). Colony-forming efficiency has also been shown to be associated with experimental metastatic potential (Price *et al*., 1986). This technique involved seeding cells in semi-solid medium containing agar and assessing the formation of colonies in this environment. 4T1 cells pre-treated with 18 μM fatty acids for 3 days were seeded in the soft agar and incubated for 10 days. Live colonies were stained with *p*-iodonitrotetrazolium chloride solution and colonies with a diameter greater than 100 μm were counted. Results are representative of duplicate experiments, completed in triplicate. Figures 3.32 and 3.33 illustrate results from the soft agar assays. All treatments caused an increase in the number of colonies formed with a significant increase in colonies formed from cells pre-treated with CLA ($p<0.01$), *c*9,*t*11-CLA ($p<0.01$) and *t*10,*c*12-CLA ($p<0.00005$).

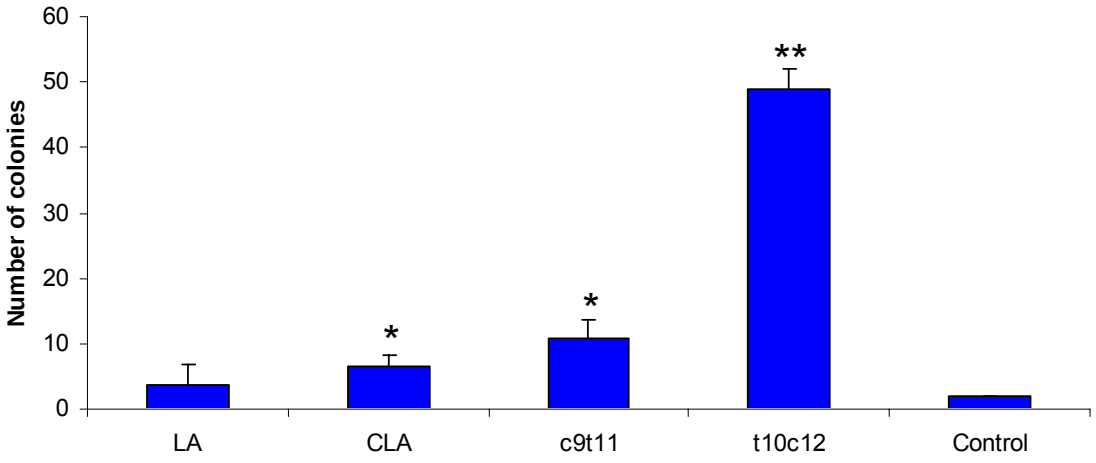

Figure 3.32 Effect of treatment with 18 μM LA, CLA, *c*9,*t*11-CLA and *t*10,*c*12-CLA for 3 days on 4T1 cell colony formation in soft agar assay. *$p<0.01$, **$p<0.00005$, Student's t-test.

The increase in colonies formed following treatment with CLA, *c*9,*t*11-CLA and *t*10,*c*12-CLA can be clearly observed in the images of the wells in Figure 3.33. The change in pH of the medium in the wells due to the growth of the colonies of cells pre-treated with *t*10,*c*12-CLA was dramatic.

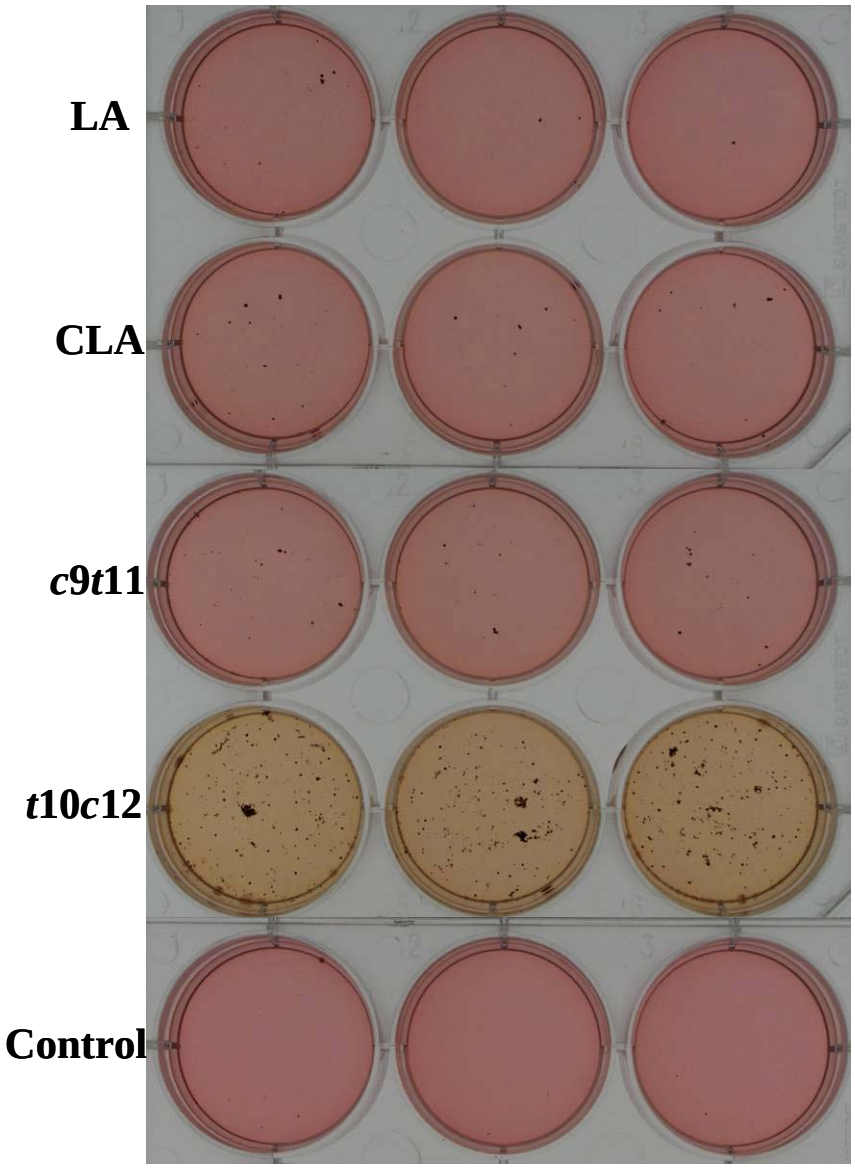

Figure 3.33 Effect of treatment with 18 μM LA, CLA, *c*9,*t*11-CLA and *t*10,*c*12-CLA for 3 days on 4T1 cell colony formation in soft agar assay. An increase in the number of colonies formed following treatment with the *t*10,*c*12-CLA isomer is clear.

3.2.10 Effect of CLA and individual isomers on levels of MMP-2 and MMP-9 mRNA

In order to investigate further the possible effect of the fatty acids on invasion and metastasis, the expression of MMP-2 and MMP-9 was examined. The 4T1 cell line was treated with 18 μM LA, CLA, *c*9,*t*11-CLA or *t*10,*c*12-CLA for 3 days. RNA was extracted from the treated cells as outlined in sections 2.2.8 and 2.2.9.1, quantified and separated on a 1.2% agarose gel as described in section 2.2.9.2. Figure 3.34 shows a picture of the agarose gel used to confirm the integrity of the RNA. The 18S and 28S sub-units could be seen clearly in all samples.

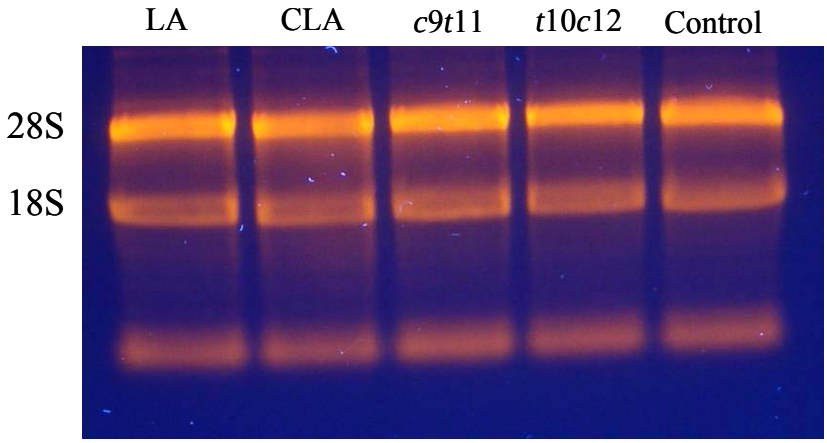

Figure 3.34 1 μg RNA from 4T1 cells treated with LA, CLA, *c*9,*t*11-CLA and *t*10,*c*12-CLA separated on a 1.2% agarose gel. The presence of the 28S and 18S sub-units was indicative of RNA integrity.

The RNA was used as a template to produce cDNA by reverse transcription as per section 2.2.9.3. The cDNA was then used to amplify sections of the actin, MMP-2 and MMP-9 genes as described in section 2.2.9.4. Figure 3.35 shows the actin PCR products. These products were used to normalise data from the densitometry of the following RT-PCR experiments. Figure 3.36 shows PCR products and densitometry analysis for MMP-2 and MMP-9. In comparison to the control, all fatty acid-treatments resulted in a decrease in the level of MMP-2 mRNA. Treatment with LA, CLA and *t*10,*c*12-CLA resulted in an increase in the levels of MMP-9 mRNA, while *c*9,*t*11-CLA caused a decrease in expression of MMP-9 mRNA (Figure 3.36).

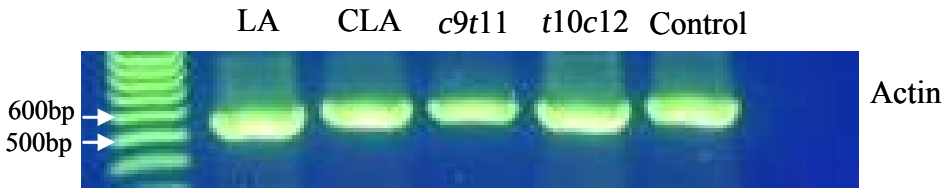

Figure 3.35 Actin RT-PCR of samples from the 4T1 cell line. The PCR product is visible at 554 bp. Densitometry values for MMP and TIMP RT-PCR were normalized to these RT-PCR products.

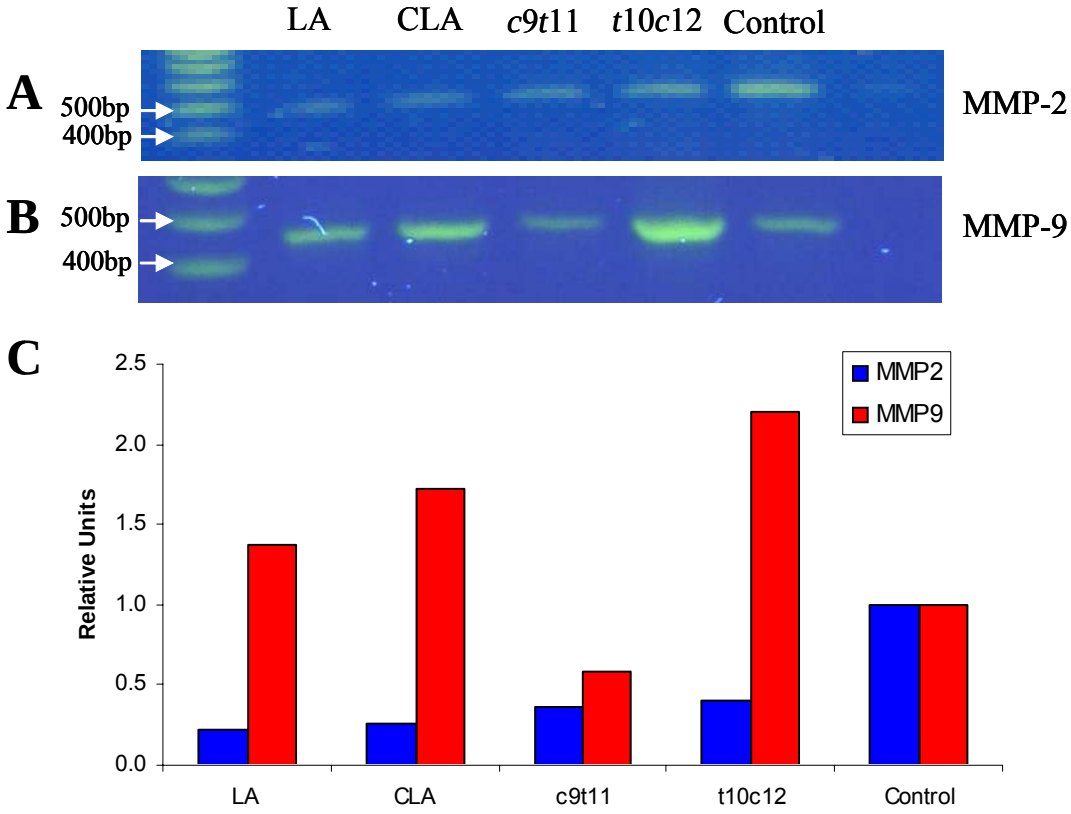

Figure 3.36 MMP-2 (A) and MMP-9 (B) RT-PCR and densitometry analysis (C) of samples from fatty acid-treated 4T1 cells. PCR products were separated on 1% agarose gels. PCR products were 475 bp and 467 bp for MMP-2 and MMP-9 respectively.

3.2.11 Effect of CLA and individual isomers on levels of MMP-9 protein in the 4T1 cell line

Following analysis of mRNA levels of MMP-2 and MMP-9 in the 4T1 cell line, protein levels were examined in conditioned medium collected from cells treated with 18 μM fatty acids for 3 days, as described in section 2.2.8. Centrifugal filter devices were used to eliminate proteins under 10 kDa to concentrate the protein samples. The total protein in the concentrated conditioned medium was quantified and an equal amount of protein was loaded for each sample and separated on a gelatin zymogram as outlined in sections 2.2.10.1 and 2.2.10.2. Gelatin zymography is a technique used to analyse gelatinase enzymes. Gelatin was incorporated into the SDS gel as a substrate for the gelatinases (MMP-2 and MMP-9). Proteins were separated on the gel, incubated to allow the enzymes to degrade the gelatin and then stained with Coomassie Blue. Upon de-staining, clear bands became visible against the blue background in the position of the gelatinases, where the gelatin had been degraded. Figure 3.37 shows a gelatin zymogram and densitometry analysis with conditioned medium samples from the 4T1 cell line, which contained 4.5 μg total protein. Mouse MMP-9 is 105 kDa in comparison to human MMP-9 at 92 kDa, as in the BHK control. MMP-9 protein levels in the 4T1 cell line were decreased following treatment with LA, and increased following treatment with CLA, *c*9,*t*11-CLA and *t*10,*c*12-CLA. No bands were observed for MMP-2 in these samples, which indicated no protein was produced or levels were so low that they were undetectable. A western blot was conducted with an antibody for MMP-9 but no bands were visible (data not shown). The antibody used was directed against human MMP-9 but the data sheet stated reactivity with mouse MMP-9 so this result was disappointing.

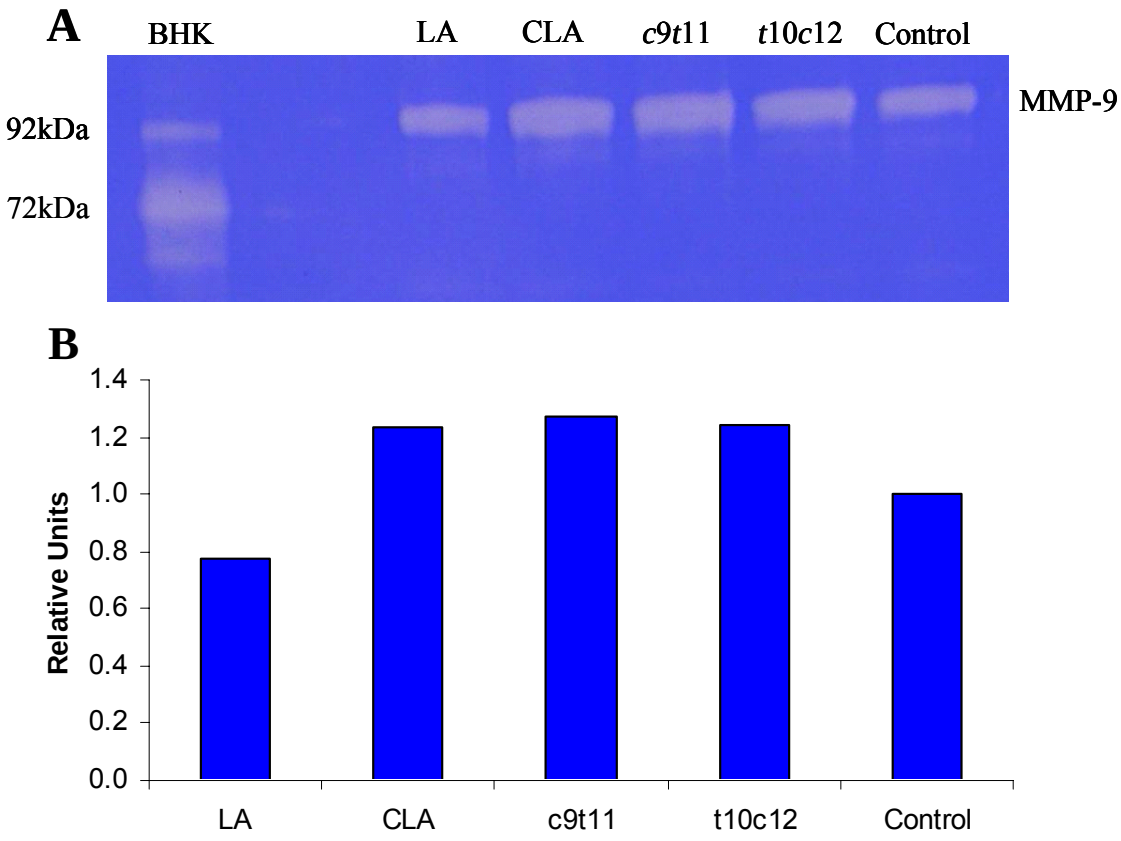

Figure 3.37 Gelatin zymography (A) and densitometry analysis (B) using concentrated conditioned medium samples from the 4T1 cell line. Conditioned medium from the BHK cell line was used as a control, as it constitutively expressed MMP-2 and was transfected with cDNA for human MMP-9. 4.5 μg total protein was loaded for the samples from the 4T1 cell line. Bands are visible at 105 kDa for murine MMP-9 in the 4T1 cell line but no MMP-2 is evident.

3.2.12 Effect of CLA and individual isomers on levels of MMP-2 protein in the Hs578T cell line

In order to investigate the effect on the levels of MMP-2 protein, conditioned medium samples from the Hs578T cell line were separated on a gelatin zymogram. Figure 3.38 shows the gelatin zymogram and densitometric analysis using samples from the Hs578T cell line, containing 5.34 μg total protein. A band for latent MMP-2 can be observed at 72 kDa, with a weak band at 66 kDa for the active form. MMP-2

protein levels in the Hs578T cell line were elevated in all fatty acid-treated cells in comparison to the control. Western blot analysis was conducted using the samples from the Hs578T cell line as outlined in section 2.2.10.4. Figure 3.39 shows the western blot and densitometric analysis using samples from the Hs578T cell line. Treatment of the Hs578T cell line with LA, CLA and the *c*9,*t*11-CLA isomer caused an increase in the protein level of MMP-2.

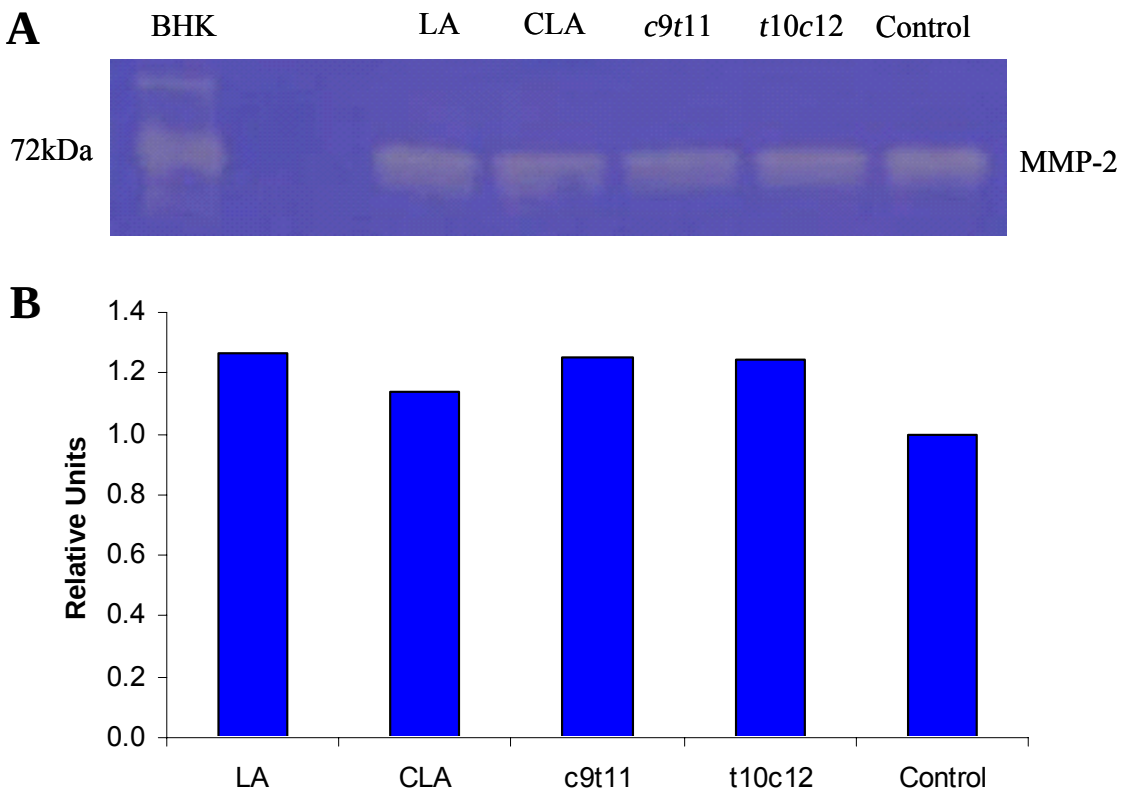

Figure 3.38 Gelatin zymography (A) and densitometry analysis (B) using concentrated conditioned medium samples from the Hs578T cell line. Conditioned medium from the BHK cell line was used as a control, as it constitutively expressed MMP-2 and was transfected with cDNA for human MMP-9. 5.34 µg total protein was loaded for samples from the Hs578T cell line. Bands were visible for latent and active MMP-2 at 66 kDa and 72 kDa respectively.

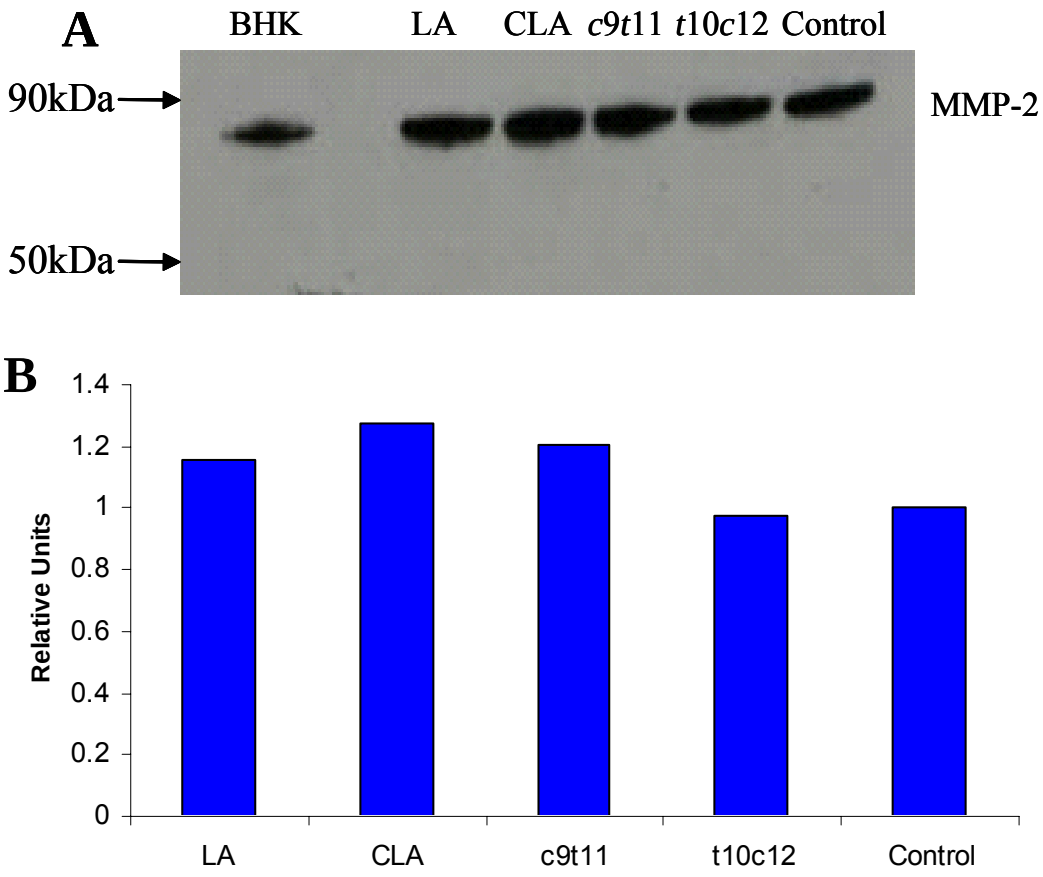

Figure 3.39 Western blot (A) and densitometry analysis (B) using conditioned medium samples from the Hs578T cell line. Conditioned medium from the BHK cell line was used as a control, as it constitutively expresses MMP-2 and is transfected with cDNA for human MMP-9. 5.34 µg total protein was loaded for samples from the Hs578T cell line. An increase in MMP-2 protein level was noted after treatment with LA, CLA and *c*9,*t*11-CLA in comparison to the control.

3.2.13 Effect of CLA and individual isomers on levels of TIMP-1 and TIMP-2 mRNA

TIMP mRNA levels were investigated by RT-PCR to determine any effect following treatment with the fatty acids. RT-PCR products and densitometry analysis are outlined in Figure 3.40. Bands were normalised to actin in Figure 3.35. All treatments resulted in a decrease in the levels of TIMP-1 mRNA, with the *t*10,*c*12-CLA isomer having the greatest effect. TIMP-2 mRNA levels decreased following treatment with LA and increased following CLA and *t*10,*c*12-CLA treatment.

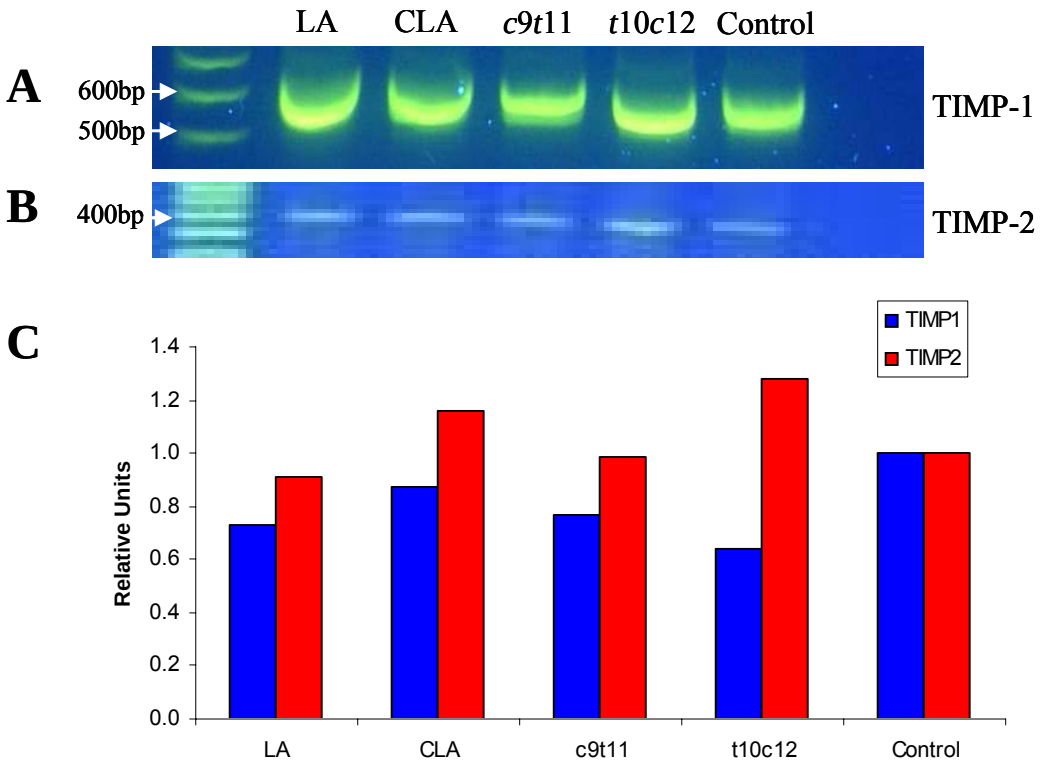

Figure 3.40 TIMP-1 RT-PCR (A), TIMP-2 RT-PCR (B) and densitometry analysis (C) of RNA extracted from fatty acid-treated 4T1 cells. PCR products were separated on 1% agarose gels. PCR products were 584 bp and 341 bp for TIMP-1 and TIMP-2 respectively.

3.2.14 Effect of CLA and individual isomers on levels of TIMP-1 and TIMP-2 protein

Reverse zymograms are used to detect TIMP proteins. They were prepared using a similar method to the gelatin zymogram, with the addition of BHK medium incorporated into the gel. Protein samples were separated on the gel, which was then incubated in substrate buffer and stained with Coomassie Blue. The BHK medium degraded the gelatin in the gel except in the region of the TIMPs, hence leaving blue bands against a white background. A reverse zymogram was used to analyse conditioned medium samples from the 4T1 cell line to determine the effect of the fatty acids on levels of TIMP-1 and TIMP-2 proteins. Unfortunately, no bands were evident in the samples from the 4T1 cell line despite a band visible for the TIMP-1 and TIMP-2 recombinant controls (data not shown).

3.3 Discussion

CLA and various isomers have been shown to have beneficial effects in relation to cancer, atherosclerosis, diabetes and obesity (Belury, 2002b). There is considerable interest in using CLA as a component in functional foods. Current levels of CLA intake in the UK are approximately 400-600 milligrams per day (Wahle *et al*., 2004). Sources with increased CLA content are desirable and the level of CLA in cow's milk can be manipulated by changes in the diet of the cows. Unsaturated fats, processed seeds, fish oils, marine algae and pasture feeding have all been shown to increase the level of CLA in milk fat (Bauman *et al*., 1999).

The aim of this chapter was to investigate the effect of a mixture of CLA isomers and the two individual isomers, *c*9,*t*11-CLA and *t*10,*c*12-CLA, on proliferation, cell cycle and apoptosis. In order to look at the modulation of metastasis, these fatty acids were investigated with regard to *in vitro* cell invasion, migration, adhesion and colony formation in soft agar. MMP and TIMP mRNA and protein levels were also analysed following treatment with the fatty acids. The CLA mixture of isomers contained *c*9,*t*11-CLA/*t*9,*c*11-CLA (~41%), *t*10,*c*12-CLA (~44%), *c*10,*c*12-CLA (~10%) and others (~5%). In order to carry out this assessment, the 4T1 cell line was chosen as it forms highly metastatic tumours in BALB/c mice. This cell line would facilitate future animal studies investigating the effect of CLA on tumourigenesis and metastasis. The Hs578T cell line was used to examine the effect of CLA in a human breast cancer cell line.

Assays for quantification of cell death were initially investigated and the Promega MTS system chosen for cytotoxicity assays (Figure 3.7). Cytotoxicity was analysed after treatment of cells for 1, 3 and 5 days. Standard curves were optimised to ensure cells were in the logarithmic growth phase for experiments (Figure 3.8 and Table 3.2). Concentrations of 18 μM (5 μg/ml) to 107 μM (30 μg/ml) were chosen for analysis. Concentrations of 10-70 μM are the physiological levels found in human serum, thus the range tested included current and elevated physiological levels (Tanmahasamut *et al*., 2004). After treatment of the 4T1 cell line for 1 day, toxicity was low except at the top concentration of CLA, at which nearly 100% cell death was exhibited (Figure 3.10). The toxicity of CLA in the 4T1 cell line was also evident after 3 and 5 days treatment (Figures 3.11 and 3.12). Despite the high toxicity of

CLA after treatment for 3 days with an IC_{50} value of 44 μM, the IC_{50} value after 5 days treatment increased to 58 μM. This did not completely reflect the toxicity of CLA over 5 days. With the exception of the toxicity level at 54 μM, the toxicity at all other concentrations mirrored that observed after 3 days treatment. The increase in the IC_{50} value was due to this dip in toxicity at 54 μM. The similarity between the toxicity of CLA after 3 and 5 days treatment was consistent with results noted in animal studies showing no increase in protection against development of mammary tumours above a certain dietary level of CLA (1%). This would indicate a threshold in the anti-cancer activity of CLA, possibly due to a limit in the metabolism of CLA into the active products (Ip *et al*., 2001 and Ip *et al*., 1996).

The *c*9,*t*11-CLA and *t*10,*c*12-CLA isomers also caused toxicity over 3 and 5 days. The *c*9,*t*11-CLA isomer had IC_{50} values of 82 μM and 78 μM over these two time points respectively (Figures 3.11, 3.12 and Table 3.3). The *t*10,*c*12-CLA isomer was less toxic than *c*9,*t*11-CLA after 3 days treatment, with an IC_{50} value of 98 μM (Figure 3.11 and Table 3.3). However, over 5 days, *t*10,*c*12-CLA was more toxic than *c*9,*t*11-CLA, with an IC_{50} of 62 μM (Figure 3.12 and Table 3.3). Again, there may be a limit to the effect of *c*9,*t*11-CLA, with no increase in toxicity observed over the extended incubation period. In experiments with the 4T1 cell line, there was no increase in cell growth following treatment with LA. Cytotoxicity was noted only at the top concentration of 107 μM after 5 days treatment, with an IC_{50} value of 100 μM established (Figure 3.12 and Table 3.3).

In the Hs578T cell line, cytotoxicity was low after treatment for 1 day and 3 days (Figures 3.13 and 3.14). IC_{50} values were not established over these time points for any treatment. After 5 days treatment, CLA caused the highest toxicity levels with an IC_{50} value of 58 μM (Figure 3.15 and Table 3.4). The *c*9,*t*11-CLA and *t*10,*c*12-CLA isomers exhibited toxicity at the highest concentration, with IC_{50} values established at 104 μM and 98 μM respectively. Treatment with LA resulted in low toxicity even at the highest concentration of 107 μM after 5 days treatment. LA caused an increase in cell growth after treatment with 71 μM for 1 day and 54 μM, 71 μM and 89 μM for 3 days (Figures 3.13 and 3.14). This correlates with published reports of increased growth up to a certain concentration, with cell death occurring at higher concentrations (Reyes *et al*., 2004).

While CLA had the same IC_{50} value in the 4T1 and Hs578T cell lines after treatment for 5 days, in general, the Hs578T cell line was more resistant to cell death than the 4T1 cells. CLA was consistently more toxic to the 4T1 and Hs578T cell lines than the individual isomers over the time ranges tested. The toxicity of *c*9,*t*11-CLA and *t*10,*c*12-CLA varied, with *c*9,*t*11-CLA more toxic than *t*10,*c*12-CLA in the 4T1 cell line after 3 days treatment, but *t*10,*c*12-CLA was more toxic after 5 days treatment in both cell lines. The toxicity exhibited by CLA would indicate a synergistic effect of the isomers in the mix. As this mixture contained 41% *c*9,*t*11-CLA/*t*9,*c*11-CLA, without specifying the amount of each, it would be interesting to investigate the toxicity of *t*9,*c*11-CLA in the future, to determine its contribution to the cytotoxicity.

Extensive studies have been conducted on the effect of CLA in the two breast cancer cell lines, MCF-7 and MDA-MB-231. Majumder *et al*. (2002) found CLA to be more effective than the individual isomers at inhibiting proliferation of the MCF-7 and MDA-MB-231 cell lines, supporting the results presented here, although the authors did not specify the concentrations tested. Maggiora *et al*. (2004) saw no effect on MCF-7 and MDA-MB-231 cell proliferation after 24 hours treatment with 5 μM, 50 μM or 200 μM CLA or LA. A decrease was observed in cell numbers of both cell lines after treatment with 50 μM and 200 μM CLA for 48 hours in comparison to the control. After 72 hours treatment, LA had no effect on cell growth in the MCF-7 cell line, but caused a slight decrease in cell growth in the MDA-MB-231 cell line. CLA treatment at all three concentrations caused a decrease in cell growth after 72 hours in the MCF-7 cell line but had a lower inhibitory effect in the MDA-MB-231 cell line. After incubation for 72 hours with CLA, the 50 μM treatment was more effective at inhibiting cell proliferation than the 200 μM treatment, indicating a limit in toxicity as observed with the results presented here.

Using the same cell lines, MCF-7 and MDA-MB-231, Tanmahasamut *et al*. (2004) examined the effects of CLA over a concentration range of 25 – 200 μM for 48 hours. This group reported 80% inhibition of MCF-7 cell growth after treatment with 200 μM CLA for 48 hours, in comparison to the results from Maggiora *et al*. (2004), with less than 33% inhibition over the same time period. Cell death was not reported in the MDA-MB-231 cell line after treatment with 200 μM CLA for 72 hours (Tanmahasamut *et al*., 2004). The individual isomers, *c*9,*t*11-CLA and

*t*10,*c*12-CLA, were also tested over 48 hours in the MCF-7 cell line. At 100 μM and 200 μM, *t*10,*c*12-CLA exhibited the highest inhibition of cell growth in comparison to CLA and *c*9,*t*11-CLA. The *c*9,*t*11-CLA isomer had no effect on the growth of the MDA-MB-231 cell line after treatment for 48 hours, while the *t*10,*c*12-CLA isomer was not tested in this cell line.

Treatment with 10 μM *c*9,*t*11-CLA isomer demonstrated the strongest inhibitory effect on growth of the MCF-7 cell line in comparison to the *t*10,*c*12-CLA isomer and CLA, after 2, 3 and 4 days (Chujo *et al*., 2003). Miller *et al*. (2003) investigated the effect of CLA from milk fat and synthetic *c*9,*t*11-CLA in the MCF-7 cell line. Milk fat containing 80.6 μM CLA inhibited growth of the MCF-7 cell line by 61%, while the synthetic *c*9,*t*11-CLA caused growth inhibition of 49%. Thus CLA and the individual isomers have caused varying toxicity to cells depending on time of incubation, concentration and cell line. In general, the MDA-MB-231 cell line was less sensitive to treatment; a fact partially explained by the negative ER status of these cells (Tanmahasamut *et al*., 2004). Both the 4T1 and Hs578T cell lines are ER negative (Banka *et al*., 2006 and ATCC), which could account for the low level of toxicity noted in the Hs578T cell line. Toxicity in the 4T1 cell line was obviously effected through other mechanisms and so this was investigated further.

The effect of CLA and the individual isomers on cell cycle kinetics was examined in the 4T1 cell line. The Guava® PCA flow cytometry system was used for these experiments. This machine has been designed for high-throughput, benchtop use with the required assays pre-programmed into the system. The cell cycle is rigorously controlled by checkpoints throughout the process to ensure mutations cannot be passed on to daughter cells. The main checkpoints occur at the latter stages of the G1 phase, during S phase and late in the G2 phase, before mitosis occurs. The G1 checkpoint, called the restriction (R) point, halts cells moving into the S phase until all the necessary proteins are synthesised for DNA replication and the DNA is checked for damages. During DNA synthesis in the S phase, replication can be halted due to depletion of nucleotide pools or misincorporation of nucleotides. At the G2 checkpoint, the DNA is once again checked to ensure replication is complete and all damage has been repaired before the cell moves into the mitosis phase (Sampath and Plunkett, 2001).

Two concentrations, 54 μM and 89 μM, were chosen to assess perturbations in the cell cycle. In comparison to control-treated cells, all treatments at the lower concentration caused a G1 arrest, and a decrease in the S and G2 phase populations (Figures 3.17 and 3.18, Table 3.5). The greatest arrests in the G1 phase were noted following treatment with 54 μM LA and *c*9,*t*11-CLA, with populations increased to 74.4% and 71.7% respectively, in comparison to the control (37%). In the control, 39.7% of the cells were in the S phase. The *c*9,*t*11-CLA isomer had the greatest effect on this phase, reducing the population to 8.2%. LA, CLA and *t*10,*c*12-CLA caused a decrease in S phase population to 12.5%, 15.4% and 24.5% respectively. The *t*10,*c*12-CLA isomer had the greatest effect on the G2 population, reducing it to 10.2%, in comparison to the control (23.2%). The *c*9,*t*11-CLA isomer caused a small reduction in G2 phase population, to 20.1%, with LA and CLA decreasing the population to 13.2% and 17.1% respectively. In the cytotoxicity experiments, 54 μM CLA caused approximately 60% cell death, while the other treatments were not toxic to the 4T1 cells. Regardless of this, CLA did not have a dramatic effect on the cell cycle in comparison to the other fatty acids.

At the higher concentration of 89 μM, an increase was also observed in the G1 phase population (Figures 3.19 and 3.20, Table 3.6). LA caused the greatest increase, with the G1 population rising to 69% compared to 35.3% for the control. Treatment with CLA, *c*9,*t*11-CLA and *t*10,*c*12-CLA increased the G1 phase population to 57.8%, 65.3% and 64% respectively. The S and G2 phase populations decreased following all treatments at the higher concentration. The S phase population dropped from 45.4% for the control to 13.5%, 29.5%, 22.8% and 20.7% following treatment with LA, CLA, *c*9,*t*11-CLA and *t*10,*c*12-CLA respectively. The G2 phase population decreased to 17.5% and 15.3% following treatment with LA and *t*10,*c*12-CLA respectively, in comparison to the control (19.3%). CLA and *c*9,*t*11-CLA caused greater decreases in G2 phase populations to 12.7% and 11.9% respectively. In comparison to the effect at 54 μM, the arrest in G1 phase was not as pronounced and the S phase population was greater following treatment with 89 μM fatty acids. This could suggest increased apoptosis from the G1 phase population at the higher concentration.

Durgam and Fernandes (1997) also reported arrest of MCF-7 cells in the G1 phase following treatment with 35 μM CLA for 3 days. 71% of the cell population

was in the G1 phase as compared to 53% of the control cells. LA, however, did not cause an increase in the G1 phase population in their experiments. In contrast, in the MDA-MB-231 cell line, no effect was noted in cell cycle kinetics following treatment with 60 μM CLA for 24 or 48 hours (Miglietta *et al*., 2006a). After 72 hours treatment, a decrease was observed in the G1 phase population, with a corresponding increase in S phase population. Our results, along with this data, would indicate that the effects of CLA on cell cycle kinetics are dependent on cell line and concentration of treatment. However, research using non-breast cancer cell lines has also shown G1 phase arrest following CLA treatment. In the HT-29 colorectal cancer cell line, dose-dependent increases in the G1 phase population were noted with increasing concentration of CLA (18/36/71 μM) following treatment for 3 days (Lim *et al*., 2005). The S and G2 phase populations decreased accordingly. Cho *et al*. (2006) looked at the effect of the *t*10,*c*12-CLA isomer on the cell cycle kinetics of the HT-29 cell line. Treatment with just 4 μM *t*10,*c*12-CLA caused a G1 phase arrest and reduction in the percentage of cells in the S and G2 phases, although the authors did not specify the duration of treatment. Liu *et al*. (2002) also saw a G1 phase arrest in the gastric adenocarcinoma cell line SGC-7901 following treatment with a range of concentrations of *c*9,*t*11-CLA over 24 and 48 hours.

Analysis of the effect of the treatment with fatty acids on apoptosis in the 4T1 cell line was conducted using an annexin V/7-AAD assay. During early apoptosis, phosphatidylserine molecules on the inner surface of the cell membrane become translocated to the outer membrane where they can bind annexin V. At later stages of apoptosis and during necrosis, the membrane integrity is compromised and the 7-AAD stain can enter the cell. Treatment of the 4T1 cells with 54 μM LA, CLA and *c*9,*t*11-CLA did not cause any significant change in the levels of apoptotic cells (Figure 3.24). The treatment with 54 μM *t*10,*c*12-CLA caused a significant increase in apoptotic cells in comparison to the control. The results for LA and *c*9,*t*11-CLA correlated with the low cytotoxicity observed following this treatment (Figure 3.11). The level of apoptosis noted in the cells treated with CLA was lower than the cell death noted in the cytotoxicity assays under the same conditions.

Following treatment at the higher concentration of 89 μM, a significant increase in apoptotic cells was noted for CLA and the *c*9,*t*11-CLA isomer (Figure 3.24). CLA treatment resulted in an increase in apoptotic cells to approximately 75%,

which correlated with the cytotoxicity exhibited after the same treatment (Figure 3.11). The *c*9,*t*11-CLA isomer caused an increase in apoptotic cells to approximately 59%, which was similar to the cell death observed in the cytotoxicity assays. The apoptotic population of cells was not significantly increased following treatment with LA or *t*10,*c*12-CLA, correlating with the results from the cytotoxicity assays.

Analysis of apoptosis following treatment with CLA has been examined by Maggiora *et al*. (2004) in the MCF-7 and MDA-MB-231 cell line. This group reported an increase in apoptosis in the MCF-7 cell line following treatment with 50 μM and 200 μM CLA for 48 hours, but little increase in the MDA-MB-231 cell line. Levels of apoptotic cells were 25% at the higher concentration of 200 μM in the MCF-7 cell line. Majumder *et al*. (2002) reported induction of apoptosis in the MCF-7 cell line following treatment with 50 μM and 100 μM CLA for 24 hours. The effect in the MDA-MB-231 cell line was not as pronounced under the same conditions. The effect of individual isomers on apoptosis has not been looked at in breast cancer cell lines. The *c*9,*t*11-CLA isomer did not cause any induction of apoptosis in the HCT116 colorectal cancer cell line after treatment with 50 μM for 72 hours (Lee *et al*., 2006). On the other hand, treatment with the *t*10,*c*12-CLA isomer doubled the percentage of apoptotic cells. Cho *et al*. (2005) also saw a doubling in the apoptotic cell population following treatment of the HT-29 colorectal cancer cell line with 4 μM *t*10,*c*12-CLA. This group reported no induction of apoptosis following treatment with the *c*9,*t*11-CLA isomer. These results, and the data presented here, confirm that CLA induced apoptosis in a number of different cell lines. The results for the individual isomers presented here did not correlate with the literature and this would indicate that the effect may be species or cell line dependent.

Metastasis of tumour cells to secondary sites of the body plays a significant role in the prognosis of the disease. Numerous factors influence this action, including the ability of the tumour cell to migrate, to invade the ECM and also to grow and divide in a new organ (Bogenrieder and Herlyn, 2003). Migration of the 4T1 cell line following treatment with CLA and the individual isomers was investigated using the Falcon™ Cell Culture Inserts. Cells were pre-treated for 48 hours with 18 μM fatty acids, then seeded into the chamber and incubated for 24 hours with treatment added. The effects on migration of this cell line are illustrated in Figures 3.25, 3.26 and 3.27. LA and CLA treatment did not result in a change in the migratory ability of the 4T1

cells. The *c*9,*t*11-CLA isomer caused an increase in migration of the cells but due to large error bars this difference was not statistically significant. Treatment with the *t*10,*c*12-CLA isomer resulted in a statistically significant decrease in migration of the 4T1 cells ($p<0.05$). These results are illustrated in the images in Figures 3.26 and 3.27.

For invasion assays, cells were treated in the same manner and seeded into BD BioCoat™ Matrigel™ Invasion Chambers. Treatment of the cells with LA and *t*10,*c*12-CLA caused a decrease in invasion, while CLA and *c*9,*t*11-CLA treatment caused an increase but these results were not statistically significant due to large error bars (Figure 3.28). The considerable standard deviations are due to inter-assay variability despite a general consistency in the results trend. This has previously been noted in our laboratory with this assay and is probably due to variations in batches of Matrigel-coated membranes. The chambers and invaded cells can be seen in the images in Figures 3.29 and 3.30. The increase in invaded cells following treatment with *c*9,*t*11-CLA can be clearly seen in these pictures.

In the ADF human glioblastoma cell line, pre-treatment with 25 μM CLA caused a decrease in cell migration and invasion after incubation for 6 hours in the chambers (Cimini *et al*., 2005). Migration and invasion were reduced to approximately 40% and 20% of the control cells respectively. Chen *et al*. (2003) looked at migration and invasion of the human gastric carcinoma cell line SGC-7901 following treatment with the *c*9,*t*11-CLA isomer. The authors pre-treated the cells for 24 hours prior to seeding, and during the 4 hour incubation in the migration chambers, resulting in a dose-dependent decrease in migration of the cells. The highest concentration of 200 μM caused inhibition of cell migration by 16% in comparison to the control. Invasion results were similar, with a dose-dependent reduction of invading cells. At the highest concentration, cell invasion was inhibited by 53.7%.

Invasion of the human gastric cell line MKN28 and the human colon cancer cell line Colo320 was investigated following treatment with 0.5 nM and 1 nM CLA (Kunayasi *et al*., 2006). Both treatments caused a decrease in invasion of the cells, with 1 nM CLA reducing invasion to 2% and 8% of the controls in the MKN28 and Colo320 cell lines respectively. The authors did not specify the duration of treatment or incubation in the invasion chambers. A recent publication looked at the effects of

the individual isomers *c*9,*t*11-CLA and *t*10,*c*12-CLA on phorbol 12-myristate 13-acetate (PMA)-induced migration of the SW480 cell line (Soel *et al*., 2007). Treatment for the 16 hour incubation in the chambers with 1 μM, 2 μM and 4 μM of the *c*9,*t*11-CLA isomer, but not the *t*10,*c*12-CLA isomer, resulted in decreased migration of the cells. Thus, all published reports to date documented a decrease in migration and invasion following fatty acids treatment, correlating with the result presented here for the *t*10,*c*12-CLA isomer. Increases in migration following *c*9,*t*11-CLA treatment and in invasion following CLA and *c*9,*t*11-CLA treatments have not previously been reported but the results detailed here were not statistically significant.

Adhesion of cells plays a major role in invasion and metastasis (Hanahan and Weinberg, 2000). Loss of adhesion to the surrounding cells and the ECM allows invasion and migration into the blood or lymph system, which facilitates cells in the process of metastasis. Treatment of the 4T1 cell line with 18 μM fatty acids for 3 days caused a decrease in adhesion of CLA-treated cells and an increase in adhesion of cells pre-treated with *c*9,*t*11-CLA and *t*10,*c*12-CLA (Figure 3.31). However, these results were not statistically significant. Adhesion of the ADF human glioblastoma cell line was investigated following treatment with 25 μM for 48 hours (Cimini *et al*., 2005). The authors reported an increase in adhesion to plastic to approximately 200% of control cells. Adhesion to gelatin and Matrigel was also increased. In contrast, adhesion of the human gastric carcinoma cell line SGC-7901 to laminin, fibronectin and Matrigel decreased in a dose-dependent manner following treatment with a range of concentrations of *c*9,*t*11-CLA (Chen *et al*., 2003).

Soft agar assays were used to test the effect of CLA and individual isomers on anchorage-independent growth of the 4T1 cell line. Growth in soft agar is regarded as an indication of tumourigenicity and has been shown to be associated with experimental metastatic potential (Price *et al*., 1986). A significant stimulatory effect on colony formation was noted following treatment with the *t*10,*c*12-CLA isomer for 3 days ($P<0.00005$) (Figure 3.32). Significant increases were also observed after CLA and *c*9,*t*11-CLA treatment ($p<0.01$). Colonies can be seen in Figure 3.33, with the growth of colonies of cells pre-treated with *t*10,*c*12-CLA having an effect on the pH of the medium. A thorough search through published literature did not reveal any reports on the effect of CLA on soft agar colony formation to date. The effect of LA on soft agar colony formation was investigated in the MCF-7 cell line (Chamras *et*

al., 2002). LA, at concentrations of 1 μM, 10 μM and 100 μM, did not have any significant effect on colony growth. Cells were treated for the two week duration of the assay.

The overall effect of the *t*10,*c*12-CLA isomer was to reduce migration and invasion of the 4T1 cell line and increase colony formation in soft agar. The decreases in migration and invasion could suggest an effect on the role of adhesion molecules in this event. CLA has been shown to modulate the activation of PPARs. The effect of CLA on PPARγ has recently been reported to influence β-catenin and E-cadherin expression in the MCF-7 cell line (Bocca *et al*., 2007). An increase in both proteins was noted along with an increase in co-precipitation of the proteins, suggesting a role for CLA in stabilisation of the β-catenin:E-cadherin complex. This could explain the migration and invasion results reported here with *t*10,*c*12-CLA and the 4T1 cell line. An increase in cell-cell adhesion would decrease migration and invasion. Further investigation along these lines is needed to confirm the mechanism of the decreased migration and invasion. Although adhesion of pre-treated cells to plastic was not affected by the treatments, adhesion to Matrigel, fibronectin and laminin could be examined.

The stimulatory effect of *t*10,*c*12-CLA on colony formation in soft agar could be further assessed using varied concentrations to determine if the effect on colony growth is dose-dependent. Molecular interactions responsible for this result could be examined by analysing changes in the Ras/Raf/ERK protein kinase pathway, which is involved in cell proliferation. Modulation by CLA of expression of proteins in this pathway has been reported in the literature (Miglietta *et al*., 2006b and Miller *et al*., 2003).

With the decrease in migration and invasion of cells following treatment with the *t*10,*c*12-CLA isomer and the increase caused by *c*9,*t*11-CLA treatment, we decided to investigate the roles of MMPs and TIMPs in these results. MMPs play a major role in the process of metastasis and the combined activity of the whole family of enzymes can degrade the ECM (Lynch and Matrisian, 2002). Following treatment of the 4T1 cells with 18 μM fatty acids, mRNA was extracted and subjected to RT-PCR. Primers for MMP-2 and MMP-9 were used to examine the levels of these gelatinase enzymes in the 4T1 cells by RT-PCR. A decrease in MMP-2 was noted after all treatments with the fatty acids, although bands were faint even after 30 cycles

of PCR (Figure 3.36). In contrast, MMP-9 levels varied in response. Following treatment with LA, CLA and *t*10,*c*12-CLA there was an increase in the level of MMP-9 mRNA. *c*9,*t*11-CLA treatment however caused a decrease in MMP-9 mRNA levels (Figure 3.36).

Gelatin zymography was used to examine the level of MMP-2 and MMP-9 proteins secreted into the conditioned medium from the cells (Figure 3.37). Bands for murine MMP-9 were observed at 105 kDa. Densitometry showed increases in MMP-9 protein in the samples from CLA, *c*9,*t*11-CLA and *t*10,*c*12-CLA-treated cells in comparison to the control. Treatment with LA caused a decrease in the level of MMP-9 protein. The effect of CLA and *t*10,*c*12-CLA treatments on MMP-9 protein levels correlated with the effect observed on mRNA levels. The MMP-9 protein levels in cells treated with LA and *c*9,*t*11-CLA had opposing results to the mRNA findings. This could indicate post-transcriptional regulation influencing the levels of protein being produced. Western blotting was conducted to confirm the MMP-9 protein levels but no bands were visible (data not shown), probably due to low affinity of the antibody for the murine protein, despite indications otherwise from the manufacturer's data sheet.

No bands were observed for MMP-2 on a gelatin zymogram, indicating that protein levels were too low for detection. The MMP-2 RT-PCR bands present in Figure 3.36 were quite faint and thus low mRNA levels could account for the low protein levels. The Hs578T cell line had previously been shown to express MMP-2 (Hughes, 2006). In order to look at the effect of the fatty acids on MMP-2 protein levels, the Hs578T cell line was treated and conditioned medium collected. Gelatin zymography using these samples showed an increase in MMP-2 protein levels following all treatments, in comparison to the control (Figure 3.38). A western blot using an anti-MMP-2 antibody confirmed the increase in protein following treatment with LA, CLA and *c*9,*t*11-CLA however, no increase was noted following treatment with *t*10,*c*12-CLA (Figure 3.39). RNA levels were not investigated in this cell line.

The TIMP molecules help to modulate MMP activity by binding non-covalently to the active MMPs (Birkedal-Hansen *et al*., 1993). Thus, the effect of CLA and the individual isomers on TIMP mRNA and protein expression was investigated. RT-PCR analysis of TIMP-1 and TIMP-2 showed varied effects on the mRNA levels (Figure 3.40). TIMP-1 mRNA levels were decreased after all treatments, with the greatest reduction observed following treatment with *t*10,*c*12-

CLA. TIMP-2 mRNA levels were reduced following treatment with LA but increased following CLA and *t*10,*c*12-CLA treatment. The bands for TIMP-2 mRNA were weak, which would correlate with the MMP-2 result, as TIMP-2 plays a role in regulating MMP-2 (Birkedal-Hansen *et al*., 1993). Unfortunately, the reverse zymogram with conditioned medium from the treated cells was not sensitive enough to detect bands for the TIMP proteins.

Cimini *et al*. (2005) looked at the effect of 25 μM CLA on MMP-2 expression on the ADF human glioblastoma cell line. Treatment for 48 hours down-regulated MMP-2 protein expression. Modulation of both MMP-2 and MMP-9 protein levels in the SGC-7901 gastric carcinoma cell line by the *c*9,*t*11-CLA isomer were investigated by gelatin zymography (Chen *et al*., 2003). A dose-dependent reduction of MMP-9 protein was noted following treatment with 25 μM, 50 μM, 100 μM and 200 μM *c*9,*t*11-CLA for 24 hours. No effect was observed on MMP-2 protein levels in the same samples. The authors also investigated the effect of the *c*9,*t*11-CLA isomer on TIMP-1 and TIMP-2 mRNA levels by RT-PCR. A dose-dependent increase in TIMP-1 and TIMP-2 mRNA was noted following treatment with 25 μM, 50 μM, 100 μM and 200 μM *c*9,*t*11-CLA for 24 hours.

A recent publication examined the effects of *c*9,*t*11-CLA and *t*10,*c*12-CLA on phorbol 12-myristate 13-acetate (PMA)-induced expression of MMP-9 protein in the SW480 cell line (Soel *et al*., 2007). The *c*9,*t*11-CLA isomer caused a dose-dependent decrease in MMP-9 protein activity as assessed by gelatin zymography. The *t*10,*c*12-CLA isomer had no effect on the activity of MMP-9. However, the isomers did not have any effect on the MMP-9 protein levels as analysed by western blot. These results and the findings presented here suggest tissue-specific effects of CLA and the isomers on the levels of MMP-2 and MMP-9. In our results, the increase in MMP-9 protein following treatment with CLA, *c*9,*t*11-CLA and *t*10,*c*12-CLA correlated with the decrease in TIMP-1 mRNA levels, as the association of these two proteins regulates MMP-9 activity (Birkedal-Hansen *et al*., 1993). Unfortunately, the reverse zymogram could not confirm the reduced protein levels of TIMP-1. The invasion results following CLA treatment correlated with the increase in MMP-9 protein levels and the decrease in TIMP-1 mRNA levels.

3.4 Summary

The effect of CLA and the individual isomers, *c*9,*t*11-CLA and *t*10,*c*12-CLA, produced interesting but varied results with regards to cytotoxicity, cell cycle kinetics, apoptosis, migration, invasion, adhesion, colony formation in soft agar and MMP/TIMP levels. CLA was the most toxic to both the 4T1 murine mammary cancer cell line and the Hs578T human breast cancer cell line in comparison to the individual isomers. Analysis of cell cycle kinetics revealed a predominant G1 phase arrest in the 4T1 cells following treatments. Migration and invasion of the 4T1 cell line was increased after treatment with *c*9,*t*11-CLA and decreased after treatment with *t*10,*c*12-CLA ($p<0.05$). Adhesion assays did not show any significant changes after treatment with the fatty acids. The *t*10,*c*12-CLA isomer had a significant effect on colony formation of the 4T1 cells in soft agar, with a 25-fold increase in colonies formed in comparison to the control ($P<0.00005$). The *c*9,*t*11-CLA isomer and CLA also increased the number of colonies formed ($p<0.01$). MMP-2 mRNA levels were reduced in the 4T1 cell line following all treatments but MMP-2 protein expression was not observed using gelatin zymography. MMP-2 protein levels in the Hs578T cell line were increased following treatment with *c*9,*t*11-CLA and *t*10,*c*12-CLA. MMP-9 mRNA and protein levels were increased following treatment with CLA and *t*10,*c*12-CLA, which correlated with decreased TIMP-1 mRNA levels. Future work in this area would focus on the effect of the *t*10,*c*12-CLA isomer on migration, invasion, adhesion and colony growth in soft agar.

Chapter 4

Biological evaluation of a series of 5-Fluorouracil and 5-Fluorouridine derivatives in breast and colorectal cancer cell lines

4.1 Introduction

4.1.1 5-Fluorouracil: Metabolism and mechanisms of action

5-Fluorouracil (5-FU) is an anti-metabolite agent, first synthesised in 1957 by replacing hydrogen with fluorine at position 5 of the uracil molecule. It was designed following the discovery that rat hepatomas utilised uracil more rapidly than normal tissues (Longley *et al.*, 2003). 5-FU and its deoxynucleoside, 5-Fluorouridine (5-FUrd), are used extensively in the treatment of a wide range of solid tumours, including colorectal, breast and gastric cancers (Figure 4.1). Treatment with 5-FU alone has response rates of only 10-15%, while combination treatments with irinotecan and oxaliplatin increase response rates to 40-50% (Longley *et al.*, 2003 and Venook, 2005).

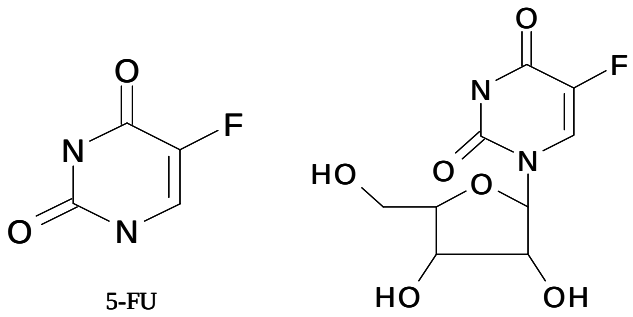

Figure 4.1 The structure of 5-FU and 5-FUrd.

Upon introduction into the body, there are two pathways which 5-FU can undertake (Figure 4.2). Approximately 80% of injected 5-FU follows the catabolic route, which involves degradation of 5-FU by the enzyme dihydropyrimidine dehydrogenase (DPD) into dihydrofluorouracil (DHFU), then α-fluoro-β-ureidopropionic acid and α-fluoro-β-alanine which are excreted from the body in the urine (Malet-Martino and Martino, 2002 and Heggie *et al.*, 1987). This primarily occurs in the liver but also in the plasma and gastrointestinal (GI) tract (Longley *et al.*, 2003). The remaining 5-FU is utilised by the anabolic route, which leads to three main mechanisms of action of toxicity; RNA misincorporation, thymidylate synthase (TS) inhibition and DNA misincorporation.

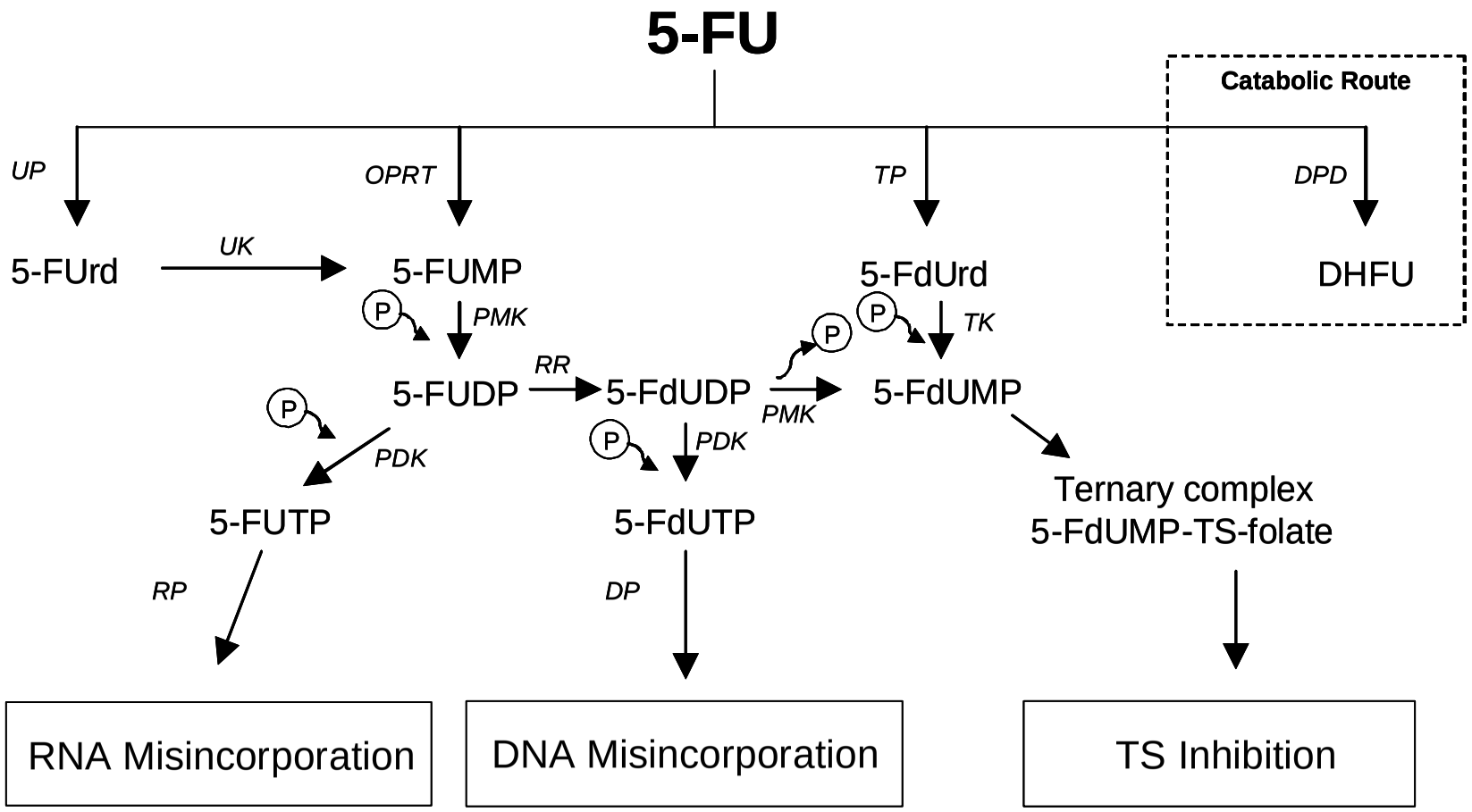

Figure 4.2 5-FU metabolism and mechanisms of action. Adapted from Longley *et al.*, 2003 and Malet-Martino and Martino, 2002.

Firstly, 5-FU can be converted to 5-FUrd by uridine phosphorylase (UP), followed by conversion to 5-Fluorouridine monophosphate (5-FUMP) by uridine kinase (UK) (Xiong and Ajani, 2004). 5-FUMP is also derived directly from 5-FU via the action of orotate phosphoribosyltransferase (OPRT). 5-FUMP can then be phosphorylated by pyrimidine monophosphate kinase (PMK) to 5-Fluorouridine diphosphate (5-FUDP), which is further phosphorylated to 5-Fluorouridine triphosphate (5-FUTP) by pyrimidine diphosphate kinase (PDK). 5-FUTP is partially responsible for the anti-cancer effect of 5-FU through RNA misincorporation. RNA polymerases (RP) insert 5-FUTP into all classes of RNA instead of uridine-5-triphosphate (UTP). Pre-ribosomal RNA (rRNA) processing to mature rRNA is inhibited, along with disruption of post-transcriptional modification of transfer RNAs (tRNAs). Complexes of small nuclear RNA (snRNA) and proteins are affected and lead to inhibition of splicing of pre-messenger RNA (mRNA) (Longley *et al*., 2003 and Malet-Martino and Martino, 2002).

Thymidine phosphorylase (TP) is involved in converting 5-FU into 5-Fluorodeoxyuridine (5-FdUrd) in the first step of the second mechanism of action, TS inhibition. Thymidine kinase (TK) phosphorylates 5-FdUrd giving 5-Fluorodeoxyuridine monophosphate (5-FdUMP). 5-FdUMP is the key molecule involved in the inhibition of TS which is the primary mode of action of 5-FU toxicity. The enzyme TS is usually involved in the conversion of deoxyuridine monophosphate (dUMP) to deoxythymidine monophosphate (dTMP), the precursor to deoxythymidine triphosphate (dTTP), which is incorporated into DNA during replication of the genome and during repair mechanisms. The reduced folate 5,10-methylenetetrahydrofolate (CH_2THF) acts as methyl donor, transferring a methyl group to the carbon 5 of dUMP to form dTMP. TS acts as a dimer, each subunit binding FdUMP and CH_2THF. The fluorine atom at position 5 of FdUMP is more tightly bound than the hydrogen of dUMP and so cannot be removed for replacement with the methyl group, thus forming a stable ternary complex of these molecules (Malet-Martino and Martino, 2002). This action sequesters TS in the cell and thereby prevents binding of dUMP, thus cutting off production of dTMP. This leads to disruption of DNA synthesis and repair, and subsequent cell death (Longley *et al*., 2003 and Malet-Martino and Martino, 2002). TS inhibition also results in dUMP accumulation in the cell, which leads to increased production of deoxyuridine triphosphate (dUTP). dUTP can be integrated into DNA in place of dTTP,

contributing to cell damage by the third mechanism of action of 5-FU, DNA misincorporation. This mechanism is also played out by the production of 5-Fluorodeoxyuridine triphosphate (5-FdUTP). By the action of enzymes ribonucleotide reductase (RR) and pyrimidine diphosphate kinase (PDK), 5-FUDP can be converted to 5-Fluorodeoxyuridine diphosphate (5-FdUDP) and then 5-FdUTP. Incorporation of uracil and 5-FdUTP into DNA causes DNA damage and cell death.

4.1.2 5-Fluorouracil resistance

Variations in expression of the numerous enzymes involved in the complex metabolism process play a major role in the efficacy of, and the resistance to, 5-FU treatment. DPD activity primarily determines the level of 5-FU that is rapidly eliminated from the body before the drug can exert any effect on the tumour cells. Variability in activity of this enzyme has been observed between patients and also between normal and tumour tissue in the one patient (Malet-Martino and Martino, 2002). High levels of DPD mRNA have been noted in various tumours and cell lines with low sensitivity to 5-FU (Kakimoto *et al*., 2005). Patients with low DPD levels can experience systemic toxicity following treatment with 5-FU while over-expression of DPD has been shown to correlate with resistance to the treatment (Longley *et al*., 2003).

TS activity and expression also has an effect on cellular sensitivity to 5-FU. The promoter of the *TS* gene is polymorphic, with variation in a 28 bp tandem repeat sequence. TSER*2 and TSER*3 promoters have 2 or 3 tandem repeats in the enhancer region respectively. *TS* promoters containing the TSER*3 sequence result in mRNA levels threefold higher than those with the TSER*2 sequence. Individuals who are homozygous for TSER*3 have been shown to be less likely to respond to 5-FU-based chemotherapy, due to the increased levels of TS (Relling and Dervieux, 2001 and Longley *et al*., 2003). TS expression is also induced following treatment with 5-FU due to a negative-feedback mechanism – free TS can bind to TS mRNA, preventing translation, thus when TS is sequestered into complexes with FdUMP, the mRNA is released to be translated, producing more TS protein (Longley *et al*., 2003). This is also a potential mechanism of resistance of cells to 5-FU.

Mutations or loss of the tumour suppressor p53 may also play a role in the development of resistance to 5-FU chemotherapy. The normal function of p53 is to induce apoptosis in cells with DNA damage. Following loss of function, these cells can avoid apoptosis and thus reduce the cellular sensitivity to 5-FU treatment (Longley *et al*., 2003). DNA MMR function similarly has an effect on response to 5-FU. Cells with low levels of MMR proteins are less sensitive to 5-FU due to lack of detection of the DNA damaging chemotherapeutic agent intended to initiate cell death (Jover *et al*., 2006).

4.1.3 Administration of 5-FU

5-FU, as a small molecule with a pK_A of 8.0, would be expected to have excellent absorption and bioavailability (Malet-Martino and Martino, 2002). However, it is rarely administered orally due to irregular absorption, possibly accounted for by the variation in levels of DPD in the GI tract. It is usually administered intravenously, either by continuous infusion (CI) or bolus infusion. The side effects or toxicities accompanying 5-FU chemotherapy vary between these two methods of administration. Patients under the bolus regimen usually experience myelosuppression, oral mucositis, diarrhoea, nausea and vomiting. These GI side-effects are a result of the conversion of 5-FU into 5-FUMP by OPRT in the GI tract. Hand-foot syndrome affects patients administered 5-FU under CI without the hematologic or GI toxicities (Malet-Martino and Martino, 2002). Prolonged exposure through CI results in TS-directed cell death while the RNA-mediated cell death is seen mainly following bolus administration of 5-FU (Xiong and Ajani, 2004, and Malet-Martino and Martino, 2002).

While remaining one of the most widely used chemotherapeutic agents, the lack of selectivity of 5-FU for tumour tissue, the short half-life in plasma (5-20 minutes), the low bioavailability due to DPD degradation and tumour cell resistance has led to numerous combination therapies and the introduction of 5-FU prodrugs in an attempt to overcome these short-comings (Malet-Martino and Martino, 2002).

4.1.4 Combination therapies of 5-FU

To improve the response rates to 5-FU, a number of combination therapies have been developed for patients. Leucovorin (5-formyltetrahydrofolate, LV) is the calcium salt of folinic acid and acts as an intracellular source of reduced folates, including CH_2THF, which is required for the formation and stabilisation of the TS-FdUMP-CH_2THF complex, thereby increasing the inhibition of TS (Longley *et al*., 2003 and Malet-Martino and Martino, 2002). Clinical trials combining 5-FU with LV showed an increase in overall response rate from 11% to 23% (Xiong and Ajani, 2004). 5-FU is now administered with LV as standard chemotherapy. Oxaliplatin is often combined with 5-FU/LV for treatment of colorectal cancer, a regimen termed FOLFOX. This drug is a platinum analog, which acts as a DNA-damaging agent (Xiong and Ajani, 2004). Irinotecan is a synthetic analogue of camptothecan and is converted to SN38, a topoisomerase inhibitor. Irinotecan treatment with 5-FU/LV is termed FOLFIRI. Irinotecan prevents the religation of DNA following cleavage by topoisomerase I by stabilising the complex formed by the enzyme and the DNA, resulting in apoptosis (Xiong and Ajani, 2004). The combination of 5-FU/LV with irinotecan and oxaliplatin has been termed FOLFOXIRI and has recently shown significant antitumour activity and allowed surgical resection of metastases in patients (Masi *et al*., 2006). Eniluracil (EU), administered in combination with 5-FU, is an irreversible inhibitor of DPD that binds to its active site, resulting in increased oral bioavailability and a prolonged half-life of 5-FU (Xiong and Ajani, 2004 and Lamont and Schilsky, 1999).

4.1.5 Prodrugs

A prodrug is a pharmacologically inactive drug, which is only modified at the tumour site to a pharmacologically active species (Denny, 2001). Prodrugs have been designed to enhance drug uptake or the pharmacokinetics. Tumour-activated prodrugs (TAP) have also recently been investigated. Prodrugs can be activated by conditions or enzymes within the cell (termed bioreductive prodrugs), by an enzyme delivered to the cell via antibody attachment (termed antibody directed enzyme prodrug therapy - ADEPT) or by an enzyme whose gene was delivered by gene therapy (termed gene directed enzyme prodrug therapy - GDEPT).

Bioreductive prodrugs can be activated by biological enzymes in the cell, with selectivity occurring due to the hypoxic conditions of tumours. In normal tissues, the reaction is incomplete or reversed due to the presence of oxygen while in the hypoxic tumour cells, the reaction is allowed to commence and the active drug is produced (Sinhababu and Thakker, 1996). ADEPT involves the delivery of a non-human enzyme to the tumour site by covalent linkage to a monoclonal antibody directed to tumour-specific antigens (Sinhababu and Thakker, 1996). GDEPT, or suicide gene therapy, delivers the gene encoding a non-human enzyme to the tumour cell where the enzyme is produced. Following targeting of the antibody-enzyme complex or the gene to the tumour cells in ADEPT and GDEPT, the prodrug is then administered to the patient. Activation of the prodrug will thus occur specifically at the tumour site (Denny, 2001).

Photodynamic therapy (PDT) is another method of activation of a prodrug. In traditional PDT, a photosensitiser is delivered to the tumour cell and, upon application of visible light, converts molecular oxygen to highly reactive oxygen species (ROS), causing cell death (Castano *et al*., 2006). Utilising this strategy with a prodrug attached to a photosensitiser would prolong the effect on the cells after exposure to the light therapy (Gray, 2005).

4.1.6 Objectives of Chapter 4

The aims and objectives of the work outlined in this chapter were to examine the biological activity of a panel of 5-FU and 5-FUrd derivatives, including five prodrugs. The compounds were synthesised and analysed as part of a structure-activity relationship (SAR) study to investigate the effect of varying components on these widely used chemotherapeutic agents. Firstly, the effect was investigated by testing the compounds in a murine mammary and a human colorectal cancer cell line to determine the levels of toxicity. The effect on proliferation of a 5-FU resistant colorectal cancer cell line was also investigated. Modulation of the cell cycle kinetics and apoptosis following treatment with the compounds was examined, to determine the molecular mechanisms involved. Assays were conducted to investigate the effects of the compounds on the migration, invasion and soft agar colony formation of the cells.

4.2 Results

5-FU and 5-FUrd derivatives were synthesised and their cytotoxicity was assessed for a range of concentrations over 3 and 5 days using the 4T1 murine mammary cancer cell line, the SW480 human colorectal cancer cell line and the HCT116 human colorectal cancer cell line. Cytotoxicity was expressed as percentage cell death in relation to cells treated with vehicle only. IC_{50} values were extrapolated from the toxicity profiles. The effect of the compounds on the cell cycle kinetics and apoptosis in the 4T1 cells was analysed using the Guava® Personal Cell Analysis (PCA) system. Invasion and migration of the 4T1 cells following treatment with the compounds was assessed. The ability of cells to form colonies in soft agar following treatment was also investigated.

4.2.1 Synthesis of 5-FU and 5-FUrd derivatives

Twelve derivatives of 5-FU and 5-FUrd were synthesised by Dr. Ian Gray and Dr. Kieran Nolan in the School of Chemical Sciences, Dublin City University (Lin *et al.*, 1986 and Gray, 2005) (Table 4.1). The compounds were analysed by nuclear magnetic resonance (NMR), and purity (>95%) confirmed. The lipophilicity value (ClogP) and size ($Å^3$) of each compound were calculated using Chem 3D Ultra 9.0 (Cambridge Software) and are listed in Table 4.1. The ClogP value gives an indication of the solubility of a compound in 1-octanol and water. If the compound is more soluble in water than 1-octanol, it will have a negative ClogP value, whereas if the reverse is the case, the ClogP value will be positive. The more negative the ClogP value, the more hydrophilic the compound and this may inhibit crossing of the cellular membranes. The more lipophilic compounds, with larger ClogP values, will interact more with the membranes and may not cross to the aqueous phase (Silverman, 1992). The size of the compounds are represented as $Å^3$.

Compounds 3-5 and 10-14 were derivatives of 5-FU while compounds 6-9 were derivatives of 5-FUrd (Table 4.1). There were 3 types of 5-FU derivatives: those with a nitro-benzyl side-chain, an ester side-chain or an acid derivative. The side-chains were linked to either the N^1 or N^3 position of 5-FU, or both (Figure 4.3). Compounds 3, 13 and 14 contained nitro-benzyl side-chains. The side-chain of

compounds 3 and 13 were joined to the N^3 of 5-FU. Compound 13 had a longer side-chain, with the nitro-benzyl part separated by a carbonate segment. Compounds 3 and 14 contained the same side-chain, the side-chain attached to both the N^1 and the N^3 positions in compound 14.

The ester group included compounds 4, 5, 10 and 11, of which, all except compound 10 contained a benzyl group. Compound 4 was a long chain methoxy ester while compound 5 was a short chain methoxy ester, both bound at the N^1 position of the 5-FU molecule. Compound 11 had the same short chain methoxy ester group as compound 5, but bound at both the N^1 and the N^3 position. Compound 10 was another short chain methoxy ester ending with a double bond between the final two carbons in the chain and without the benzyl group. Compound 12 was an acid derivative, with no benzyl group (Table 4.1).

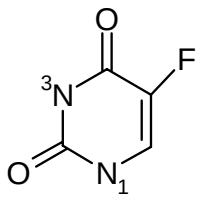

Figure 4.3 Structure of 5-Fluorouracil demonstrating positions of N^1 and N^3 where the side-chains were bound in the derivatives. (Gray, 2005)

The 5-FUrd derivatives contained nitro-benzyl side-chains and a taxol-derived side-chain. Compounds 6 and 9 had the same nitro-benzyl side-chain as the 5-FU derivatives, compounds 3 and 14. This nitro-benzyl group was at position N^3 of 5-FUrd with the sugar bound at the N^1 position. Compounds 7, 8 and 9 all had protected secondary hydroxyl groups C-2 and C-3 of the sugar. This eliminated any possibility of unwanted side reactions with these hydroxyls. Compound 7 contained a side chain which is a derivative of the side chain found in Taxol, (2R, 3S)-N-benzoyl-3-phenylisoserine.

Compounds 3, 6, 9, 13 and 14 were designed as prodrugs, pharmacologically inactive drugs which can be activated at the site of action. Removal of the nitro-benzyl side-chain releases the active 5-FU molecule.

Table 4.1 Names, molecular weights, lipophilicity values (ClogP), sizes ($Å^3$) and structures of 5-FU and 5-FUrd derivatives. (ND=Not determined)

Cmpd	Chemical Name	MW	ClogP	$Å^3$	Structure
1	5-Fluorouracil	130	-0.577	67.4	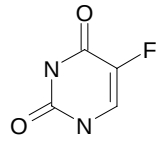
2	5-Fluorouridine	262	-1.74	185	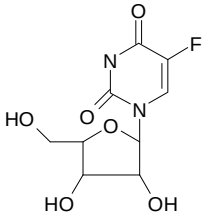
3	3-(p-nitrobenzyl)-5-Fluorouracil	265	1.62	159	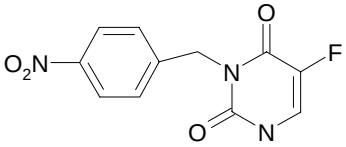
4	Hexanedioic Acid Benzylester-5-Fluorouracil Methyl ester	378	ND	ND	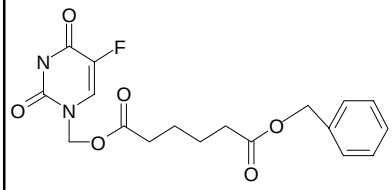
5	1-Benzyloxycarbonyl oxymethyl-5-Fluorouracil	294	0.984	190	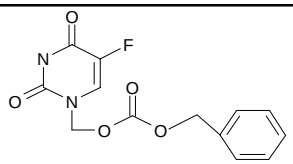
6	N3-(p-nitrobenzyl)-5-Fluorouridine	397	-1.15	283	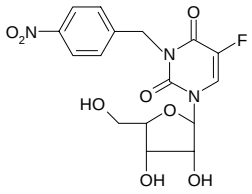
7	2',3'-isopropylidene-5'-O-((-4''S,5''R)-N-acetyl-2'',2''-dimethyl-4''-phenyl-1'',3''-oxazolidine-5''-carboxylate)-fluorouridine	547	ND	ND	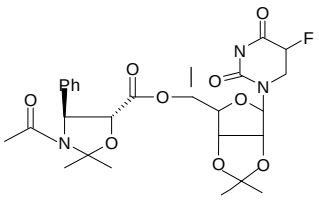

Table 4.1 (Continued) Names, molecular weights, lipophilicity values (ClogP), sizes ($Å^3$) and structures of 5-FU and 5-FUrd derivatives. (ND=Not determined)

Cmpd No.	Chemical Name	MW	ClogP	Å ^{3}	Structure
8	2,3-isopropylidene-5-Fluorouridine	301	-0.61	231	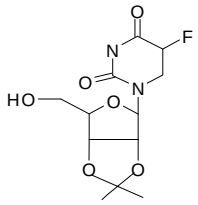
9	2,3-Isopropylidene-N3-(p-nitrobenzyl)-5-Fluorouridine	436	0.0287	ND	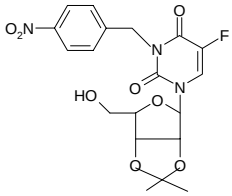
10	1-Alloxycarbonyloxy methyl-5-Fluorouracil	244	0.31	142	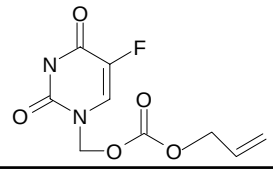
11	1,3-benzyloxycarbonyl oxymethyl-5-Fluorouracil	458	0.715	ND	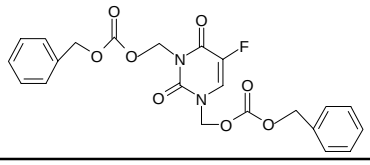
12	Acid derivative of 5-FU	204	-1.36	112	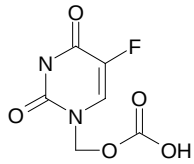
13	3-(p-nitrobenzyloxy carbonyl)-5-Fluorouracil	309	0.658	182	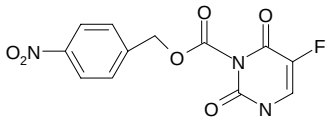
14	1,3-bis-(p-nitrobenzyl)-5-Fluorouracil	400	2.87	283	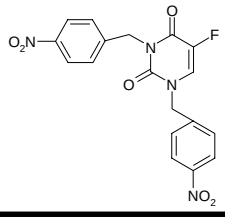

4.2.2 Cytotoxicity of 5-FU and 5-FUrd derivatives in the 4T1 murine mammary cancer cell line

Initial experiments were conducted in the 4T1 cell line. Results are from a minimum of duplicate experiments, completed in triplicate. Cytotoxicity assays were set up as described in Section 2.2.2. Cells were seeded in triplicate and allowed to attach overnight before treatment was added. Standard curves were set up for each assay to ensure cells were in the exponential phase of growth for the experiments. Cells for treatment were seeded at the second highest point on the standard curve. The x-axis of each cytotoxicity graph is on a logarithmic scale to show clearly the range of concentrations tested. Figure 4.4 shows the cytotoxicity results for 5-FU and the nitro-benzyl derivatives of 5-FU, compounds 3, 13 and 14, after treatment for 3 days. The parent compound 5-FU showed dose-dependent cytotoxicity and was the most toxic to the 4T1 cells, with an IC_{50} value of 0.35 μM (Table 4.2). Greater than 80% cell death was seen from 4 μM and higher. The toxicity profile of compound 3 mirrored that of 5-FU but was less toxic, with an IC_{50} value of 0.71 μM. Compound 13 showed toxicity from approximately 11 μM upwards. However, its IC_{50} value of 40 μM was two orders of magnitude higher than 5-FU (Table 4.2). Compound 14, on the other hand, showed low toxicity even up to 250 μM, the highest concentration tested.

The cytotoxicity of the ester derivatives of 5-FU are shown in Figure 4.5. Compound 10, with the short chain methoxy ester ending with a double bond, showed dose-dependent cytotoxicity, with a low IC_{50} value of 0.037 μM, an order of magnitude lower than the parent 5-FU (Table 4.2). Compound 11 showed increased toxicity in the 4T1 cells compared with 5-FU, with an IC_{50} value of 0.21 μM. Compounds 4 and 5 were also highly toxic, with IC_{50} values of 0.63 μM and 0.34 μM respectively. Figure 4.6 shows toxicity for compound 12, the acid derivative of 5-FU, which mirrored very closely the toxicity profile of the parent compound, with the same IC_{50} value of 0.35 μM.

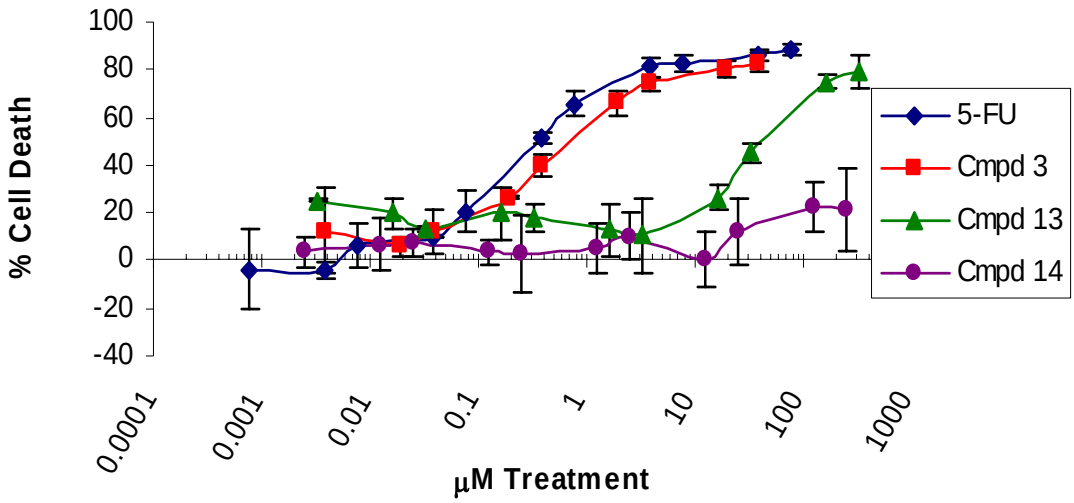

Figure 4.4 Cytotoxicity of the nitro-benzyl derivatives of 5-FU in the 4T1 cell line after treatment for 3 days. 5-FU showed the highest toxicity towards the cells with compound 3 marginally lower in toxicity. Compound 13 showed toxicity only from 4 µM upwards and low toxicity was seen for compound 14 up to the highest concentration tested, 250 µM.

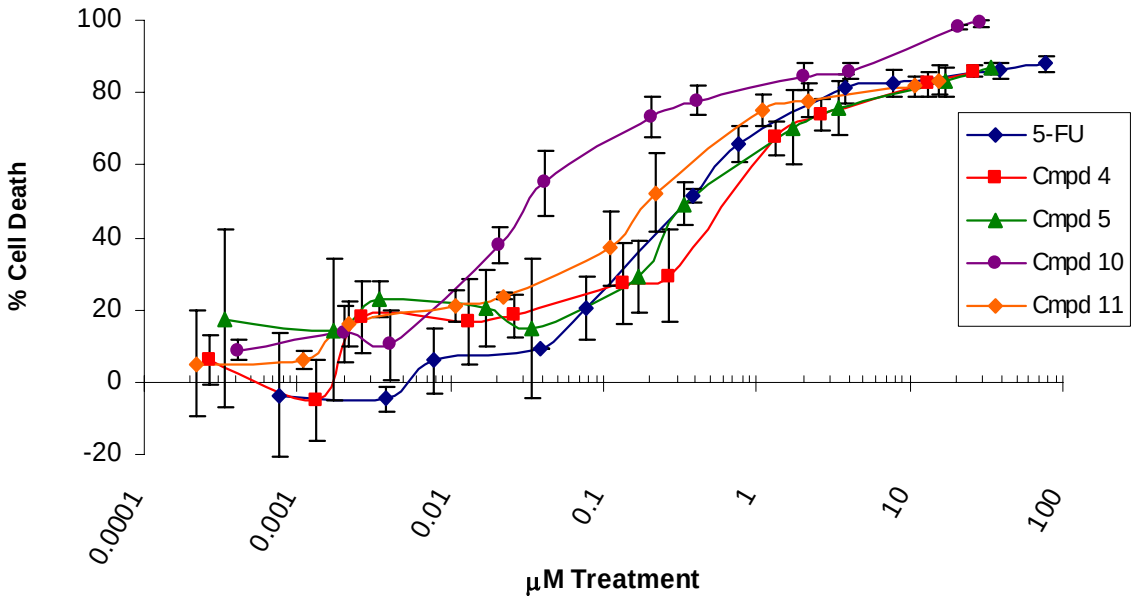

Figure 4.5 Cytotoxicity of the ester derivatives of 5-FU in the 4T1 cell line after treatment for 3 days. Compound 10 showed the highest toxicity towards the 4T1 cells. Compound 11 was also more toxic than 5-FU, with compounds 4 and 5 marginally less toxic.

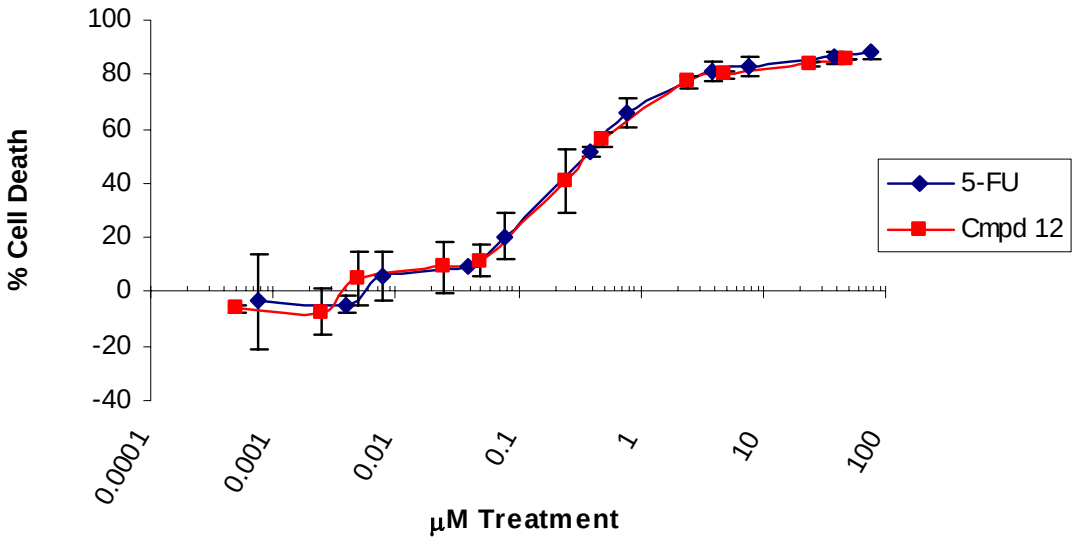

Figure 4.6 Cytotoxicity of the acid derivative of 5-FU in the 4T1 cell line after treatment for 3 days. The toxicity profile of compound 12 mirrored that of 5-FU very closely, showing considerable toxicity from 0.04 µM upwards.

The cytotoxicity results for the derivatives of the nucleoside, 5-FUrd, are shown in Figure 4.7. 5-FUrd was very toxic, with an IC_{50} value of 0.018 µM, revealing higher toxicity than 5-FU and also the 5-FU derivatives - compounds 10, 11 and 12. However, all of the 5-FUrd derivatives, compounds 6, 7, 8 and 9, showed low toxicity, and IC_{50} values were not established for these compounds at the range of concentrations tested.

Figure 4.8 shows the cytotoxicity profiles of 5-FU compounds 3 and 14 and 5-FUrd compounds 6 and 9, which all have the same nitro-benzyl side-chain. Despite the similar side-chain, the only compound which showed a significant level of cytotoxicity was compound 3, the 5-FU derivative with the nitro-benzyl side-chain attached at the N^3 position in the 5-FU molecule.

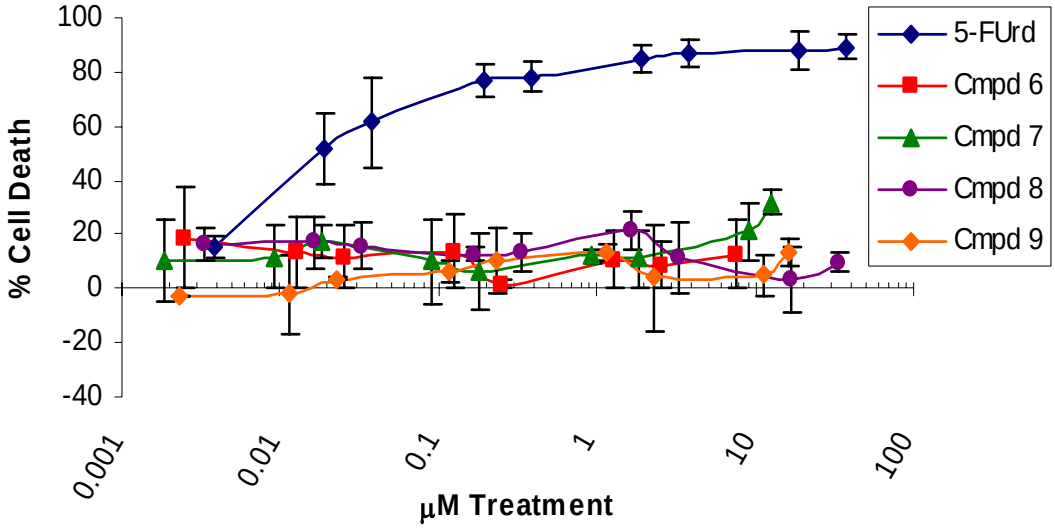

Figure 4.7 Cytotoxicity of the 5-FUrd derivatives in the 4T1 cell line after treatment for 3 days. 5-FUrd was toxic to the 4T1 cells from 0.004 µM upwards, compared to the derivatives, which showed low toxicity over the range of concentrations tested.

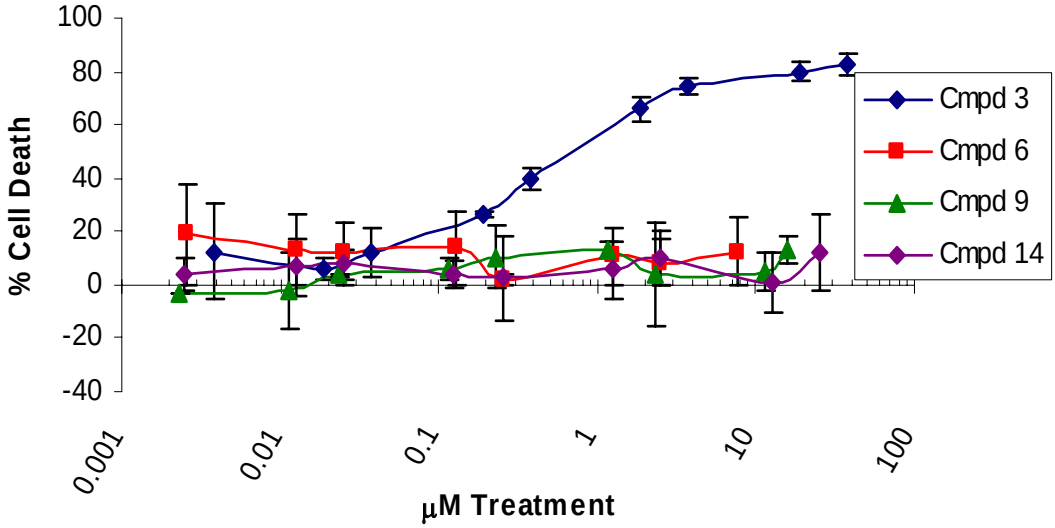

Figure 4.8 Cytotoxicity of the nitro-benzyl derivatives of 5-FU and 5-FUrd in the 4T1 cell line after treatment for 3 days. Despite having the same side-chain, compound 3 was the only derivative which showed toxicity in the 4T1 cells.

Cytotoxicity of the compounds was also tested in the 4T1 cell line over 5 days. For the sake of clarity, the individual graphs of cytotoxicity over 5 days are not shown but IC_{50} values were calculated and are listed in Table 4.2. The 5 day cytotoxicity analysis showed similar patterns, with 5-FU, compounds 3, 4, 5, 10, 11 and 12 all having low IC_{50} values. Compounds 4, 5 and 10 showed the most toxicity with IC_{50} values of 0.02 µM, 0.022 µM and 0.014 µM respectively, all approximately one order of magnitude lower than the parent 5-FU (IC_{50}: 0.17µM). Compounds 3 and 11 had similar toxicity to 5-FU, with IC_{50} values of 0.11 µM and 0.1 µM respectively, while compound 12 was less toxic with an IC_{50} value of 0.31 µM. 5-FU derivatives 13 and 14 showed low toxicity, with IC_{50} values two and three orders of magnitude higher than 5-FU respectively. The IC_{50} value for 5-FUrd was not established in the range tested, with greater than 50% cell death seen from the lowest concentration tested, 0.004 µM (Table 4.2). 5-FUrd derivatives 6, 7, 8 and 9 again showed low toxicity. IC_{50} values were not established for compounds 6, 8 and 9, over the range of concentrations tested. The IC_{50} value for compound 7 was established at 5.7 µM, considerably higher than the IC_{50} value for the parent 5-FUrd.

Table 4.2 IC_{50} values of the 5-FU and 5-FUrd derivatives in the 4T1 murine mammary cancer cell line after treatment for 3 and 5 days.

IC_{50} Values 4T1 Cell Line (µM)					
	3 Days	**5 Days**		**3 Days**	**5 Days**
5-FU	0.35±0.03	0.17±0.06	**5-FUrd**	0.018±0.004	<0.004[a]
Cmpd 3	0.71±0.22	0.11±0.13	**Cmpd 6**	>7.6[b]	>7.6[b]
Cmpd 4	0.63±0.16	0.02±0.009	**Cmpd 7**	>12.8[b]	5.7±4.7
Cmpd 5	0.34±0.1	0.022±0.006	**Cmpd 8**	>33[b]	>33[b]
Cmpd 10	0.037±0.015	0.014±0.006	**Cmpd 9**	>16.1[b]	>16.1[b]
Cmpd 11	0.21±0.1	0.1±0.08			
Cmpd 12	0.35±0.08	0.31±0.26			
Cmpd 13	40±7	16±7			
Cmpd 14	>250[b]	150±7			

Mean ± SD
(a) IC_{50} value not established, lower than range of concentrations tested
(b) IC_{50} value not reached up to highest concentration tested

4.2.3 Cytotoxicity of the 5-FU and 5-FUrd derivatives in the SW480 human colorectal cancer cell line

The SW480 cell line was derived from a human colorectal adenocarcinoma. Cytotoxicity was assayed after treatment for 3 and 5 days, IC_{50} values were established and are listed in Table 4.3. Results are from a minimum of duplicate experiments, completed in triplicate. The nitro-benzyl derivatives of 5-FU caused a similar level of toxicity, after treatment for 3 days, to that observed in the 4T1 cell line (Figure 4.9). Compound 3 was less toxic than 5-FU, with IC_{50} values of 11 µM and 4.9 µM respectively. Compounds 13 and 14 showed no toxicity over the range of concentrations tested, however, due to limited availability of compounds, concentrations could not be tested to as high a concentration as with the 4T1 cell line. The ester derivatives, compounds 10 and 11, were again more toxic than the parent 5-FU after treatment for 3 days (Figure 4.10). The IC_{50} value of compound 10 (0.38 µM) was greater than one order of magnitude less than that of the parent 5-FU (Table 4.3). Compounds 4 and 5 were slightly less toxic than 5-FU with IC_{50} values of 7.8 µM and 7.1 µM respectively (Table 4.3). The IC_{50} value of compound 12, the acid derivative, was 5.1 µM, again with a toxicity profile which mirrored 5-FU (Figure 4.11).

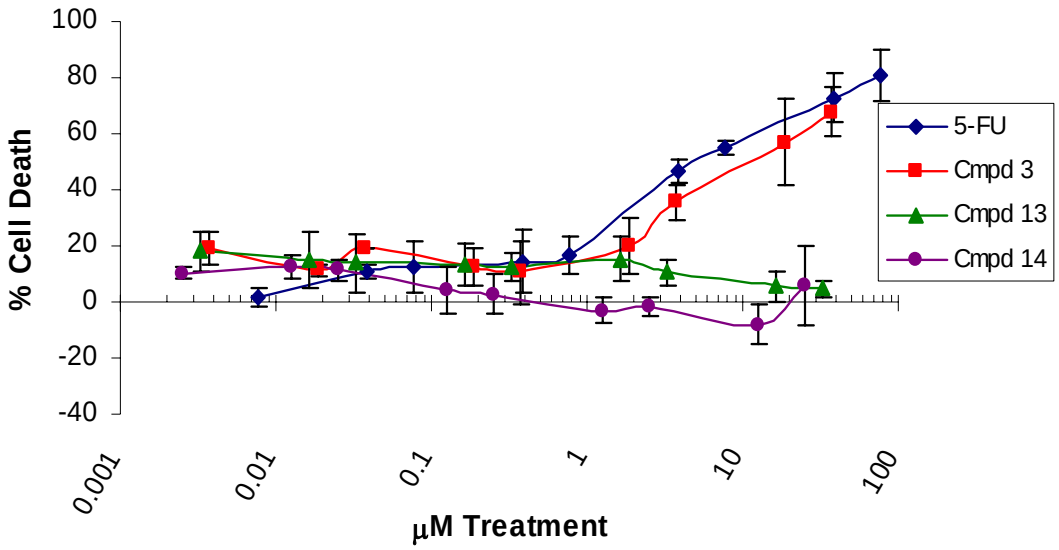

Figure 4.9 Cytotoxicity of the nitro-benzyl derivatives of 5-FU in the SW480 cell line after treatment for 3 days. 5-FU and compound 3 showed toxicity from 1 µM upwards. Compounds 13 and 14 showed low toxicity over the range of concentrations tested.

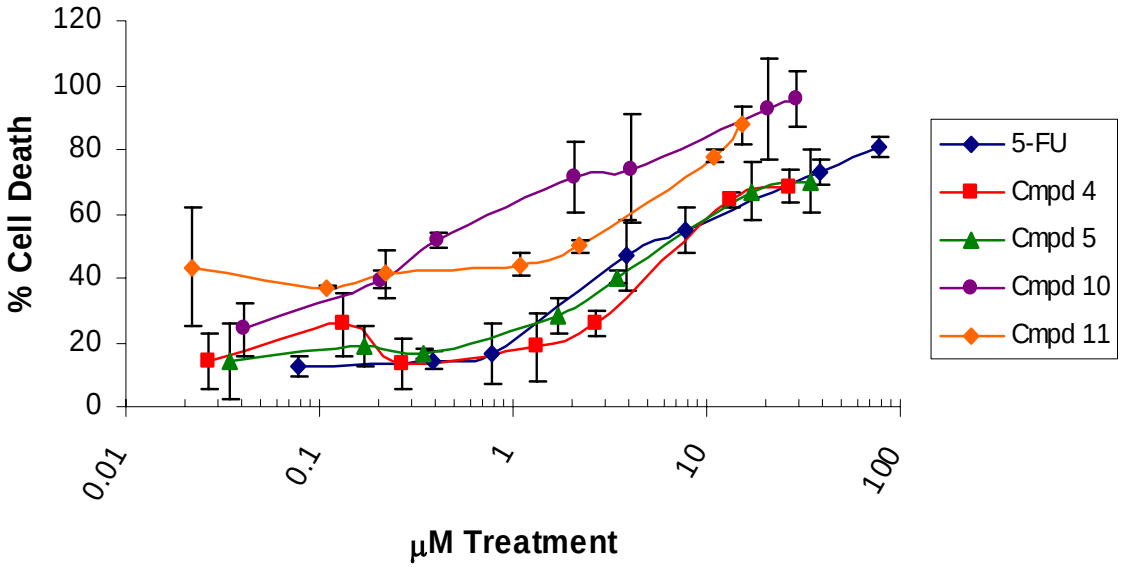

Figure 4.10 Cytotoxicity of the ester derivatives of 5-FU in the SW480 cell line after treatment for 3 days. Compounds 10 and 11 showed the highest toxicity in the SW480 cells. 5-FU, compound 4 and compound 5 showed similar toxicity profiles.

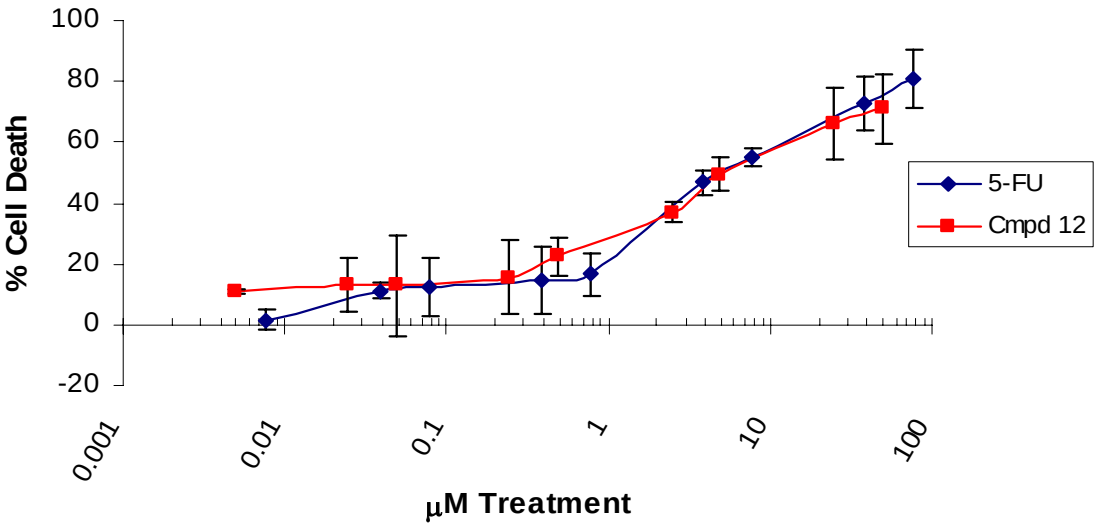

Figure 4.11 Cytotoxicity of the acid derivative of 5-FU in the SW480 cell line after treatment for 3 days. A similar cytotoxic response to the treatment was seen for both 5-FU and compound 12.

The 5-FUrd derivatives, compounds 6, 7, 8 and 9 showed low toxicity over the range of concentrations tested over 3 days (Figure 4.12 and Table 4.3). The IC_{50} value for 5-FUrd after treatment for 3 days was 0.37 µM, more toxic than 5-FU or the 5-FU derivatives, although compound 10 had a similar IC_{50} value of 0.38 µM.

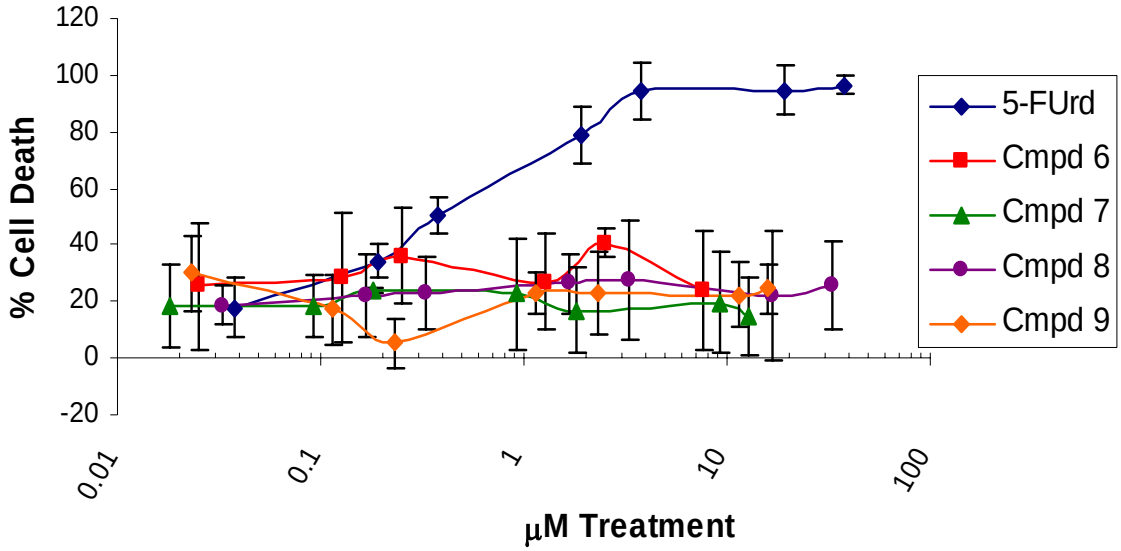

Figure 4.12 Cytotoxicity of the 5-FUrd derivatives in the SW480 cell line after treatment for 3 days. 5-FUrd showed toxicity from 0.04 µM, reaching 100% cell death at approximately 3 µM. The 5-FUrd derivatives showed low toxicity over the range of concentrations tested.

After treatment for 5 days, similar results were seen with IC_{50} values for compounds 10 and 11 (0.22 µM and 1.2 µM) lower than the parent 5-FU (2.6 µM) (Table 4.3). Compound 5 also had a lower IC_{50} value of 2.4 µM after treatment for 5 days. Compounds 3 (IC_{50}: 3.5 µM), 4 (IC_{50}: 4.3 µM) and 12 (IC_{50}: 3 µM) were less toxic than 5-FU (Table 4.3). After treatment for 5 days, 5-FUrd had an IC_{50} value of 0.25 µM, with only the 5-FU derivative, compound 10, being more toxic. The 5-FUrd derivatives, compounds 6-9, had low toxicity over the range of concentrations tested.

Table 4.3 IC_{50} values of the 5-FU and 5-FUrd derivatives in the SW480 human colorectal cancer cell line after treatment for 3 and 5 days.

IC_{50} Values SW480 Cell Line (μM)					
	3 Days	**5 Days**		**3 Days**	**5 Days**
5-FU	4.9±1.2	2.6±0.5	**5-FUrd**	0.37±0.28	0.25±0.005
Cmpd 3	11±12.4	3.5±1.04	**Cmpd 6**	>7.6[a]	>7.6[a]
Cmpd 4	7.8±0.85	4.3±2.1	**Cmpd 7**	>12.8[a]	>12.8[a]
Cmpd 5	7.1±5.3	2.4±0.75	**Cmpd 8**	>33[a]	>33[a]
Cmpd 10	0.38±0.47	0.22±0.1	**Cmpd 9**	>16.1[a]	>16.1[a]
Cmpd 11	2.05±0.8	1.2±0.4			
Cmpd 12	5.1±0.2	3±0.45			
Cmpd 13	>32[a]	>32[a]			
Cmpd 14	>25[a]	>25[a]			

Mean±SD

(a) IC_{50} value not reached up to highest concentration tested

4.2.4 Cytotoxicity of 5-FU derivatives in the HCT116 parental and 5-FU resistant cell lines

The HCT116 parental and 5-FU resistant cell lines were kindly provided by Professor Patrick G. Johnston, Department of Oncology, Cancer Research Centre, Queen's University Belfast, Belfast, Northern Ireland. The HCT116 parental (HCT(P)) cell line was a human colorectal carcinoma cell line. The HCT116 5-FU-resistant (HCT(R)) cell line was established from the HCT(P) cell line by repeated exposure to stepwise increasing concentrations of 5-FU (Boyer *et al.,* 2004). The IC_{50} values for 5-FU after treatment for 3 days was increased 3-fold following this treatment, from 4.3 μM to 12.7 μM. The 5-FU resistant cell line was sub-cultured in medium supplemented with 2 μM 5-FU to maintain this selection (Boyer *et al.*, 2004). These cell lines were acquired to determine the toxicity of selected 5-FU derivatives.

The cytotoxicity of 5-FU, 5-FUrd and selected 5-FU compounds was analysed over 3 and 5 days using the parental and resistant cell lines (Table 4.4). The results are from triplicate treatments. The IC_{50} value for HCT(P) after treatment for 3 days was 4.5 μM, similar to that established by Boyer *et al*. (2004). The IC_{50} value for the 5-FU resistant cell line was only 2-fold higher in our experiments, at 9 μM (Figure 4.13 and Table 4.4). A decrease in this ratio indicates increased sensitivity of the resistant cell line to the treatment. If the ratio of IC_{50} values was less than 1, the resistant cell line was more sensitive to the treatment than the parental cell line. Of the derivatives tested, treatment with compounds 4 and 10 resulted in the lowest ratio of IC_{50} values between the parental and resistant cell lines at 1.7 (Figure 4.13, 4.14 and Table 4.4). 5-FUrd had a 1.44-fold difference while compounds 3 and 5 had fold differences of 1.83 and 2.33 respectively. Compounds 11, 13 and 14 showed low toxicity and IC_{50} values were not established over the range of concentrations tested (Figure 4.14 and Table 4.4).

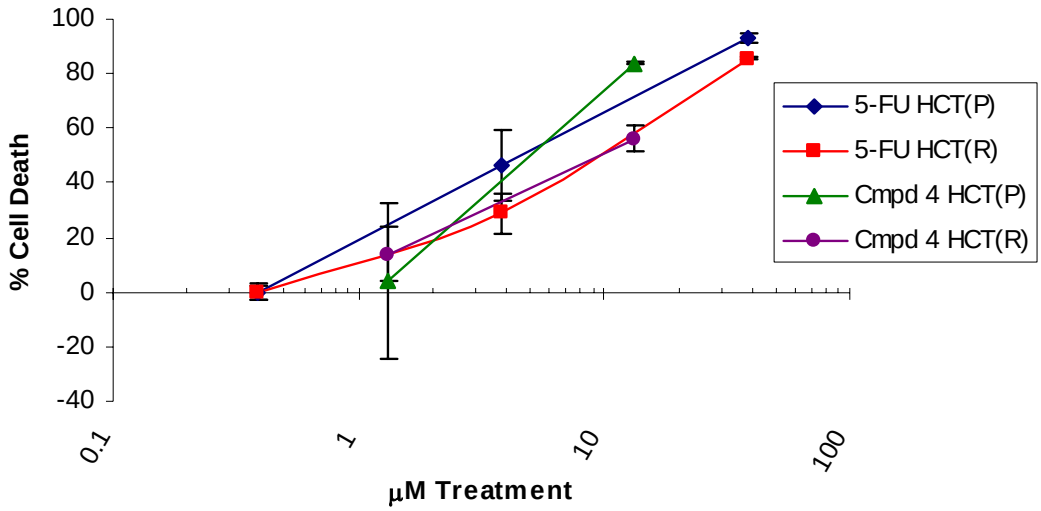

Figure 4.13 Cytotoxicity of 5-FU and compound 4 in the HCT(P) and HCT(R) cell lines after treatment for 3 days. The IC_{50} value of 5-FU in the resistant cell line was 2-fold higher than in the parental cell line. Compound 4 had a ratio of 1.7 between the IC_{50} values for the parental and resistant cell line.

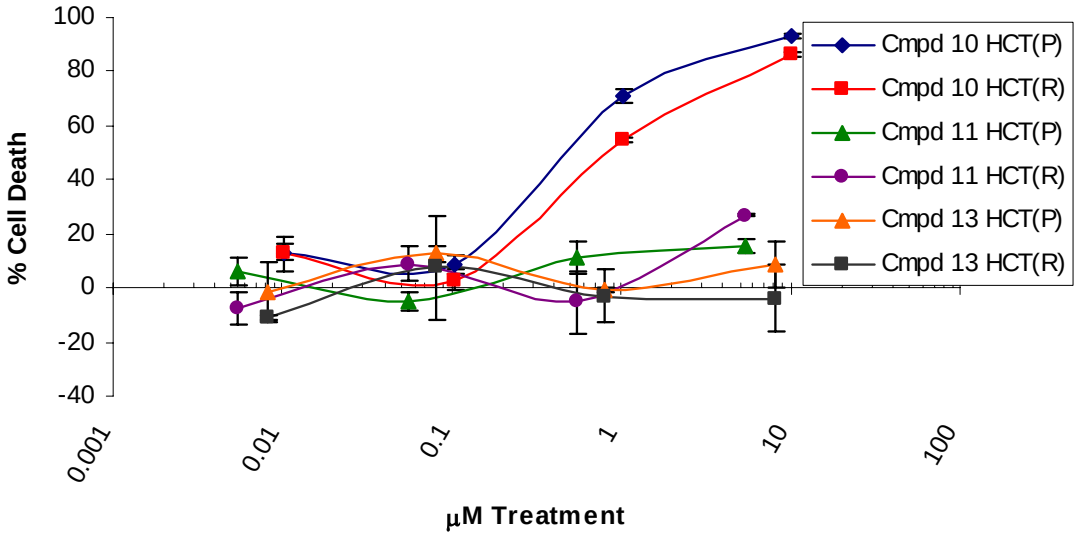

Figure 4.14 Cytotoxicity of compounds 10, 11 and 13 in the HCT(P) and HCT(R) cell lines after treatment for 3 days. Compound 10 showed toxicity from 0.1 µM upwards, with IC_{50} values of 0.47 µM and 0.8 µM for the parental and resistant cell lines respectively. Compounds 11 and 13 showed low toxicity over the range of concentrations tested.

After treatment for 5 days, there was a 4-fold difference in IC_{50} value between the parental and resistant cell line for 5-FU (Table 4.4). 5-FUrd was extremely toxic in both cell lines over 5 days. The IC_{50} values of 0.062 μM and 0.053 μM for the parental and resistant cell lines respectively gave a ratio of 0.86. This indicates that the resistant cell line was unexpectedly more sensitive to the 5-FUrd than the parental cell line (Table 4.4). For the 5-FU derivatives, all four compounds that exhibited toxicity showed lower ratios than for the 5-FU treatment. The ratio of IC_{50} values for compounds 3 and 10 were 1.13 and 0.89, again indicating the resistant cell line was relatively more sensitive to these derivatives than to 5-FU. This would also suggest the HCT(R) cells were more sensitive to compound 10 than the HCT(P) cells.

Table 4.4: IC_{50} values of the 5-FU derivatives and 5-FUrd in the HCT(P) and HCT(R) cell lines after treatment for 3 and 5 days.

IC_{50} Values HCT116 Parental & Resistant Cell Lines (μM)						
	3 Days			**5 Days**		
	HCT(P)	**HCT(R)**	**Fold[a]**	**HCT(P)**	**HCT(R)**	**Fold[a]**
5-FU	4.5±2.3	9±2.3	2.00	1.2±0.15	4.8±0.9	4.00
5-FUrd	0.16±0.05	0.23±0.01	1.44	0.062±0.004	0.053±0.04	0.86
Cmpd 3	7.1±1.7	13±3.8	1.83	7±0.38	7.9±0.95	1.13
Cmpd 4	5.3±2	9±3.1	1.70	3.9±0.8	5±1.96	1.28
Cmpd 5	4.3±1.5	10±0.15	2.33	4.6±1	6.6±0.89	1.44
Cmpd 10	0.47±0.03	0.8±0.01	1.70	0.47±0.02	0.42±0.03	0.89
Cmpd 11	>5.5[b]	>5.5[b]		>5.5[b]	>5.5[b]	
Cmpd 13	>8.1[b]	>8.1[b]		>8.1[b]	>8.1[b]	
Cmpd 14	>6.3[b]	>6.3[b]		>6.3[b]	>6.3[b]	

Mean ± SD
(a) Fold = fold increase in resistance
(b) IC_{50} value not reached up to highest concentration tested

4.2.5 Guava® cell cycle analysis of 4T1 cells following treatment with 5-FU and 5-FU derivatives

4T1 cells were treated with 0.1 μM and 1 μM 5-FU and 5-FU derivatives for 3 days, and then assessed on the Guava® PCA. These concentrations were chosen because the IC_{50} values for the majority of the compounds fell between these two points and would therefore, give a good indication of the effect on the cell cycle with increasing toxicity. Results are representative of three independent experiments. Data was analysed using Multicycle software (Phoenix Flow Systems, CA) to determine the cell cycle stages. Figure 4.15 shows the cell cycle analysis for 5-FU and compounds 3, 4, 5, 10, 11, 13 and 14 at 0.1 μM. Figure 4.16 and Table 4.5 summarise these results. Control cells were treated with the equivalent amount of DMSO used in the treatments. In the control sample, the majority of the cell population was in the G1 phase (44.1%), with 38.1% in S phase and 17.9% in G2 phase (Figures 4.15 and 4.16). Following treatment with 5-FU at 0.1 μM, an increase was seen in the percentage of cells in the G2 phase (35.4%), with a reduction of cells in G1 phase to 28.1% and S phase to 36.5%.

Compounds 3 and 5 caused a decrease in G1 cell population and an increase in the G2 phase population after treatment with 0.1 μM (Figures 4.15 and 4.16). Compound 4 caused a decrease in the G1 and S phase populations and an increase in G2 phase population. Compound 10 had a considerable effect on the cell cycle even after treatment with 0.1 μM, with the S phase increasing to 92.4%, G2 decreasing to 0% and the G1 population to 7.6% (Figures 4.15 and 4.16). Compound 11 also caused an increase in the cell population in the S and G2 phases following treatment with 0.1 μM (Figures 4.15 and 4.16). Treatment with compounds 13 and 14 had little effect on the cell cycle. For compound 13, 0.1 μM of treatment led to a slight decrease in G1 phase, with corresponding small increases in S and G2 phases. Compound 14 caused an increase in G1 and S phase cell populations with a decrease in G2 cell population following 0.1 μM treatment (Figures 4.15 and 4.16).

Treatment with 5-FU at the higher concentration of 1 μM caused a complete reduction in the S phase cell population to 0% (Figures 4.17 and 4.18, Table 4.6). The G1 phase accounted for 62.4% of the cell population and G2 phase 37.6% (Figures 4.17 and 4.18, Table 4.6). Treatment with 1 μM of compounds 3, 4 and 5

resulted in a dramatic decrease in S phase population. Compounds 3, 4 and 5 caused a decrease in the S phase population to 0%, 3% and 0.7% respectively (Figures 4.17 and 4.18, Table 4.6). Upon treatment with 1 μM of compound 10, 28.8% of the cell population were in the G1 phase and 71.2% in the S phase (Figures 4.17 and 4.18, Table 4.6). 1 μM of treatment with compound 11 caused an increase in G1 cell population and a decrease in the S phase cell population (Figures 4.17 and 4.18, Table 4.6). Exposure to 1 μM of compound 13 and compound 14 resulted in an increase in the G2 population (Figures 4.17 and 4.18, Table 4.6).

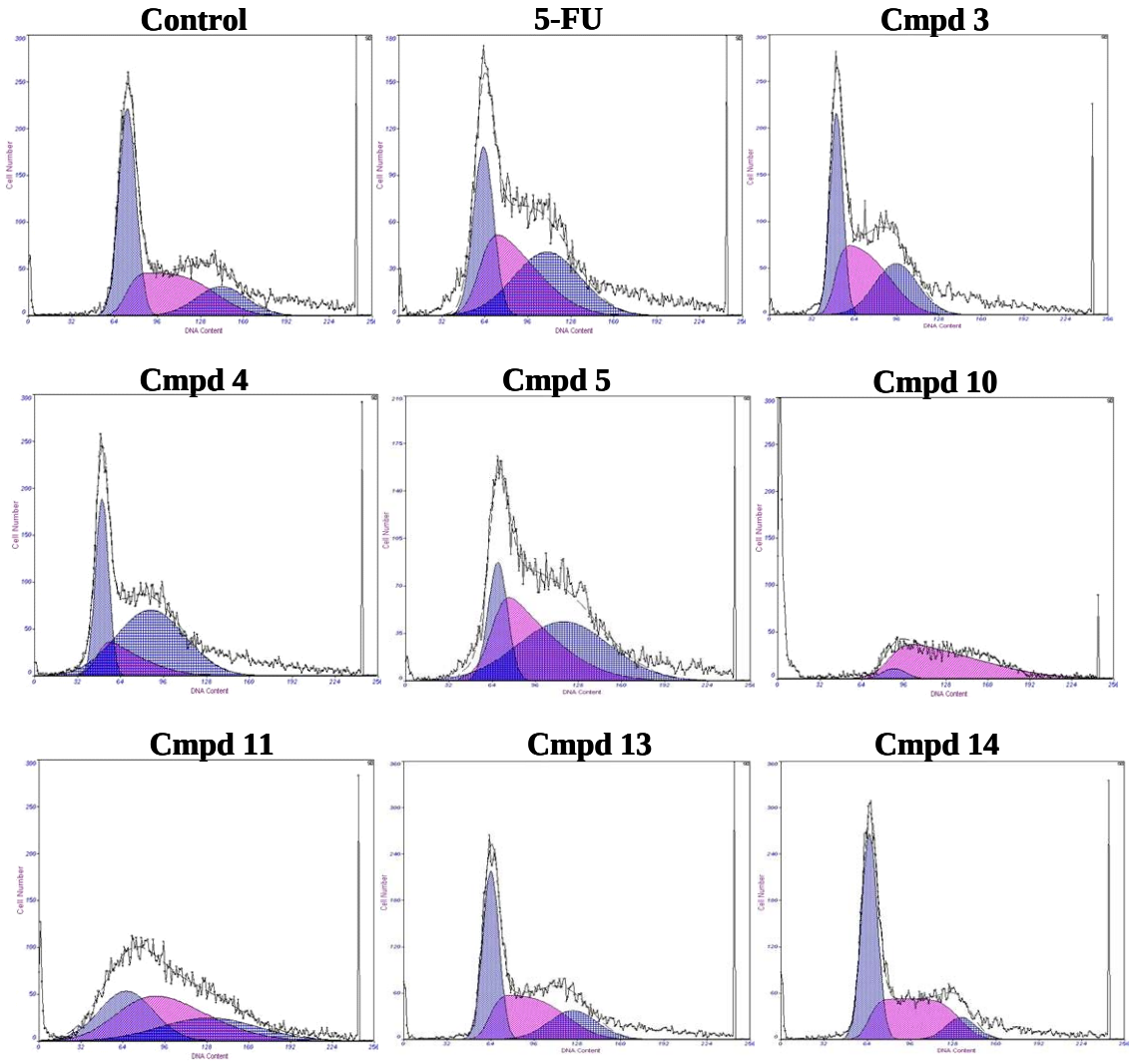

Figure 4.15 Cell cycle analysis of 4T1 cells following treatment for 3 days with 0.1 μM 5-FU and 5-FU derivatives. X-axis shows DNA content, y-axis represents counts of cells. G1 phase is in light blue, S phase in pink and G2 phase in dark blue.

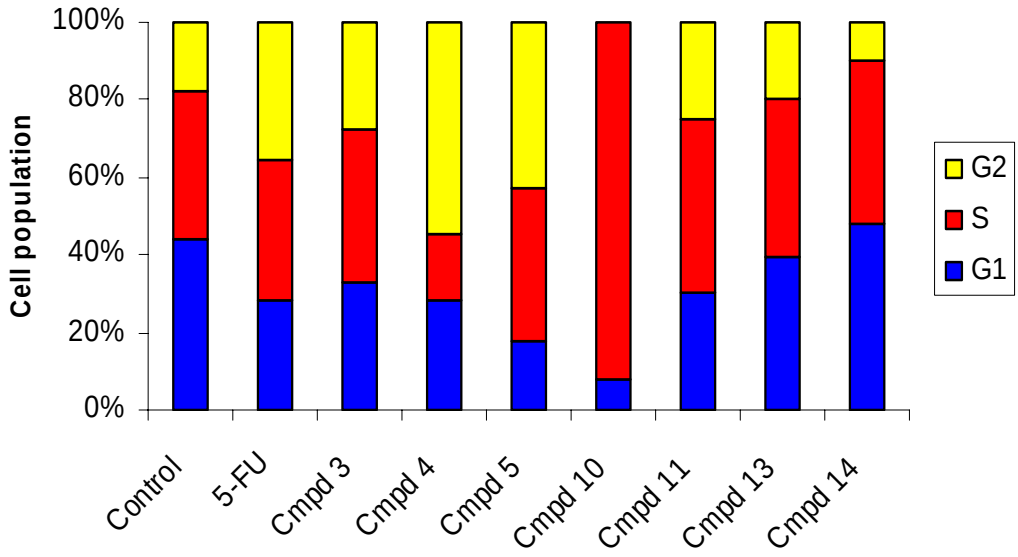

Figure 4.16 Cell cycle analysis of 4T1 cells following treatment for 3 days with 0.1 μM 5-FU and derivatives. 5-FU, compounds 3, 4, 5, 11 and 13 all caused an increase in the percentage of cells in the G2 phase. Compound 10 treatment resulted in a complete reduction of cells in the G2 phase. Compound 14 showed slight increase of cells in G1 phase.

Table 4.5 Percentages of cell cycle populations following treatment with 0.1 μM 5-FU and 5-FU derivatives for 3 days.

Cell Cycle Analysis: 0.1 μM			
	G1 (%)	S (%)	G2 (%)
Control	44.1	38.1	17.9
5-FU	28.1	36.5	35.4
Cmpd 3	32.6	40.0	27.3
Cmpd 4	28.2	17.5	54.3
Cmpd 5	18.1	38.9	43.0
Cmpd 10	7.6	92.4	0.0
Cmpd 11	30.3	44.6	25.1
Cmpd 13	39.4	40.6	20.1
Cmpd 14	47.7	42.7	9.5

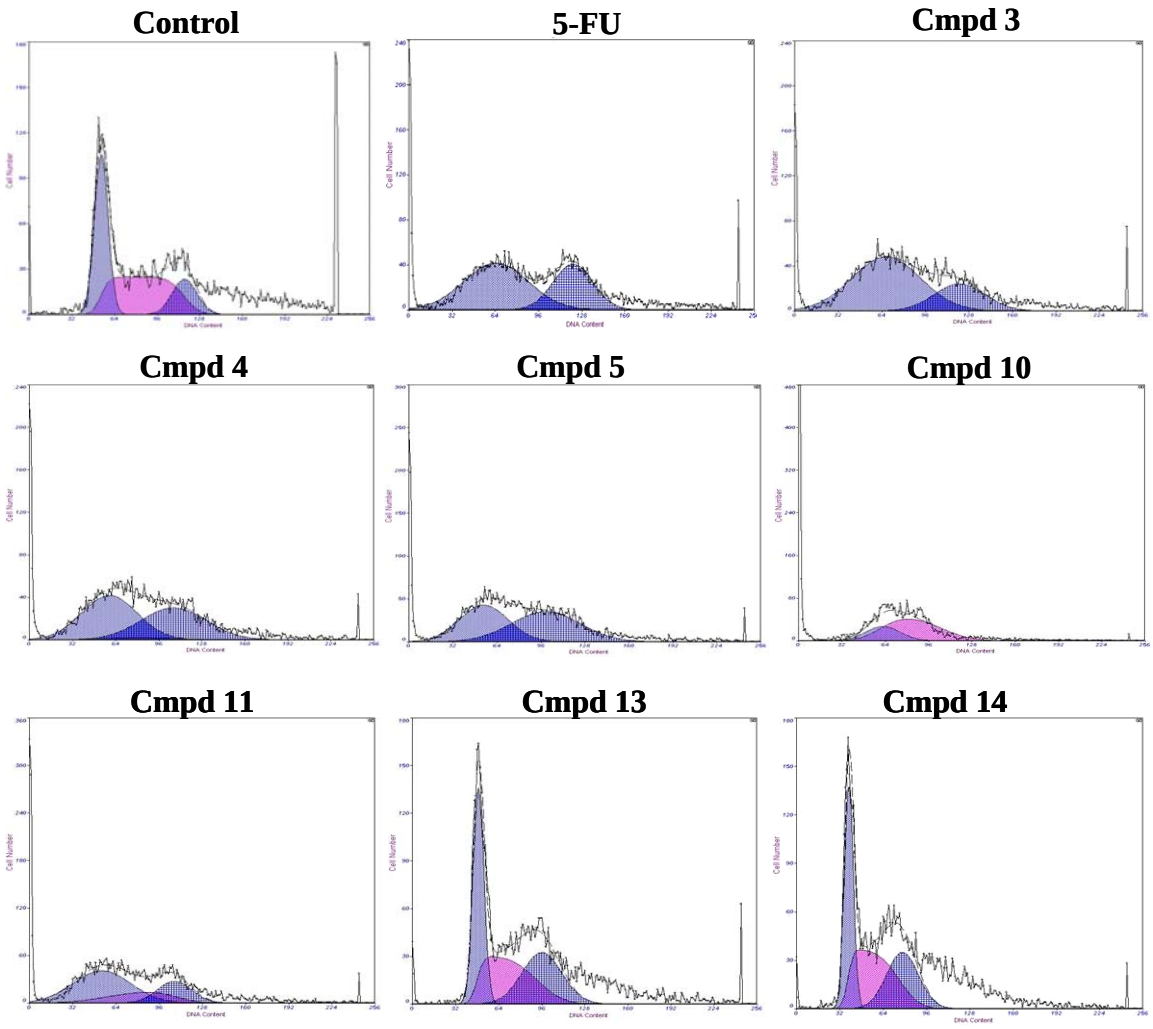

Figure 4.17 Cell cycle analysis of 4T1 cells following 3 days treatment with 1 μM 5-FU and 5-FU derivatives. X-axis shows DNA content, y-axis represents counts of cells. G1 phase is in light blue, S phase in pink and G2 phase in dark blue.

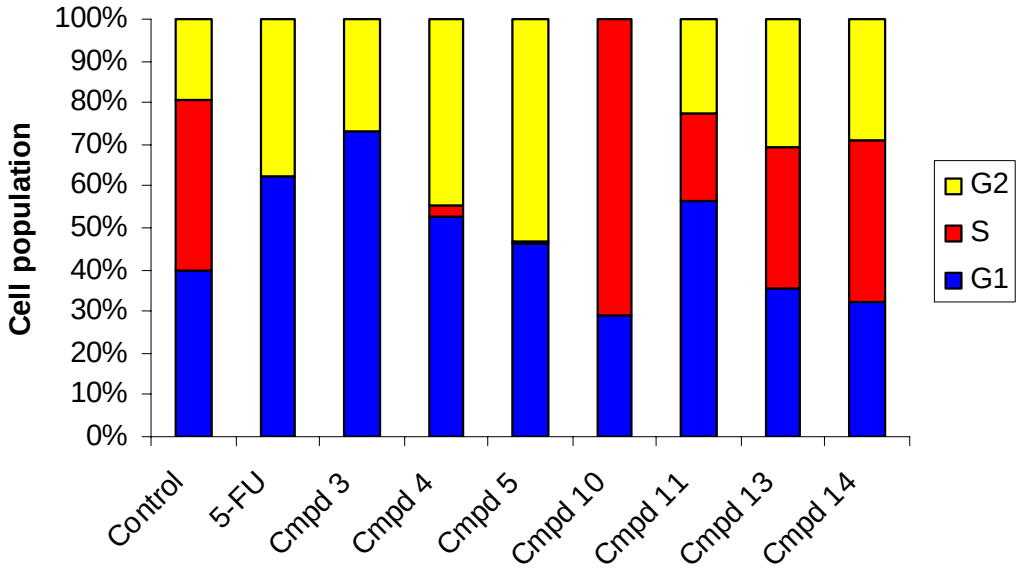

Figure 4.18 Cell cycle analysis of 4T1 cells following treatment for 3 days with 1 μM 5-FU and derivatives. 5-FU, compounds 3, 4, 5 and 11 caused a decrease in S phase population and an increase in the G1 and G2 populations. Compound 10 caused a complete reduction in G2 cell population. Compounds 13 and 14 showed minimal effect on the cell cycle.

Table 4.6 Percentages of cell cycle populations following treatment with 1 μM 5-FU and 5-FU derivatives for 3 days.

Cell Cycle Analysis: 1 μM			
	G1 (%)	S (%)	G2 (%)
Control	39.9	40.5	19.6
5-FU	62.4	0.0	37.6
Cmpd 3	73.1	0.0	26.9
Cmpd 4	52.4	3.0	44.6
Cmpd 5	46.1	0.7	53.2
Cmpd 10	28.8	71.2	0.0
Cmpd 11	56.4	20.8	22.7
Cmpd 13	35.2	34.2	30.5
Cmpd 14	32.4	38.9	28.8

4.2.6 Guava® apoptosis analysis of 4T1 cells following treatment with 5-FU and 5-FU derivatives

The 4T1 cell line was treated with 0.1 μM and 1 μM of 5-FU and 5-FU derivatives in order to investigate the effect on apoptosis. Figures 4.19 and 4.20 shows the apoptosis analysis results from cells treated for 3 days with 0.1 μM and 1 μM of 5-FU and 5-FU derivatives. Results are representative of three independent experiments. Figure 4.21 summarises the data, illustrating the percentage of annexin V positive cells, which includes both early and late apoptotic cells and also necrotic cells. The x-axis and y-axis represent Annexin V and 7-AAD staining respectively. Healthy cells without any dye are seen in the lower left quadrant of the dot-plots in Figure 4.19, while cells undergoing apoptosis move firstly into the lower right quadrant (following translocation of phosphatidylserine molecule from inner to outer surface to cell membrane) and then move to the upper right quadrant (following breach of the integrity of the membrane). Cells undergoing necrosis move from the lower left quadrant to the upper right quadrant without moving into the lower right quadrant.

The control-treated cells showed 8-9% annexin V-positive cells, with the bulk of the cell population evident in the lower left quadrant of the dot-plot (Figure 4.19). For the parent compound, 5-FU, approximately 12% apoptotic cells were noted following treatment with 0.1 μM, increasing to approximately 45% after treatment with 1 μM ($p<0.05$) (Figures 4.19 and 4.20). The movement of the cell population from the lower left quadrant into the lower and upper right quadrants can be observed following treatment with 1 μM (Figure 4.20). Compounds 3, 4 and 5 showed similar effects on the 4T1 cells, with 10-12% annexin V-positive cells after treatment with 0.1 μM and 25-30% following treatment with 1 μM ($p<0.05$) (Figures 4.19 and 4.20). Treatment with compounds 10 and 11 resulted in the highest level of apoptotic cells following the 0.1 μM treatment, at 45% and 24% of the cell population respectively. This result for compound 10 was statistically significant in relation to the control cells and also in relation to the 5-FU-treated cells ($p<0.01$) (Figure 4.21). After treatment with 1 μM of both these compounds only a small increase in apoptosis was seen, to 46% and 29% (Figures 4.20 and 4.21). Compounds 13 and 14 at 0.1 μM and 1 μM showed low levels of apoptosis, below 10%, similar to the control-treated cells. This

result was statistically significant ($p<0.01$) in relation to the 5-FU treated cells at 1 μM.

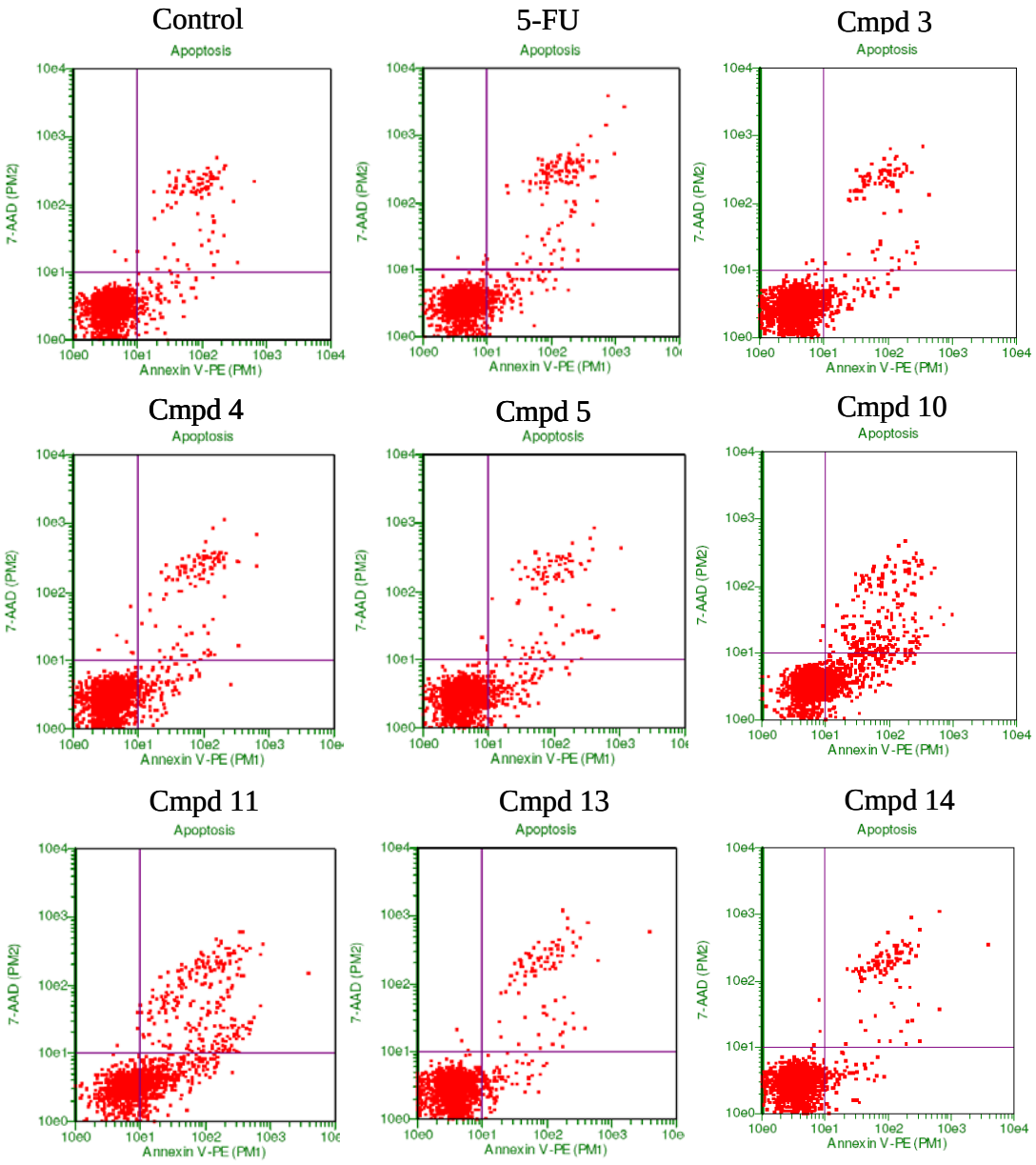

Figure 4.19 Apoptosis analysis of 4T1 cells following treatment for 3 days with 0.1 μM 5-FU and 5-FU derivatives. Cells in the lower left quadrant are not stained with either dye. Cells undergoing apoptosis move firstly into the lower right quadrant then move to the upper right quadrant.

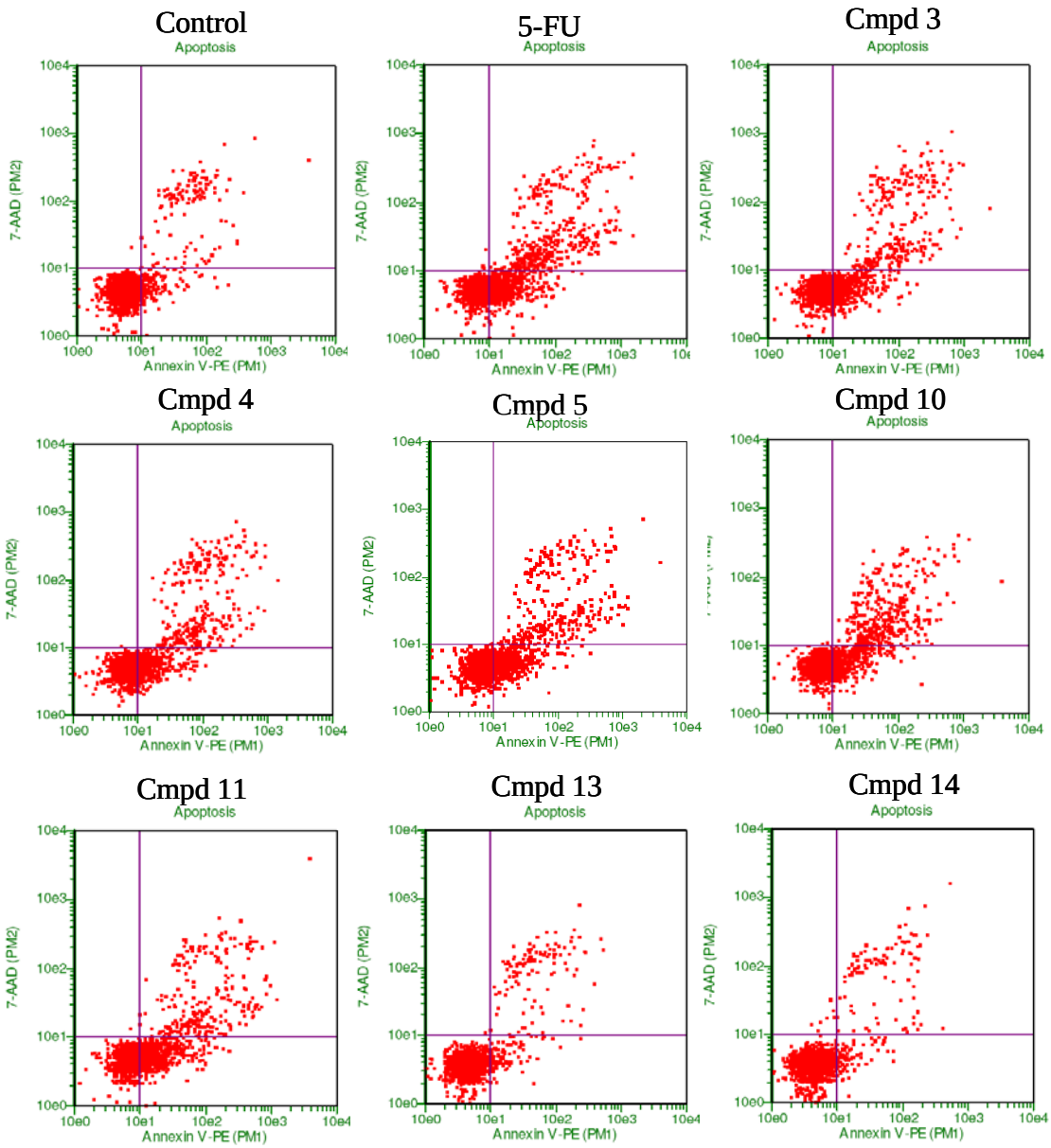

Figure 4.20 Apoptosis analysis of 4T1 cells following treatment for 3 days with 1 μM 5-FU and 5-FU derivatives. An increased number of cells can be seen in the lower and upper right quadrants following treatment with 5-FU and compounds 3, 4, 5, 10 and 11.

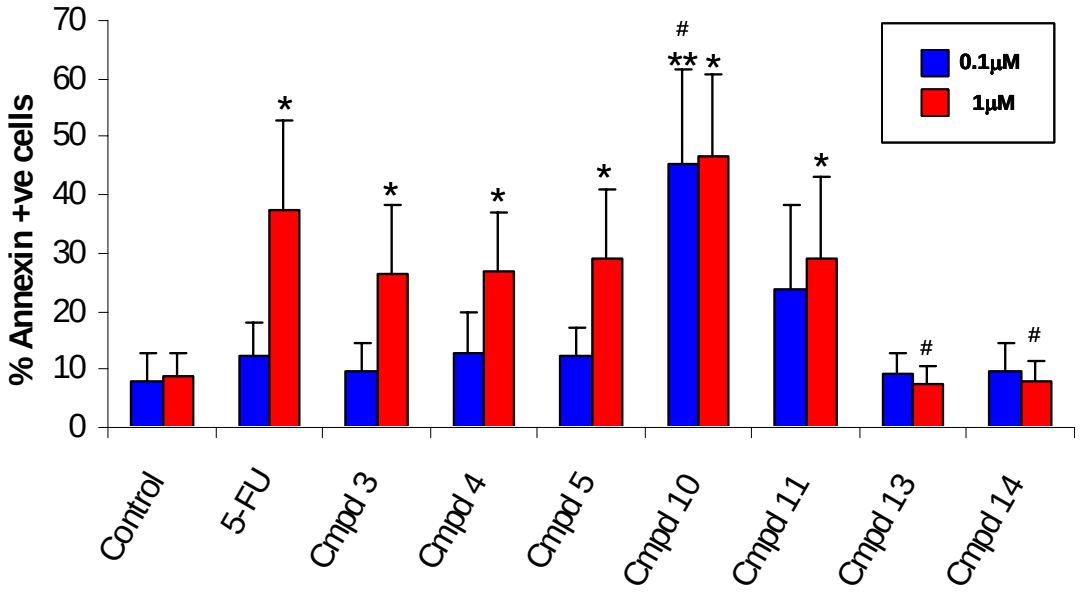

Figure 4.21 Apoptosis analysis of 4T1 cells following treatment for 3 days with 0.1 μM and 1 μM 5-FU and 5-FU derivatives. Graph indicates the percentage of annexin positive cells, giving an indication of early and late apoptotic cell population and necrotic cell population. * p-value<0.05 in relation to control, ** p-value<0.01 in relation to control, # p-value<0.01 in relation to 5-FU treated cells, Student's t-test.

4.2.7 Effect of 5-FU and 5-FU derivatives on migration of the 4T1 cell line

To determine the effect of 5-FU and derivatives on the migratory capabilities of 4T1 cells, *in vitro* migration assays were conducted and analysed as per section 2.2.5. Results are from duplicate experiments, completed in triplicate. Cells were initially pre-treated in 25 cm^2 cell culture flasks with 0.5 nM of the compound for 48 hours, then trypsinised and seeded into Falcon™ Cell Culture Inserts, with treatment added, incubated for 24 hours and the level of migration quantified. This concentration of compound was chosen to ensure minimal toxicity for all compounds (<10% cell death) in order to determine effects that were due to changes in migratory or invasive ability rather than cell death. Figure 4.22 shows the results for the migration assay. In comparison to control-treated cells, the percentage of cells migrating through the membrane was increased following treatment with 5-FU and the derivatives. 5-FU and compounds 3, 4, 13 and 14 caused the largest increases in migration (Figure 4.22). The increase seen for compounds 3 (82%), 4 (84%) and 14 (51%) were significant in comparison to the control-treated cells (36%) ($p<0.001$, $p<0.01$, $p<0.05$ respectively) (Table 4.7).

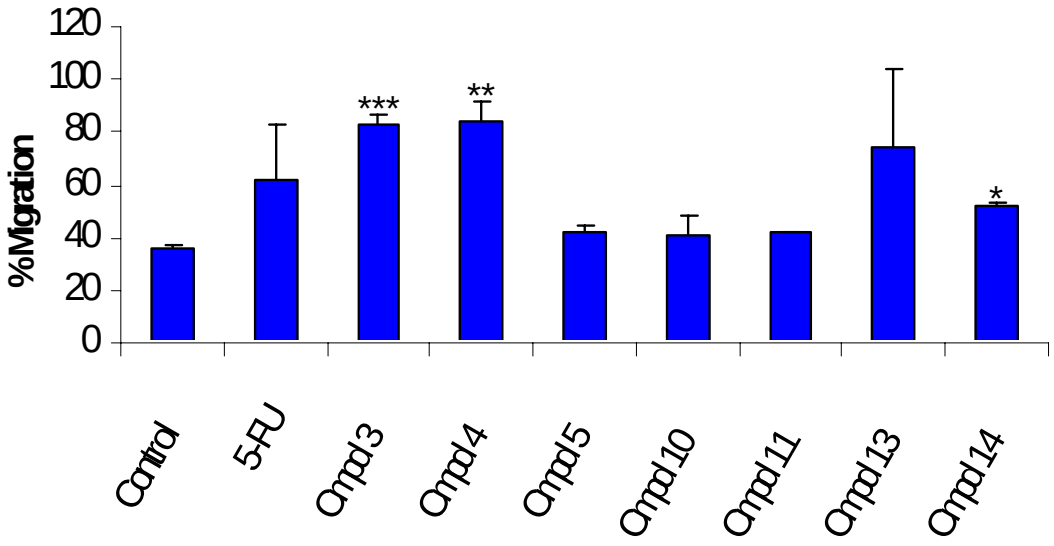

Figure 4.22 Effect of treatment with 0.5 nM 5-FU and 5-FU derivatives for 3 days on migration of the 4T1 cell line. Treatment with 5-FU, compounds 3, 4, 13 and 14 resulted in increased invasion of the cells. *$p<0.05$, *$p<0.01$, ***$p<0.001$, Student's t-test.

Figure 4.23 shows photographs of the migratory cells which have been fixed and stained on the underside of the membrane. A clear increase can be seen in the cells treated with 5-FU and compounds 3, 4, 13 and 14, in comparison to the control-treated cells.

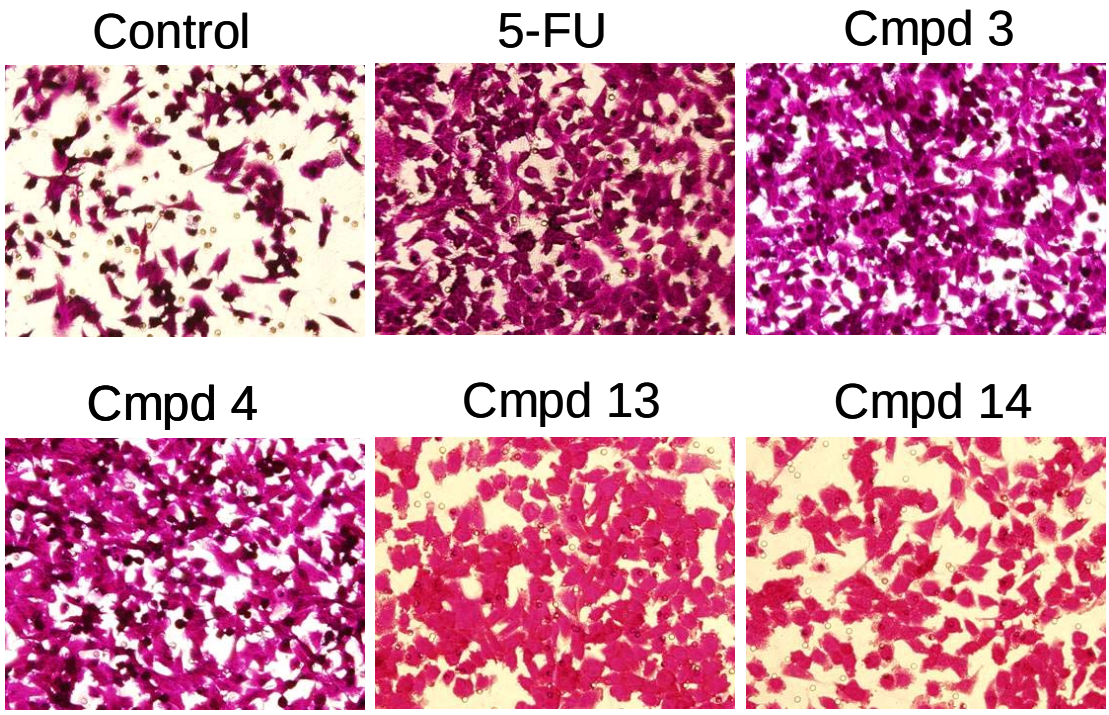

Figure 4.23 Falcon™ cell culture inserts following fixing and staining of the membrane with crystal violet. A clear increase in the number of cells that have migrated can be seen for the populations treated with 5-FU and 5-FU derivatives in comparison to the control-treated cells.

4.2.8 Effect of 5-FU and 5-FU derivatives on invasion of the 4T1 cell line

Invasion assays were set up in the same manner as migration assays. Unlike the Falcon™ Cell Culture Inserts, the BD BioCoat™ Matrigel™ Invasion Chambers contained a layer of Matrigel on the top of the membrane, which must be degraded by the cells before they can move through the pores. Results are from duplicate experiments, completed in triplicate. Figure 4.24 illustrates the effect of 5-FU and 5-FU derivatives on invasion of the 4T1 cell line. The control-treated cells showed 15% invasion after 24 hours (Table 4.7). Treatment with 0.5 nM of 5-FU and 5-FU derivatives caused an increase in invasion in comparison to the control. Compounds 3 and 4 resulted in the greatest increases in invasion of the cells, with a statistically significant result for compound 4 (51%, $p<0.05$). Figure 4.25 shows pictures of the membranes with a clear increase in the number of cells that had invaded following treatment with 5-FU and compounds 3 and 4. Table 4.7 summarises the migration and invasion data.

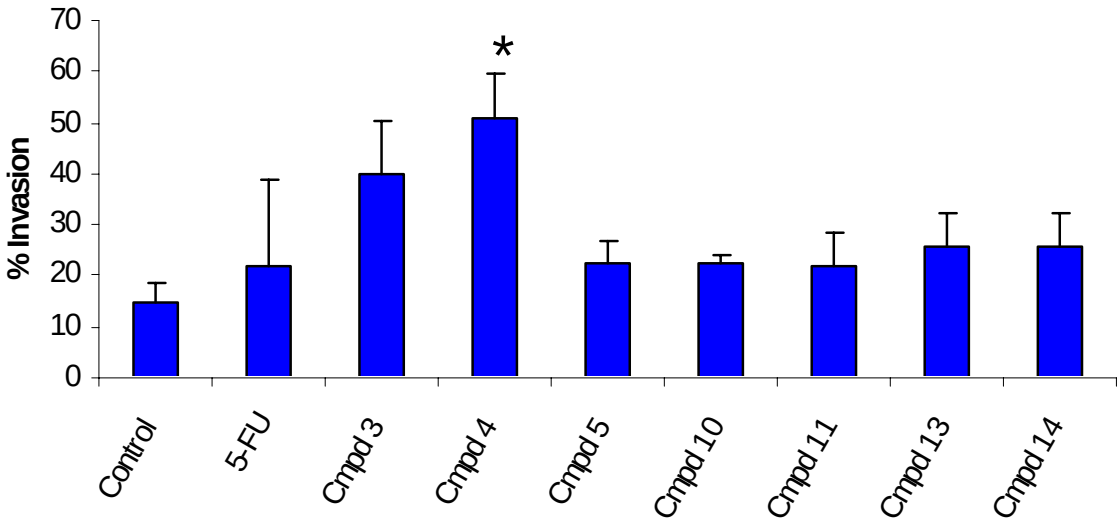

Figure 4.24 Effect of treatment with 0.5 nM 5-FU and 5-FU derivatives for 3 days on invasion of the 4T1 cell line. Invasion of cells increased following treatment with 5-FU, compounds 3 and 4. *$p<0.05$, Student's t-test.

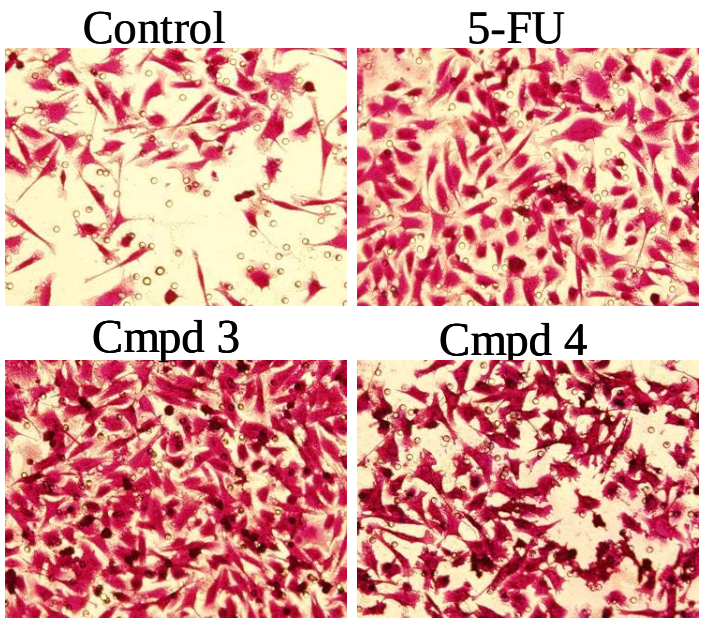

Figure 4.25 BD BioCoat™ Matrigel™ Invasion Chambers following fixing and staining of the membrane with crystal violet. A clear increase in the number of cells that have invaded can be seen for the populations treated with 5-FU and compounds 3 and 4 in comparison to the control-treated cells.

Table 4.7 Migration and invasion data for 4T1 cell line following treatment with 5-FU and 5-FU derivatives for 3 days.

	Migration (%)	**Invasion (%)**
Control	36 ± 2	15 ± 4
5-FU	62 ± 22	22 ± 17
Cmpd 3	82 ± 5***	40 ± 11
Cmpd 4	84 ± 8**	51 ± 9*
Cmpd 5	42 ± 3	23 ± 4
Cmpd 10	42 ± 7	22 ± 2
Cmpd 11	42 ± 0.5	22 ± 7
Cmpd 13	74 ± 30	26 ± 7
Cmpd 14	51 ± 2*	26 ± 7

*p<0.05, **p<0.01, ***p<0.001, Student's t-test

4.2.9 Effect of 5-FU and 5-FU derivatives on colony formation of the 4T1 cell line in soft agar

Soft agar assays are used to test the anchorage-independent growth of cells which is a possible indication of tumourigenicity and is used to assess the efficacy of anticancer compounds. A compound is considered efficacious if treatment results in a reduction in the number of colonies to below 30% of that in the control sample (Fiebig *et al.*, 2004). This technique involved seeding cells in semi-solid medium containing agar and assessing the formation of colonies in this environment. 4T1 cells pre-treated with 0.5 nM 5-FU derivatives for 3 days were seeded in the soft agar and incubated for 10 days. Live colonies were stained with p-Iodonitrotetrazolium chloride solution and colonies with a diameter greater than 100 μm were counted. Results are from duplicate experiments, completed in triplicate. Cells pre-treated with compounds 5 and 14 led to an increase in the number of colonies formed, while cells pre-treated with compounds 11 and 13 showed a decrease in the number of colonies formed, in comparison to the control-treated cells (Figure 4.26). However, none of these results were found to be statistically significant and none of the compounds showed a reduction to below 30% of the control.

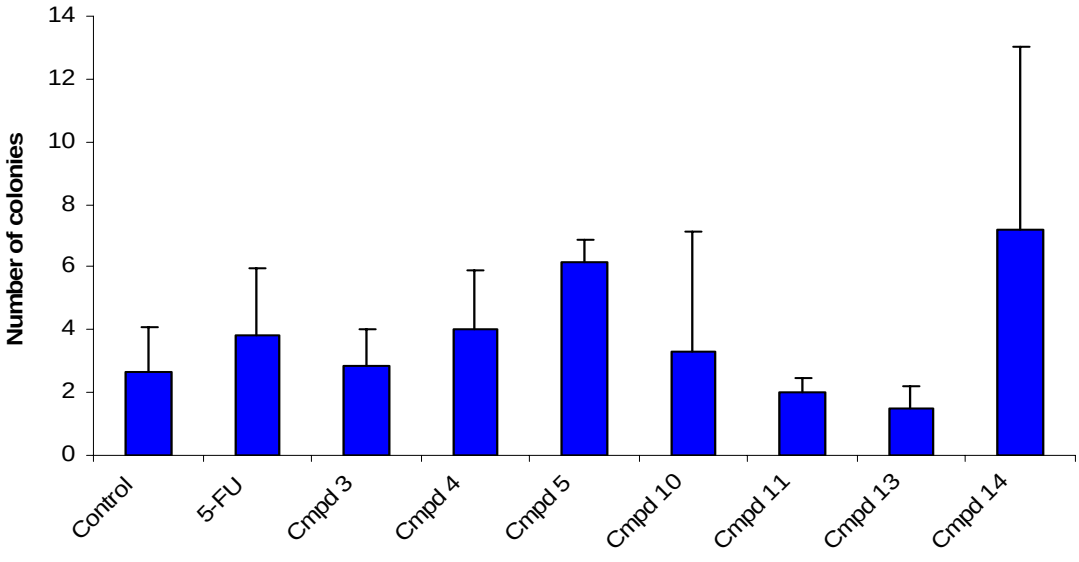

Figure 4.26 Effect of treatment with 0.5 nM 5-FU and 5-FU derivatives for 3 days on 4T1 cell colony formation in soft agar assay. In comparison to the control, treatment with compounds 11 and 13 resulted in a decrease in the number of colonies formed. Compounds 5 and 14 caused the largest increase in number of colonies formed.

4.3 Discussion

5-FU has been used extensively in chemotherapy for the treatment of a range of cancers over several decades. Despite its widespread use, response rates are still only 40-50% following combination treatments (Longley *et al*., 2003 and Venook, 2005). More efficacious drugs are required to increase patient survival. Drugs that specifically target the tumour would reduce side-effects of therapy, improving the quality of life of patients, and allow higher doses to be administered. Toward this end, a number of derivatives of 5-FU and its nucleoside, 5-FUrd, were synthesised and examined for their effect on proliferation, cell cycle kinetics, apoptosis, migration, invasion and the ability to form colonies in soft agar. The aim of the design and synthesis of these compounds was to gain insight into the effect of various additions and modifications to 5-FU and 5-FUrd on toxicity and mechanisms of action of the drugs. As such, this work was part of a SAR study to refine structural requirements for biological activity of the compounds.

Eight derivatives of 5-FU and 4 derivatives of 5-FUrd were synthesised, including nitro-benzyl, ester and acid derivatives. The nitro-benzyl derivatives, compounds 3, 6, 9, 13 and 14 were designed as prodrugs, with the nitro-benzyl side-chain to be cleaved by reductases within the cell, yielding 5-FU and quinone methide, which would also be toxic to the cells, via formation of DNA adducts (Wang *et al*., 2005). The prodrug aspect will be further investigated in chapter 5. Initial cytotoxicity testing of all compounds was conducted in the 4T1 murine mammary cancer cell line. The nitro-benzyl derivatives of 5-FU showed different toxicities towards the cells, with compound 3 marginally less toxic than 5-FU, compound 13 considerably less toxic and compound 14 showing low toxicity over the range of concentrations tested (Figure 4.4 and Table 4.2). Unfortunately, compound 14 could not be tested to higher concentrations as this would have resulted in a final concentration of greater than 0.1% DMSO. As these three compounds were designed as prodrugs, the lower toxicity of compounds 13 and 14 was not surprising. Low toxicity, below 20%, was seen for compound 14 up to 254 μM, due to the presence of two nitro-benzyl side-chains attached at both the N^1 and N^3 positions of 5-FU. Addition of these two side-chains increased the lipophilicity (ClogP value) and size of this compound in comparison to 5-FU (Table 4.1). Attachment of a side-chain to the

N^1 position interferes with formation of the corresponding nucleoside, preventing bonding with the sugar (Figure 4.27). For 5-FU, this meant the toxicity via production of 5-FUTP, 5-FdUTP and 5-FdUMP was prevented, hence the lack of effect of compound 14 on the cells.

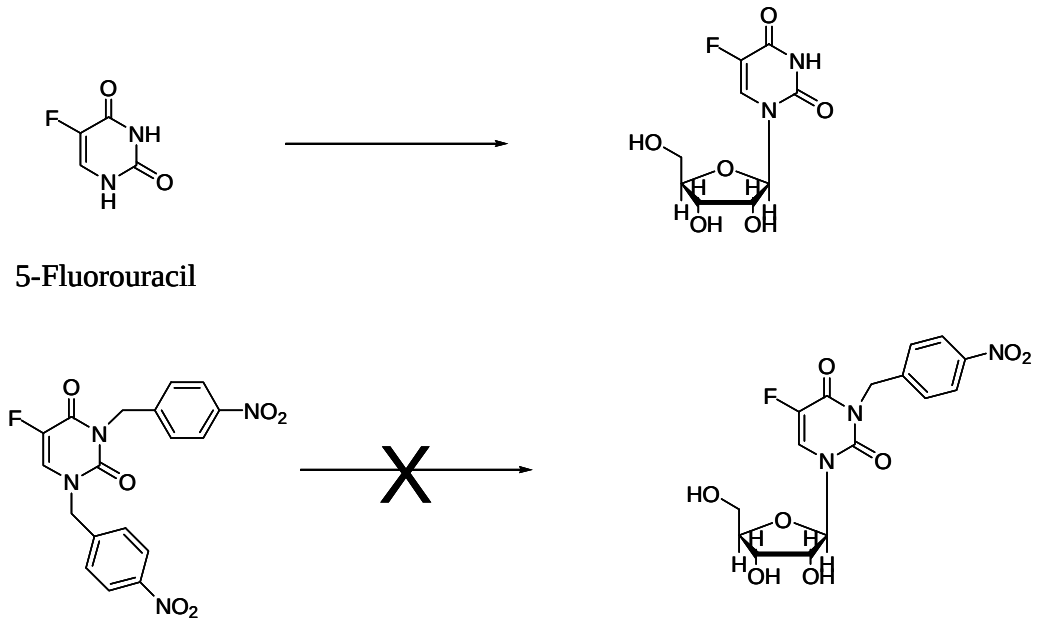

Figure 4.27 Formation of nucleosides from 5-FU and compound 14. The nitro-benzyl side-chain attached to the N^1 position in compound 14 blocks addition of the sugar.

Compound 3 had considerable toxicity despite the nitro-benzyl side chain at the N^3 position. Addition of this side-chain resulted in a lipophilicity value and size of 1.62 and 159 $Å^3$ respectively (Table 4.1). As the N^1 position of this compound was not bound by a side-chain, the compound was still be able to form the corresponding nucleoside, as depicted in Figure 4.28. Thymidylate synthase attacks the carbon atom next to the N^1 position, and the nitro-benzyl side-chain would not hinder this process, thus this molecule is most likely exhibiting its toxicity via thymidylate synthase inhibition, like the parent 5-FU (Figure 4.28). Since it may form the nucleoside, this compound may also cause cytotoxicity via misincorporation

into DNA and RNA. The addition of the nitrobenzyloxycarbonyl side-chain to the N^3 position in compound 13 suppressed toxicity of 5-FU up to approximately 10 μM after 3 days. The ClogP value and size of this compound was 0.658 and 182 $Å^3$ respectively (Table 4.1). The side-chain would not hinder the formation of the nucleoside but would affect the reaction with the thymidylate synthase complex (Figure 4.28). This compound would be less reactive to attack by the enzyme complex due to the extended conjugation of the carbamate linkage (Figure 4.29).

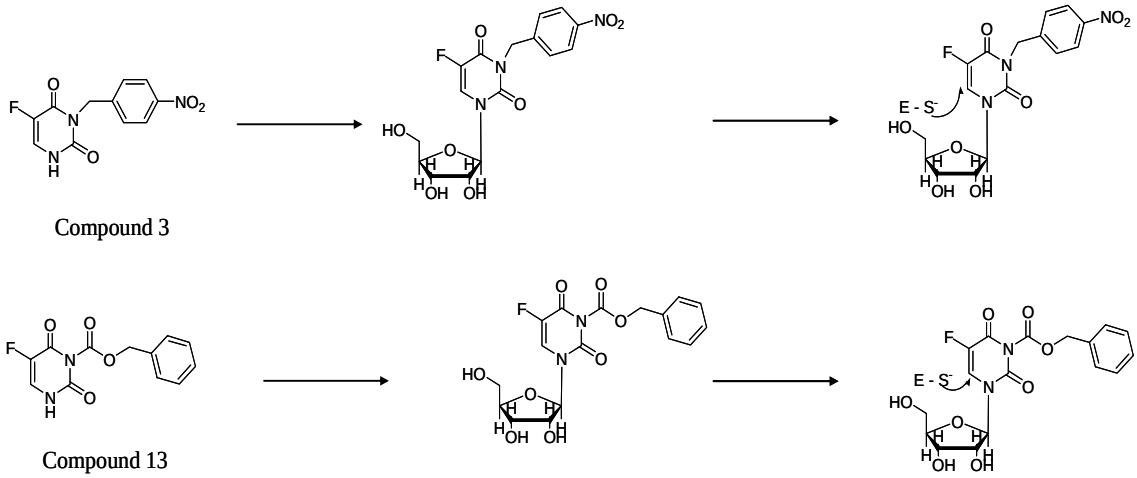

Figure 4.28 Formation of nucleosides from compounds 3 and 13. $E\text{-}S^-$ represents thymidylate synthase enzyme.

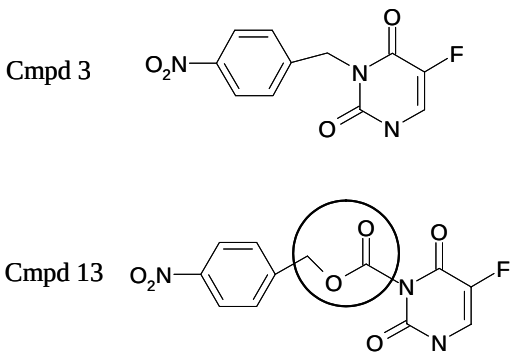

Figure 4.29 Extended conjugation due to carbamate linkage of compound 13 would hinder reaction with the thymidylate synthase enzyme, in comparison to compound 3.

The ester derivatives of 5-FU, compounds 4, 5, 10 and 11, were all toxic to the 4T1 cells, with similar, if not lower, IC_{50} values to 5-FU (Figure 4.5 and Table 4.2). The ester side-chains were introduced to increase the lipophilicity of the drug, resulting in increased absorption by the cells. As can be seen from Table 4.1, the ClogP values have were increased in compounds 5, 10 and 11 with a corresponding increase in size. The ClogP value and size of compound 4 were unfortunately not determined. Compound 10, with an allyloxycarbonylmethyl group attached at the N^3 position, was extremely toxic to the cells with an IC_{50} value one order of magnitude lower than 5-FU. Compound 11 had a benzyloxycarbonylmethyl side-chain attached at both the N^1 and N^3 positions and was also more toxic than 5-FU, with an IC_{50} value after 3 days treatment of 0.21 μM. Compound 5 had this same side-chain attached at just the N^1 position and had an IC_{50} value of 0.34 μM after 3 days treatment. Compound 4 had a longer methoxy ester chain attached to the N^1 position, and exhibited toxicity marginally less than 5-FU, with an IC_{50} value of 0.63 μM after treatment for 3 days.

The toxic nature of these compounds indicated increased uptake of the drug and also rapid cleavage of the side-chains following addition to the cells. Inclusion of the ester side-chain allowed the bond between the N^1 of 5-FU and the first carbon of the side-chain to become more labile to chemical/enzyme hydrolysis, as illustrated in Figure 4.30 with compounds 11 and 5. Compounds 4 and 10 underwent the same hydrolysis reaction. The increased lipophilicity would have caused greater absorption of the compounds, resulting in the increased toxicity observed with compounds 10 and 11 in comparison to the parent 5-FU molecule. The free side-chains of these compounds may also have contributed to the toxicity seen in the cells. The double bond at the end of the side-chain of compound 10 would increase the toxicity of this side-chain (Thomas, 2000). The acid derivative, compound 12, exhibited toxicity in the 4T1 cells which strikingly mirrored that of the parent 5-FU. Again, for this molecule, rapid hydrolysis of the side-chain to release 5-FU would account for the toxicity seen in the cells.

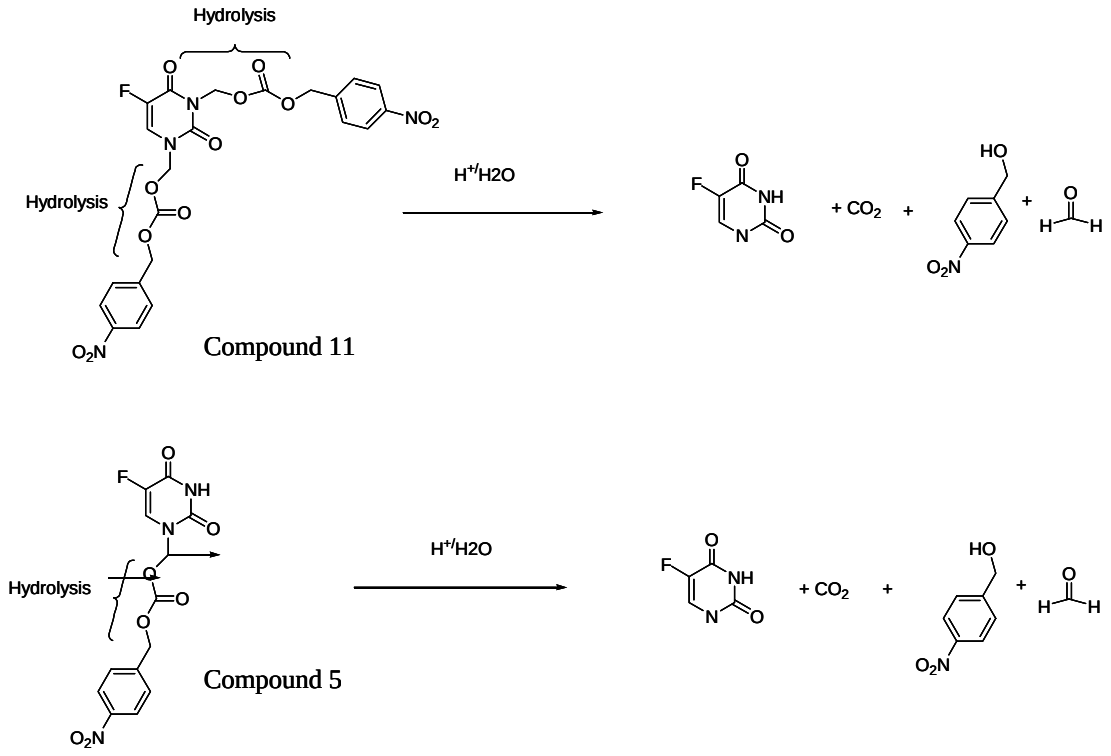

Figure 4.30 Hydrolysis of the carbamate bridge of side-chains in compounds 11 and 5.

5-FUrd proved to be very toxic to the cells, with an IC_{50} value of 0.018 μM after treatment for 3 days, in comparison to 0.35 μM for 5-FU (Table 4.2). This was due to the fact that 5-FUrd in effect skips a step in the anabolism of 5-FU, and was available to be immediately utilised by UK for conversion to 5-FUMP, followed by further phosphorylation to 5-FUDP and 5-FUTP, leading to RNA misincorporation. 5-FUDP can also be reduced to 5-FdUDP and from there can follow the pathways to effect DNA misincorporation and TS inhibition (Figure 4.1). All of the derivatives of 5-FUrd showed low toxicity (Figure 4.7 and Table 4.2). Addition of the side-chains increased the ClogP values and size of compounds 6, 8 and 9. These values could not be determined for compound 7. Compound 8 had the C-2 and C-3 hydroxyl groups of the sugar protected in comparison to the parent 5-FUrd (Table 4.1). This modification alone prevented the toxicity of the molecule. Compound 6 had the nitro-benzyl group attached to the N^3 of the 5-FUrd and again this modification caused the reduction of toxicity of this molecule. Compound 9 was a combination of compounds 8 and 6 – with both the protected C-2 and C-3 hydroxyl groups and the

nitro-benzyl group at the N^3 position, and showed minimal toxicity to the 4T1 cell line, due to a combination of the two modifications. Compounds 8 and 9, despite the protection of the C-2 and C-3 hydroxyl groups, would still be able to form the triphosphate molecule, as the C-5 hydroxyl is still available to form bonds with the phosphate groups. However, upon incorporation into RNA, the strand could not be elongated as the C-2 hydroxyl group would not be free to bind to the next nucleotide in the chain. They would also be unable to form 5-FdUMP, 5-FdUDP or 5-FdUTP as the C-3 hydroxyl group could not be removed by RR. Thus the mechanisms of action of 5-FU were prevented by the protection of the hydroxyl groups. Compound 7 had the protected C-2 and C-3 hydroxyl groups and had a Taxol-derived side-chain attached to the C-5 of the sugar. This side-chain should enhance diffusion of the compound into the cell but would also prevent binding of the phosphate groups to the sugar, thus having a negative effect on formation of the nucleotides, 5-FUMP, 5-FUDP or 5-FUTP.

The lack of toxicity of compound 6 was interesting but puzzling at the same time, as compound 6 was in fact the nucleoside of compound 3. Compound 3 had an IC_{50} value of 0.71 μM in the 4T1 cell line after treatment for 3 days, while compound 6 exhibited no toxicity up to 7.6 μM, the highest concentration available for testing. One possibility for the difference in toxicity is the lipophilicity and size of the compounds. Compound 3 had a ClogP value of 1.62 and a size of 159 $Å^3$, whereas compound 6 had a ClogP value of -1.15 and a size of 283 $Å^3$. The decrease in lipophilicity and increase in the size of compound 6 could affect the uptake of the compound and consequently the toxicity.

The cytotoxicity of these compounds was also tested in the SW480 human colorectal cancer cell line. Toxicity profiles were similar to those in the 4T1 cell line with IC_{50} values being generally higher. Of the nitro-benzyl derivatives, compound 3 had an IC_{50} value of 11 μM after treatment for 3 days, in comparison to 4.9 μM for 5-FU. Compounds 13 and 14 showed low toxicity with no IC_{50} values established over the ranges tested. Compounds 10 and 11, the ester derivatives, were again more toxic than 5-FU and compounds 4 and 5 were slightly lower in toxicity than 5-FU. This would indicate that the rapid hydrolysis of the side-chain was also occurring in this cell line. The acid derivative, compound 12, and the 5-FUrd derivatives all had similar effects on the SW480 cell line as in the 4T1 cell line.

Resistance of tumour cells to 5-FU is a major factor influencing response rates following treatment. Numerous different enzymes are involved in the anabolism and catabolism of 5-FU in the body and varying levels and activity of these enzymes can affect resistance to therapy (Longley *et al.*, 2003 and Boyer *et al*., 2004). Selected compounds were tested on the HCT(P) and HCT(R) cell lines. The HCT(R) cell line was established following repeated exposure to stepwise increasing concentrations of 5-FU, resulting in a 3-fold increase in the IC_{50} value observed (Boyer *et al*., 2004). Analysis of the cytotoxicity of the 5-FU derivatives in the resistant cell line could possibly identify if any of the compounds could overcome resistance due to an alternative mechanism of cytotoxicity towards the cells, and could possibly highlight strategies to do so. Molecular analysis of the 5-FU resistant cell line revealed a reduction in the levels of TP mRNA, the enzyme which processes 5-FU to 5-FdUrd, and an increase in TK mRNA (Boyer *et al*., 2004). TK salvages thymidylate from exogenous thymidine when the intracellular supplies are low. There was no difference in the levels of DPD, TS, UK, or UP mRNA between the parental and resistant cell lines (Boyer *et al*., 2004).

After treatment for 3 days, the IC_{50} value of 5-FU in the parental cell line was 4.5 μM and two-fold higher, 9 μM, in the resistant cell line (Table 4.4). The IC_{50} value in the HCT(R) cell line was lower than the IC_{50} of 12.7 μM reported by Boyer *et al*. (2004). After treatment for 5 days, the ratio of IC_{50} values had increased to 4-fold. 5-FUrd exhibited the most toxicity towards the parental and resistant cell lines, with 3 day IC_{50} values of 0.16 μM and 0.23 μM respectively, giving a ratio of 1.44. After 5 days treatment, the ratio of IC_{50} values had decreased to 0.86 for 5-FUrd (Table 4.4). A decreased ratio would indicate an increase in sensitivity of the resistant cell line to the treatment. IC_{50} values were not established for compounds 11, 13 and 14 after treatment for 3 or 5 days. This was surprising for compound 11 as the IC_{50} values in the SW480 colorectal cancer cell line had been established as 2.05 μM and 1.2 μM after treatment for 3 and 5 days respectively.

The nitro-benzyl derivative, compound 3, showed toxicity after treatment for 3 and 5 days, with ratios of IC_{50} values of 1.83 and 1.13 respectively. Compound 10 had an IC_{50} value of 0.47 μM in the HCT(P) cell line, and 0.8 μM in the HCT(R) cell line after treatment for 3 days. These values are greater than one order of magnitude lower than the IC_{50} values for 5-FU. The ratio of the IC_{50} values for compound 10

was 1.7. After treatment for 5 days, however, the IC_{50} value had not decreased in the HCT(P) cell line, while the IC_{50} value for the HCT(R) cell line was established as 0.42 μM, and the ratio had consequently decreased to 0.89. This indicates increased sensitivity of HCT(R) cell line to this compound and could reflect a different mechanism of action of toxicity. Compound 4 had ratios of IC_{50} values of 1.7 and 1.28 after 3 and 5 days treatment respectively, while compound 5 had a ratio of 2.33 after treatment for 3 days and 1.44 after treatment for 5 days. The derivatives with the ester side-chains, compounds 4, 5 and 10, were seen to have high toxicity in the 4T1 and SW480 cell lines. The decrease in ratio may be due to the increased uptake of the compounds and toxicity exhibited by the side-chains of these compounds. Also, it is a possibility that the compounds are not deactivated as efficiently by the catabolic enzyme DPD, resulting in increased toxicity in the resistant cell lines.

Following analysis of the cytotoxicity of the derivatives, we wanted to investigate the mechanisms involved in this process and also to look at the effect on migration, invasion and colony formation in soft agar. The 5-FU nitro-benzyl and ester derivatives were chosen for the remaining experiments, due to availability of larger quantities of these compounds. Firstly, the effect of the derivatives on cell cycle kinetics and apoptosis was investigated. The Guava® PCA system was used for these experiments. This machine has been designed for high-throughput, benchtop use with the required assays pre-programmed into the system. For the cell cycle analysis, the Multicycle software uses a more accurate method than the Guava® software for deciphering the populations in the different stages. This software uses an algorithm which assumes the G1/G0 and G2/M phases have normal distribution and subsequently calculates the S phase population accordingly.

The effect of 5-FU on the cell cycle has been investigated by a number of groups. Marchal *et al*. (2004) looked at the effect of 5-FU on the breast cancer cell line, MCF-7. Following treatment with 2.75 μM 5-FU for 48 hours, a decrease in the number of cells in G0/G1 phase (68% to 58%) and in G2/M phase (12% to 2%), and a corresponding increase in S phase population (20% to 39%) was observed in comparison to the control cells. Boyer *et al*. (2004) investigated the effect of 1 μM, 5 μM and 10 μM 5-FU on the colorectal cancer cell line HCT116, after treatment for 3 days. They noted an S phase arrest after treatment with 1 μM and a G2/M phase arrest after treatment with 5 μM and 10 μM. Upon cell cycle analysis with the DLD-

1, LoVo and SW620 colorectal cancer cell lines, Tokunaga *et al*. (2000) concluded three modes of cell growth modulation following treatment with 5-FU. The drug was seen to cause both a loss of, and an accumulation in, the S phase population; a G2/M block; and arrest in the G1/S border; depending on the cell line and the concentration of treatment. Li *et al*. (2004) treated the NA and HSC-4 oral cancer cell lines with 1 mg/ml and 10 mg/ml of 5-FU (7.7 mM and 77 mM) and observed late G1/early-S phase accumulation over 8-24 hours. The effect of 5-FU on DNA synthesis, through the inhibition of TS and misincorporation into DNA, will manifest itself in the S phase while RNA misincorporation of 5-FU occurs in the G1 phase (Li *et al.*, 2004). The different regimens of administration of 5-FU to patients may even have an effect on the perturbation of the cell cycle, with continuous infusion exhibiting toxicity through TS inhibition while bolus administration resulted in RNA inhibition (Xiong and Ajani, 2004).

In the work presented here, 5-FU treatment at 0.1 μM showed mainly an increase in the number of cells in G2 phase and a decrease in the G1 cell population (Figures 4.15 and 4.16, Table 4.5). Following treatment with 1 μM 5-FU, 62% of cells were in G1 phase and the remaining were in G2 phase, with no cells in S phase (Figures 4.17 and 4.18, Table 4.6). These results would indicate that following treatment with the lower concentration of 5-FU, cells were still moving into the S phase for DNA replication but there was a pause before mitosis due to the cell damage, causing a build-up of cells in G2 phase. At the higher concentration, cells were no longer moving into the S phase, possibly due to RNA misincorporation, and were arrested in G1 and G2 phases. Compounds 3, 4 and 5 had similar effects on the cell cycle kinetics. Treatment with compound 11 at 0.1 μM resulted in a decrease in G1 phase and increases in S and G2 phases, indicating S phase and G2 phase arrest. The higher concentration of 1μM caused an accumulation of cells in G1 (56.4%), possibly due to RNA misincorporation of 5-FU.

Compound 10 had the most dramatic effect on the cells, with 92.4% of cells in S phase and 7.6% cells in G1 phase after treatment with 0.1 μM. After treatment with 1 μM of compound 10, 71.2% of the cell population were in S phase with 28.8% in G1 phase (Figures 4.17 and 4.18, Table 4.6). This indicated inhibition of replication of DNA in the S phase due to extensive DNA damage, with the cells unable to proceed to the G2 phase due to their arrest and subsequent death. Hence, it would

appear that compounds 3, 4, 5 and 11 were having more of an effect on both RNA misincorporation and DNA synthesis, as the cells were arresting in G1 phase but also appeared to be pausing before mitosis, probably due to errors in DNA replication which would have occurred during S phase. Compound 10 appeared to be affecting mainly DNA synthesis in the S phase, with damaged cells accumulating in this phase. Treatment with 0.1 μM and 1 μM of compounds 13 and 14 had little effect on the cell cycle. This would correlate with the cytotoxicity data, with low levels of cell death seen at these two concentrations.

This analysis showed that the 5-FU derivatives were affecting different aspects of the cell cycle. Arrest in G1, S and G2 phases was seen depending on the concentration and compound. Numerous molecules play a role in the complex process of regulation of the cell cycle, including the cyclins and cyclin-dependent kinases (CDKs). The G1 checkpoint is regulated by cyclins D and E, and Cdk2 and Cdk4, with p21, Rb and p53 also playing roles in determining cell cycle progression or arrest (Sampath, 2001). Progression through S phase checkpoints is determined by cyclin A, Chk1, Chk2, Cdc25A and Cdk2. Cyclin B, Cdk1, Chk1, Chk2 and Cdc25C play a role in G2 checkpoint regulation (Sampath, 2001). Had time and resources allowed, further investigation into the effect of the 5-FU derivatives on the levels of these key players of cell cycle progression would have been an interesting topic.

Apoptosis of the cell is accompanied by many morphological changes, including nuclear chromatin condensation, fragmentation of DNA, cell shrinkage, collapse of the mitochondrial membrane potential and changes at the cell surface. This is a controlled process, hence also known as programmed-cell death. In contrast, necrosis results in uncontrolled swelling, followed by rupture of the plasma membrane, and non-specific DNA degradation (Brown and Attardi, 2005). Changes at the cell surface of apoptotic cells allow the annexin V assay to monitor this occurrence. Early in apoptosis, the phosphatidylserine molecule moves from the inner membrane to the outer membrane of the cell surface. Annexin V binds to this molecule on the outer membrane. When used in conjunction with 7-AAD, which enters cells late in apoptosis or during necrosis, an indication of the populations of cells going through early and late apoptosis and necrosis can be monitored.

Marchal *et al*. (2004) subjected MCF-7 breast cancer cells to 2.75 μM 5-FU and monitored the effect on apoptosis after treatment for 6, 12 and 24 hours. After 6

hours of treatment, 66% of cells were undergoing apoptosis, with 38% in the early stage and 28% in the late stage. Following 12 and 24 hours treatment, the percentage of cells undergoing apoptosis was still 66%, with varying amounts in early and late stages. Espinosa *et al*. (2005), using the same cell line, observed 57% and 53% apoptotic cells following treatment with 2.75 μM for 24 and 48 hours. In our work, the control cells showed approximately 10% apoptotic cells, with 5-FU treatment increasing this to 12% and 37% for 0.1 μM and 1 μM, respectively (Figures 4.19-4.21). Treatment with 0.1 μM compound 10 caused an increase in cells undergoing apoptosis (45%), with compound 11 increasing the apoptotic population to 24%. The result for compound 10 was statistically significant in relation to both the control cells and the 5-FU treated cells ($p<0.01$). The remaining compounds, at 0.1 μM, showed minimal effect on apoptosis of the cells.

Treatment with 1 μM of the derivatives resulted in a more dramatic effect on apoptosis (Figure 4.20). Compounds 3, 4 and 5 showed an increase in apoptotic cells to 26-29%. Treatment with compounds 10 and 11 resulted in increases to 46% and 29% respectively. These results were all statistically significant in relation to the result for the control cells ($p<0.05$). Treatment with compounds 13 and 14 had minimal effect in comparison to the control-treated cells, however their results were statistically significant in relation to the 5-FU treated cells ($p<0.01$). These results reflected those seen in the cytotoxicity data, although the percentage of apoptotic cells does not seem to reach the corresponding percentage cell death values across the spectrum of results. The levels of apoptosis were higher in the work of Marchal *et al*. (2004) than seen in our work, which could be explained by the different concentrations used.

There are two different apoptotic pathways that cells undergo following death-inducing signals. The extrinsic pathway is mediated by receptors on the cell membrane including CD95 and TNF-related apoptosis-inducing ligand (TRAIL) receptors, which interact with intracellular proteins such as Fas-associated death domain (FADD) and caspase-8 to induce the caspase cascade (Fulda and Debatin, 2006). Intrinsic pathway activation occurs following disruption of the mitochondrial membrane, releasing cytochrome *c*, apoptosis inducing factor (AIF) and Smac/DIABLO into the cytosol. Subsequent caspase activation leads to apoptosis of the cell. These two pathways may also run concurrently and have an accumulative

effect on the progress to cell death. p53 protein plays a role in both pathways, with p53-inducible elements in the promoter region of the gene encoding the CD95 protein, involved in the extrinsic pathway. In the intrinsic pathway, p53 can play a role in relaying DNA damage signals to the mitochondria and can also activate the expression of pro-apoptotic Bcl-2 proteins (Fulda and Debatin, 2006). Considering the fact that the 4T1 cell line is p53-null, this would be an interesting area of investigation to pursue in future work – to elucidate the proteins involved in apoptosis induced by the 5-FU derivatives.

Metastasis of tumour cells to secondary sites of the body plays a significant role in the prognosis of the disease. Numerous factors influence this action, including the ability of the tumour cell to migrate, to invade the ECM and also to grow and divide in a new organ (Bogenrieder and Herlyn, 2003). 5-FU is used in chemotherapy for metastatic cancers, thus we wanted to investigate the possible effects of these new compounds on migration, invasion and colony formation in soft agar. Cells were pre-treated with 0.5 nM 5-FU and 5-FU derivatives for 48 hours before being seeded into Falcon™ cell culture inserts (migration) or BD BioCoat™ Matrigel™ Invasion Chambers, with further treatment, and incubated for 24 hours. Cells that succeeded in migrating or invading through the pores of the membrane were fixed, stained with crystal violet and the stain eluted out with glacial acetic acid and absorbance read.

Surprisingly, given the fact that 5-FU was already used extensively in chemotherapy for primary and metastatic tumours, the literature regarding its effect on *in vitro* migration and invasion was not extensive. 5-FU has been shown to have a varied effect on the migration of cells, with no effect seen at lower concentrations (<1 μg/ml/<7.7 μM) and inhibition noted at concentrations of 1 μg/ml (7.7 μM) and higher (Gordon *et al.*, 2005). Warusavitarne *et al*. (2006) observed no significant difference in the rate of invasion of HCT116, LoVo, LIM1215 and KM12C cell lines which were seeded into the chambers in media containing 50 μM 5-FU and incubated for 24 hours. Liang *et al*. (2004) established a 5-FU resistant variant from the human squamous cell line DLKP by pulse selection with 2 ng/ml (15.4 nM) over 4 months. This cell line was shown to be significantly more invasive after 48 hours than the parental cell line ($p<0.001$).

In this work, the sub-lethal dose of 0.5 nM caused only increases in cell

migration in comparison to the control-treated cells (Figures 4.22 and 4.23). 5-FU and compounds 3, 4, 13 and 14 showed an increase in the number of cells that migrated through the membrane, with the results for compounds 3, 4 and 14 being statistically significant. For the invasion assay, all the treatments of 0.5 nM resulted in an increase in the number of cells that invaded (Figures 4.24 and 4.25). Compounds 3 and 4 had the greatest effect on invasion, with the result for compound 4 being statistically significant ($p<0.05$). There are numerous players that have a role in the processes of migration, invasion and anchorage-independent growth, including enzymes such as the MMPs and cell adhesion molecules such as integrins and cadherins (Egeblad and Werb, 2002 and Cavallaro and Christofori, 2004). However, as there was no significant reduction observed in the migration or invasion of the 4T1 cells following treatment with the 5-FU derivatives, this area of investigation was not pursued.

Colony formation in soft agar is used to investigate possible anticancer agents and their effect on the proliferative capacity of cancer cells. Fiebig *et al*. (2004) looked at the effect of a number of chemotherapeutic agents, including 5-FU, on the growth of human tumour xenografts in soft agar. The colon carcinoma xenograft was not affected by treatment with 0.2 μg/ml (1.5 μM) or 0.6 μg/ml (4.6 μM) 5-FU while the lung carcinoma xenograft showed a reduction of colony counts to between 30 and 50% of the control after 0.2 μg/ml and below 10% after 0.6 μg/ml treatment. Our results showed a decrease in the numbers of colonies formed after treatment with compounds 11 and 13, although the results were not significant and the colony counts were not below 30% of the control (Figure 4.26). 5-FU and compounds 4, 5 and 14, however, caused an increase in the number of colonies formed in the soft agar, although these results were not significant. The work of Fiebig *et al*. (2004) was to test the resistance of the xenografts to treatments in comparison to the response of the patient and so they used a higher concentration than in our experiments. Further investigation in this area could have examined the effect of different concentrations of the 5-FU derivatives. Alternatively, the assay could be changed to allow the formation of the colonies in the soft agar followed by treatment with the derivatives, rather than the pre-treatment method used in this work.

Investigation of the cytotoxicity of the 5-FU and 5-FUrd derivatives generated interesting results, with compound 10 proving the most toxic of the compounds, even

more toxic than the parent 5-FU. The remaining ester derivatives, compounds 4, 5 and 11, were found to be highly toxic compounds also, with increased lipophilicity due to the side-chains. Analogues of compound 10 are currently being synthesised to investigate further the structural components underlying its toxicity. Conversely, the lack of toxicity seen with the prodrugs of 5-FU (compounds 13 and 14) and 5-FUrd (compounds 6 and 9) towards the 4T1 and SW480 cell lines showed promise as activation of these prodrugs could lead to toxicity in the tumour cell environment. Thus, this avenue of investigation was followed – methods of activation and toxicity of the activated prodrugs (Chapter 5).

4.4 Summary

Twelve derivatives of 5-FU and 5-FUrd were synthesised and tested for cytotoxic properties using the 4T1 and SW480 cell lines. Varying responses were noted, from low toxicity (compounds 6-9, 13 and 14) to increased toxicity (compounds 10 and 11) compared to the parent compounds. Cytotoxicity results using the HCT116 parental and resistant cell lines showed an increase in sensitivity of the resistant cell line to the 5-FU derivatives (compounds 3, 4 and 10). Cell cycle analysis of the 4T1 cell line revealed two different modes of action – arrest during the S phase (compound 10) or arrest in G1 and G2 phases (compounds 3, 4, 5 and 11). Apoptosis analysis showed a significant increase following treatment with 1 μM 5-FU, compounds 3, 4, 5, 10 and 11, and correlated with the cytotoxicity data. Investigation of the effect of the derivatives on migration of the 4T1 cell line resulted in a significant increase following treatment with compounds 3, 4 and 14. Invasion assays also showed compound 4 caused a significant increase in invasion of the 4T1 cells. There was no significant effect on growth of colonies of treated 4T1 cells in soft agar assays. This aspect of analysis of the compounds was not pursued following these results. Having identified a number of prodrug-designed compounds with low toxicity (compounds 6, 9, 13 and 14) this area was focused on for further study.

Chapter 5

Prodrug derivatives of 5-Fluorouracil and 5-Fluorouridine: Analysis of activation and cytotoxicity

5.1 Introduction

5.1.1 Tumour-activated prodrugs

Prodrugs are pharmacologically inactive drugs that are transformed into an active metabolite which exhibits pharmacological effects. They were first described by Albert (1958) and can be designed to overcome inadequate pharmacokinetic or pharmacodynamic properties such as chemical instability, poor solubility or poor absorption, but also to target the drug to the site of action (Ettmayer *et al*., 2004). The latter type, termed tumour-activated prodrugs (TAP) in relation to cancer therapy, will be concentrated on here. TAPs come in the form of bioreductive or enzyme targeted prodrugs. Bioreductive prodrugs can be activated by specific intracellular conditions including hypoxia or increased tissue- or cell-specific enzymes. Prodrugs can also be activated by enzymes in enzyme prodrug therapy (EPT), in which case the enzymes are delivered to the cell via three different mechanisms: antibody-directed (ADEPT), gene-directed (GDEPT) or virus-directed (VDEPT) (Denny, 2001).

In general, there are three domains present in a TAP referred to as a trigger, a linker and an effector (Figure 5.1). The trigger undergoes selective metabolism at the site of action. The linker deactivates the drug until metabolism of the trigger. The effector is the active drug and exerts the cytotoxic effect on the tissue when released. The effector should have a suitable half-life to cause sufficient cell death, while it should also be capable of diffusion to neighbouring cells to exhibit a bystander effect i.e. the death of neighbouring cells which have not activated the prodrug themselves (Denny, 2001).

Figure 5.1 Structure of tumour-activated prodrug, with three domains; trigger, linker and effector.

General properties of a prodrug are as follows: (a) it must distribute efficiently to the tumour site, (b) it must be selectively metabolised to a cytotoxic agent in the tumour only, and (c) it should be able to exhibit a bystander effect but without toxicity to neighbouring tissues or diffusion into the circulatory system (Denny, 2001 and Xu and McLeod, 2001). The released drug should be at least 100-fold more toxic than the prodrug in order to result in significant therapeutic gain (Greco and Dachs, 2001).

5.1.2 Bioreductive prodrugs

Bioreductive prodrugs are activated by intracellular conditions such as selective enzyme expression, hypoxia and pH differences. Increased gene expression of specific enzymes in tumour tissue as well as low extracellular pH conditions have been examined in relation to prodrugs. Hypoxia, however, has been the main area of research for bioreductive prodrugs. Hypoxia, or low oxygen tension, occurs within a tumour when oxygen demand exceeds oxygen supply (Airley *et al*., 2000). Oxygen levels in normal cells can vary between 3.1 and 8.7% while tumours can have oxygen levels as low as 0.01% (Kizaka-Kondoh *et al*., 2003). Breast cancer tumours reportedly have a median oxygen level of 1.4% (Brown and Wilson, 2004). If a cell in a tumour is greater than 50 μm from a capillary, it is hypoxic. A complete lack of oxygen, anoxia, occurs if a cell is greater than 145 μm from a blood supply (Airley *et al*., 2000). Hypoxic regions occur as a tumour increases in size but also due to the poorly developed vascular system in solid tumours. Two types of hypoxia exist within a tumour: chronic and acute. Chronic hypoxia occurs due to the distance of the cell from the nearest blood vessel, although these cells can still survive and proliferate (Kizaka-Kondoh *et al*., 2003). Acute or transient hypoxia is a result of temporary shut down of blood vessels (Kizaka-Kondoh *et al*., 2003 and Denny, 2001). Hypoxic conditions in a tumour are associated with resistance to chemotherapeutic and radiation treatment, and a metastatic phenotype (Sinhababu and Thakker, 1996 and Brown and Wilson, 2004).

Hypoxia-selective prodrugs are generally substrates for enzymes present in all cells of the body. However, in normal tissues the reaction is incomplete or reversed

due to the presence of oxygen while in the hypoxic tumour cells the reaction is allowed to commence and the active drug is produced (Figure 5.2) (Sinhababu and Thakker, 1996). The prodrugs need to have effective extracellular distribution in order to reach the hypoxic cells distant from the blood vessels. After activation however, the drugs should have a short half-life so that they do not diffuse into neighbouring tissues or into the circulatory system.

The enzymes involved in activation of prodrugs include cytosolic reductases (carbonyl reductase, DT-diaphorase, xanthine oxidase, aldehyde oxidase), mitochondrial reductases (dihydrolipoamide dehydrogenase, cytochrome b5 reductase, succinate dehydrogenase) and microsomal reductases (NADPH-cytochrome reductase, cytochrome P450) (Smyth and Orsi, 1989). The majority of these enzymes are one-electron reductases. DT-diaphorase (also known as NQO1 – NAD(P)H-quinone oxidoreductase) and cytochrome P450 are two-electron reductases and carbonyl reductase can act as both a one-electron and two-electron reductase (Patterson, 2002 and Williams *et al*., 2001).

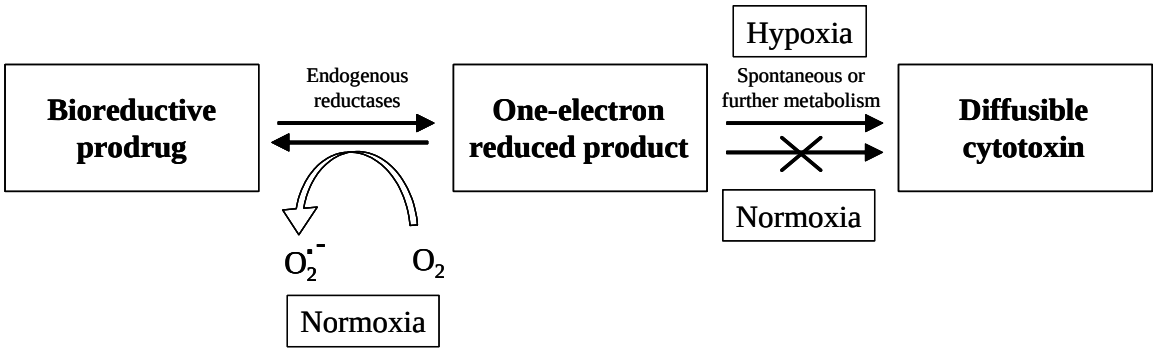

Figure 5.2 Mechanism of prodrug activation under hypoxia. Adapted from Denny, 2001 and Airley *et al*., 2000.

There are four types of bioreductive drugs activated under hypoxia: quinones, aromatic N-oxides, aliphatic N-oxides and nitroaromatics/nitroheterocyclics (Denny, 2001 and Airley *et al*., 2000). Cytochrome P450 reductase activates quinones by one-electron reduction to the semi-quinone radical anion. Following reduction, subsequent fragmentation to a DNA cross-linking species generates toxicity in cells (Denny, 2001). Tirapazamine (TPZ, 3-aminobenzotriazine-1,4-di-*N*-oxide) is an aromatic *N*-oxide which has shown promising results in conjunction with cisplatin in phase II and III trials in head and neck cancer and non-small cell lung cancer (Figure 5.3A) (Brown and Wilson, 2004). Under hypoxic conditions, TPZ undergoes a one-electron reduction to an oxidising radical that leads to DNA double-strand breaks, single-strand breaks and base damage (Kizaka-Kondoh *et al*., 2003 and Maluf *et al*., 2006). Cytochrome P450 and cytochrome P450 reductase are the enzymes responsible for this activation (Denny, 2001). AQ4N (1,4-bis-{[2-(dimethyl-amino-N-oxide)ethyl]amino}-5,8-dihydroxyanthracene-9,10-dione), an aliphatic N-oxide, is also a promising bioreductive agent. AQ4N is activated to AQ4 (1,4-bis-{[2-(dimethyl-amino)ethyl]amino}-5,8-dihydroxyanthracene-9,10-dione) under hypoxic conditions. AQ4 intercalates with DNA and blocks Topoisomerase II action (Figure 5.3B) (Kizaka-Kondoh *et al*., 2003). AQ4N is activated by two-electron reduction by the CYP3A isoenzyme of the cytochrome P450 family (Patterson, 2002). Nitroaromatics undergo six-electron reduction in cells by flavin-containing enzymes (Figure 5.3C) (Sinhababu and Thakker, 1996).

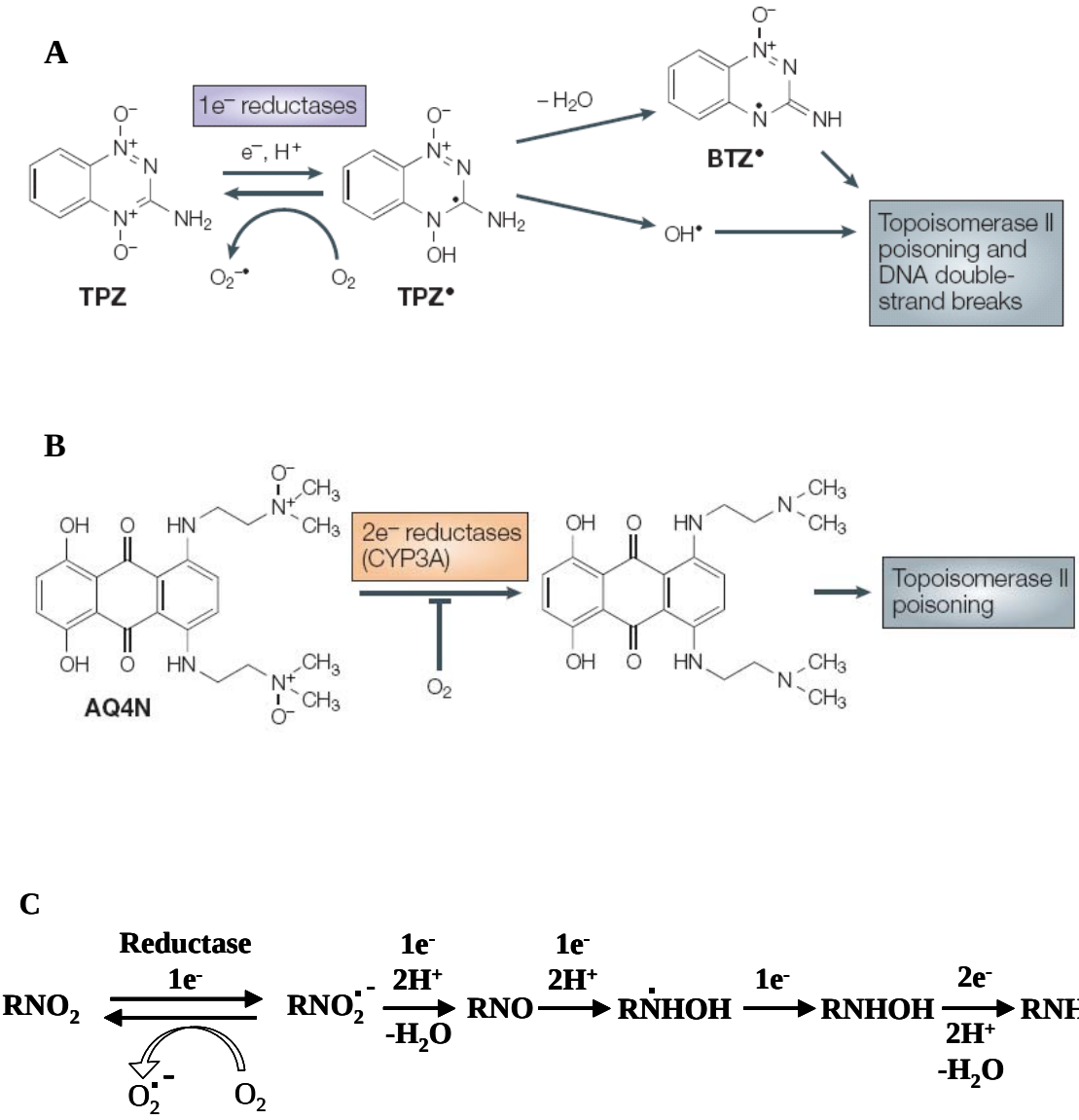

Figure 5.3 Structure and metabolism of prodrugs Tirapazamine (A) and AQ4N (B). From Brown and Wilson, 2004. (C) Nitroaromatic six-electron reduction. Adapted from Sinhababu and Thakker, 1996.

5.1.3 Antibody-Directed, Gene-Directed and Virus-Directed Enzyme Prodrug Therapy

ADEPT involves covalent linkage of a non-human enzyme to a monoclonal antibody that is directed against a tumour antigen. The prodrug must not be a substrate of any other human enzyme to avoid activation and toxicity in alternative sites of the body. The enzyme-antibody conjugate must be allowed to localise to the tumour and clear from normal tissue before the prodrug is administered. Following administration, the prodrug is activated by the enzyme at the site of the tumour only (Figure 5.4A) (Sinhababu and Thakker, 1996). There are a number of criteria to be fulfilled in order to maximise this therapy. Specificity of the antibody to the tumour cells is crucial and the enzyme-antibody conjugate must not be immunogenic (Sinhababu and Thakker, 1996). The prodrug should be limited in its ability to enter cells before activation, this maximises the pool of prodrug to be acted on extracellularly (Denny, 2001). The active drug must be able to diffuse into the tumour cells to exhibit its cytotoxic action. This would also result in a bystander effect as the prodrug is activated extracellularly and the active drug may then diffuse to neighbouring cells, without the need for each individual cell to express the antigen or to attract the antibody-enzyme conjugate. Conversely, limited diffusion to within the tumour is vital to avoid toxicity of neighbouring tissues. The half-life of the active drug would have an impact on this (Sinhababu and Thakker, 1996 and Denny, 2001).

GDEPT and VDEPT both focus on delivering a gene encoding a non-human enzyme into the tumour cell wherein the enzyme is produced (Figure 5.4B) (Ettmayer *et al*., 2004 and Rooseboom *et al*., 2004). In VDEPT, gene targeting is achieved by using viral vectors, most commonly retroviruses or adenoviruses, while in GDEPT, or suicide gene therapy, a non-viral vector is used for delivery of the gene (Rooseboom *et al*., 2004). For both systems, the vector delivering the gene must be taken up by the cells and subsequent stable expression of the enzyme is essential. The enzyme itself should not exhibit toxicity towards the cells (Kizaka-Kondoh *et al*., 2003).

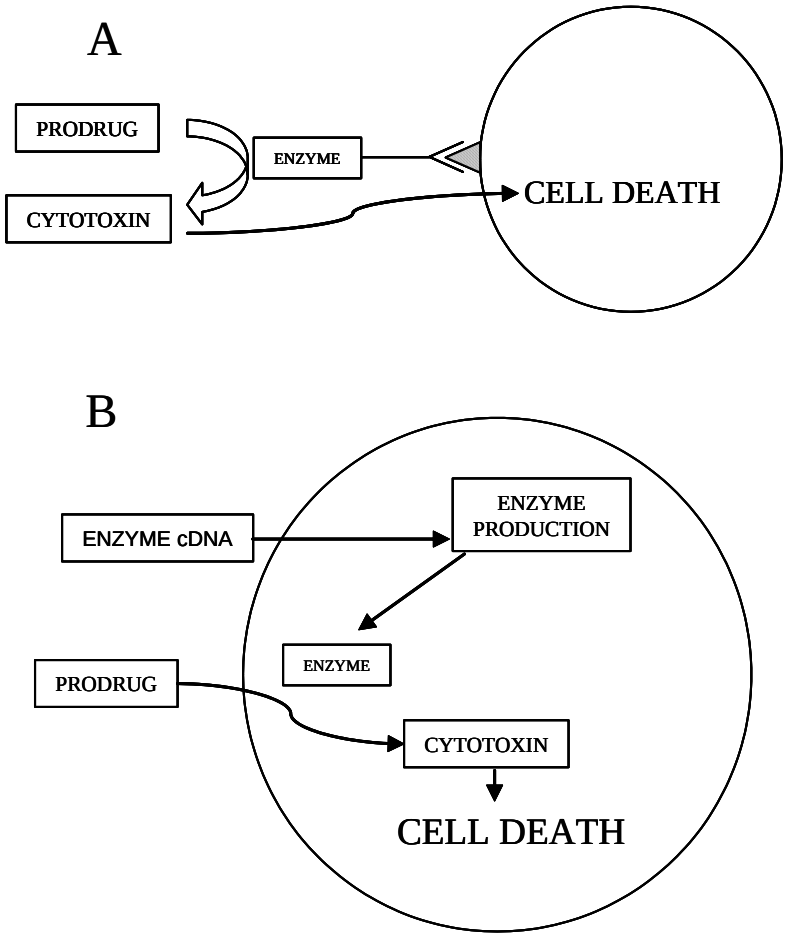

Figure 5.4 Diagrammatical illustrations of ADEPT (A) and GDEPT/VDEPT (B).

In GDEPT and VDEPT, it is necessary for the prodrug to enter the cell in order to undergo activation. The active drug must be able to diffuse to neighbouring cells to exhibit a bystander effect as gene delivery will not have occurred in 100% of cells (Rooseboom *et al*., 2004). Challenges to this system include selective delivery of the gene to the tumour tissue, immunogenic reaction to the DNA, and insertional mutagenesis (Ettmayer *et al*., 2004). A problem for VDEPT is that retroviral vectors only target dividing cells, and within a tumour, this constitutes only approximately 6-20% of the cells (Ettmayer *et al*., 2004). One advantage of the GDEPT/VDEPT system over ADEPT, however, is the requirement of the majority of enzymes for a co-factor, which are generally available intracellularly (Xu and McLeod, 2001). The literature at times refers to GDEPT even when viral vectors are used for delivery, hence VDEPT could in fact be considered a form of GDEPT.

5.1.4 CB1954 and Nitroreductase

CB1954 (5-aziridinyl-2,4-dinitrobenzamide) is an example of a prodrug activated by the *Escherichia coli* nitroreductase (NTR) enzyme. Initially, CB1954 was noted to be effective in the treatment of tumours in rats. CB1954 was activated by high levels of the DT-diaphorase enzyme present in the rat cells. However, this unfortunately did not translate to humans, as CB1954 was a considerably poorer substrate for the human form of the DT-diaphorase enzyme (Denny, 2001). The difference in reactivity between the enzymes from the two species was found to be caused by a one amino acid change at position 104 of the protein sequence (Denny, 2003). A related form, NQ02, which has no known physiological function, was found to have latent activity but only in the presence of the co-factor, dihydronicotinamide riboside (NRH) (Knox *et al*., 2003). This co-factor was expensive and time-consuming to make, making this an unattractive combination. An NRH substitute, EP-0152R has been selected for development with NQ02 (Denny, 2003).

CB1954 is, however, efficiently reduced by the *E. coli* NTR, a 24 kDa enzyme that uses NADH or NADPH as substrate and catalyses the reduction of nitro groups to hydroxylamine groups (Denny, 2003 and Rooseboom *et al*., 2004). This enzyme is a product of the *nfsB* gene in *E. coli* and is an oxygen-insensitive flavin mononucleotide (FMN)-containing NTR. NTR functions as a homodimer, with a FMN molecule attached to each monomer (Denny, 2003). Reduction by NTR occurs by a substituted enzyme (ping-pong) mechanism – firstly, reduction of FMN occurs by NADH or NADPH, followed by reduction of the CB1954 substrate by the FMN (Searle *et al*., 2004). CB1954 is a weak monofunctional alkylator but reduction produces a potent DNA cross-linking agent (Greco and Dachs, 2001). Reduction can occur at either the 2- or 4-nitro group, giving a mixture of hydroxylamines. The 4-hydroxylamine is converted by cellular thioesters, such as acetyl coenzyme A, to the active metabolite which cross-links with DNA, exerting the main cytotoxic effect (Figure 5.5) (Denny, 2001 and 2003). This cross-link is unique, with the 4-hydroxylamine reacting with the C8 position of deoxyguanosine, while the aziridine group reacts with the opposing strand of DNA (Denny *et al*., 2003). The 2-hydroxylamine also exhibits some toxicity through formation of DNA adducts (Brown and Wilson, 2004). A major advantage of CB1954 is that the activated drug

is able to kill proliferating and non-proliferating cells (Greco and Dachs, 2001). Also, the hydroxylamine metabolites of CB1954 have been shown to be able to cross cell membranes freely and thus a bystander effect is possible for this drug (Xu and McLeod, 2001).

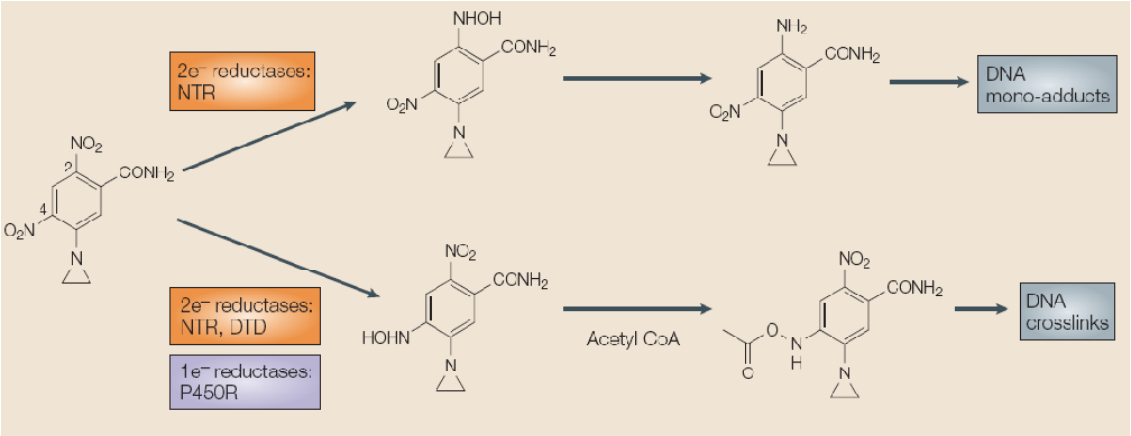

Figure 5.5 Structure of prodrug CB1954 (left), used in enzyme prodrug therapy with NTR enzyme, and activation to 2-hydroxylamine (top pathway) and 4-hydroxylamine (bottom pathway). (From Brown and Wilson, 2004.)

The CB1954/NTR combination has been tested with various approaches to GDEPT and VDEPT. *In vitro* testing of the CB1954/NTR system showed a dramatic increase in toxicity in NTR-expressing cell lines, with up to 2000-fold increase in IC_{50} values (Weedon *et al*., 2000). Phase I trials have been completed testing the individual components of a VDEPT system (Chung-Faye *et al*., 2001 and Palmer *et al*., 2004). Chung-Faye *et al*. (2001) administered intravenously (i.v.) varying concentrations of CB1954 as a single agent, to thirty patients with gastrointestinal malignancies. This was to determine toxicity and pharmacokinetics of the prodrug alone before administration with the NTR. The highest dose level was 37.5 mg/m^2 and all three patients in this treatment group experienced dose-limiting toxicities (DLTs). It was concluded from this trial that a lower i.v. dose of 24 mg/m^2 at 3-weekly intervals was the safest regimen (Chung-Faye *et al*., 2001). Palmer *et al*. (2004) constructed CTL102, a replication-deficient adenovirus vector, containing the *E. coli nfsB* gene. This was administered to patients with liver cancer to determine

primarily toxicity, and secondly, expression of the NTR, immune response and pharmacokinetics. A maximum dose of 5 x 10^{11} virus particles, administered intratumourally, was well tolerated with no DLTs observed. Immunohistochemical staining of resected tumour sections showed expression of the NTR in the tumour cells (Palmer *et al*., 2004). The authors have now moved on to test these two components together, with intratumoural CTL102 administration 48 hours prior to i.v. administration of CB1954. To date no further publications or results from this clinical trial have been published.

A phase I clinical trial in prostate cancer was also conducted using CTL102 and CB1954 (James *et al*., 2004). Intraprostatic injection of CTL102 has been reported as feasible and safe in the 16 patients treated. Expression of the NTR was seen in tumour and stroma using immunohistochemistry staining of resected tissue. One patient was injected with the virus and administered i.v. CB1954, and exhibited no significant toxicities and a fall in PSA levels by >50% after one month. No further results have been published to date.

5.1.5 Current 5-FU prodrugs

There are a number of prodrugs of 5-FU in use today, with an emphasis on oral administration in order to improve quality of life for patients. These include Capecitabine and Ftorafur. Capecitabine (N^4-pentyloxycarbonyl-5-deoxy-5-fluorocytidine) is a prodrug of 5-FU which is taken orally without degradation by DPD in the GI tract (Figure 5.6) (Xiong and Ajani, 2004). It is acted on in the liver by carboxylesterase to produce 5-deoxy-5-fluorocytidine (5-DFCR). Cytosine deaminase (CD) is highly expressed in the liver and solid tumours. CD converts 5-DFCR to 5-deoxy-5-fluorouridine (5-DFUR) which is then converted to 5-FU by TP and/or UP. TP and UP are generally more active in tumour tissue than in normal tissue, thus resulting in an increased level of 5-FU being released in the tumour cells (Longley *et al*., 2003 and Xiong and Ajani, 2004). Capecitabine is indicated for patients whose cancer progresses after anthracycline and taxane therapy (Kakimoto *et al*., 2005 and Awada *et al*., 2003).

Ftorafur (FT, 1-(2-tetrahydrofuryl)-5-Fluorouracil) is a mixture of two stereoisomers (Figure 5.6). FT is converted to 5-FU by two mechanisms, cleavage of

the C2'-N1' bond which occurs in the cytosol by thymidine phosphorylase, or hepatic microsomal oxidation at the C5' position by cytochrome P450 enzymes (Xiong and Ajani, 2004 and Rooseboom *et al*., 2004). It is generally administered as a Uracil/Ftorafur (UFT) formulation, combining a 4:1 molar ratio of uracil with Ftorafur. The uracil in this combination saturates DPD, thus allowing 5-FU to avoid degradation (Longley *et al*., 2003). This combination has fewer side-effects than 5-FU during clinical use, is reliably absorbed and, with a half-life of 5-12 hours in circulation, produces sustained high plasma levels of 5-FU (Lamont and Schilsky, 1999). The term S1 is used for another combination therapy with the prodrug FT, in conjunction with 5-chloro-2,4-dihydroxypyrimidine (CDHP) and potassium oxonate (OXO). CDHP is an inhibitor of DPD, 180 times more potent than uracil, enhancing the efficacy of 5-FU by limiting degradation by DPD. OXO inhibits phosphorylation of 5-FU by OPRT in the GI tract, which is one of the main causes of toxicity (Malet-Martino and Martino, 2002).

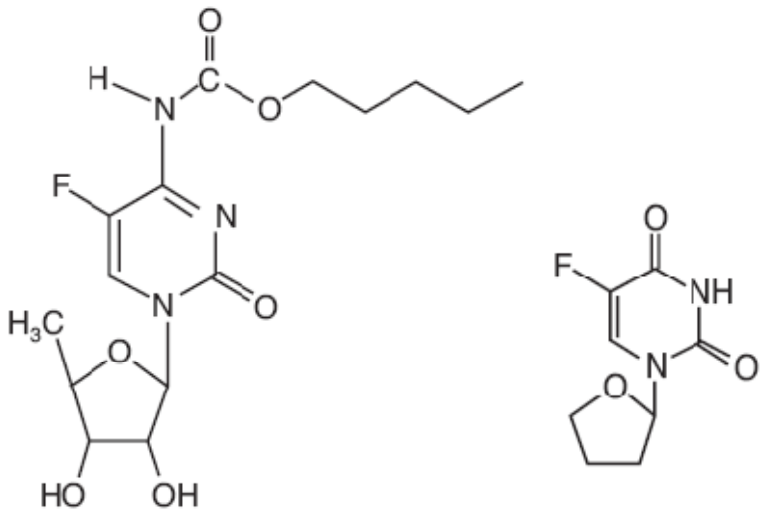

Figure 5.6 Structure of N^4-pentyloxycarbonyl-5-deoxy-5-fluorocytidine (Capecitabine, left) and 1-(2-tetrahydrofuryl)-5-Fluorouracil (Ftorafur, right), prodrugs of 5-FU.

5.1.6 Chemistry of prodrugs 3, 6, 9, 13 and 14

Compounds 3, 6, 9, 13 and 14 were designed as prodrugs, with a nitro-benzyl side-chain attached to the parent 5-FU or 5-FUrd. These prodrugs have three components essential to their function: trigger, linker and effector. In the case of these compounds, the nitro group acts as the trigger, the benzyl group is the linker and the effector is 5-FU or 5-FUrd, as illustrated in Figure 5.7 with a diagram of compound 3. Activation of these prodrugs involves reduction of the nitro group, which causes conformational changes in the benzyl group and subsequent cleavage of the bond between the parent 5-FU or 5-FUrd and the linker/trigger section. Figure 5.8 demonstrates the activation of compound 3, with the final result showing free 5-FU and quinone methide, another toxic molecule which forms DNA adducts (Wang *et al*., 2005).

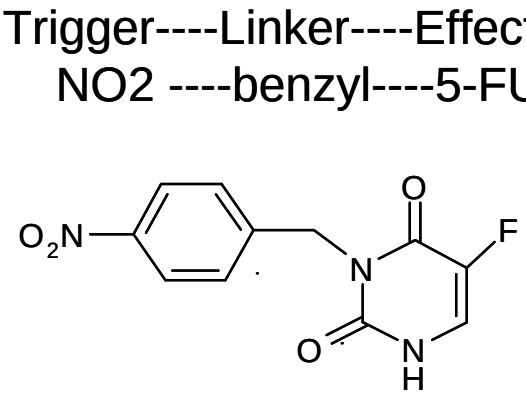

Figure 5.7 Structure of compound 3. The nitro group acts as trigger, the benzyl group is a linker and 5-FU is the effector component.

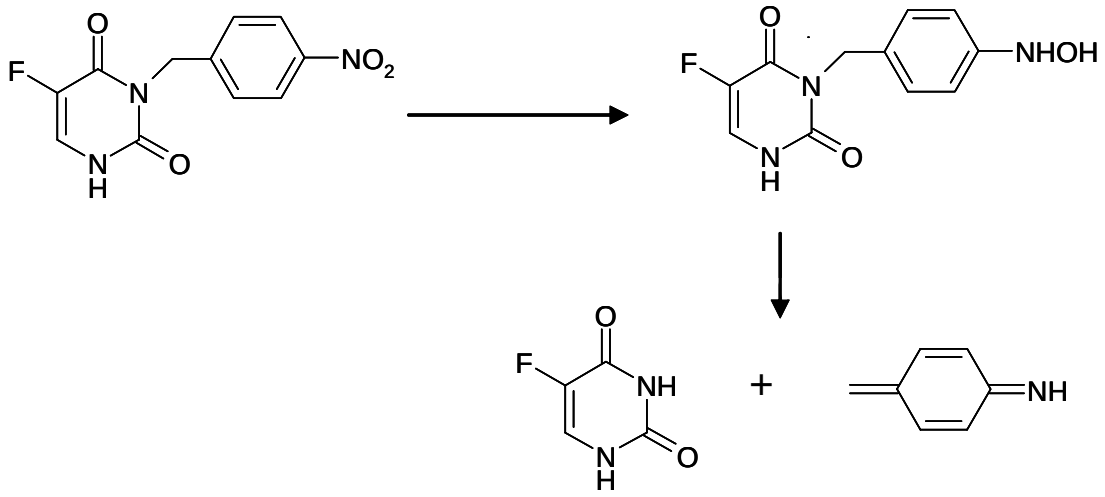

Figure 5.8 Activation of compound 3. Reduction of the nitro group to –NHOH results in cleavage of the bond between the benzyl linker group and 5-FU, releasing 5-FU and quinone methide.

5.1.7 Objectives of Chapter 5

The possibility of using targeted therapies for cancer patients could improve the outcome of the disease. Prodrugs may decrease side-effects in patients and offer more efficacious treatments. Activation of the 5-FU and 5-FUrd prodrugs 3, 6, 9, 13 and 14 and their corresponding toxicity was the focus of this chapter. Hypoxia-induced activation was initially analysed using the 4T1 and SW480 cell lines to investigate activation by endogenous one-electron reductases. Enzyme activation using *E. coli* NTR was then tested, firstly by using recombinant protein in a multi-well enzyme assay. These assays allowed investigation of the enzyme kinetics using NTR. Following this, a cell line expressing NTR was tested with the prodrugs and a known substrate. Liquid chromatography in conjunction with mass spectrometry was used to analyse activation of the prodrugs in the NTR-expressing cells. The cDNA for NTR was amplified in bacteria and used to transfect a human colorectal cancer cell line. Establishment of a transfected cell line allowed testing of the compounds in human tumour cells.

5.2 Results

5.2.1 Activation of prodrugs by hypoxia in the 4T1 cell line

Prodrugs can be activated under hypoxic conditions by reduction to an intermediate molecule which is further modified to produce the pharmacologically active drug. The selectivity to hypoxic cells occurs due to back-oxidation of the intermediate molecule to the original compound in the presence of oxygen (Brown and Wilson, 2004). In order to investigate activation of the 5-FU and 5-FUrd prodrugs, cytotoxicity experiments were set up and then incubated under hypoxic conditions (2% O_2). The first step in this series of experiments was to determine any detrimental effect of the hypoxic conditions on the cell line. The growth of the 4T1 cell line was monitored after 24, 48 and 72 hours incubation at 5% CO_2, 2% O_2. Experiments were carried out in triplicate. Figure 5.9 shows that there was minimal detrimental effect on the growth of this cell line over the three time points examined when compared to growth of the cells under normoxic conditions (20% O_2).

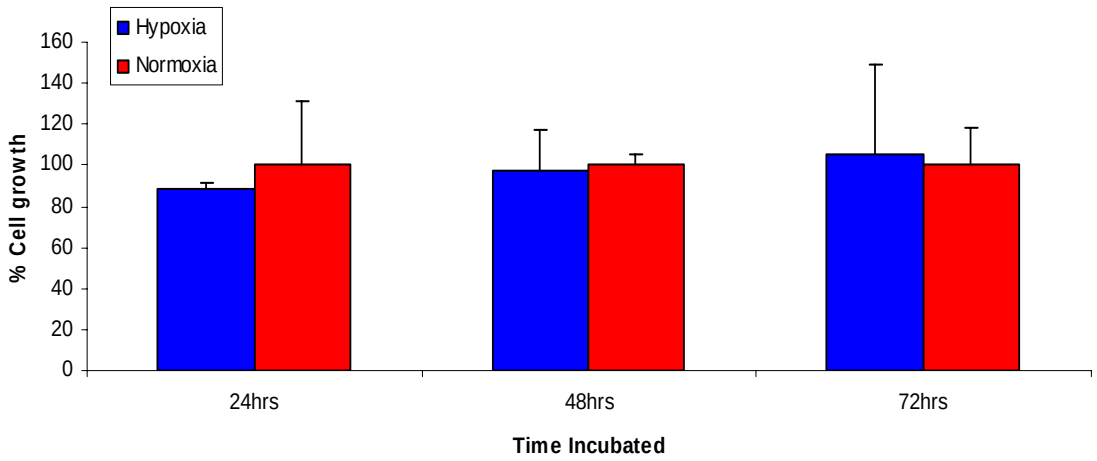

Figure 5.9 4T1 cell growth profile under hypoxic (2% O_2) and normoxic (20% O_2) conditions over 24, 48 and 72 hours to assess toxicity to the cells.

Compounds 13 and 14 were chosen for the initial investigation of toxicity in the 4T1 cell line. Cells were seeded in 96-well plates as per section 2.2.3 and allowed to attach overnight in normoxic conditions. The compounds were then added to the cells and incubated for 3 days. Assays were incubated in hypoxic conditions for 3 or 24 hours and then transferred to normoxic conditions for the remaining time, or they were incubated in the hypoxic conditions for 72 hours. Assays incubated in normoxic conditions were placed in a standard 37°C, 5% CO_2 incubator for 3 days. The level of cell death caused by the compounds was quantified using the MTS assay. Assays were carried out in triplicate. Figure 5.10 shows the results for compound 13. Over the full range of concentrations, 0.0003 μM to 323 μM, the cells under the four different conditions corresponded closely to one another. Low toxicity was observed up to approximately 10 μM for the cells in normoxia and 3 and 24 hours hypoxia, with the cell death rising up to approximately 80% at the top concentration of 323 μM. The cells incubated in hypoxic conditions for 72 hours showed no toxicity up to approximately 50 μM.

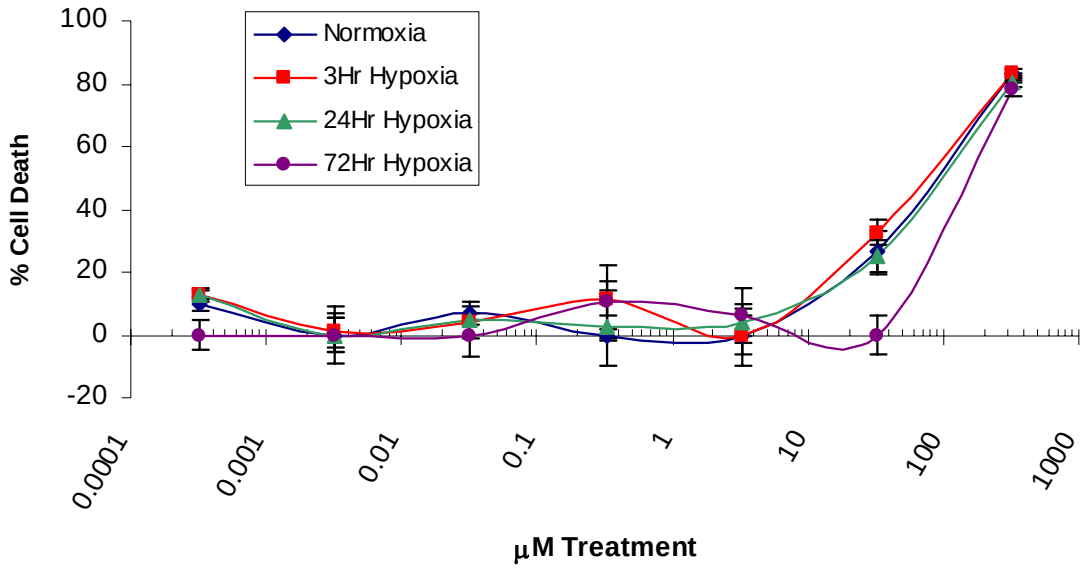

Figure 5.10 Cytotoxicity of compound 13 in the 4T1 cell line after treatment for 3 days, under normoxic conditions and following exposure to 3, 24 and 72 hours hypoxia (2% O_2).

Compound 14 caused low toxicity over the range of concentrations tested, 0.00025 μM to 250 μM, with no difference noted between the different conditions (Figure 5.11).

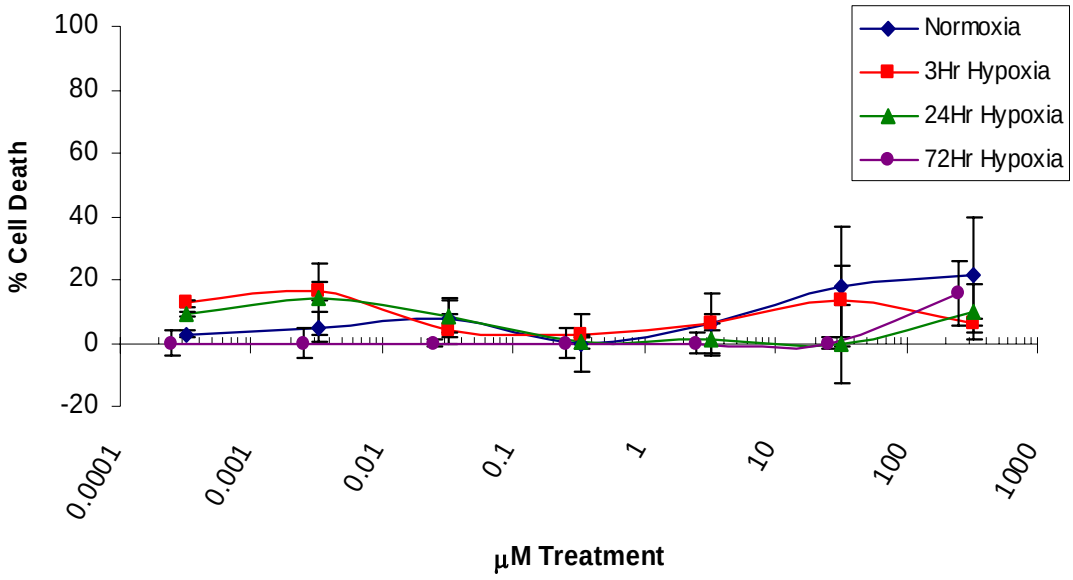

Figure 5.11 Cytotoxicity of compound 14 in the 4T1 cell line after treatment for 3 days, under normoxic conditions and following exposure to 3, 24 and 72 hours hypoxia (2% O_2).

Although no activation appeared to be occurring with compounds 13 and 14, compounds 3, 6 and 9 were then tested under hypoxic conditions for 72 hours. Compound 3 had shown toxicity previously against the 4T1 and SW480 cell lines (Sections 4.2.2 and 4.2.3). However, the possibility of increased toxicity under hypoxic conditions was examined. Figure 5.12 shows the results for this compound, with no difference in toxicity seen between the cells incubated in normoxic conditions and those exposed to hypoxia for 72 hours. Compounds 6 and 9, both 5-FUrd derivatives, caused low toxicity in the 4T1 and SW480 cell lines (Sections 4.2.2 and 4.2.3). Exposure of cells to these compounds while incubated under hypoxia for 72 hours did not cause an increase in cytotoxicity in the 4T1 cell line (Figure 5.13).

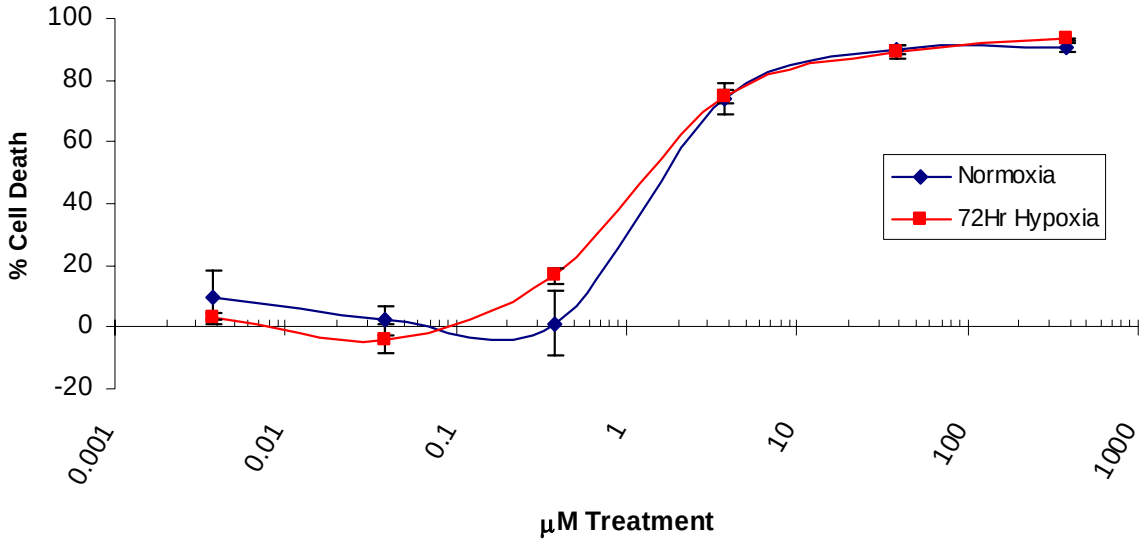

Figure 5.12 Cytotoxicity of compound 3 in the 4T1 cell line after treatment for 3 days, under normoxic conditions and following exposure to 72 hours hypoxia (2% O_2).

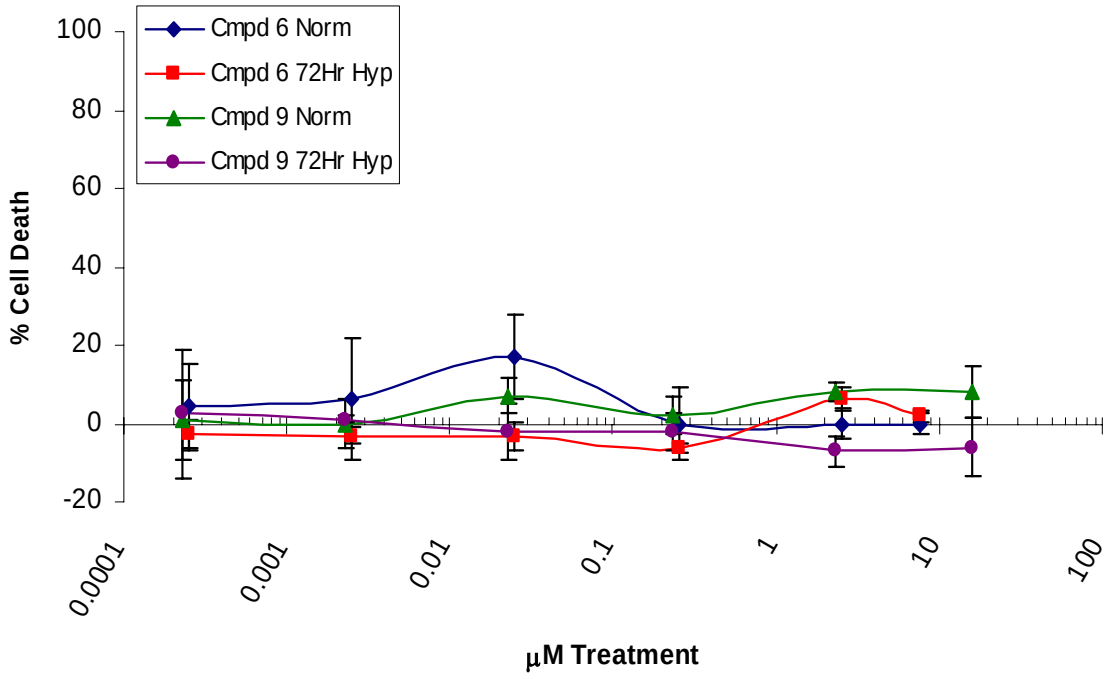

Figure 5.13 Cytotoxicity of compounds 6 and 9 in the 4T1 cell line after treatment for 3 days, under normoxic conditions and following exposure to 72 hours hypoxia (2% O_2).

5.2.1.2 Activation of prodrugs by hypoxia in the SW480 cell line

Activation and cytotoxicity of these prodrugs was examined in the SW480 colorectal cancer cell line following 72 hours exposure to hypoxic conditions. This cell line was initially tested to ensure the hypoxia alone did not cause cell death (Figure 5.14). Assays were carried out in triplicate. Incubation for 48 and 72 hours caused an increase in the growth of the SW480 cells, but no decrease in cell growth was seen. No significant difference was seen in the toxicity of these compounds under hypoxic conditions over 72 hours. Figure 5.15 shows the toxicity profile for compound 3 which showed toxicity towards the cells but no increase in toxicity under hypoxic conditions. Figure 5.16 shows the toxicity of compounds 6 and 9 after exposure to hypoxia for 72 hours. No increase in toxicity was exhibited after incubation for 72 hours with compounds 6 and 9 under hypoxic conditions. Compounds 13 and 14 did not exhibit an increase in toxicity after incubation under hypoxic conditions for 72 hours (data not shown). Hence, no activation was evident for prodrugs 3, 6, 9, 13 and 14 following exposure to hypoxic conditions over 3 days. This was possibly due to the fact that the majority of reductase enzymes in cells are one-electron reductases and these compounds appear to require two-electron reductases for activation. Since the two-electron reductases in mammalian cells are unlikely to reach the reduction potential required to reduce the nitro trigger, a known reductase with the ability to reach low reduction potentials was examined.

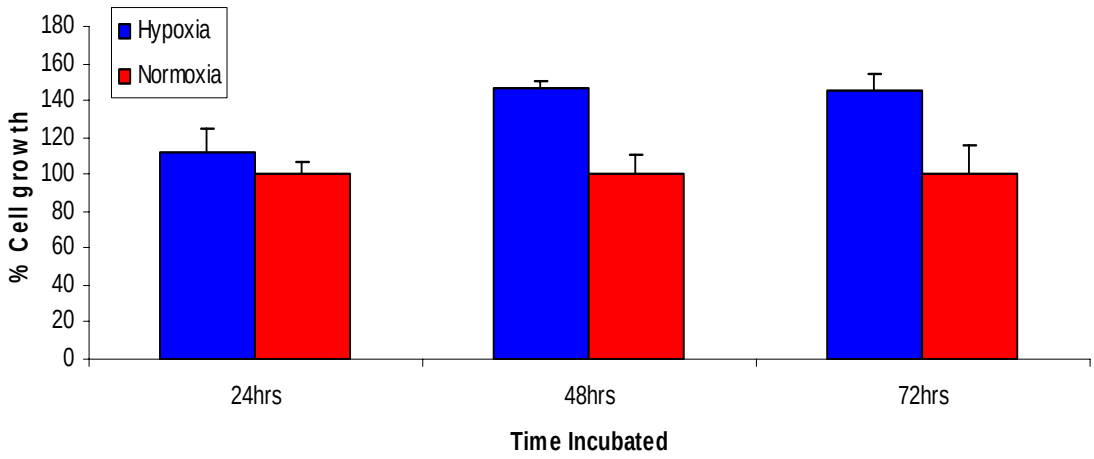

Figure 5.14 SW480 cell growth profile under hypoxic (2% O_2) and normoxic (20% O_2) conditions over 24, 48 and 72 hours to assess toxicity to the cells.

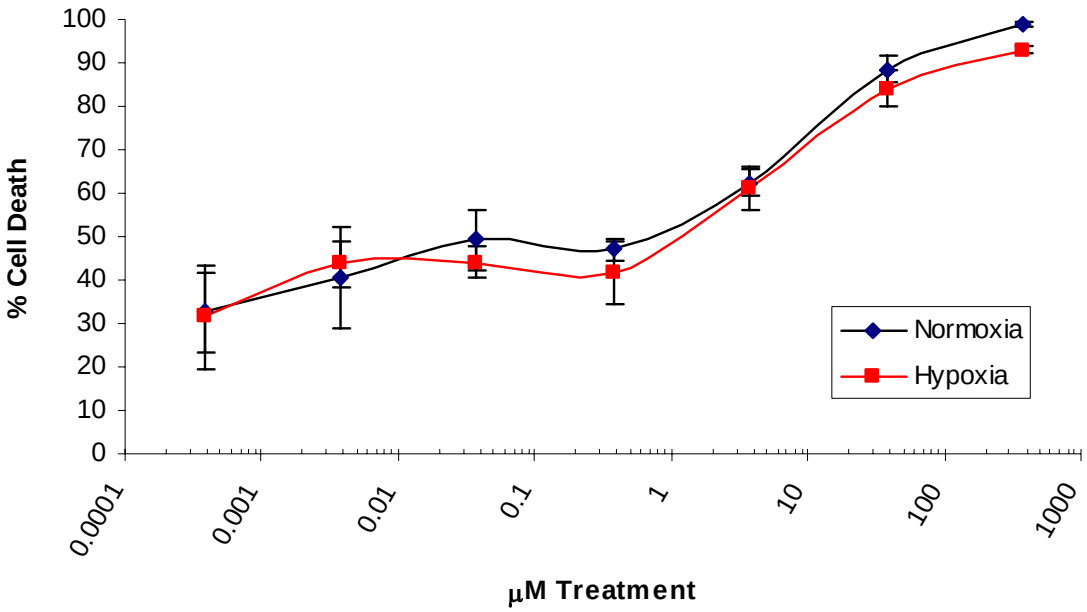

Figure 5.15 Cytotoxicity of compound 3 in the SW480 cell line after treatment for 3 days, under normoxic conditions and following exposure to 72 hours hypoxia (2% O_2).

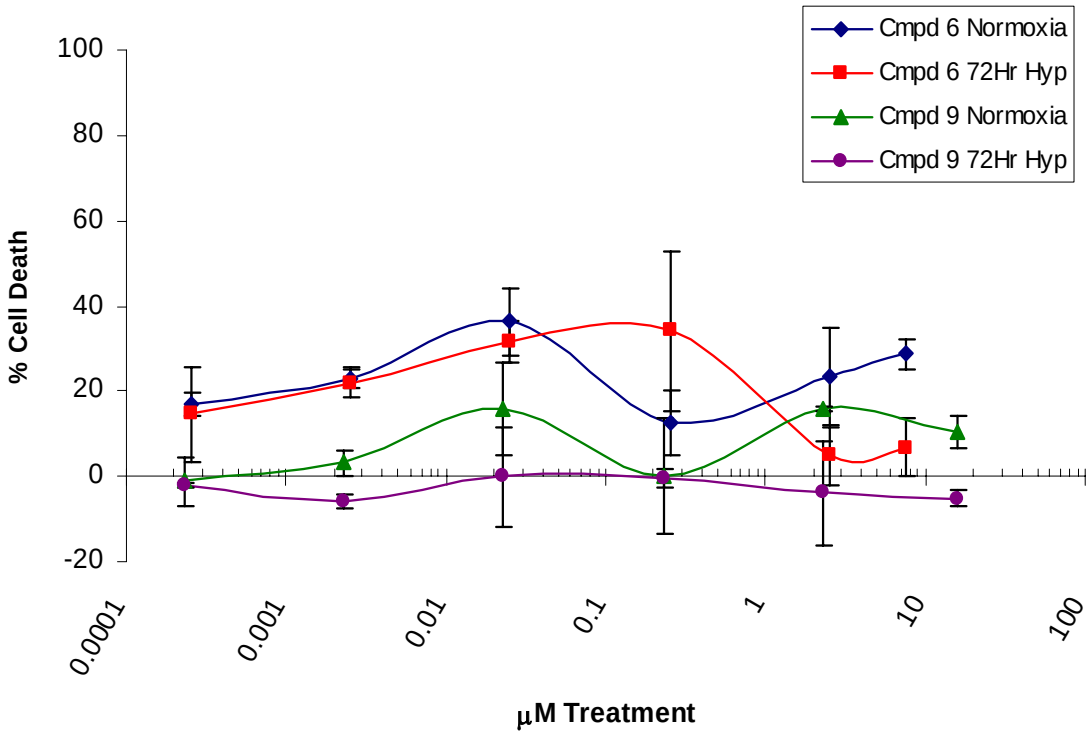

Figure 5.16 Cytotoxicity of compounds 6 and 9 in the SW480 cell line after treatment for 3 days, under normoxic conditions and following exposure to 72 hours hypoxia (2% O_2).

5.2.2 Analysis of prodrug compounds as substrates for *Escherichia coli* nitroreductase

E. coli NTR is a two-electron reductase which is known to activate nitroaromatic compounds including CB1954 (Parkinson *et al*., 2000). In order to test if the prodrugs 3, 6, 9, 13 and 14 were substrates for this enzyme, the recombinant enzyme was purchased in powder form from Sigma Aldrich for use in a simple enzyme assay with NADH as co-factor. CB1954 was also purchased from Sigma Aldrich and used as a control substrate. Following optimisation experiments with CB1954, concentrations of 500 µM NADH, 3 µg/ml NTR and 200 µM substrate were chosen (data not shown). The reaction with the substrate was set up and monitored by the decrease in absorbance of NADH at 340 nm over a period of 60 minutes, as per section 2.2.11.1. Figure 5.17 shows the results from the enzyme assays. A reduction in the absorbance at 340 nm was seen for all compounds. CB1954 and compound 9 showed the most dramatic change in absorbance over the 60 minutes.

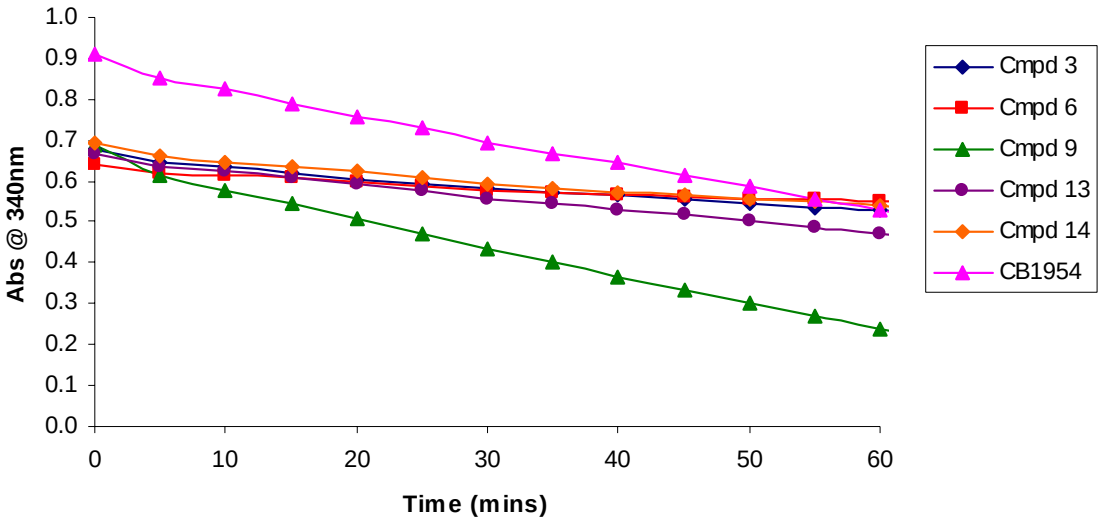

Figure 5.17 Enzyme assay to determine if prodrugs were substrates for *E. coli* NTR. CB1954 was used as a control, as it is a known substrate for NTR. Absorbance of NADH at 340 nm was monitored over a period of 60 minutes.

Although compound 9 looked the most promising in the enzyme assay outlined in Figure 5.17 there was a limited amount of this compound available for kinetic analysis therefore the more abundant compounds 13 and 14 were used. Assays were conducted using a range of substrate concentrations and the absorbance of NADH measured after 1 hour. A plot of substrate concentration [S] versus rate (velocity, v) yields the Michaelis-Menton curve. The Lineweaver-Burk, Hanes-Woolf, Eadie-Hofstee plots as well as the non-linear regression software Enzfitter (Elsevier Biosoft) were used to calculate the Michaelis constant (K_m), V_{max} and catalytic constant (k_{cat}) from this data. The K_m value is the concentration required to reach half the maximum velocity (V_{max}) of the enzyme or the concentration at which half of the active sites are filled. K_m is related to how well the substrate binds the enzyme - the lower the K_m value, the greater the affinity for the enzyme (Matthews and van Holde, 1990). However, the greater the affinity for the enzyme, the slower the reaction will proceed and this will affect the k_{cat} value. k_{cat}, or the turnover number, measures the number of molecules of substrate that are converted to product by one enzyme site per second. The K_m and V_{max} (maximum velocity) are determined from the plots as described in Table 5.1.

Table 5.1 Details of the Lineweaver-Burk, Hanes-Wolf and Eadie-Hofstee plots for determination of K_m and V_{max}.

Plot	x-axis	y-axis	x=0	y=0
Lineweaver-Burk	1/[S]	1/v	$y=1/V_{max}$	$x=-1/K_m$
Hanes-Wolf	[S]	[S]/v	$y=K_m/V_{max}$	$x=-K_m$
Eadie-Hofstee	v/[S]	v	$y=V_{max}$	$x=V_{max}/K_m$

Determination of k_{cat} was then calculated from the equation:

$$k_{cat} = V_{max} / E_t$$

where E_t was the total enzyme, and was calculated as follows:

Concentration used in reaction ($g.ml^{-1}$) / Molecular weight ($g.mole^{-1}$) = E_t ($mole.ml^{-1}$)

For these experiments, 3μg/ml enzyme was used, with molecular weight of 24,000 $g.mole^{-1}$. Thus:

$$E_t\ (mole.ml^{-1}) = 3 \times 10^{-6}\ g.ml^{-1} / 24{,}000\ g.mole^{-1} = 1.25 \times 10^{-10}\ mole.ml^{-1}$$

Compound 13 showed excellent correlation between the substrate concentrations and velocity in the plots. Figure 5.18 shows the Michaelis-Menton curve for compound 13 when substrate concentration was plotted against the velocity of the reaction. The Lineweaver-Burk plot of 1/[S] versus 1/v gave a straight line with a correlation co-efficient (R^2 value) of 1 (Figure 5.19). The correlation co-efficient for the Hanes-Woolf plot of [S] versus [S]/v was 0.998 (Figure 5.20). Figure 5.21 shows the Eadie-Hofstee plot of v/[S] versus v, giving a straight line with correlation co-efficient of 0.9828. The Hanes-Woolf plots for compound 14 and CB1954 gave straight lines with correlation co-efficients of 0.9951 and 0.9973 respectively (Figures 5.22 and 5.23).

The values for K_m and k_{cat} calculated from the plots and using the Enzfitter software are shown in Table 5.2. The K_m values for compounds 13, 14 and CB1954 were 48.17 μM, 13.47 μM and 9.66 μM respectively. This would indicate that the nitroreductase enzyme has the highest affinity for CB1954, followed closely by compound 14. The k_{cat} value of 76427 sec^{-1} for compound 13 means that this substrate is converted to product at a faster rate than compound 14 or CB1954, with k_{cat} values of 29857 sec^{-1} and 52195 sec^{-1} respectively. The k_{cat}/K_m ratio indicates the catalytic efficiency of the reaction, taking into account both the affinity of the substrate for the enzyme and the rate of reaction. The more efficient the reaction, the greater the value of k_{cat}/K_m. In this case, the efficiency of reactions appears to be in the order CB1954>compound 14>compound 13. This is due to a combination of high affinity but also moderate turnover for CB1954, whereas compound 13 had lower affinity with high turnover, and compound 14 had high affinity and low turnover.

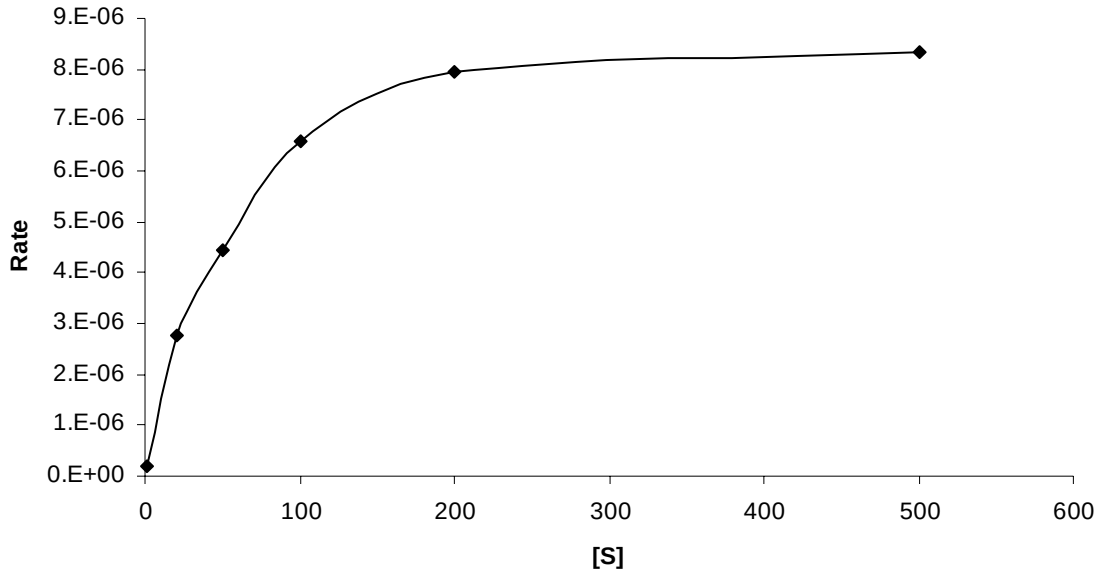

Figure 5.18 Substrate concentration versus velocity for compound 13 yielded the Michaelis-Menton hyperbola.

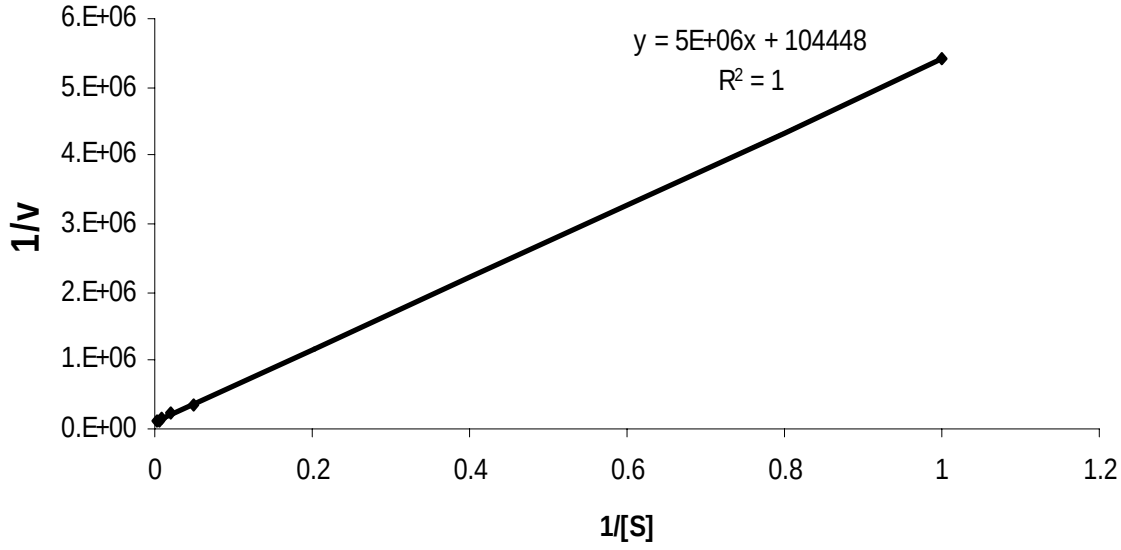

Figure 5.19 Lineweaver-Burk plot for compound 13 with 1/[S] versus 1/v. The correlation co-efficient (R^2) value was 1.

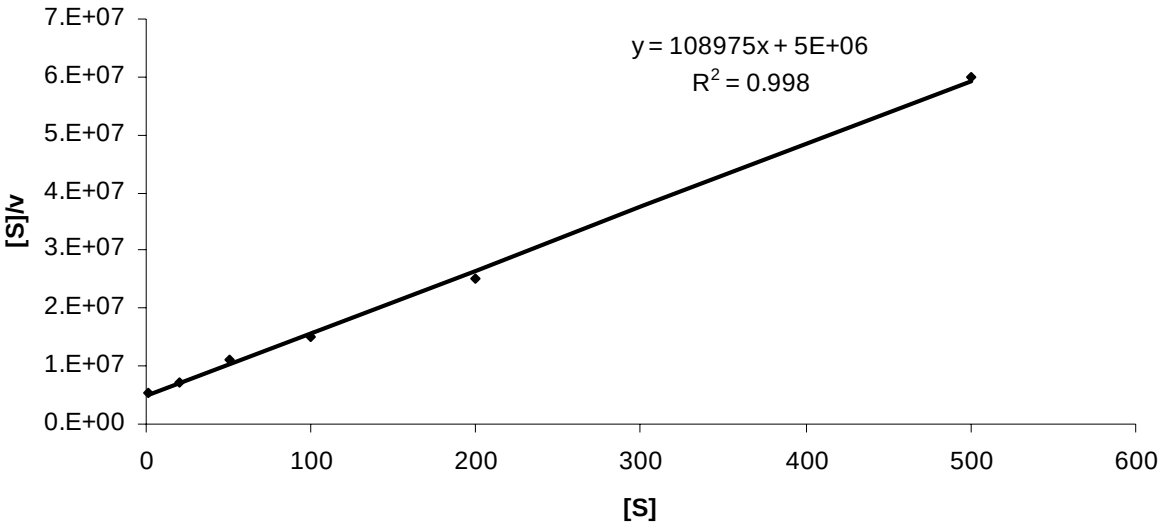

Figure 5.20 Hanes-Woolf plot for compound 13 with [S] versus [S]/v. The correlation co-efficient (R^2) value was 0.998.

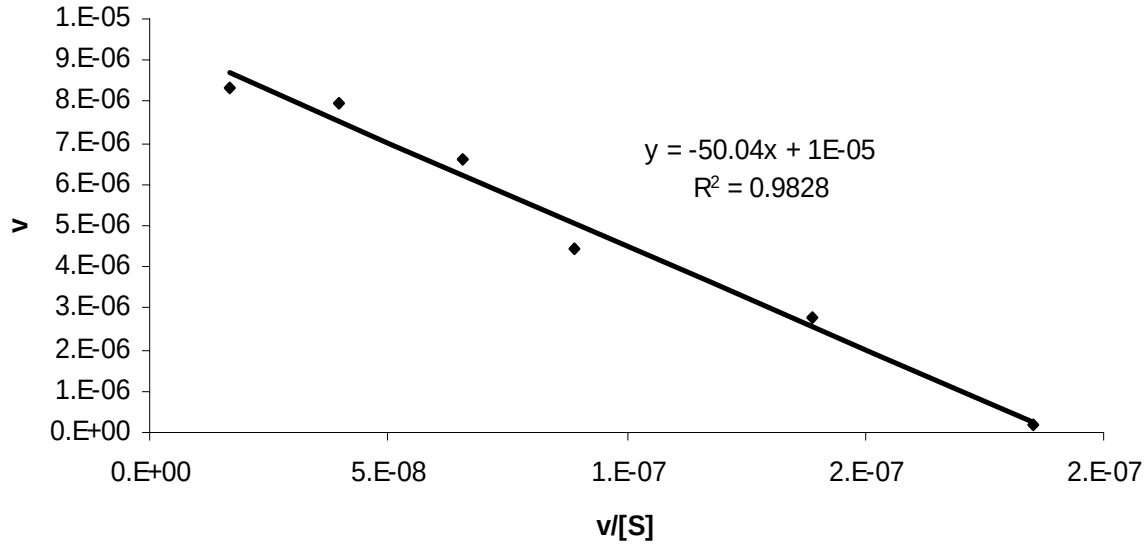

Figure 5.21 Eadie-Hofstee plot for compound 13 with v/[S] versus v. The correlation co-efficient (R^2) value was 0.9828.

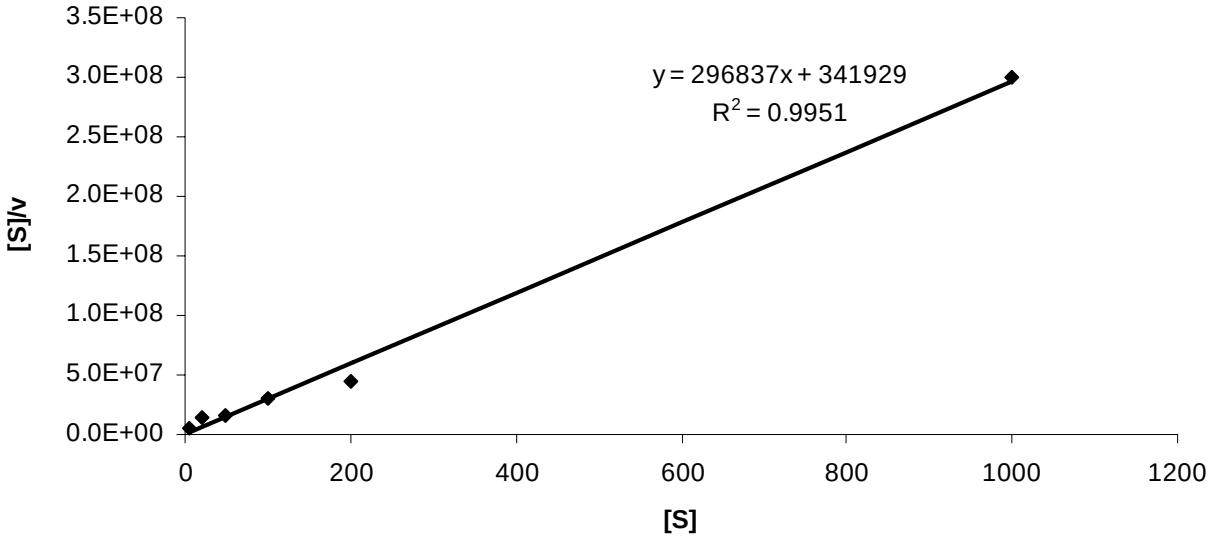

Figure 5.22 Hanes-Woolf plot for compound 14 with [S] versus [S]/v. The correlation co-efficient (R^2) value was 0.9951.

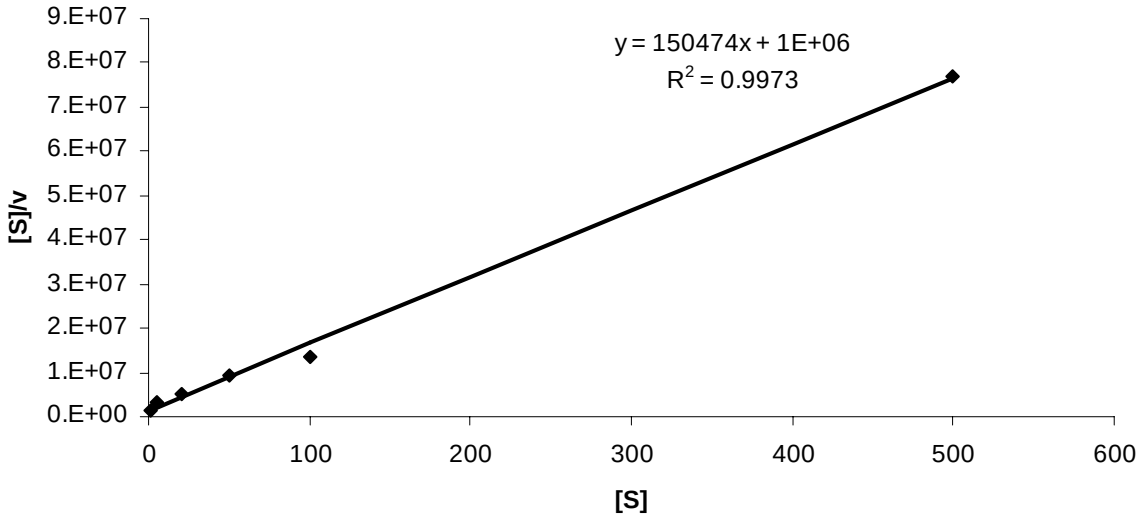

Figure 5.23 Hanes-Woolf plot for CB1954 with [S] versus [S]/v. The correlation co-efficient (R^2) value was 0.9973.

Despite the fact that CB1954 reacts more efficiently with the enzyme in comparison to compounds 13 and 14, these results were still encouraging. CB1954 is a known substrate with great potential for therapeutic purposes in conjunction with the nitroreductase enzyme. Compounds 13 and 14 showed enough activity with the enzyme to warrant moving forward to activation within cells.

Table 5.2 K_m and k_{cat} values for compounds 13, 14 and CB1954, calculated using the Lineweaver-Burk, Hanes-Woolf, Eadie-Hofstee graphs and the Enzfitter program.

	Lineweaver-Burk	Hanes-Woolf	Eadie-Hofstee	Enzfitter	Average	Std Dev	k_{cat}/K_M ($sec^{-1}M^{-1}$)
Cmpd 13							
K_M (μM)	47.87	45.88	50.04	48.88	48.17	1.76	1.59E+09
k_{cat} (sec^{-1})	76593	73411	80000	75702	76427	2733	
Cmpd 14							
K_M (μM)	13.92	1.15	16.97	21.85	13.47	8.84	2.22E+09
k_{cat} (sec^{-1})	27841	26952	32000	32636	29857	2876	
CB1954							
K_M (μM)	5.09	6.65	10.43	16.49	9.66	5.07	5.40E+09
k_{cat} (sec^{-1})	40733	53165	56000	58883	52195	7990	

5.2.3 NTR activity in V79 Chinese hamster lung fibroblast cell line lysates

Following analysis of the compounds with the *E. coli* NTR enzyme, a cell line expressing this protein, and a control cell line, were obtained from Morvus Technologies. The V79 Chinese hamster lung fibroblast cell line had been transfected with the cDNA for the NTR enzyme and was designated V79-NTR (Friedlos *et al*., 1998). The control cell line was transfected with the control vector and was designated V79-C. These two cell lines were maintained in the selection agent, puromycin. To firstly confirm activity of the NTR enzyme in this cell line, an enzyme assay was conducted using cell lysates as per section 2.2.11.2. Cells were trypsinised, centrifuged and lysed by a freeze-thaw method. The cell lysate was added to a mixture of the substrate CB1954 and the co-factor NADH and the

absorbance of NADH monitored at 340 nm over 60 minutes. Figure 5.24 shows the results from the enzyme assay using the cell lysates. The total protein added to the reaction was 15.33 μg, 18 μg and 8.8 μg for the V79-NTR, V79-C and 4T1 cell lines respectively. The lysate from the V79-NTR cell line caused an obvious decrease in the absorbance of NADH as the reaction proceeded. The lysate from theV79-C cell line caused a small decrease in absorbance over the 60 minutes (Figure 5.24). The 4T1 cell line was used as a control as it did not express the NTR enzyme and accordingly, the lysate caused a small decrease in absorbance. The specific activity was calculated from these assays, using the molar absorption coefficient of NADH (6.3×10^3 $mole^{-1}$ cm^{-1}). The specific activity of the NTR enzyme was 0.1578 Units/mg for the V79-NTR cell line. For the V79-C and 4T1 cell lines, the specific activity was significantly lower, at 0.0013 Units/mg and 0.0037 Units/mg respectively. Thus, NTR enzyme activity in the V79-NTR cell line was confirmed and the activation of the prodrugs was next tested using cytotoxicity assays.

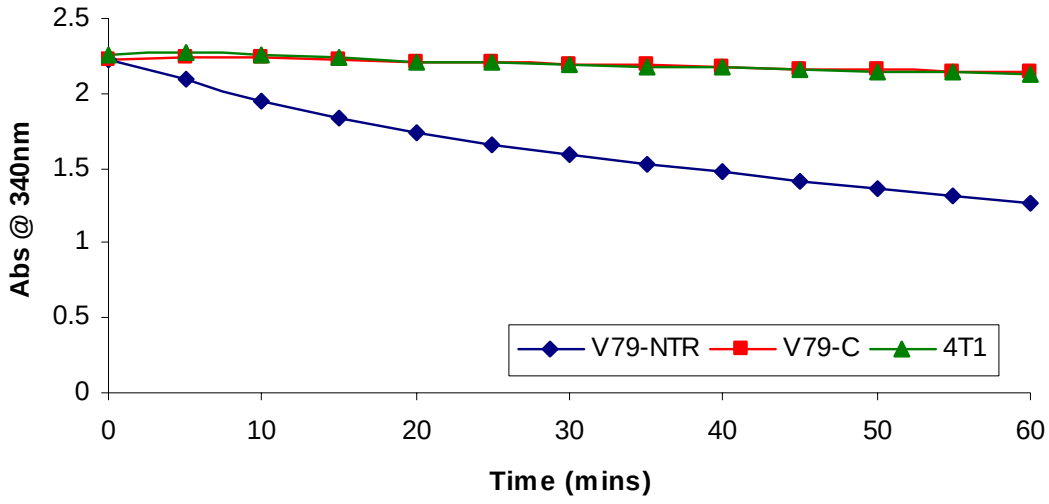

Figure 5.24 Enzyme assay using lysates from the V79-NTR, V79-C and 4T1 cell lines to test activity of NTR with known substrate CB1954. The quantity of total protein in the lysates was 15.33 μg, 18 μg and 8.8 μg respectively.

5.2.4 Cytotoxicity of prodrugs in the V79 Chinese hamster lung fibroblast cell line

Cytotoxicity of the known substrate, CB1954, and the prodrugs, 3, 6, 9, 13 and 14 was investigated in the V79-C and V79-NTR cell lines. Results are from a minimum of duplicate experiments, carried out in triplicate. Figure 5.25 shows the cytotoxicity of CB1954 over 3 days. The difference in toxicity in the two cell lines was extremely dramatic. In the V79-C cell line, no toxicity was observed up to 40 μM, with toxicity then rising to approximately 80% cell death at 397 μM. In contrast, at the lowest concentration tested, 0.00397 μM, approximately 40% cell death was noted in the V79-NTR cell line. The IC_{50} value of the V79-C cell line was 190 μM, over 27,000-fold higher than the IC_{50} value of 0.007 μM for the V79-NTR cell line (Table 5.3).

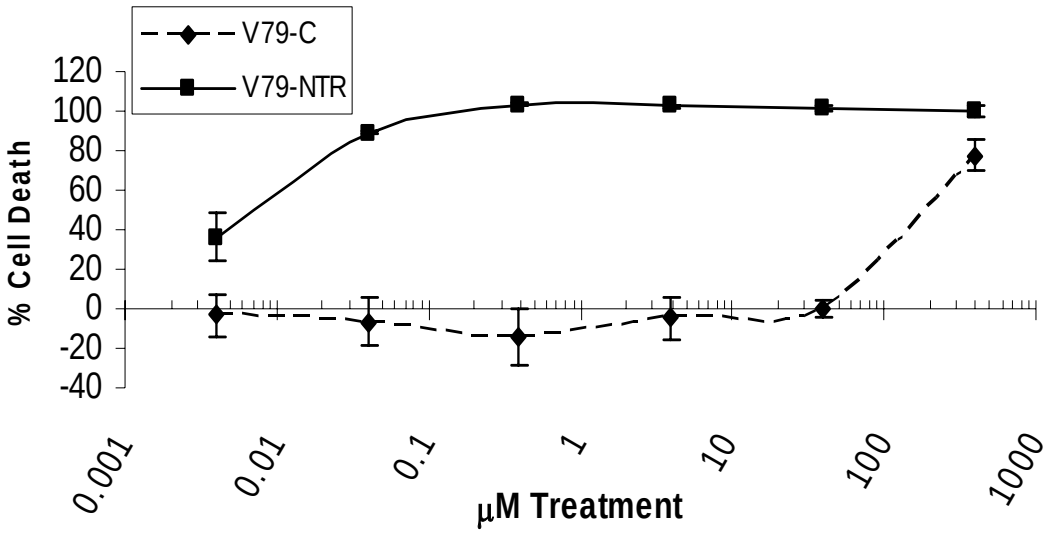

Figure 5.25 Cytotoxicity of CB1954 in the V79-C and V79-NTR cell lines after treatment for 3 days.

Treatment with compound 3 did not cause a difference in toxicity between the two cell lines, V79-C and V79-NTR. Figure 5.26 shows the cytotoxicity profile over 3 days, with compound 3 exhibiting cell death from a concentration of approximately 0.4 μM and higher in both cell lines. The IC_{50} values over 3 days for V79-C and

V79-NTR were 9 μM and 7.5 μM respectively, giving a ratio of 1.2 (Table 5.3). The ratio of IC_{50} values increased slightly to 1.9 after 5 days treatment (Table 5.3). Compound 6 showed promising results after 3 days treatment, with greater toxicity in the V79-NTR cell line in comparison to the V79-C cell line at a concentration of 25 μM (Figure 5.27). However, this was not maintained at the higher concentration of 252 μM or after 5 days treatment (Figures 5.27 and 5.28). The ratio of IC_{50} values was 10.63 and 0.97 for 3 and 5 days respectively (Table 5.3).

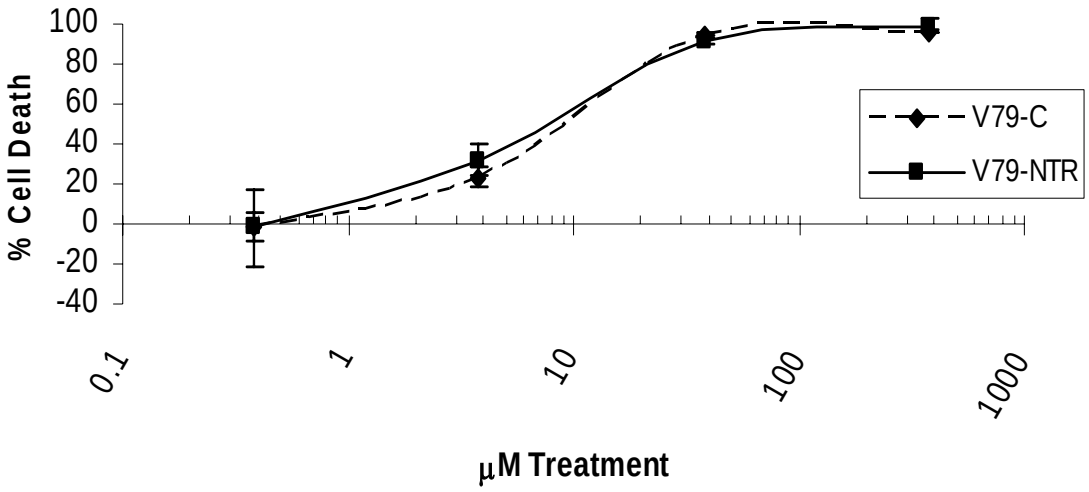

Figure 5.26 Cytotoxicity of compound 3 in the V79-C and V79-NTR cell lines after treatment for 3 days.

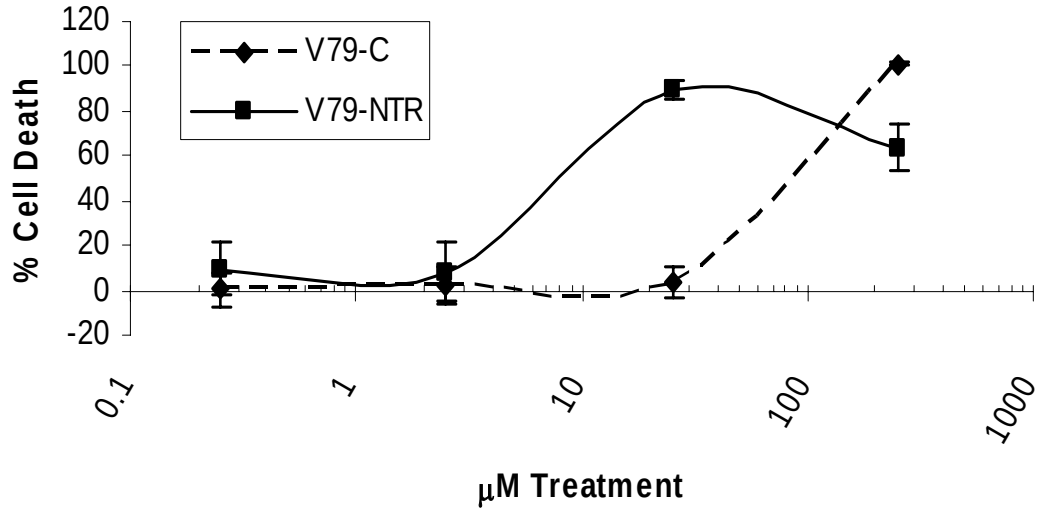

Figure 5.27 Cytotoxicity of compound 6 in the V79-C and V79-NTR cell lines after treatment for 3 days.

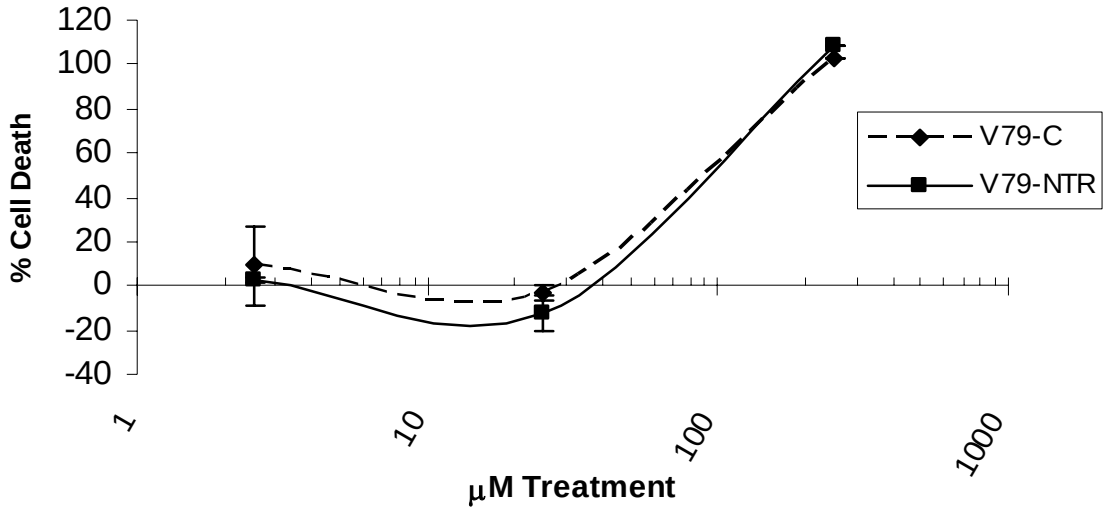

Figure 5.28 Cytotoxicity of compound 6 in the V79-C and V79-NTR cell lines after treatment for 5 days.

Compound 9 showed low toxicity in the V79-C cell line, with a maximum of 35% cell death observed over 3 days (Figure 5.29). In contrast, the V79-NTR cell line showed no toxicity over this time scale. IC_{50} values were not reached after treatment for 3 and 5 days.

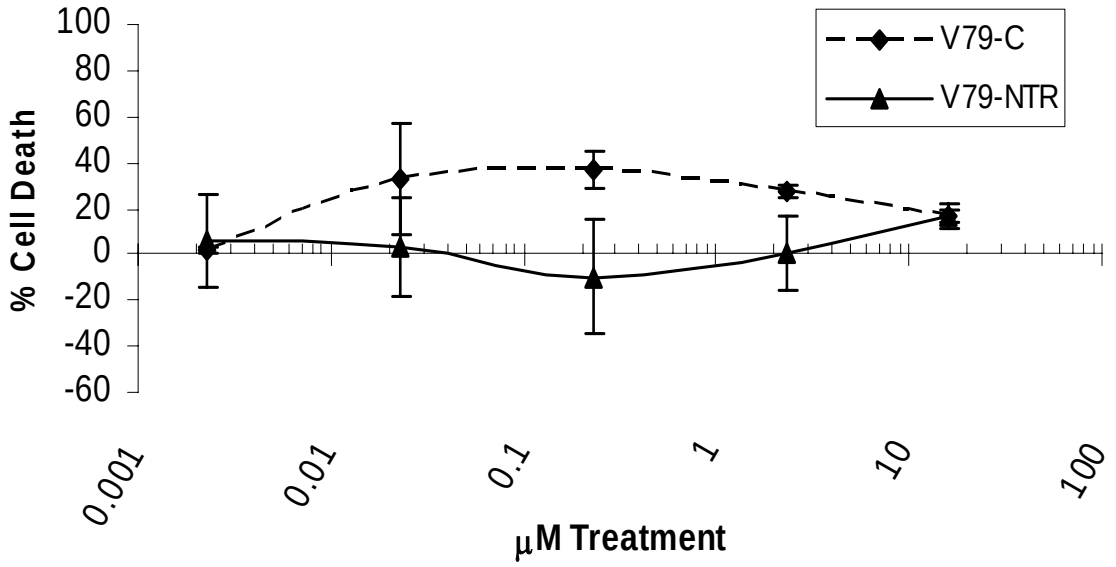

Figure 5.29 Cytotoxicity of compound 9 in the V79-C and V79-NTR cell lines after treatment for 3 days.

Figure 5.30 and 5.31 shows the results for compound 13 over 3 and 5 days respectively. Treatment with compound 13 for 3 days caused more toxicity in the V79-NTR cell line than the control cell line, with 100% cell death seen in the V79-NTR cells after treatment with 323 μM (Figure 5.30). The maximum cell death observed for the V79-C cell line was approximately 50% at 323 μM, the top concentration tested. The ratio of IC_{50} values for 3 days treatment was 4.89. Over 5 days, a more dramatic difference was seen between the two cell lines, with no toxicity seen in the V79-C cell line, up to 323 μM (Figure 5.31). An IC_{50} value of 54 μM was established for the V79-NTR cell line but the IC_{50} value was not reached for the V79-C cell line. The ratio of IC_{50} values was thus greater than 5.98 (Table 5.3). These results appear to indicate activation of the prodrug 13 by the NTR enzyme in the V79-NTR cell line.

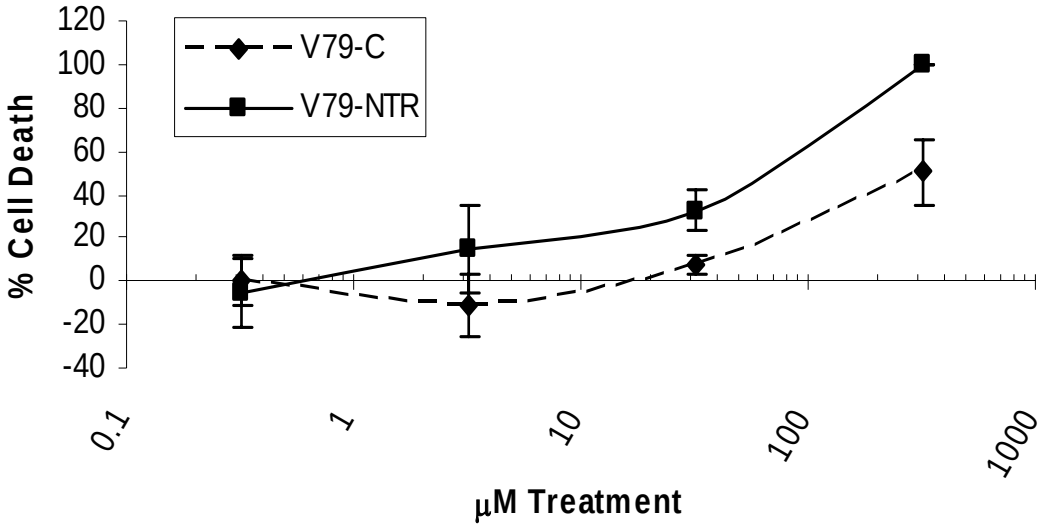

Figure 5.30 Cytotoxicity of compound 13 in the V79-C and V79-NTR cell lines after treatment for 3 days.

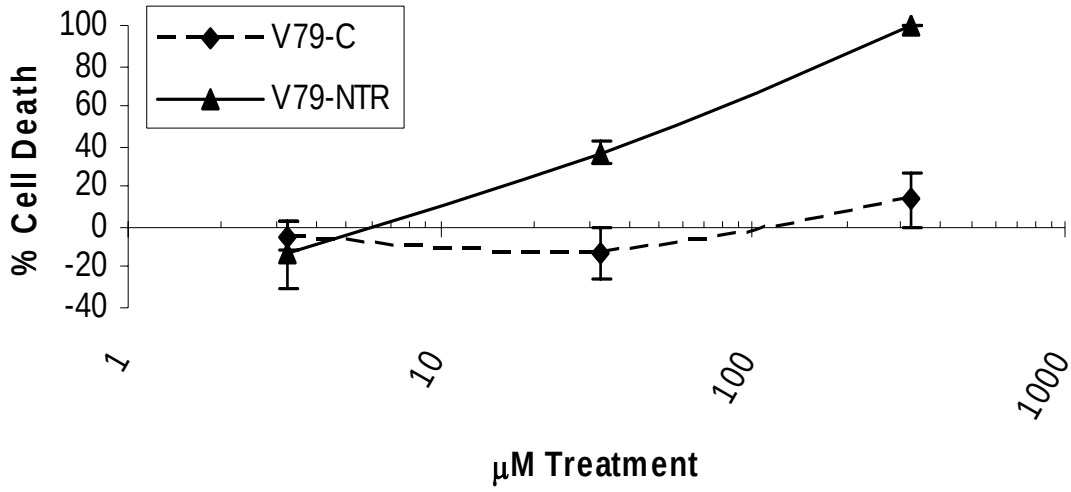

Figure 5.31 Cytotoxicity of compound 13 in the V79-C and V79-NTR cell lines after treatment for 5 days.

Compound 14 showed a dramatic difference in cytotoxicity over 3 days (Figure 5.32). No toxicity was seen in the V79-C cell line over the range of concentrations tested (0.25-250 μM). Toxicity in the V79-NTR cell line was evident from 2.5 μM, with approximately 40% cell death occurring. At 25 μM and 250 μM, 100% cell death was observed. The IC_{50} value in the V79-NTR cell line was established as 3.4 μM over 3 days. The ratio of IC_{50} values was greater than 73.5, but a more accurate ratio could not be calculated as the IC_{50} value was not reached for the V79-C cell line. Similar toxicity was observed over 5 days for the V79-NTR cell line (Figure 5.33). Over 50% cell death was noted at 2.5 μM and 100% cell death was again evident after treatment with 25μM and 250 μM. However, there was also an increase in toxicity in the control cell line, with approximately 40-50% cell death occurring after treatment with 25 μM and 250 μM. The IC_{50} values were established as 33 μM and 1.8 μM for the V79-C and V79-NTR cell lines respectively, giving a ratio of 18.33 (Table 5.3).

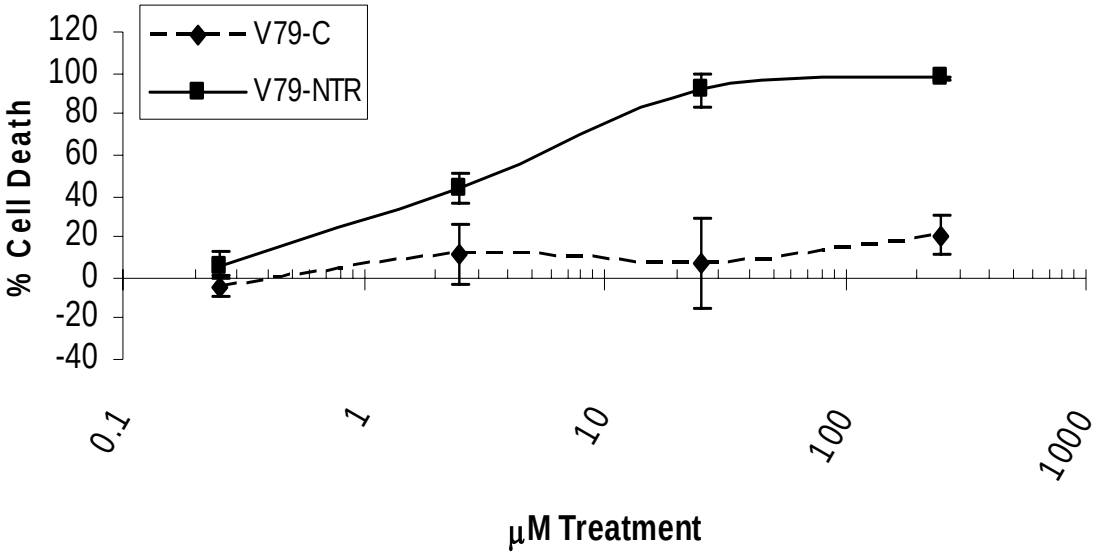

Figure 5.32 Cytotoxicity of compound 14 in the V79-C and V79-NTR cell lines after treatment for 3 days.

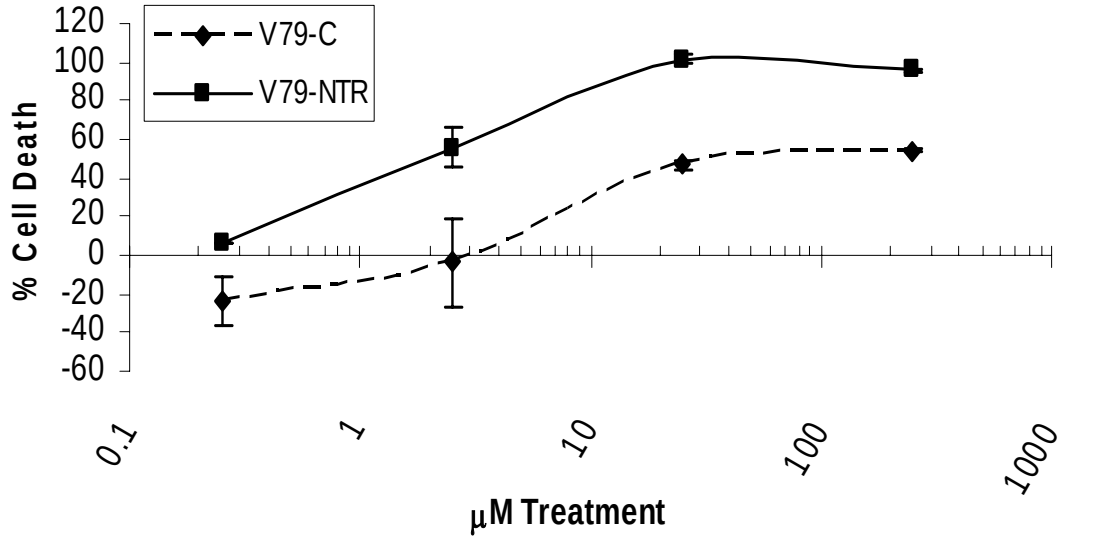

Figure 5.33 Cytotoxicity of compound 14 in the V79-C and V79-NTR cell lines after treatment for 5 days.

Table 5.3 IC_{50} values and ratios for prodrugs 3, 6, 9, 13, 14 and CB1954 in the V79-C and V79-NTR cell lines after treatment for 3 and 5 days.

IC_{50} Values V79-C & V79-NTR Cell Lines (μM)						
	3 Days			**5 Days**		
	V79-C	**V79-NTR**	**Fold**	**V79-C**	**V79-NTR**	**Fold**
Cmpd 3	9±1.05	7.5±1.49	1.2	11±1.2	5.8±1.01	1.9
Cmpd 6	85±6.2	8±2.83	10.63	88±7.8	91±8.54	0.97
Cmpd 9	>16.1[a]	>16.1[a]	-	>16.1[a]	>16.1[a]	-
Cmpd 13	323±54	66±30	4.89	>323[a]	54±7.07	>5.98[b]
Cmpd 14	>250[a]	3.4±1.27	>73.5[b]	33±3	1.8±0.2	18.33
CB1954	190±25	0.007±0.002	27143			

Mean ± SD

(a) IC_{50} value not reached up to highest concentration tested

(b) Undetermined IC_{50}, therefore highest concentration tested was used to calculate ratio and thus was an underestimate.

Following cytotoxicity analysis with the V79-C and V79-NTR cell lines, compounds 13 and 14 showed the most promise as activated prodrugs in the presence of the nitroreductase-expressing cell line. The next step was to confirm the activation of the prodrug as being the cause of this increased toxicity.

5.2.5 Liquid Chromatography-Mass Spectrometry Analysis

In order to confirm the activation of the prodrugs, samples were analysed by liquid chromatography-mass spectrometry (LC-MS). Dr. Rachel Wall and Dr. Robert O'Connor of the National Institute for Cellular Biotechnology (NICB) developed the method and ran the samples. Media was collected from cells exposed to 75 μM prodrug 13 as described in section 2.2.12.1. Analysis was carried out as described in section 2.2.12.2. Figure 5.34 shows the mass spectrometric analysis of 5-FU and compound 13 in their pure forms, with peaks of 130 and 310 m/z at 4.1 and 9.5 minutes respectively. Two controls were used, the first was a sample of compound 13 that was added to media and immediately frozen until analysis, the second was a sample of compound 13 that was added to media, incubated at 37°C for 5 days and then frozen for analysis. Figure 5.35 shows the mass spectrometric analysis of these two control samples. Figure 5.35 A and C show background noise, with the absence of a peak for 5-FU and B and D show peaks for compound 13 at 9.5 minutes. This proves activation of compound 13 was not occurring in the media alone.

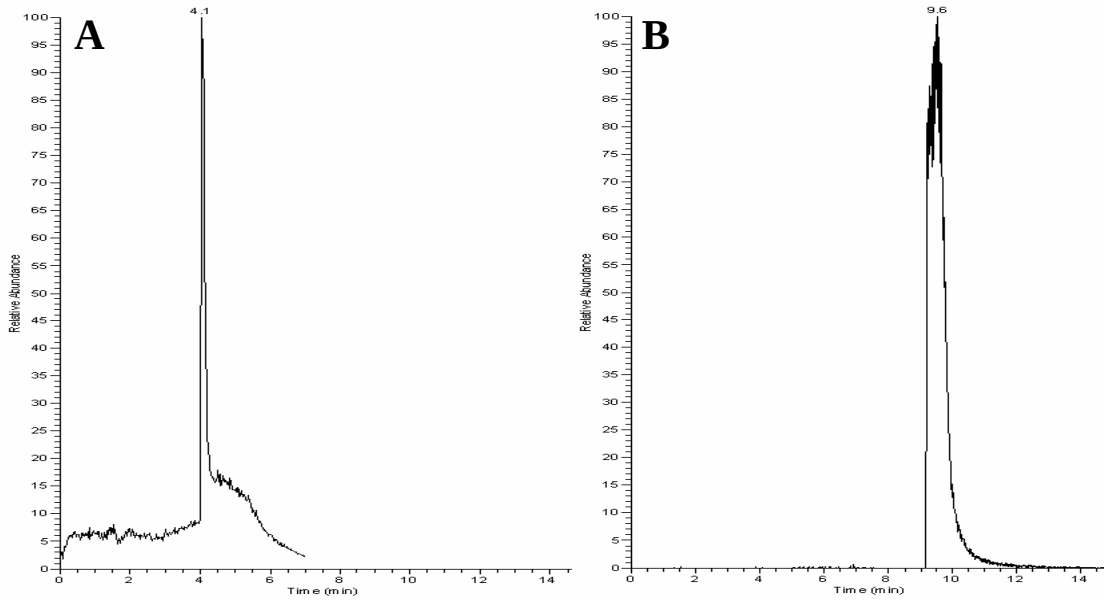

Figure 5.34 Mass spectrometric analysis of 5-FU (A) and compound 13 (B), appearing as peaks at m/z 130 and 310.

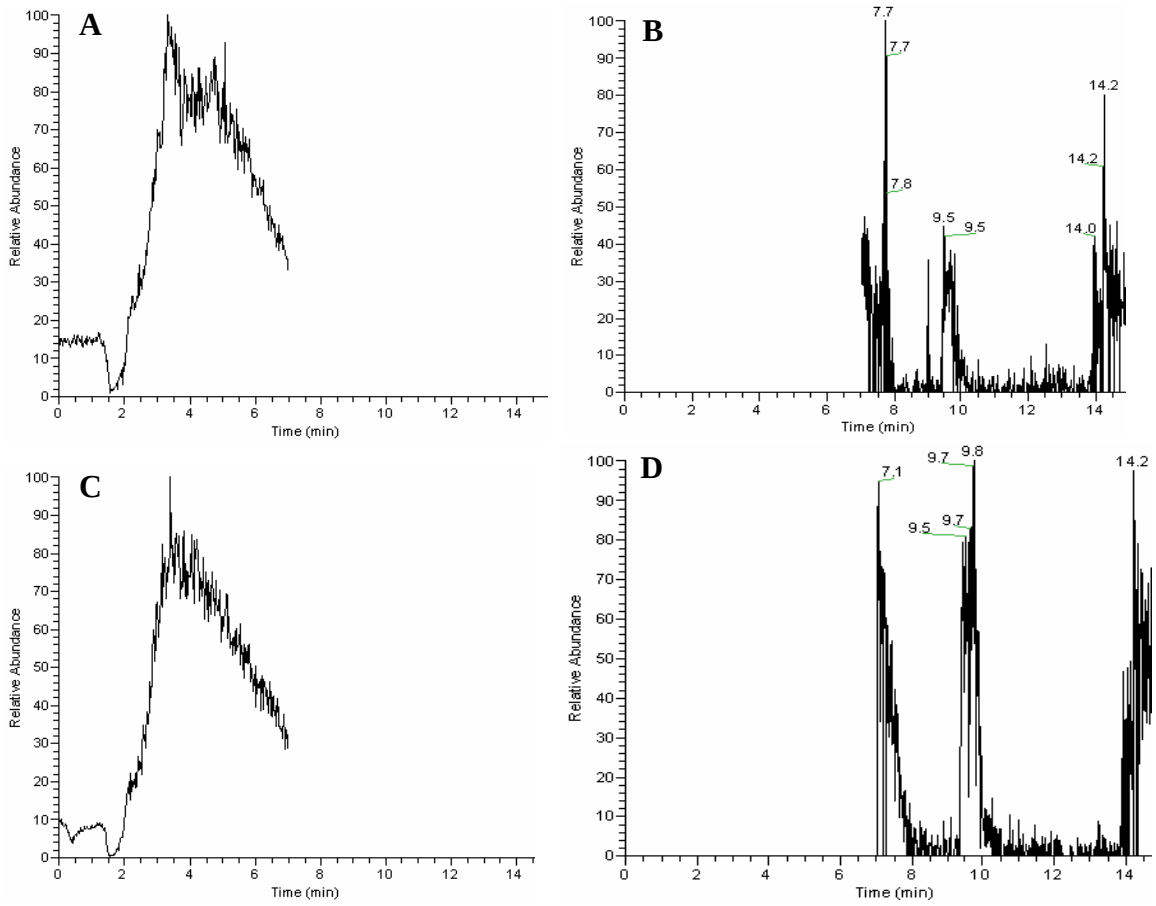

Figure 5.35 Mass spectrometric analysis of controls, A and B – compound 13 added to media and frozen immediately, C and D – compound 13 added to media, incubated at 37°C for 5 days and then frozen.

Figure 5.36 shows mass spectrometric analysis of samples from the V79-C (top) and V79-NTR (bottom) cells. Compound 13 was added to cells at 75 μM and incubated at 37°C for 5 days. The media was then removed and frozen for analysis. There was no 5-FU peak in the sample from the V79-C cells (Figure 5.36 A) while there was a peak for compound 13 evident at 9.5/9.7 minutes (Figure 5.36 B). For the V79-NTR cells, however, there was a peak of 5-FU at 4.4 minutes (Figure 5.36 C), with a clear absence of the peak for compound 13 at 9.5 minutes (Figure 5.36 D). This would indicate activation of compound 13 to 5-FU after incubation with the V79-NTR cell line for 5 days.

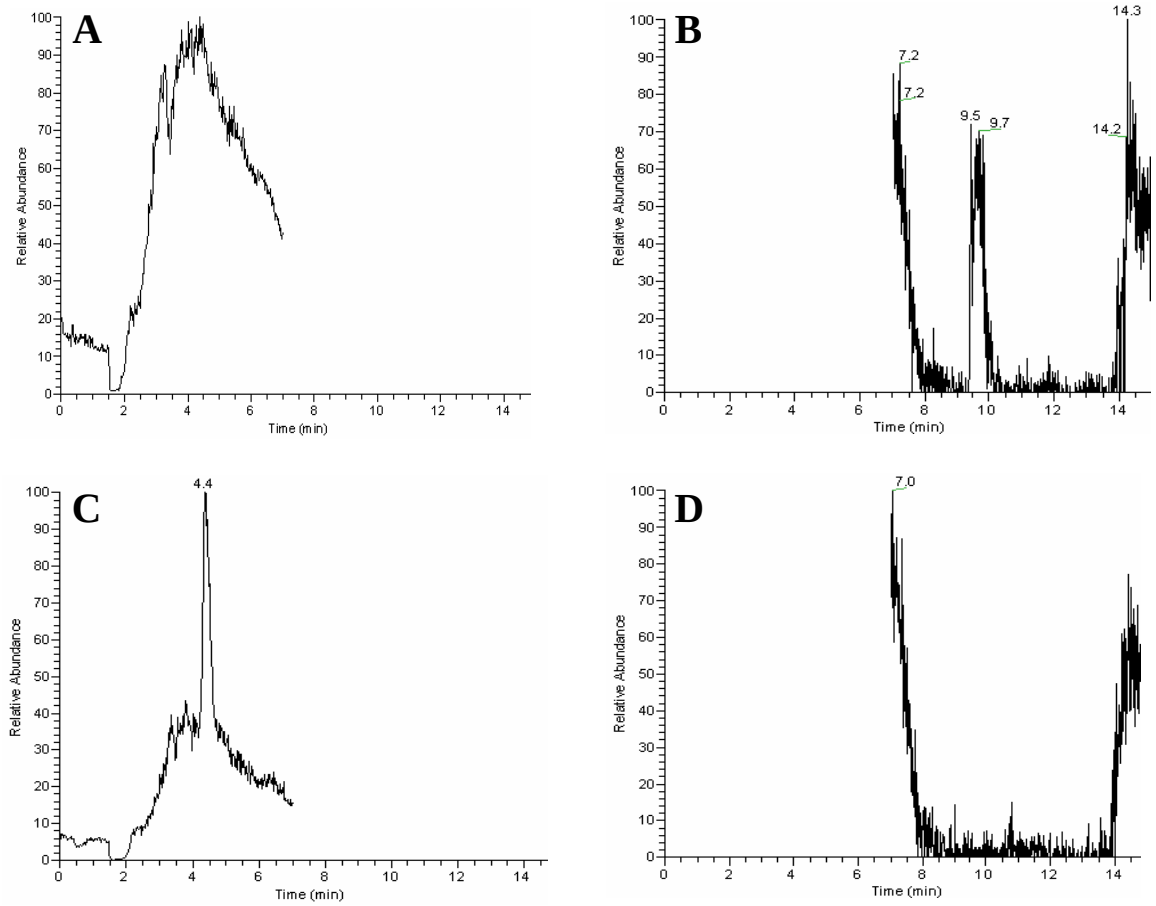

Figure 5.36 Mass spectrometric analysis of 5-FU and compound 13 after incubation with the V79-C (A and B) and V79-NTR (C and D) cell lines for 5 days. A peak of 5-FU is evident in graph C while in the same sample, the peak for compound 13 (D) has disappeared.

Unfortunately, mass spectrometric analysis of the cell pellets was not possible due to lack of sensitivity and rapid metabolism of 5-FU in the cells. Had time and resources allowed, mass spectrometric analysis of all the prodrugs would have been interesting to examine. However, from the data above confirming the release of 5-FU from the prodrug 13, it was decided to pursue the activation of the compounds by the NTR enzyme in the cancer cell environment.

5.2.6 Plasmid Preparations

The F179 and F184 plasmids were kindly provided by Dr Steve Hobbs, CRUK Centre for Cancer Therapeutics, UK. The F179 plasmid, 5.7 kb in size, was the control plasmid and contained an ampicillin resistance gene for selection in *E.coli* and the puromycin resistance gene for selection in mammalian cells (See Appendix A for plasmid map). The F184 plasmid, 6.3 kb in size, contained the cDNA for the NTR enzyme under the control of a cytomegalovirus (CMV) promoter, along with the resistance genes previously mentioned for the F179 plasmid (See Appendix A for plasmid map). The plasmids were provided on sterile discs of filter paper and thus the DNA had to be extracted and transformed into competent bacteria which were cultured to obtain working volumes of the plasmid DNA, as per section 2.2.13. Following preparations of the plasmid DNA, restriction digests were carried out as per section 2.2.13.3. F179 plasmid was digested with Eco RI, which cleaves at two sites in the plasmid, giving two DNA segments of 2.5 kb and 3.2 kb (Figure 5.37). F184 plasmid was digested with Bam HI and Xho I enzymes. Bam HI cleaves at one site and Xho I cleaves at two sites in the plasmid, in combination giving 3 fragments of DNA of 0.7 kb, 2.5 kb and 3.2 kb (Figure 5.38).

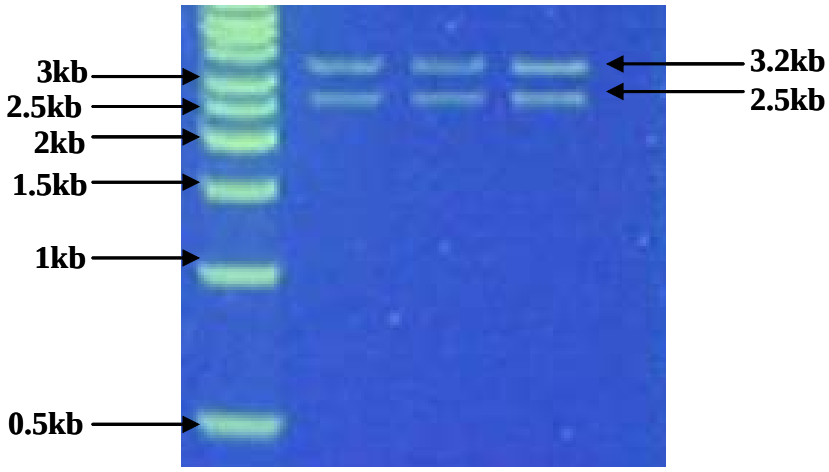

Figure 5.37 Restriction digest of F179 plasmid using Eco RI enzyme, showing two bands of 2.5 kb and 3.2 kb for three separate preparations.

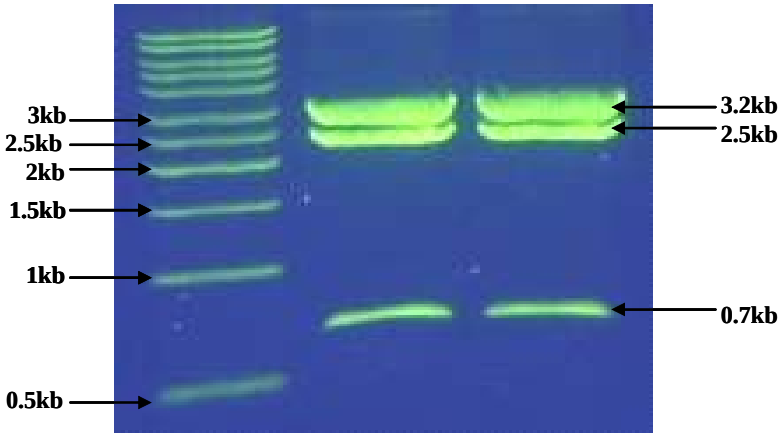

Figure 5.38 Restriction digest of F184 plasmid using Bam HI and Xho I enzymes, showing three bands of 0.7 kb, 2.5 kb and 3.2 kb for two separate preparations.

5.2.7 Transfection of the NTR gene into colon cancer cell lines

The SW480 cell line was the obvious choice for transfection of the plasmids, as the toxicity had previously been examined in this cell line and previous transfections of this cell line in our group had been successful (Murray *et al*., 2004). However, despite numerous attempts at transfection using varying cell numbers and ratios of plasmid DNA to transfection reagent, a stable cell line could not be established. The stocks of this cell line in the lab had tested positive for mycoplasma and new stocks had been purchased from the ATCC prior to the transfection attempt. Despite having fresh, mycoplasma-negative stocks, the transfection was not successful and another avenue was pursued. The HCT116 colorectal carcinoma cell line was chosen for transfection of the F179 and F184 plasmids. Firstly, transfection efficiency of this cell line was investigated using the pCH110 plasmid (See Appendix A for plasmid map), which contained the *lac Z* gene encoding the β-galactosidase protein. This plasmid was transfected into the HCT116 cell line and activity determined using X-gal (as per Section 2.2.14.1), which reacts with β-galactosidase to turn the transfected cells blue (Figure 5.39). Transfection efficiency (percentage of blue cells of total cells) was calculated as 9.7% from the 200X photograph (Figure 5.39).

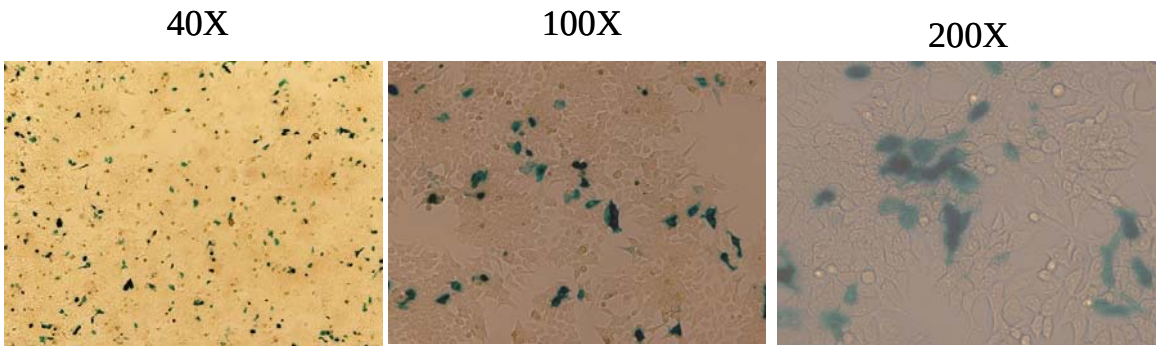

Figure 5.39 Transfection efficiency of the HCT116 cell line as illustrated by the blue staining of cells due to the interaction of β-galactosidase in transfected cells with X-gal. Photographs were taken at different magnifications using an Olympus DP70 camera.

Following confirmation of the transfection efficiency of the HCT116 cell line, the F179 and F184 plasmids were transfected into the cells successfully on the first attempt. Puromycin was used to select the cells containing the plasmids, as per section 2.2.14.2. Two different populations containing each plasmid were established. The presence of the plasmids in the cells was confirmed by PCR using DNA extracted from the cells as per section 2.2.14.3 (Figure 5.40). RT-PCR using mRNA extracted from the cells confirmed the production of NTR mRNA (Figure 5.41). The levels of NTR mRNA were similar in the HCT116 cells transfected with the F184 plasmid and the V79-NTR cells (Figure 5.41). Once cell populations were established and the presence of the plasmid confirmed, the cells were used for testing the prodrugs. The transfected cell lines were designated HCT-C (containing F179) and HCT-NTR (containing F184).

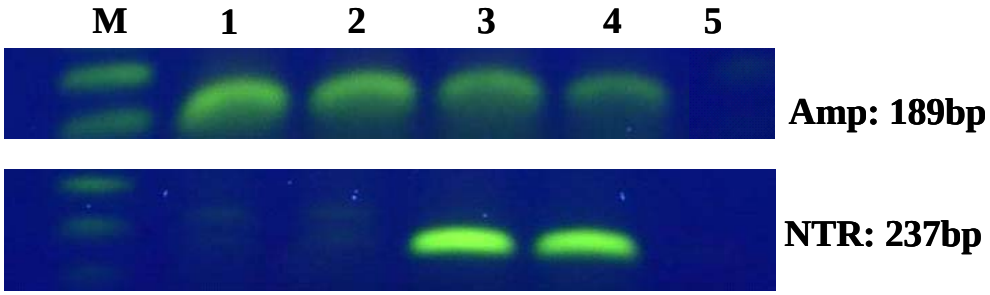

Figure 5.40 PCR products from F179 and F184 plasmids from transfected HCT116 cell lines for ampicillin (top) and NTR (bottom). M: Marker, Lane 1: F179(A), Lane 2: F179(B), Lane 3: F184(A), Lane 4: F184(B), Lane 5: Control (H_2O).

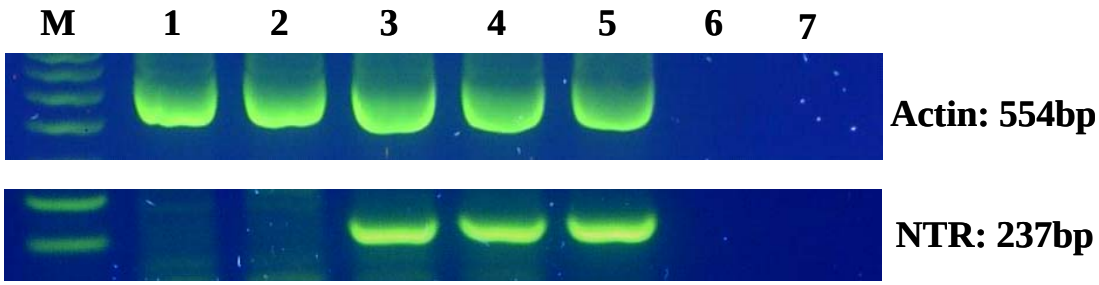

Figure 5.41 RT-PCR products from F179 and F184 plasmids for actin and NTR. M: Marker, Lane 1: F179(A), Lane 2: F179(B), Lane 3: F184(A), Lane 4: F184(B), Lane 5: V79-NTR, Lane 6: RT negative control, Lane 7: control (H_2O).

5.2.8 Cytotoxicity of prodrugs in the HCT-C and HCT-NTR cell lines

The prodrugs, 3, 6, 9, 13 and 14 were tested on the established cell lines HCT-C and HCT-NTR. Cytotoxicity was assayed three times, in triplicate. Figure 5.42 shows the toxicity of compound 3 in these two cell lines after treatment for 3 and 5 days. No significant difference in toxicity was seen between the HCT-C and HCT-NTR cell lines. The IC_{50} values and ratios are listed in Table 5.4. The ratio of IC_{50} values for compound 3 was 0.92 and 0.6 for 3 and 5 days respectively. Treatment with compound 6 only showed toxicity at the highest concentration used but caused no difference in toxicity between the two cell lines (Figure 5.43). The IC_{50} value was not reached in the HCT-NTR cell line after 3 days treatment and thus the fold difference was less than 0.6 but an exact ratio could not be established. After 5 days treatment, a ratio 1.3 was calculated between the two IC_{50} values (Table 5.4).

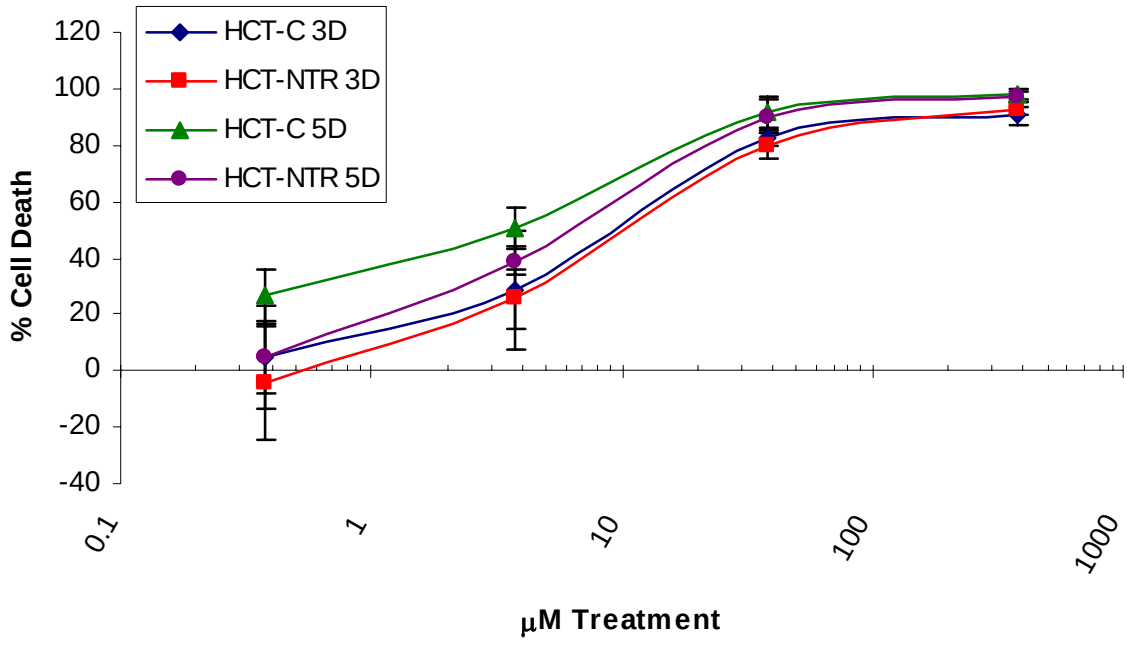

Figure 5.42 Cytotoxicity of compound 3 in the HCT-C and HCT-NTR cell lines after treatment for 3 days (3D) and 5 days (5D).

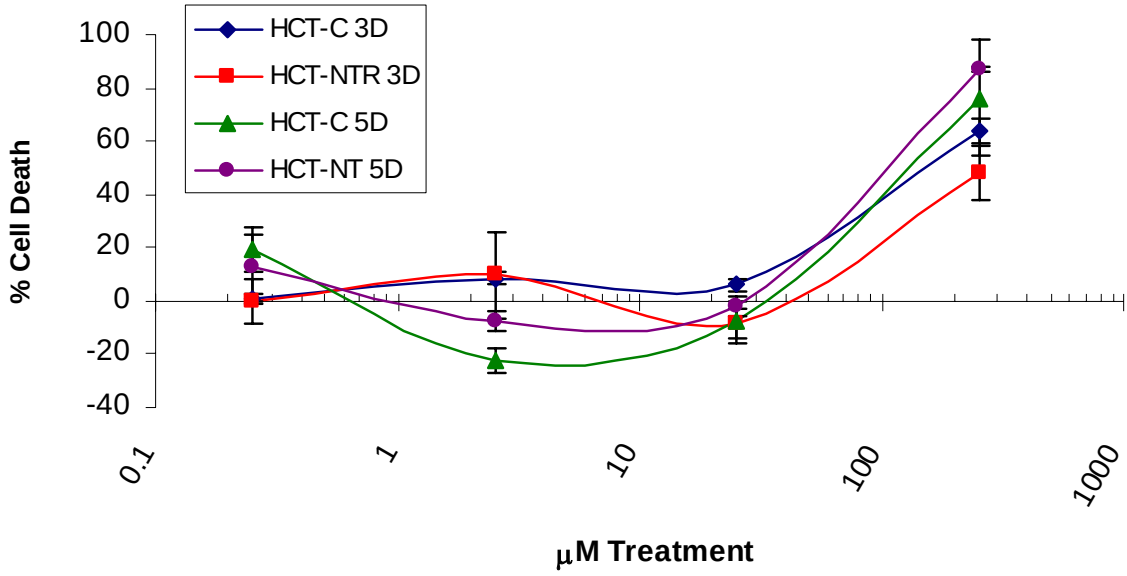

Figure 5.43 Cytotoxicity of compound 6 in the HCT-C and HCT-NTR cell lines after treatment for 3 days (3D) and 5 days (5D).

Compound 9 showed low toxicity over the range of concentrations tested, with IC_{50} values not reached for either treatment times (Figure 5.44). After treatment for 3 days, compound 13 showed low toxicity in both cell lines, with no increased toxicity in the HCT-NTR cell line, and IC_{50} values were not reached for this time point (Figure 5.45 and Table 5.4). After treatment for 5 days, a small increase in toxicity in the HCT-NTR cell line was noted in comparison to the control, at the top concentration of 323 μM. The IC_{50} values were 320 μM and 200 μM for the HCT-C and HCT-NTR cell lines, giving a ratio of 1.6. Low toxicity was observed after treatment with compound 14 (Figure 5.46). There was no significant increase in the toxicity exhibited in the HCT-NTR cell line. After treatment for 3 days, IC_{50} values of 200 μM and 248 μM were established, giving a ratio of 0.8, but the IC_{50} values were not reached for the 5 day treatment (Table 5.4). Cytotoxicity of CB1954 was examined with the HCT-C and HCT-NTR cell lines (Figure 5.47). There was an increase in toxicity in the HCT-NTR cell line at one concentration for each time point, but this was not consistent over the range of concentrations tested. The ratio of IC_{50} values was 0.98 and 2.22 for 3 and 5 days respectively (Table 5.4).

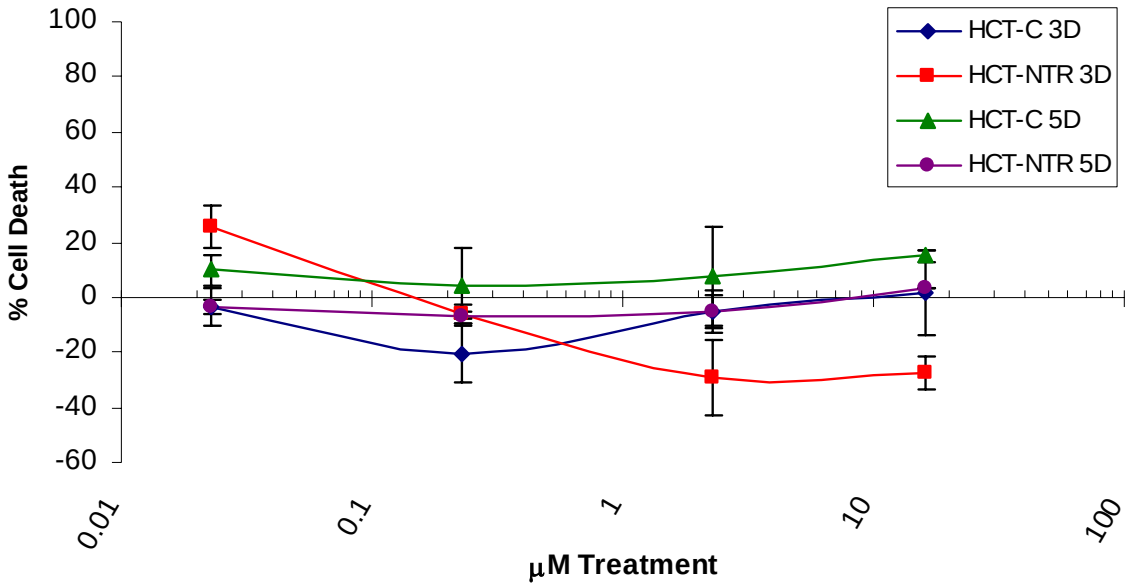

Figure 5.44 Cytotoxicity of compound 9 in the HCT-C and HCT-NTR cell lines after treatment for 3 days (3D) and 5 days (5D).

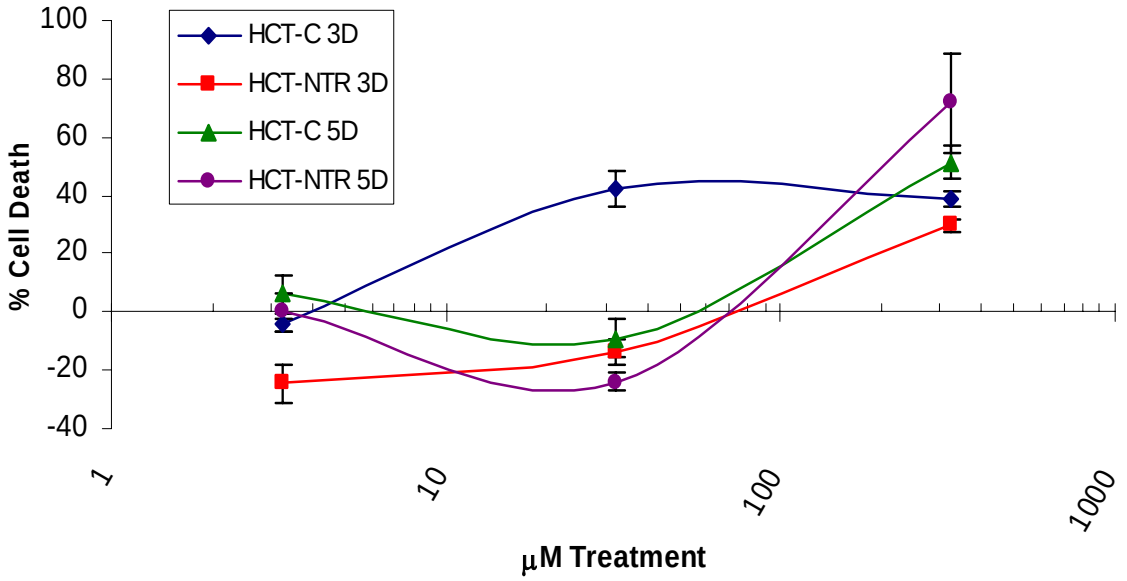

Figure 5.45 Cytotoxicity of compound 13 in the HCT-C and HCT-NTR cell lines after treatment for 3 days (3D) and 5 days (5D).

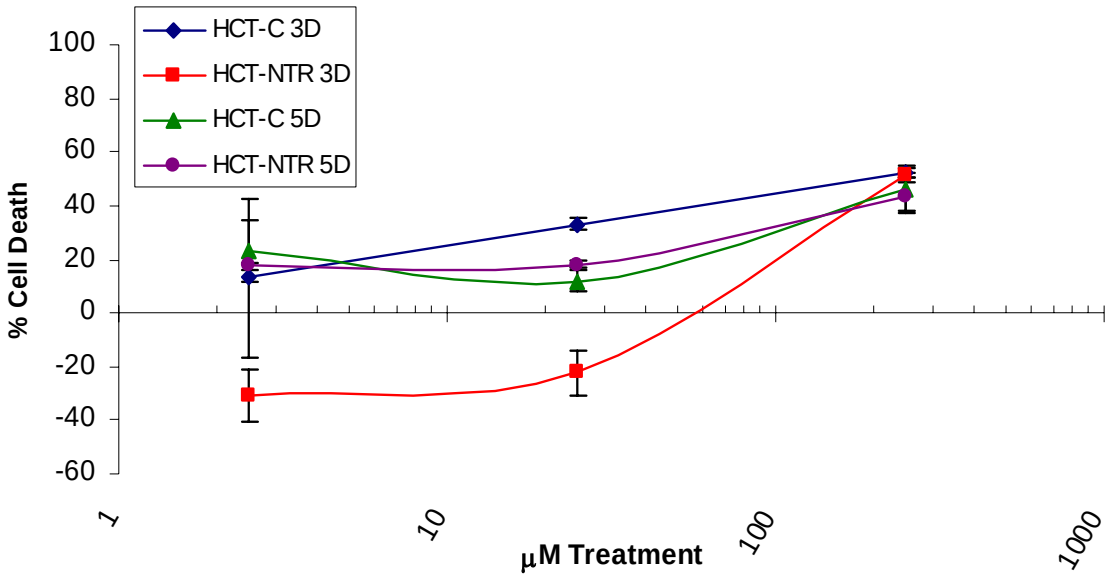

Figure 5.46 Cytotoxicity of compound 14 in the HCT-C and HCT-NTR cell lines after treatment for 3 days (3D) and 5 days (5D).

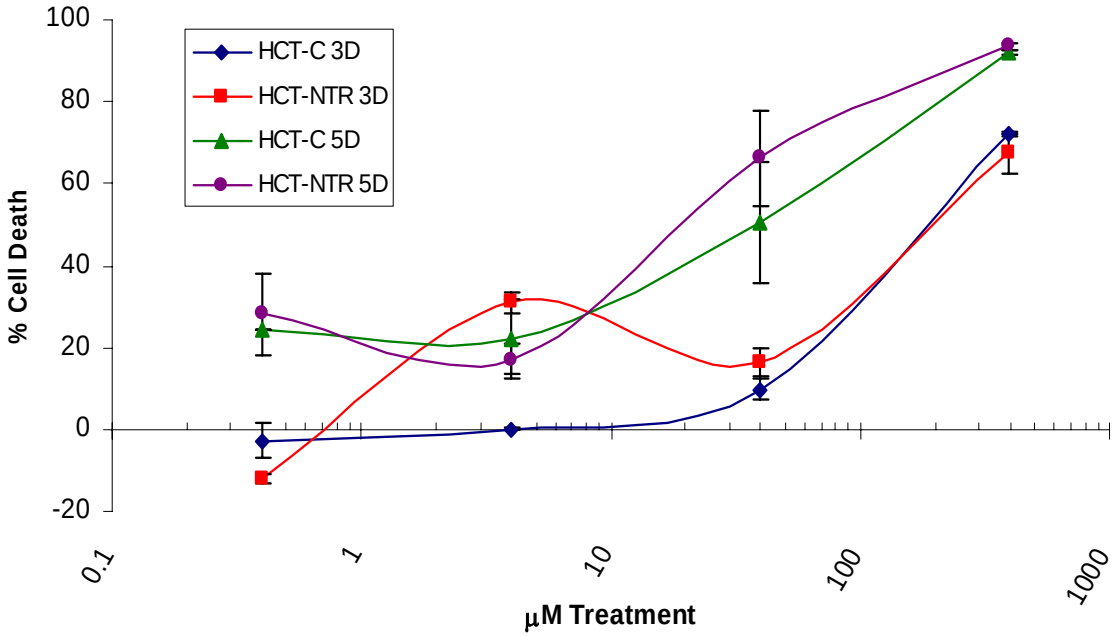

Figure 5.47 Cytotoxicity of CB1954 in the HCT-C and HCT-NTR cell lines after treatment for 3 days (3D) and 5 days (5D).

Table 5.4 IC_{50} values and ratios for prodrugs 3, 6, 9, 13, 14 and known substrate CB1954 in the HCT-C and HCT-NTR cell lines after treatment for 3 and 5 days.

IC_{50} Values HCT-C & HCT-NTR Cell Lines (μM)						
	3 Days			**5 Days**		
	HCT-C	**HCT-NTR**	**Fold**	**HCT-C**	**HCT-NTR**	**Fold**
Cmpd 3	9.5±4.5	10.3±2.3	0.92	3.7±1.78	6.2±1.04	0.60
Cmpd 6	150±14.14	>252[a]	<0.6[b]	140±81	105±7	1.33
Cmpd 9	>16.1[a]	>16.1[a]	-	>16.1[a]	>16.1[a]	-
Cmpd 13	>323[a]	>323[a]	-	320±107	200±70	1.6
Cmpd 14	200±50	248±1	0.8	>250[a]	>250[a]	-
CB1954	194±3.6	197±15.28	0.98	40±24	18±12	2.22

Mean ± SD
(a) IC_{50} value not reached up to highest concentration tested
(b) Undetermined IC_{50}, therefore highest concentration tested was used to calculate ratio and thus was an overestimate.

5.2.9 HCT-C and HCT-NTR Enzyme Assays

Activity of the NTR enzyme in the newly established cell line, HCT-NTR, was investigated using cell lysates as described in section 2.2.11.2. Lysates from HCT-NTR and HCT-C cell pellets were tested with CB1954 for activity. Figure 5.48 shows an enzyme assay using 100 μg total protein, with no activity evident in the HCT-NTR cell line (Table 5.5: Experiment A). The amount of total protein was increased to approximately 300 μg but still little activity was seen in the NTR-expressing HCT cell line, and was mirrored by the HCT-C cell line (Table 5.5: Experiment B). Table 5.5 contains the specific activity values calculated in the cell lysates used in these assays. In experiment A, the V79-NTR cell line showed greater than 20 times more specific activity than the HCT cell lines. The HCT-C cell line surprisingly showed higher specific activity than the HCT-NTR cell line but the values for both were low. The V79-NTR cell line had lower specific activity in experiment B. The specific activity for the HCT-NTR and HCT-C cell lines were

approximately half that of the V79-NTR cell line, with the control cell line again having slightly more activity than the NTR cell line.

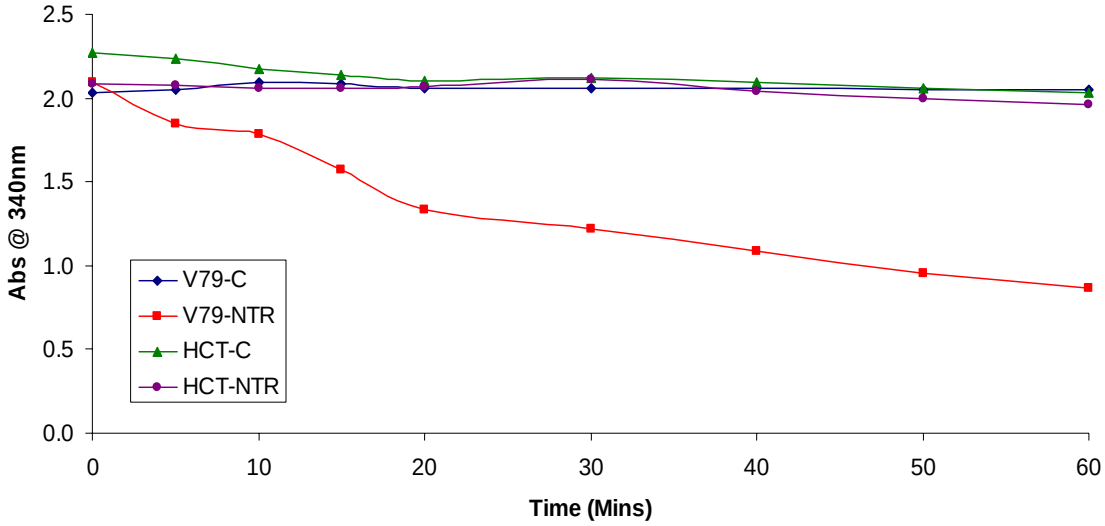

Figure 5.48 Enzyme assay using cell lysates from the V79-C, V79-NTR, HCT-C and HCT-NTR cell lines to test activity of NTR with CB1954. 100 μg protein from the cell pellets was used in this assay (Experiment A).

Table 5.5 Specific activity of nitroreductase enzyme in lysates in experiments A and B.

Specific Activity (Units/mg)		
	Experiment A	**Experiment B**
V79-C	0.000035	-
V79-NTR	0.010252	0.000851
HCT-C	0.000588	0.000461
HCT-NTR	0.000310	0.000326

In order to examine the levels of NTR protein being produced in the HCT-NTR cell line, extracts were run on an SDS gel (Figure 5.49). A positive control showed a band at 24 kDa for NTR protein (Lane 2, Figure 5.49). However, no bands were seen in any other samples run. V79-NTR (Lane 3) and V79-C (Lane 4) samples appeared to be slightly degraded, with no distinct protein bands visible. Samples from the HCT-NTR cell lines (Lanes 5 and 6) unfortunately did not show a band for the NTR protein.

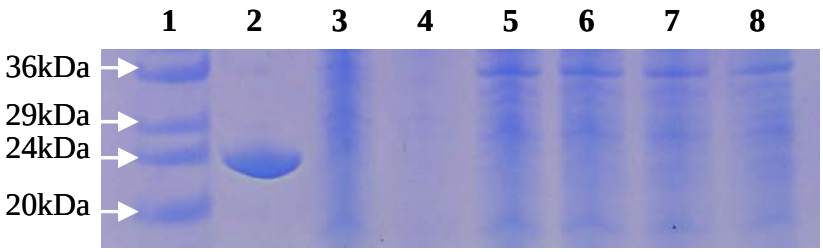

Figure 5.49 SDS gel with protein samples from V79 and HCT cell lines. Lane 1: SigmaMarker^{TM}, Lane 2: Positive control for NTR, band visible at 24 kDa, Lane 3: V79-NTR, Lane 4: V79-C, Lanes 5 and 6: HCT-NTR, Lanes 7 and 8: HCT-C. 35 μg total protein was loaded for each sample.

5.3 Discussion

The aim of this chapter was to examine the activation of the 5-FU and 5-FUrd prodrugs. These compounds were designed as bioreductive prodrugs so activation by hypoxia was first investigated. Prodrugs 3, 6, 9, 13 and 14 were tested under hypoxic conditions (2% O_2) and compared to control conditions of normoxia (20% O_2). Both the 4T1 and the SW480 cell line showed little negative effect when cultured in hypoxia for up to 72 hours (Figures 5.9 and 5.14). The SW480 cell line in fact showed an increase in cell growth, probably due to activation of anti-apoptotic proteins in response to the hypoxia (Kizaka-Kondoh *et al*., 2003). Incubation of the 4T1 cell line with varying concentrations of the prodrugs under hypoxic conditions for up to 72 hours showed no increase in toxicity in comparison to cells in normoxic conditions (Figures 5.10-5.13). Compound 13 showed toxicity towards the 4T1 cells at the higher concentrations but this was also exhibited under normoxia (Figure 5.10). Compound 14 showed low toxicity over the range of concentrations tested under both hypoxic and normoxic conditions (Figure 5.11). Compound 3, as seen previously in chapter 4, was toxic to the cells from concentrations greater than 1 μM, but showed no difference under the normoxic and hypoxic conditions (Figure 5.12). Low toxicity was seen after treatment with compounds 6 and 9 over 3 days (Figure 5.13).

Cytotoxicity assays under hypoxic conditions with the SW480 cell line also showed no difference in toxicity after treatment with the prodrugs (Figures 5.15 and 5.16). These combined results led to the conclusion that the prodrugs were not being activated under hypoxic conditions. A known hypoxia-activated prodrug, for example Tirapazamine, could have been used as a control to confirm that hypoxic levels were actually reached within the cells (Brown and Wilson, 2004). Activation at a lower percentage of oxygen (1% or 0.1%) could have been examined, however these facilities were not available for these experiments. These *in vitro* results were not necessarily an indication of the possible efficacy *in vivo*. Initial investigations in the case of AQ4N showed no activation in cultured tumour cells (Patterson and McKeown, 2000). Activation in culture was only achieved when experiments were supplemented with liver microsomal fractions (Patterson and McKeown, 2000). Freshly excised tumour tissue could also activate AQ4N under hypoxic conditions, but only up to 24 hours after excision (Hejmadi *et al*., 1996 and Patterson *et al*.,

2000). This was due to the down-regulation of cytochrome P450 in cell culture conditions (Patterson and McKeown, 2000).

The reductase enzymes responsible for the activation of prodrugs under hypoxic conditions are predominantly one-electron reductases (Williams *et al*., 2001). Thus, the lack of activation of the 5-FU and 5-FUrd prodrugs could be due to the requirement of two electron reductases, of which, cytochrome P450 has previously been shown to be down-regulated in culture. Further investigation along this avenue would have required supplementation of assays with cytochrome P450. However, activation by NTR and a GDEPT approach was also attractive.

NTR, an *E.coli* enzyme of 24 kDa, is a two-electron reductase which has previously been used to activate prodrugs such as CB1954 (Denny, 2001). This enzyme was tested with the nitrobenzyl prodrugs using an enzyme assay which monitored the rate of reaction by the decrease in absorbance of NADH at 340 nm. Compounds 9 and 13 appeared to be good substrates of the enzyme (Figure 5.17). Non-linear regression software Enzfitter and the linear plots, Lineweaver-Burk, Hanes-Woolf and Eadie-Hofstee, were used to calculate k_{cat} and K_m values using data from a range of assays varying substrate concentration and reaction time (Figures 5.18-5.23). The K_m values decreased in order, compound 13 (48.17 μM)>compound 14 (13.47 μM)>CB1954 (9.66 μM). CB1954 thus had the highest affinity for this enzyme. The k_{cat} values showed compound 13 had the highest turnover (76,427 sec^{-1}) followed by CB1954 (52,195 sec^{-1}) and compound 14 (29,857 sec^{-1}).

k_{cat}/K_m ratios incorporate both of these values and give an indication of the overall efficiency of the reaction. CB1954 and NTR proved to be the most efficient combination, with k_{cat}/K_m ratio of 5.4×10^9 $sec^{-1}M^{-1}$ (Table 5.2). This was not surprising considering the fact that CB1954 is in clinical trials with this enzyme. The k_{cat}/K_m values for compounds 13 and 14 were 1.59×10^9 and 2.22×10^9 $sec^{-1}M^{-1}$ respectively, approximately 30% and 40% of the efficiency of the CB1954/NTR system. Reported K_m and k_{cat} values for CB1954 were 862 μM and 6 sec^{-1} respectively (Rooseboom *et al.*, 2004). These are considerably different values compared to the results obtained here. The published results for CB1954/NTR are from a 1992 paper (Anlezark *et al.*, 1992). The authors used CB1954 provided by the Institute of Cancer Research and extracted NTR from *E. coli* B cell paste, as opposed to the CB1954 and NTR from Sigma-Aldrich used in the experiments presented here.

They also used a lower enzyme concentration (2 μg/ml), substrate concentration (100 μM) and a different buffer. These differences in the experimental system would have an impact on the calculations of these values. While our enzyme assay was a crude system, it allowed comparison between the known substrate CB1954 and our prodrugs, compounds 13 and 14.

Activity of the prodrugs in cell lines expressing the *E. coli* NTR enzyme was investigated next. A Chinese hamster lung fibroblast cell line transfected with the cDNA for NTR (V79-NTR) and the control cell line (V79-C) were obtained from Morvus Technologies. Total protein extracts from the V79 cell lines were first used to assess activity of the cellular enzyme. Activity in the V79-NTR cell line was evident with a sharp decrease in the absorbance of NADH in comparison to the control cell line and the 4T1 cell line (Figure 5.24). Specific activity for the V-79 cell line was 0.1578 Units/mg in comparison to 0.0013 Units/mg for the control cell line. According to Morvus Technologies product information, specific activity should be 0.02 Units/mg cell protein for the V79-NTR cell line and <0.0001 Units/mg cell protein for the V79-C cell line. Our calculations differed by one order of magnitude for both, however there was still a greater than 100-fold difference in the specific activities so activity in the V79-NTR cell line was confirmed.

Following this confirmation of the activity of the cellular enzyme, cytotoxicity in the V79-NTR and V79-C cell lines was examined. The cytotoxicity profile of CB1954 illustrated the considerable difference in response to this prodrug in the two cell lines (Figure 5.25). The ratio of IC_{50} values in the V79-C and V79-NTR cell lines for CB1954 was 27,143 (Table 5.3). According to Morvus Technologies, a greater than 7,000-fold difference can be seen between the two IC_{50} values. Higher ratios have previously been reported for this system, with up to 100,000-fold increase in toxicity (Knox *et al.*, 1992). Compound 3 showed toxicity in both the V79-C and V79-NTR cell lines, indicating that this prodrug was not activated by the NTR enzyme (Figure 5.26). Considering the toxicity noted previously with compound 3, this was not a surprising result; however, the possibility of increased toxicity in the presence of NTR had to be examined. Figure 5.27 illustrates the toxicity seen following treatment for 3 days with compound 6. There was a difference in toxicity at 25 μM, with no cell death observed in the V79-C cell line and approximately 90% cell death in the V79-NTR cell line. Despite this, at the top concentration of 252 μM,

compound 3 caused a higher percentage of cell death in the V79-C cell line than in the V79-NTR cell line. Also, no increase in toxicity was observed in the V79-NTR cell line after 5 days treatment with the same compound (Figure 5.28).

Compound 9, despite appearing to be a good substrate for the NTR enzyme (Figure 5.17), exhibited low toxicity over 3 and 5 days and IC_{50} values were not reached (Figure 5.29). However, considering the structure of compound 9, if the nitroreductase cleaved the nitro-benzyl side-chain, the structure of compound 8 would remain, with the protected C-2 and C-3 in the sugar (Figure 5.50). This component has been shown in chapter 4 to block activity of 5-FU. Thus, cleavage may be occurring but the 5-FUrd product was not toxic. Compound 13 caused an increase in toxicity in the V79-NTR cell line after treatment for both 3 and 5 days, with the ratio of IC_{50} values of 4.89 and greater than 5.98 respectively (Figures 5.30 and 5.31). Compound 14 showed promising results, causing 100% cell death in the V79-NTR cell line after treatment with 25 μM for 3 days (Figure 5.32). In the V79-C cell line, low toxicity was observed up to the top concentration of 250 μM. The ratio of IC_{50} values over 3 days was greater than 73.5, a considerable ratio between the two cell lines (Table 5.3). Over 5 days, compound 14 was more toxic to the V79-NTR cell line, with an IC_{50} value of 1.8 μM. However, the V79-C cell line also showed some toxicity, with an IC_{50} value of 33 μM, giving a ratio of 18.33 (Figure 5.33).

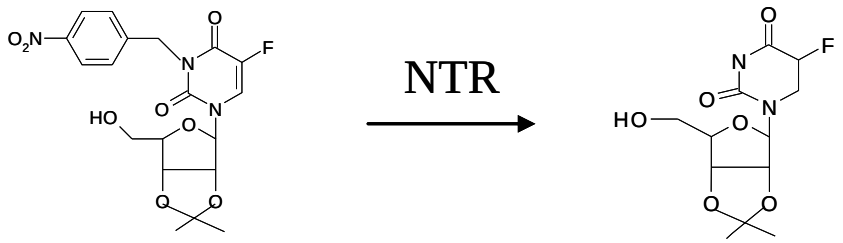

Compound 9 Compound 8

Figure 5.50 Nitroreductase activation of compound 9 would give rise to compound 8.

Greco and Dachs (2001) stated that for significant therapeutic gain, the released cytotoxin should exhibit at least 100-fold more toxicity than the prodrug. Of the 5-FU and 5-FUrd prodrugs designed here, the most promising results from

cytotoxicity assays using the V79 cell lines were for compound 14, with greater than 73.5-fold increase in IC_{50} values over 3 days in the NTR-expressing cell line. Compound 13 also showed encouraging results, with an increase in toxicity over both 3 and 5 days in the V79-NTR cell line. Compound 3 had shown toxicity towards all cell lines tested to date and the results with the V79-C and V79-NTR cell lines were not surprising. Compound 6 had a ratio of IC_{50} values of 10.63 after 3 days treatment however; this was only 0.97 after 5 days. IC_{50} values were not reached for compound 9, which had proven to be a good substrate for the NTR enzyme in the enzyme assays. However, as illustrated in Figure 5.50, the reaction of compound 9 with NTR would produce compound 8 which has previously shown low toxicity, thus, compound 9 may be a good substrate but the resulting toxicity is not occurring.

Mass spectrometry is a powerful analytical technique that can be used to elucidate the structure and chemical properties of molecules. Mass spectrometers measure the mass-to-charge (m/z) ratio of ionised molecules. Liquid chromatography mass spectrometry (LC-MS) separates compounds chromatographically before they are introduced to the ion source and mass spectrometer. In order to confirm activation of compound 13 with the release of 5-FU, mass spectrometry was conducted using compound 13 as it was the most abundant compound. The assay was developed and optimised in the NICB, DCU. Samples of media from the V79-C and V79-NTR cell lines were analysed after treatment with 75 μM of compound 13 for 5 days. Controls mixing compound 13 with media with and without 5 day incubation showed no 5-FU peaks (Figure 5.35). The media removed from the V79-C cells showed a peak for compound 13 (Figure 5.36 B), with no peak appearing for 5-FU (Figure 5.36 A). The sample taken from the V79-NTR cell line had no peak for compound 13 (Figure 5.36 D), with a peak at 4.4 minutes for 5-FU (Figure 5.36 C), indicating release of the free 5-FU from the prodrug 13. Figure 5.51 illustrates this activation of compound 13 by nitroreductase, releasing 5-FU, CO_2 and quinone methide. These results confirm the activation of compound 13 in the V79-NTR cell line and supported the basis of these compounds as NTR-activated prodrugs. The nitroreductase inhibitor, dicoumarol, could be used in experiments as further confirmation that the nitroreductase activation was causing the increased cytotoxicity.

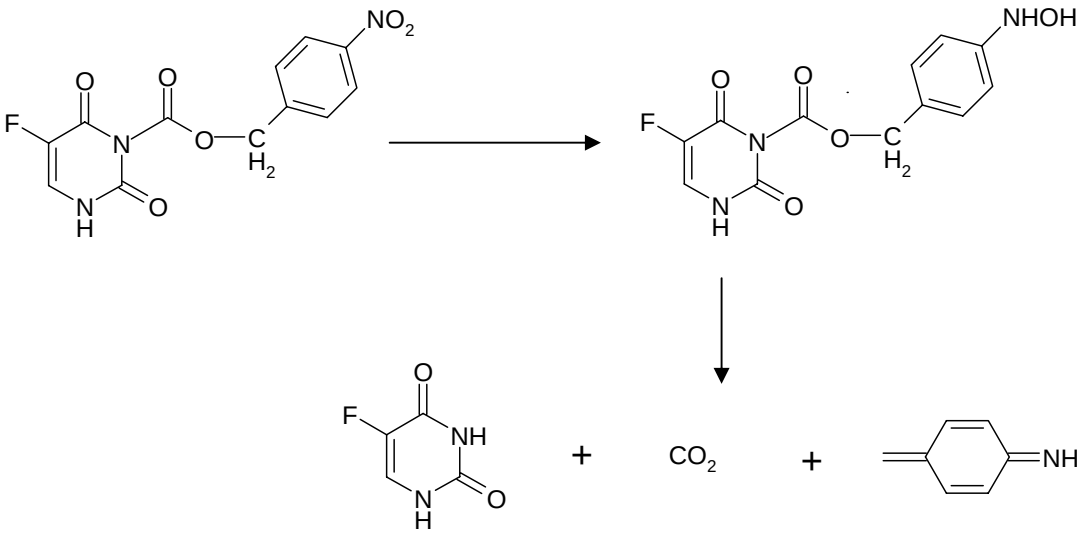

Figure 5.51 Activation of compound 13. Reduction of the nitro group to –NHOH results in cleavage of the bond between the benzyl linker group and the 5-FU, releasing 5-FU, CO_2 and quinone methide.

Once we had successfully shown activation of the prodrugs, we wanted to test the compounds in human cancer cell lines. The cDNA for *E. coli* NTR was obtained and transfected into the HCT116 colorectal cancer cell line. Development of the HCT-C and HCT-NTR cell lines enabled cytotoxicity testing of the prodrugs using a colorectal cancer cell line over-expressing the NTR enzyme. Despite problems in attempts to transfect the plasmids into the SW480 cell line, transfection using the HCT116 cell line was very successful. Transfection efficiency in this cell line was established as 9.7% using the β-galactosidase reporter gene (Figure 5.39). Two pooled populations were established containing each plasmid. The presence of the plasmid and production of the NTR mRNA in these populations was confirmed by PCR and RT-PCR respectively (Figures 5.40 and 5.41). Bands for NTR RT-PCR products in the V79-NTR (lane 5, Figure 5.41) and the HCT-NTR cell lines (lanes 3 and 4, Figure 5.41) were similar, confirming production of the NTR mRNA. However, cytotoxicity of the prodrugs with the HCT-C and HCT-NTR cell lines did not achieve the results anticipated. No increase in toxicity was observed in either of the duplicate HCT-NTR cell lines. Compound 3 showed toxicity over 3 and 5 days in

both the HCT-C and HCT-NTR cell lines (Figure 5.42). This was not surprising as the same result was seen with the V79 cell lines. Compound 6 showed toxicity over 3 and 5 days at the highest concentration tested but this was in both cell lines, so no increase was seen in the HCT-NTR cell line (Figure 5.43). Compound 9 showed no toxicity over the range of concentrations tested (Figure 5.44).

Compound 13 and 14 showed the most promising results in the V79 toxicity experiments. However, the results using the HCT cell lines were disappointing with no increase in toxicity in the HCT-NTR cell line. Compound 13 exhibited lower toxicity than in the V79-NTR cell line, with IC_{50} values not reached over 5 days, and IC_{50} values of 320 μM and 200 μM established over 5 days for the HCT-C and HCT-NTR cell lines respectively (Figure 5.45). Compound 14 also showed low toxicity; with IC_{50} values of 200 μM and 248 μM established over 3 days for the control and NTR-expressing cell lines respectively (Figure 5.46). These results indicated that no activation of the prodrugs was occurring in the HCT-NTR cell lines. To investigate this further, CB1954 was tested with the HCT-C and HCT-NTR cell lines. Toxicity was noted in both HCT cell lines at the highest concentration, 397 μM, after 3 days treatment, the equivalent to that seen in the V79-C cell line (Figures 5.47 and 5.25). No increase in the level of cell death was seen in the HCT-NTR cell line. Higher toxicity levels were observed after treatment for 5 days but no increase was evident in the HCT-NTR cell line (Figure 5.47). These results unfortunately supported the suggestion that activation of the prodrugs by the NTR enzyme was not occurring in the HCT-NTR cell lines.

To confirm this, enzyme assays were carried out using cell extracts from each of the cell lines. Experiments with 100 μg total cell protein showed no activity in the HCT-NTR cell line (Figure 5.48). V79-NTR cell extracts were used as a control and showed specific activity of 0.01 Units/mg, while the HCT-C and HCT-NTR showed specific activity of 5.88×10^{-4} and 3.1×10^{-4} Units/mg respectively (Table 5.5 Experiment A). Increasing the amount of total protein added to the reaction mixture did not increase the specific activity of V79-NTR (data not shown and Table 5.5 Experiment B). Specific activity was higher in the HCT-C cell line than the HCT-NTR cell line but both values were very low, at 4.61×10^{-4} Units/mg and 3.26×10^{-4} Units/mg respectively. The values for specific activity for the V79-NTR cell line were considerably lower than in previous experiments (Figure 5.24). The lack of

activity in the V79-NTR cell pellet was probably due to their storage at -20°C for a number of months. The enzyme could thus have been inactivated, accounting for the loss of activity.

Unfortunately, the overall conclusion from the HCT-C/HCT-NTR cytotoxicity and the enzyme assays using cell lysates was that, despite confirmation of production of the NTR mRNA in the HCT-NTR cell line, active enzyme was not being produced. There are two possible reasons for this, firstly, translation of the mRNA was not taking place or secondly, the NTR protein was being produced but it was not active. An SDS gel with samples from the HCT-NTR cell lines did not however show evidence of the NTR protein but it was not clear in the V79-NTR sample either (Figure 5.49). A western blot could have been performed to confirm the presence of the NTR protein, and would have been more sensitive than the SDS gel. However, no commercial antibody is available for the NTR enzyme, and even if the presence of the protein had been confirmed, this would not have guaranteed activity of the enzyme. Individual clones were not selected based on expression or enzyme activity hence, the populations established were polyclonal. Selection of monoclonal populations by serial dilution and screening the clones could have established a population of high-expressing cells and subsequent toxicity analysis could have been more informative.

Alternatively, sub-cloning the cDNA into another vector could have given higher expression levels. The F184 plasmid contained a cytomegalovirus (CMV) promoter/enhancer region. The human elongation factor-1α (EF-1α) promoter is a stronger promoter and would give higher expression levels (Wurm and Bernard, 1999). In the F184 plasmid the puromycin resistance gene and the NTR gene were not coupled so the translation of their mRNA was not linked. Hence, production of the puromycin resistance product could be present in cells without production of the NTR enzyme. A growth advantage in the clones producing only the puromycin resistance protein over those producing both puromycin resistance protein and NTR protein could have occurred. For future experiments, a plasmid producing a bicistronic transcript of both genes would ensure selection of cells that were producing both proteins. The V79-NTR cells obtained from Morvus Technologies had been transfected with such a bicistronic vector. However, Morvus Technologies only recommended maintaining the enzyme expressing cells for up to 10 passages, as

the enzyme production gradually decreases (personal communication from Morvus Technologies). The cytotoxicity and enzyme assays were carried out using early passages, but the decrease in enzyme production indicated that the expression was not stable. If the NTR protein was being produced within the cells, the activity could have been inhibited by incorrect protein folding, inhibition of dimer formation or a lack of co-factors. Although expression and activity was seen in the V79-NTR cell line, conditions in the HCT116 cell line may not have been conducive to activity.

Despite these disappointing results with the HCT-NTR cell line, the cytotoxicity and mass spectrometry data from the V79 cell lines indicated nitroreductase-mediated activation of the prodrugs 13 and 14. The potential use of these compounds in a GDEPT system needs to be further examined. Mass spectrometry analysis of the media from cells treated with compounds 3, 6 and 14 could be conducted. This may reveal details behind the toxicity seen for compound 3 without nitroreductase activity. No activation of compound 6 was evident and mass spectrometry would confirm this. Compounds 13 and 14 should be used as lead compounds for the development of more active prodrugs. In the long term, they could be tested *in vivo* in mice using a GDEPT approach. Delivery of the NTR gene to the cells would initially be tested in mice to confirm production of the enzyme in the target cells. Administration of the prodrug alone would then examine any endogenous activation of the prodrugs or dose-limiting toxicities. Following these two initial steps, both NTR and prodrug administration would be investigated for efficacy. This work combines to provide a proof of concept for the de-activation of 5-FU by addition of a nitro-benzyl side-chain, which acts as an efficient trigger to release the drug upon exposure to the NTR enzyme.

5.4 Summary

Activation of the prodrugs 3, 6, 9, 13 and 14 was analysed firstly under hypoxic conditions, using the 4T1 and SW480 cell lines. Treatment of the cells with prodrug for up to 72 hours under hypoxic conditions did not increase toxicity of the compounds. Enzyme activation using the *E. coli* NTR enzyme was examined in a simple multi-well plate format, monitoring oxidation of NADH as the reaction proceeded, and also with cell extracts from pellets of NTR-expressing cells. Compounds 9 and 13 appeared to be good substrates for the enzyme. Analysis of compounds 13 and 14 using enzyme kinetics plots allowed calculation of k_{cat} and K_m values. Compound 13 had a high turnover rate of substrate (75,702 sec^{-1}) but compound 14 had a higher overall efficiency value as indicated by a k_{cat}/K_m ratio of 2.22E9. Cytotoxicity assays using the V79 cell lines showed compounds 13 and 14 to have increased toxicity in the NTR-expressing cells, indicating activation to the active drug. The IC_{50} value of compound 14 was greater than 73.5-fold higher in the N79-NTR cell line in comparison to the V79-C cell line over 3 days. Mass spectrometry confirmed that activation of compound 13 was occurring. A clear 5-FU peak was evident after analysis of media from the V79-NTR cells which had been exposed to compound 13 for 5 days. The cDNA for the NTR gene was acquired, amplified and transfected into the HCT116 colorectal cancer cell line and mRNA production confirmed. However, in cytotoxicity experiments with prodrugs no increase in cell death was observed in the HCT-NTR cells in comparison to the HCT-C cells. No activity was noted in enzyme assays using cell extracts either. Despite these disappointing results with the HCT116 cell line, the results from the V79-NTR cell line and the mass spectrometry would still suggest compounds 13 and 14 are potential prodrugs for used in a GDEPT system with NTR. Optimisation of the expression of the NTR in the HCT116 cell line and further analysis of activation, followed by animal studies should prove the efficacy of these prodrugs.

Chapter 6

Summary and Conclusions

6.1 Summary and conclusions

It is predicted that by the year 2020 there will be over 28,000 new cancer cases annually in Ireland (National Cancer Forum, 2006). Widespread screening programmes, better detection methods and improved treatment regimes are urgently required. Future prospects for cancer treatments are looking promising, with research into all aspects of cancer initiation, progression and metastasis to the fore of scientific endeavour. Proteomic and genomic technologies have increased our understanding of the molecular changes that occur as cancer develops and are important tools in this area. The major objectives of this thesis were to investigate the feasibility of using a dietary component, CLA, and novel derivatives of a standard chemotherapeutic agent, 5-FU, as anti-cancer and anti-metastatic agents.

CLA comprises a group of positional and geometric isomers of the fatty acid LA and has previously been shown to have beneficial effects against cancer, obesity, diabetes and atherosclerosis (Pariza *et al*., 2000). A mixture of CLA isomers ('CLA'), two individual isomers, *c*9,*t*11-CLA and *t*10,*c*12-CLA, and LA were tested for cytotoxicity in the 4T1 murine mammary cancer cell line and the Hs578T human breast cancer cell line. Treatment with CLA caused the highest level of toxicity in the 4T1 cell line after 1, 3 and 5 days. The *c*9,*t*11-CLA isomer was more toxic than the *t*10,*c*12-CLA isomer after treatment for 3 days, while after 5 days *t*10,*c*12-CLA treatment resulted in greater cell death. Low toxicity was observed following treatment with LA, except at the highest treatment concentration of 107 μM after 5 days. There appeared to be a threshold with regards to the cytotoxicity of CLA and *c*9,*t*11-CLA, with little increase in cell death observed from 3 to 5 days treatment. This was supported by results in animal studies which showed a maximal response to dietary levels of 1% CLA in comparison to 1.5% CLA (Ip *et al*., 2001 and Ip *et al*., 1996). Cytotoxicity was lower in the Hs578T cell line than in the murine cell line. CLA exhibited the highest toxicity after treatment for 5 days, while the *t*10,*c*12-CLA isomer had more of an effect than the *c*9,*t*11-CLA isomer. The lower responsiveness of the Hs578T cell line could be due to its negative ER status (Tanmahasamut *et al*., 2004). However, despite the negative ER status of the 4T1 murine mammary cancer cell line, cytotoxicity was noted at higher levels than in the Hs578T cell line, indicating different mechanisms of action independent of ER interaction.

In order to determine the mechanism of action of cytotoxicity, cell cycle kinetics and apoptosis levels were analysed in the 4T1 cell line following treatment with the fatty acids. Treatment with two different concentrations, 54 μM and 89 μM, resulted predominantly in a G1 phase arrest of the cells (Figures 3.17 and 3.19). Treatment at the higher concentration did not cause as great an arrest as at the lower concentration, possibly indicating apoptosis of cells from the G1 population. A significant increase in apoptosis was noted at the higher concentration of CLA and the *c*9,*t*11-CLA isomer in comparison to the control ($p<0.05$). These results, along with the cytotoxicity data, indicated a role for CLA as an anti-cancer agent. Its presence in dairy foods such as cow's milk and cheese, with elevated levels possible through variations in the cow's diet, would allow the use of CLA as a biologically active supplement of a functional food (O'Shea *et al*., 1998).

The effects of CLA and the individual isomers on *in vitro* cell migration, invasion and soft agar colony formation were varied. Treatment of the 4T1 cells with CLA had no effect on migration, increased invasion (not significant), and caused a significant increase in colony formation in soft agar ($p<0.01$). The *c*9,*t*11-CLA isomer caused an increase in migration, invasion and colony formation in soft agar ($p<0.01$). Treatment with the *t*10,*c*12-CLA isomer resulted in decreased migration and invasion of the 4T1 cell line and caused a significant increase in colony formation in soft agar ($p<0.00005$).

In order to investigate these effects on migration, invasion and colony formation in soft agar, the level of MMPs and TIMPs in treated cells was examined. An increase in MMP-9 mRNA and protein levels, and a decrease in TIMP-1 mRNA levels following treatment with CLA explains the increased invasion of the 4T1 cells. The level of MMP-9 protein was increased and TIMP-1 mRNA levels were decreased in the 4T1 cells following treatment with *c*9,*t*11-CLA, again possibly playing a role in the increased migration and invasion. Treatment with *t*10,*c*12-CLA resulted in increased MMP-9 protein and mRNA levels and decreased TIMP-1 mRNA levels.

The increase in invasion, colony formation in soft agar and MMP-9 protein levels in the 4T1 cell line following treatment with CLA and the *c*9,*t*11-CLA isomer would not support their use as anti-metastatic agents. The *t*10,*c*12-CLA isomer however, caused a decrease in migration and invasion but significantly increased colony formation in soft agar. MMP-9 mRNA and protein levels were increased

following treatment with *t*10,*c*12-CLA along with a decrease in TIMP-1 mRNA levels. These results would indicate a role of other factors in the down-regulation of migration and invasion of the 4T1 cells, possibly including cell adhesion molecules. An up-regulation in cell adhesion molecules such as E-cadherin could contribute to inhibition of migration and invasion. No difference in adhesion of the cells after treatment with the fatty acids was observed, however this was only examined on plastic and this result would not necessarily reflect adhesion to other cells or ECM components such as laminin or fibronectin. The effect of *t*10,*c*12-CLA on colony formation in soft agar needs further analysis. Possible areas of interest would be the Ras/Raf/ERK pathway which is involved in cell proliferation. Unfortunately time restrictions did not allow these areas to be pursued further as part of this thesis but it is hoped this work will be continued in the near future. Overall, the rationale for using CLA and the isomers as anti-metastatic agents was not convincing from these results. Future studies on the anti-cancer activity of CLA should monitor the effects on invasion and migration of the cells as metastasis-promoting properties would not be beneficial to patients.

The promotion of migration, invasion and formation of colonies in soft agar in the 4T1 cancer cells reported in this work could be a species-specific effect. CLA has been noted to have a varied effect on PPAR-responsive genes in mice in comparison to rats. Belury *et al*. (1997) reported increased mRNA levels of acyl-CoA oxidase, fatty acid binding protein and cytochrome P4504A1 in the livers of female SENCAR mice fed 0.5%, 1% and 1.5% CLA in the diet. In contrast, Moya-Camarena *et al*. (1999) did not note any effect on mRNA levels of these enzymes in female Sprague-Dawley rats. Opposing effects on blood insulin in mice and rats have also been noted (Pariza *et al*., 2001).

The ability of CLA to enhance the efficacy of other chemotherapeutic agents is also under investigation in our laboratory. Fatty acids have previously been reported to modulate toxicity of anti-cancer treatments. Menendez *et al*. (2004) noted increased toxicity in the MDA-MB-231 cell line following treatment with DHA and the taxanes, Taxol and Taxotere. A synergistic interaction between GLA and vinorelbine was also reported by the same group in the MCF-7 cell line (Menendez *et al*., 2002). A prodrug incorporating DHA and paclitaxel was reported to have promising results in phase I clinical trials in patients with advanced solid tumours (Wolff *et al*., 2003). However, results of a phase II trial of this DHA-paclitaxel

conjugate in oesophago-gastric cancers were not convincing enough to warrant further studies (Jones *et al*., 2007). In a phase II trial using DHA-paclitaxel in combination with carboplatin to treat patients with advanced solid tumours, the authors reported one partial response and 10 patients with stable disease, warranting further investigation of DHA-paclitaxel in combination regimens (Harries *et al*., 2004). The ability of CLA to modulate the effect of chemotherapeutic agents needs examination, with close monitoring of the promotion of metastasis.

5-FU is one of the most widely used anti-cancer agents for solid tumours (Malet-Martino and Martino, 2002). It is commonly administered as part of a combination treatment regime but response rates in advanced CRC are generally still below 50% (Longley *et al*., 2003). These low response rates and side-effects such as myelosuppression and GI toxicities warrant investigation into more effective therapies. Twelve novel derivatives of 5-FU and 5-FUrd were synthesized and tested as part of a SAR study. Cytotoxicity of all compounds was tested in the 4T1 cell line and the SW480 cell line, with similar results obtained in both cell lines. The nitro-benzyl derivatives of 5-FU caused varied toxicity after treatment for 3 days. Compound 3 was less toxic than the parent 5-FU, compound 13 only caused toxicity at the higher concentrations and treatment with compound 14 resulted in low toxicity over the range of concentrations tested. These compounds were designed as prodrugs so the lower toxicity of compounds 13 and 14 was expected. The toxicity of compound 3 however, was unexpected and was probably due to binding and inhibition of thymidylate synthase. Of the ester derivatives, compounds 10 and 11 were more toxic than the parent 5-FU, with compound 10 exhibiting 10-fold greater toxicity than the parent drug. Compounds 4 and 5 had similar toxicity to 5-FU. The ester side-chains caused an increase in lipophilicity of these compounds and this would have resulted in greater absorption of the compounds into the cells. The side-chains would also have been rapidly hydrolysed within the cell to yield 5-FU, resulting in toxicity. This modification of 5-FU has thus proven to be successful in improving the toxicity of the drug. Further modifications of compound 10 are currently being conducted by Dr. Nolan's group and testing will begin shortly.

The 5-FUrd derivatives caused low toxicity in both cell lines over the range of concentrations tested, with the modifications to structure completely suppressing the toxicity of the parent drug. The protected C-2 and C-3 hydroxyl groups of the sugar in compounds 7, 8 and 9 prevented toxicity of these compounds. Compound 6 did

not have protected groups but did not exhibit toxicity, however, the size and lipophilicity of this compound would have affected its uptake into the cells.

Testing of the compounds in a 5-FU resistant cell line, HCT(R), was conducted to determine if these compounds could bypass the resistance mechanisms present in these resistant cells. After treatment for 3 days, 5-FUrd and compounds 3, 4 and 10 all had lower fold-differences between the parental and resistant cell lines, indicating an increased sensitivity to these treatments in the resistant cell line in comparison to 5-FU. Over 5 days, treatment with 5-FUrd and compounds 3, 4, 5 and 10 all had lower ratios than 5-FU. Compound 10 in particular proved quite toxic in the HCT(P) and HCT(R) cell lines, with IC_{50} values 10-fold lower than the parent 5-FU. The ratio of IC_{50} values was 0.89 over 5 days, indicating higher sensitivity in the resistant cell line than in the parental cell line. Thus, this compound had escaped the resistance mechanisms of the HCT(R) cell line and caused greater toxicity than in the parental cells.

Following the cytotoxicity results, investigation of cell cycle kinetics and apoptosis was conducted. Cell cycle analysis showed the most dramatic effects following treatment with compounds 4 and 10 at 0.1 μM for 3 days. Compound 4 caused a marked increase in the G2 phase population while treatment with compound 10 resulted in an S phase arrest (Figure 4.16). Treatment at the higher concentration of 1 μM caused elimination of S phase cells and G1 phase arrest for 5-FU, compounds 3, 4 and 5. Compound 10 at the higher concentration also caused an S phase arrest, with complete elimination of the G2 phase population. These results demonstrated different mechanisms of action for these compounds. The arrest in the G2 phase at lower concentrations indicates damage to DNA during replication and a subsequent pause for repair before mitosis. Arrest in the G1 phase at the higher concentrations, with elimination of the S phase indicates cells were not beginning DNA replication possibly due to RNA misincorporation. The S phase arrest noted after treatment with compound 10 would indicate extensive DNA damage during replication and subsequent cell death before cells reached the G2 phase of the cell cycle. Apoptosis levels in the cells following treatment with 0.1 μM compound 10 confirmed the high cytotoxicity noted with this derivative. Treatment with 1 μM of 5-FU, compounds 3, 4, 5, 10 and 11 all caused significant increases in the level of apoptotic cells.

The effect of a selected number of derivatives on migration, invasion and colony formation in soft agar of the 4T1 cell line was examined but unfortunately no significant decrease was observed in any of these properties. Treatment with compounds 3, 4 and 14 resulted in significant increases in migration of the cells, while invasion was also significantly increased following treatment with compound 4 (Figures 4.22 and 4.24). This pro-invasive effect has previously been reported following pulse selection with 5-FU in the DKLP cell line (Liang *et al*., 2004). Thus these compounds would not be candidates for anti-metastatic approaches to therapy and this aspect requires monitoring in future studies.

The nitro-benzyl derivatives of 5-FU and 5-FUrd were designed as prodrugs, with cleavage of the side-chain releasing the toxic parent molecule. The activation of these prodrugs was first examined using hypoxic conditions, to determine if the increase in one-electron reductases in the hypoxic environment could cleave the nitro-benzyl groups. Cytotoxicity of the prodrugs, compounds 3, 6, 9, 13 and 14, was examined under hypoxic conditions using the 4T1 and the SW480 cell lines. No increase in toxicity was observed following incubation with the compounds under hypoxic conditions for 3 days. Therefore, an alternative approach to activation of the compounds was investigated. An *E. coli* enzyme, NTR, was tested with the compounds for activity. Compounds 9 and 13 showed the most promise after enzyme assays (Figure 5.17). Enzyme kinetic analysis with compounds 13 and 14, along with a known substrate for the enzyme CB1954, revealed compound 13 had the highest k_{cat} value, an indication of the rate of conversion of substrate to product. The K_m values showed CB1954 to have the greatest affinity for the enzyme but this was followed closely by compound 14.

A cell line which was stably transfected with the cDNA for NTR (V79-NTR) and the control cell line (V79-C) were obtained to test activation by the NTR enzyme in the cellular environment. Testing of cell lysates with CB1954 confirmed cellular NTR activity (Figure 5.24). Cytotoxicity testing in the V79 cells over 3 and 5 days did not show any increase in cell death for compound 3 or compound 9. Compound 3 had exhibited cytotoxicity in the absence of activation so this was not unexpected. Compound 9 had appeared to be a good substrate for the enzyme but the protected C-2 and C-3 hydroxyls of the sugar would have prevented toxicity even when the nitro-benzyl group was removed. Compound 6 showed promising results over 3 days but this unfortunately did not extend to the 5 day treatment. Compounds 13 and 14

showed the most promising results, with toxicity increased in the V79-NTR cell line. After treatment for 3 days with compound 14, a greater than 73-fold increase in IC_{50} value was noted between the two cell lines (Table 5.2).

The cytotoxicity results in the V79 cell lines were encouraging and confirmation of the activation of compound 13 was investigated using mass spectrometry. Medium removed from the V79-C and V79-NTR cells which had been incubated with compound 13 for 5 days was analysed. The V79-C media sample showed a peak for compound 13 but no peak for 5-FU (Figure 5.36 A and B). The media sample which had been incubated with the V79-NTR cell line had no peak for compound 13 and a peak for 5-FU, indicating activation of the prodrug to the parent drug (Figure 5.36 C and D). These results supported the theory that the increased toxicity within the V79-NTR cells was due to activation of the prodrugs to 5-FU.

The cDNA for the NTR enzyme was obtained from Dr. Steve Hobbs (CRUK) in order to transfect into a cancer cell line and test the prodrugs in this environment. The plasmid was successfully amplified in bacteria and transfected into the HCT116 colorectal cancer cell line. However, cytotoxicity testing of the prodrugs in the newly developed HCT-NTR and HCT-C cell lines did not show a difference between the two cell lines. No NTR activity was observed in enzyme assays with CB1954 using cell lysates from these cell lines. Protein analysis by SDS gel electrophoresis did not confirm the presence of the enzyme in the HCT-NTR cells. Unfortunately an antibody to *E. coli* NTR was not commercially available and we were unable to perform a western blot. While the presence of the NTR mRNA had been confirmed in the transfected cells using RT-PCR, translation into the protein or activity of the enzyme was compromised within these cells. These final results were disappointing but do not detract from the results in the V79 cell lines and the activation shown by mass spectrometry. These prodrugs have provided evidence for the proof of concept of the ability of the nitro-benzyl side-chain to suppress toxicity of the 5-FU drug. The NTR enzyme in the V79-NTR cells was shown to activate the prodrugs by cleavage of this group. The prodrug compounds 13 and 14, will be used as lead compounds for further development of a GDEPT approach to anti-cancer therapy.

CLA and 5-FU derivatives have proven to be strong anti-cancer agents. The development of functional foods will see major growth in the 21st century (Riezzo *et al.*, 2005). In theory, increased levels of CLA in dairy products would provide a simple delivery method of this anti-cancer component. Thus CLA would be part of a

dietary approach to anti-cancer therapies. Further monitoring of the pro-metastatic properties of CLA is warranted before full confidence in this anti-cancer agent can be confirmed. More effective chemotherapeutic agents such as the 5-FU derivatives will also be required to tackle the growing cancer incidence in this country. Compound 10 proved a highly toxic drug against the cell lines used in this study. The 5-FU prodrugs are examples of more targeted treatments to cancer cells. A focus on combining these two elements for future therapies would be extremely beneficial for the cancer patient.

6.2 Future work

- Further investigation into the effect of the *t*10,*c*12-CLA isomer on invasion, migration and colony formation in soft agar is warranted. It would be interesting to investigate a possible dose-dependent effect of this isomer on the colony growth by varying the concentrations used for treatment. Analysis of adhesion to various substrates following treatment could provide insight into the mode of action. At the molecular level, the effect on cell adhesion molecules, such as E-cadherin and β-catenin, and on the Ras/Raf/ERK pathway might also provide information on the mechanism of action. Examination of the effects of CLA and the individual isomers on invasion and migration in human cancer cell lines would shed more light on whether this was a species-specific phenomenon.
- The structure activity relationship study of the 5-FU and 5-FUrd derivatives has provided crucial information with regards to the toxicity of these compounds. The design of the 5-FUrd derivatives demonstrated the ability to completely suppress the cytotoxic effect of the parent compound. The ester derivatives proved very toxic to the cancer cell lines, with compound 10 exhibiting 10-fold greater toxicity than 5-FU. Further modifications to this compound are currently being made and will be tested *in vitro*. Future animal studies with this compound and derivatives will be conducted to investigate the efficacy *in vivo*.
- The nitro-benzyl prodrugs, in particular compounds 13 and 14, showed promising results with NTR activation. The use of these lead compounds with NTR in a GDEPT approach to anti-cancer therapy will be further examined. Optimisation of a NTR-expressing cancer cell line is required for further testing. An improved bicistronic vector and cloning out of individual high-expressing transfected cells should tackle this problem. Testing of these prodrugs along with a gene delivery system in animal studies would examine their efficacy *in vivo*. In the clinical setting, testing of the gene delivery system would be the first step to confirm production of the enzyme. This would be followed by administration of the prodrug alone to determine any DLTs or activation in the tissues, before co-administration of the gene and the prodrug.

- Design of 5-FU prodrugs for activation by one-electron reductases, which are up-regulated in hypoxic cells, would eliminate the gene therapy aspect required with the NTR-activated prodrugs. This approach would take advantage of the presence of hypoxic conditions within tumours to modify the prodrugs.

Chapter 7

Bibliography

Ahmad, A. and Hart, I.R. (1997) Mechanisms of metastasis. *Critical Reviews in Oncology/Hematology* **26**: 163-173.

Airley, R.E., Monaghan, J.E. and Stratford, I.J. (2000) Hypoxia and disease: opportunities for novel diagnostic and therapeutic prodrug strategies. *The Pharmaceutical Journal* **264**: 666-673.

Albert, A. (1958) Chemical aspects of selective toxicity. *Nature* **182**: 421-423.

Al-Hajj, M., Wicha, M.S., Benito-Hernandez, A., Morrison, S.J. and Clarke M.F. (2003) Prospective identification of tumorigenic breast cancer cells. *Proceedings of National Academy of Sciences* **100**: 3983-3988.

Anlezark, G.M., Melton, R.G., Sherwood, R.F., Coles, B., Friedlos, F. and Knox, R.J. (1992) The bioactivation of 5-(aziridin-1-yl)-2,4-dinitrobenzamide (CB1954) – I: Purification and properties of a nitroreductase anzyme from *Escherichia coli* – a potential enzyme for antibody-directed enzyme prodrug therapy (ADEPT). *Biochemical Pharmacology* **44**: 2289-2295.

Aro, A., Mannisto, S., Salminen, I., Ovaskainen, M.L., Kataja, V. and Uusitupa, M. (2000) Inverse association between dietary and serum conjugated linoleic acid and risk of breast cancer in postmenopausal women. *Nutrition and Cancer* **38**: 151-157.

Awada, A., Cardoso, F., Atalay, G., Giuliani, R., Mano, M. and Piccart, M.J. (2003) The pipeline for new anticancer agents for breast cancer treatment in 2003. *Critical Reviews of Oncology/Haematology* **48**: 45-63.

Banka, C.L., Lund, C.V., Nguyen, M.T.N., Pakchoian, A.J., Mueller, B.M. and Eliceiri, B.P. (2006) Estrogen induces lung metastasis through a host compartment-specific response. *Cancer Research* **66**: 3667-3672.

Banni, S., Petroni, A., Blasevich, M., Carta, G., Cordeddu, L., Murru, E., Melis, M.P., Mahon, A. and Belury, M.A. (2004) Conjugated linoleic acids (CLA) as precursors of a distinct family of PUFAs. *Lipids* **39**: 1143-1146.

Bauman, D.E., Baumgard, L.H., Corl, B.A. and Griinari, J.M. (1999) Biosynthesis of conjugated linoleic acid in ruminants. *Proceedings of the American Society of Animal Science 1999 Annual Meeting* E30.

Belury, M.A., Moya-Camarena, S.Y., Liu, K.L. and Vanden Heuvel, J.P. (1997) Dietary conjugated linoleic acid induces peroxisome-specific enzyme accumulation and ornithine decarboxylase activity in mouse liver. *Journal of Nutritional Biochemistry* **8**: 579-584.

Belury, M.A. (2002a) Inhibition of carcinogenesis by conjugated linoleic acid: potential mechanisms of action. *Journal of Nutrition* **132**: 2995-2998.

Belury, M.A. (2002b) Dietary conjugated linoleic acid in health: Physiological effects and mechanisms of action. *Annual Review of Nutrition* **22**: 505-531.

Birkedal-Hansen, H., Moore, W.G.I., Bodden, M.K., Windsor, L.J., Birkedal-Hansen, B., DeCarlo, A. and Engler, J.A. (1993) Matrix metalloproteinases: A review. *Critical Reviews in Oral Biology and Medicine* **4**: 197-250.

Bissell, M.J. and Radisky, D. (2001) Putting tumours in context. *Nature Reviews Cancer* **1**: 46-54.

Bocca, C., Bozzo, F., Francica, S., Colombatto, S. and Miglietta, A. (2007) Involvement of PPARγ and E-cadherin/β-catenin pathway in the antiproliferative effect of conjugated linoleic acid in MCF-7 cells. *International Journal of Cancer* **121**: 248-256.

Bogenrieder, T. and Herlyn, M. (2003) Axis of evil: molecular mechanisms of cancer metastasis. *Oncogene* **22**: 6524-6536.

Boyer, J., McLeon, E.G., Arorri, S., Wilson, P., McCulla, A., Carey, P.D., Longley, D.B. and Johnston, P.G. (2004) Characterization of p53 wild-type and null isogenic colorectal cancer cell lines resistant to 5-Fluorouracil, Oxaliplatin and Irinotecan. *Cancer Research* **10**: 2158-2167.

Brown, J.M. and Wilson, W.R. (2004) Exploiting tumour hypoxia in cancer treatment. *Nature Reviews Cancer* **4**: 437-447.

Brown, J.M. and Attardi, L.D. (2005) The role of apoptosis in cancer development and treatment response. *Nature Reviews Cancer* **5**: 231-237.

Buzdar, A.M., Ibrahim, N.K., Francie, D., Booser, D.J., Thomas, E.S., Theriault, R.L., Pusztai, L., Green, M.C., Arun, B.K., Giordano, S.H., Cristofanilli, M., Frye, D.K., Smith, T.L., Hunt, K.K., Singletary, S.E., Sahin, A.A., Ewer, M.S., Buchholz, D. and Hortobagyi, G.N. (2005) Significantly higher pathologic complete remission rate after neoadjuvant therapy with Trastuzumab, paclitaxel, and epirubicin chemotherapy: Results of a randomized trial in human epidermal growth factor receptor 2- Positive operable breast cancer. *Journal of Clinical Oncology* **23**: 3676-3685.

Campo, J., Comber, H. and Gavin, A.T. (2004) All Ireland Cancer Statistics 1998-2000. *Northern Ireland Cancer Registry/National Cancer Registry*.

Castano, A.P., Mroz, P. and Hamblin, M.R. (2006) Photodynamic therapy and anti-tumour immunity. *Nature Reviews Cancer* **6**: 535-545.

Cavallaro, U. and Christofori, G. (2004) Cell adhesion and signalling by cadherins and Ig-CAMs in cancer. *Nature Reviews Cancer* **4**: 118-132.

Chajes, V., Lavillonniere, F., Ferrari, P., Jourdan, M.L., Pinault, M., Maillard, V., Sebedio, J.L. and Bougnoux, P. (2002) Conjugated linoleic acid content in breast adipose tissue is not associated with the relative risk of breast cancer in a population of French patients. *Cancer Epidemiology, Biomarkers and Prevention* **11**: 672-673.

Chajes, V., Lavillonniere, F., Maillard, V., Giraudeau, B., Jourdan, M.L., Sebedio, J.L. and Bougnoux, P. (2003) Conjugated linoleic acid content in breast adipose tissue of breast cancer patients and the risk of metastasis. *Nutrition and Cancer* **45**: 17-23.

Chambers, A.F., Groom, A.C. and MacDonald, I.C. (2003) Dissemination and growth of cancer cells in metastatic sites. *Nature Reviews Cancer* **2**: 563-572.

Chamras, H., Ardashian, A., Heber, D. and Glaspy, J.A. (2002) Fatty acid modulation of MCF-7 human breast cancer cell proliferation, apoptosis and differentiation. *Journal of Nutritional Biochemistry* **13**: 711-716.

Chen, B.Q., Yang, Y.M., Gao, Y.H., Liu, J.R., Xue, Y.B., Wang, X.L., Zheng, Y.M., Zhang, J.S. and Liu, R.H. (2003) Inhibitory effects of *c*9,*t*11-conjugated linoleic acid on invasion of human gastric carcinoma cell line SGC-7901. *World Journal of Gastroenterology* **9**: 1909-1914.

Cho, H.J., Kim, W.K., Jung, J.I., Kim, E.J., Lim, S.S., Kwon, D.Y. and Park, J.H.Y. (2005) *Trans*-10,*cis*-12, not *cis*-9,*trans*-11, conjugated linoleic acid decreases ErbB3 expression in HT-29 human colon cancer cells. *World Journal of Gastroenterology* **11**: 5142-5150.

Cho, H.J., Kim, E.J., Lim, S.S., Kim, M.K., Sung, M.K., Kim, J.S. and Park, J.H.Y. (2006) *Trans*-10,*cis*-12, not *cis*-9,*trans*-11, conjugated linoleic acid inhibits G1-S progression in HT-29 human colon cancer cells. *Journal of Nutrition* **136**: 893-898.

Chujo, H., Yamasaki, M., Nou, S., Koyanagi, N., Tachibana, H. and Yamada, K. (2003) Effect of conjugated linoleic acid isomers on growth factor-induced proliferation of human breast cancer cells. *Cancer Letters* **202**: 81-87.

Chung-Faye, G., Palmer, D., Anderson, D., Clark, J., Downes, M., Baddeley, J., Hussain, S., Murray, P.I., Searle, P., Seymour, L., Harris, P.A., Ferry, D. and

Kerr, D.J. (2001) Virus-directed, enzyme prodrug therapy with nitroimidazole reductase: a phase I and pharmacokinetic study of its prodrug, CB1954. *Clinical Cancer Research* **7**: 2662-2668.

Cimini, A.M., Cristiano, L., Colafarina, S., Benedetti, E., Di Loreto, S., Festuccia, C., Amicarelli, F., Canuto, R.A. and Ceru, M.P. (2005) PPARγ-dependent effects of conjugated linoleic acid on the human glioblastoma cell line (ADF). *International Journal of Cancer* **117**: 923-933.

Cocquyt, V. and Van Belle, S. (2005) Lobular carcinoma *in situ* and invasive lobular cancer of the breast. *Current Opinion in Obstetrics and Gynecology* **17**: 55-60.

Connolly, J.M., Gilhooly, E.M. and Rose, D.P. (1999) Effects of reduced dietary linoleic acid intake, alone or combined with an algal source of docosahexanoic acid, on MDA-MB-231 breast cancer cell growth and apoptosis in nude mice. *Nutrition and Cancer* **35**: 44-49.

Cross, S.S. and Bury, J.P. (2003) Molecular biology in diagnostic histopathology: Part II – cell adhesion molecules. *Current Diagnostic Pathology* **9**: 313-321.

Curran, S. and Murray, G.I. (2000) Matrix metalloproteinases: molecular aspects of their roles in tumour invasion and metastasis. *European Journal of Cancer* **36**: 1621-1630.

Das, U. (2006) Essential fatty acids: biochemistry, physiology and pathology. *Biotechnology Journal* **1**: 420-439.

de la Chapelle, A. (2004) Genetic predisposition to colorectal cancer. *Nature Reviews Cancer* **4**: 769-780.

Denny, W.A. (2001) Prodrug strategies in cancer therapy. *European Journal of Medicinal Chemistry* **36**: 577-595.

Denny, W.A. (2003) Produgs for gene-directed enzyme-prodrug therapy (suicide gene therapy). *Journal of Biomedicine and Biotechnology* **1**: 48-70.

Durgam, V.R. and Fernandes, G. (1997) The growth inhibitory effect of conjugated linoleic acid on MCF-7 cells is related to estrogen response system. *Cancer Letters* **116**: 121-130.

Egeblad, M. and Werb, Z. (2002) New functions for the matrix metalloproteinases in cancer progression. *Nature Reviews Cancer* **2**: 161-174.

Espinosa, A., Marchal, J.A., Aranega, A., Gallo, M.A., Aiello, S. and Campos, J. (2005) Antitumoural properties of benzannelated seven-membered 5-fluorouracil derivatives and related open analogues. Molecular markers for apoptosis and cell cycle dysregulation. *Il Farmaco* **60**: 91-97.

Ettmayer, P., Amidon, G.L., Clement, B. and Testa, B. (2004) Lessons learned from marketed and investigational prodrugs. *Journal of Medicinal Chemistry* **47**:2393-2404.

Fiebig, H.H., Maier, A. and Burger, A.M. (2004) Clonogenic assay with established human tumour xenografts: correlation of *in vitro* to *in vivo* activity as a basis for anticancer drug discovery. *European Journal of Cancer* **40**: 802-820.

Fisher, J.F. and Mobashery, S. (2006) Recent advances in MMP inhibitor design. *Cancer Metastasis Reviews* **25**: 115-136.

Friedlos, F., Court, S., Ford, M., Denny, W.A. and Springer, C. (1998) Gene-directed enzyme prodrug therapy: quantitative bystander cytotoxicity and DNA damage induced by CB1954 in cells expressing bacterial nitroreductase. *Gene Therapy* **5**: 105-112.

Fulda, S. and Debatin, K-M. (2006) Extrinsic versus intrinsic apoptosis pathways in anticancer chemotherapy. *Oncogene* **25**: 4798-4811.

Geho, D.H., Bandle, R.W., Clair, T. and Liotta, L.A. (2005) Physiological mechanisms of tumor-cell invasion and migration. *Physiology* **20**: 194-200.

Gordon, S.R., Climie, M. and Hitt, A.L. (2005) 5-Fluorouracil interferes with actin organisation, stress fiber formation and cell migration in corneal endothelial cells during wound repair along the natural basement membrane. *Cell Motility and the Cytoskeleton* **62**: 244-258.

Grady, W.M. (2006) Molecular basis for subdividing hereditary colon cancer? *Gut* **54**:1676-1678.

Gray, I.J. (2005) Synthesis of new 5-Fluorouracil photosensitiser conjugates for use as prodrugs in the photodynamic therapy for cancer. PhD thesis, Dubin City University.

Greco, O. and Dachs, G.U. (2001) Gene directed enzyme/prodrug therapy of cancer: historical appraisal and future prospectives. *Journal of Cellular Physiology* **187**: 22-36.

Greenwald, P. (1999) Role of dietary fat in the causation of breast cancer: point. *Cancer Epidemiology, Biomarkers and Prevention* **8**: 3-7.

Ha, Y.L., Grimm, N.K. and Pariza, M.W. (1987) Anticarcinogens from fried ground beef: beat-altered derivatives of linoleic acid. *Carcinogenesis* **8**: 1881-1887.

Ha, Y.L., Storkson, J. and Pariza, M.W. (1990) Inhibition of benzo(*a*)pyrene-induced mouse forestomach neoplasia by conjugated dienoic derivatives of linoleic acid. *Cancer Research* **50**: 1097-1101.

Hanahan, D. and Weinberg, R.A. (2000) The hallmarks of cancer. *Cell* **100**: 57-70.

Harries, M., O'Donnell, A., Scurr, M., Reade, S., Cole, C., Judson, I., Greystoke, A., Twelves, C. and Kaye, S. (2004) Phase I/II study of DHA-paclitaxel in

combination with carboplatin in patients with advanced malignant solid tumours. *British Journal of Cancer* **91**: 1651-1655.

Harris, M.A., Hansen, R.A., Vidsudhiphan, P., Koslo, J.L., Thomas, J.B., Watkins, B.A. and Allen, K.G.D. (2001) Effects of conjugated linoleic acids and docosahexanoic acid on rat liver and reproductive tissue fatty acids, prostaglandins and matrix metalloproteinase production. *Prostaglandins, Leukotrienes and Essential Fatty Acids* **65**: 23-29.

Heggie, G.D., Sammadossi, J.P., Cross, D.S., Hunter, W.J. and Diasio, R.B. (1987) Clinical pharmacokinetics of 5-Fluorouracil and its metabolites in plasma, urine and bile. *Cancer Research* **47**: 2203-2206.

Hejmadi, M.V., McKeown, S.R., Friery, O.P., McIntyre, I.A., Patterson, L.H. and Hirst, D.G. (1996) DNA damage following combination of radiation with the bioreductive drug AQ4N: possible selective toxicity to oxic and hypoxic tumour cells. *British Journal of Cancer* **73**: 499-505.

Hendon, S.E. and DiPalma, J.A. (2005) U.S. practices for colon cancer screening. *Keio Journal of Medicine* **54**: 179-183.

Heppner, G.H., Miller, F.R. and Shekhar, P.V.M. (2000) Nontransgenic models of breast cancer. *Breast Cancer Research* **2**: 331-334.

Hidalgo, M. and Eckhardt, S.G. (2001) Development of matrix metalloproteinase inhibitors in cancer therapy. *Journal of the National Cancer Institute* **93**: 178-193.

Hubbard, N.E., Lim, D. and Erickson, K.L. (1998) Alteration of murine mammary tumorigenesis by dietary enrichment with n-3 fatty acids in fish oil. *Cancer Letters* **124**: 1-7.

Hubbard, N.E., Lim, D., Summers, L. and Erickson, K.L. (2000) Reduction of murine mammary tumor metastasis by conjugated linoleic acid. *Cancer Letters* **150**: 93-100.

Hubbard, N.E., Lim, D. and Erickson, K.L. (2003) Effect of separate conjugated linoleic acid isomers on murine mammary tumorigenesis. *Cancer Letters* **190**:13-19.

Hughes, L. (2006) Development, characterisation and gene expression profiling of a novel more invasive variant established from the human breast cancer cell line Hs578T. PhD thesis, University College Dublin.

Igarashi, M. and Miyazawa, T. (2001) The growth inhibitory effect of conjugated linoleic acid on a human hepatoma cell line, HepG2, is induced by a change in fatty acid metabolism, but not the facilitation of lipid peroxidation in the cells. *Biochimica et Biophysica Acta* **1530**: 162-171.

Ingvarsson, S. (1999) Molecular genetics of breast cancer progression. *Seminars in Cancer Biology* **9**: 277-288.

Ip, C., Chin, S.F., Scimeca, J.A. and Pariza, M.W. (1991) Mammary cancer prevention by conjugated dienoic derivative of linoleic acid. *Cancer Research* **51**: 6118-6124.

Ip, C., Singh, M., Thompson, H.J. and Scimeca, J.A. (1994) Conjugated linoleic acid suppresses mammary carcinogenesis and proliferative activity of the mammary gland in the rat. *Cancer Research* **54**: 1212-1215.

Ip, C., Scimeca, J.A. and Thompson, H. (1995) Effect of timing and duration of dietary conjugated linoleic acid on mammary cancer prevention. *Nutrition and Cancer* **2**: 241-247.

Ip, C., Briggs, S.P., Haegele, A.D., Thompson, H.J., Storkson, J. and Scimeca, J.A. (1996) The efficacy of conjugated linoleic acid in mammary cancer prevention

is independent of the level or type of fat in the diet. *Carcinogenesis* **17**: 1045-1050.

Ip, C., Jiang, C., Thompson, H.J. and Scimeca, J.A. (1997) Retention of conjugated linoleic acid in the mammary gland is associated with tumor inhibition during the post-initiation phase of carcinogenesis. *Carcinogenesis* **18**: 755-759.

Ip, C., Banni, S., Angioni, E., Carta, G., McGinley, J., Thompson, H.J., Barbano, D. and Bauman, D. (1999) Conjugated linoleic acid-enriched butter fat alters mammary gland morphogenesis and reduces cancer risk in rats. *Journal of Nutrition* **129**: 2135-2142.

Ip, C., Dong, Y., Thompson, H.J., Bauman, D.E. and Ip, M.M. (2001) Control of rat mammary epithelium proliferation by conjugated linoleic acid. *Nutrition and Cancer* **39**: 233-238.

James, N.D., Patel, P., Mautner, V., Young, J.G., Hull, D., Searle, P., Leung, H.Y., Ellis, J., Wallace, M. and Young, S. (2004) A clinical trial of virus-directed enzyme prodrug therapy (VDEPT) using adenovirus encoded nitroreductase (ntr) and CB1954 in patients with localised prostate cancer (PCa). *Journal of Clinical Oncology* **22**: 4572.

Jiang, W.G., Bryce, R.P. and Horrobin, D.F. (1998) Essential fatty acids: molecular and cellular basis of their anti-cancer action and clinical implications. *Critical Reviews in Oncology/Hematology* **27**: 179-209.

Jones, R.J. Hawkins, R.E., Eatock, M.M., Ferry, D.R., Eskens, F.A.L.M., Wilke, H.J. and Evans, T.R.J. (2007) A phase II open-label study of DHA-paclitael (Taxoprexin) by 2-h intravenous infusion in previously untreated patients with locally advanced or metastatic gastric or oesophageal adenocarcinoma. *Cancer Chemotherapy and Pharmacology*, Epub ahead of publication.

Jover, R., Zapater, P., Castells, A., Llor, X., Andreu, M., Cubiella, J., Pinol, V., Xicola, R.M., Bujanda, L., Rene, J.M., Clofent, J., Bessa, X., Morillas, J.D.,

Nicolas-Perez, D., Paya, A. and Alenda, C. (2006) Mismatch repair status in the prediction of benefit from adjuvant fluorouracil chemotherapy in colorectal cancer. *Gut* **55:** 848-855.

Kakimoto, M., Uetake, H., Osanai, T., Shirota, Y., Takagi, Y., Takeshita, E., Toriya, Y., Danenberg, K., Danenberg, P.V. and Sugihara, K. (2005) Thymidylate synthase and dihydropyrimidine dehydrogenase gene expression in breast cancer predicts 5-FU sensitivity by a histocultural drug sensitivity test. *Cancer Letters* **223**: 103-111.

Kalirai, H. and Clarke, R. (2006) Human breast epithelial stem cells and their regulation. *Journal of Pathology* **208**: 7-16.

Kim, E.J., Holthuizen, P.E., Park, H.S., Ha, Y.L., Jung, K.C. and Park, J.H.Y. (2002) *Trans*-10,*cis*-12-conjugated linoleic acid inhibits Caco-2 colon cancer cell growth. *American Journal of Physiology – Gastrointestinal and Liver Physiology* **283**:G357-G367.

King, R.J.B. (2000) Invasion and metastasis. *Cancer Biology*, 2nd Edition.

Kizaka-Kondoh, S., Inoue, M., Harada, H. and Hiraoka, M. (2003) Tumour hypoxia: A target for selective cancer therapy. *Cancer Science* **94**: 1021-1028.

Knox, R.J., Friedlos, F., Sherwood, R.F., Melton, R.G. and Anlezark, G.M. (1992) The bioactivation of 5-(aziridin-1-yl)-2,4-dinitrobenzamide (CB1954) – II: A comparison of an *Escherichia coli* nitroreductase and Walker DT diaphorase. *Biochemical Pharmacology* **44**: 2297-2301.

Knox, R.J., Burke, P.J., Chen, S. and Kerr, D.J. (2003) CB 1954: From the Walker tumour to NQO2 and VDEPT. *Current Pharmaceutical Design* **9**: 2091-2104.

Kunayasi, H., Yoshida, K., Sasaki, T., Sasahira, T., Fujii, K. and Ohmori, H. (2006) Conjugated linoleic acid inhibits peritoneal metastasis in human gastrointestinal cancer cells. *International Journal of Cancer* **118**: 571-576.

Lacroix, M., Toillon, R-A. and Leclercq, G. (2004) Stable 'portrait' of breast tumours during progression: data from biology, pathology and genetics. *Endocrine-Related Cancer* **11**: 497-522.

Lamont, E.B. and Schilsky, R.L. (1999) The oral fluoropyrimidines in cancer chemotherapy. *Clinical Cancer Research* **5**: 2289-2296.

Larsson, S.C., Bergkvist, L. and Wolk, A. (2005) High-fat dairy food and conjugated linoleic acid intakes in relation to colorectal cancer incidence in the Swedish Mammography Cohort. *American Journal of Clinical Nutrition* **82**: 894-900.

Lazo, J.S. and Larner, J.M. (1998) Chapter 45: Individual antineoplastic drugs. *Human Pharmacology: Molecular to clinical.* Mosby 3rd edition. Editors: Brody, T.M., Larner, J. and Minneman, K.P.

Lee, K.W., Lee, H.J., Cho, H.Y. and Kim, Y.J. (2005) Role of the conjugated linoleic acid in the prevention of cancer. *Critical Reviews in Food Sciences and Nutrition*. **45**: 135-144.

Lee, S.H., Yamaguchi, K., Kim, J.S., Eling, T.E., Safe, S., Park, Y. and Baek, S.J. (2006) Conjugated linoleic acid stimulates an anti-tumorigenic protein NAG-1 in an isomer specific manner. *Carcinogenesis* **27**: 972-981.

Li, M-H., Ito, D., Sanada, M., Odani, T., Hatori, M., Iwase, M. and Nagumo, M. (2004) Effect of 5-Fluorouracil on G1 phase cell cycle regulation in oral cancer cell lines. *Oral Oncology* **40**: 63-70.

Liang, Y., McDonnell, S. and Clynes, M. (2002) Examining the relationship between cancer invasion/metastasis and drug resistance. *Current Cancer Drug Targets* **2**: 257-277.

Liang, Y., O'Driscoll, L., McDonnell, S., Doolan, P., Oglesby, I., Duffy, K., O'Connor, R. and Clynes, M. (2004) Enhanced *in vitro* invasiveness and drug resistance with altered gene expression patterns in a human lung carcinoma cell

line after pulse selection with anticancer agents. *International Journal of Cancer* **111**: 484-493.

Lim, D.Y., Tyner, A.L., Park, J.B., Lee, J.Y., Choi, Y.H. and Park, J.H.Y. (2005) Inhibition of colon cancer cell proliferation by the dietary compound conjugated linoleic acid is mediated by the CDK inhibitor $p21^{CIP1/WAF1}$. *Journal of Cell Physiology* **205**: 107-113.

Lin, T.S., Wang, L., Antonini, I., Cosby, L.A., Shiba, D.A., Kirkpatrick, D.L. and Sartorelli, A.C. (1986) (*o*- and *p*-Nitrobenzyloxycarbonyl)-5-fluorouracil derivatives as potential conjugated bioreductive alkylating agents. *Journal of Medicinal Chemistry* **29**: 84-89.

Liu, J.R., Chen, B.Q., Yang, Y.M., Wang, X.L., Xue, Y.B., Zheng, Y.M. and Liu, R.H. (2002) Effect of apoptosis on gastric adenocarcinoma cell line SGC-7901 induced by *cis*-9,*trans*-11-conjugated linoleic acid. *World Journal of Gastroenterology* **8**: 999-1004.

Longley, D.B., Harkin, D.P. and Johnston, P.G. (2003) 5-Fluorouracil: Mechanisms of action and clinical strategies. *Nature Reviews Cancer* **3**: 330-338.

Lynch, C.C. and Matrisian, L.M. (2002) Matrix metalloproteinases in tumor-host cell communication. *Differentiation* **70**: 561-573.

Maggiora, M., Bologna, M., Ceru, M.P., Possati, L., Angelucci, A., Cimini, A., Miglietta, A., Bozzo, F., Margiotta, C., Muzio, G. and Canuto, R.A. (2004) An overview of the effect of linoleic and conjugated-linoleic acids on the growth of several human tumor cell lines. *International Journal of Cancer* **112**: 909-919.

Maillard, V., Bougnoux, P., Ferrari, P., Jourdan, M.L., Pinault, M., Lavillonniere, F., Body, G., Le Floch, O. and Chajes, V. (2002) N-3 and n-6 fatty acids in breast adipose tissue and relative risk of breast cancer in a case-control study in Tours, France. *International Journal of Cancer* **98**: 78-83.

Majumder, B., Wahle, K.W.J., Moir, S., Schofield, A., Choe, S.N., Farquharson, A., Grant, I and Heys S.D. (2002) Conjugated linoleic acids (CLAs) regulate the expression of key apoptotic genes in human breast cancer cells. *FASEB Journal* **16**: 1447-1449.

Malet-Martino, M. and Martino, R. (2002) Clinical studies of three oral prodrugs of 5-Fluorouracil (Capecitabine, UFT, S-1): A Review. *The Oncologist* **7**: 288-323.

Maluf, F.C., Leiser, A.L., Aghajanian, C., Sabbatini, P., Pezzulli, S., Chi, D.S., Wold, J.K., Levenback, C., Loh, E. and Spriggs, D.R. (2006) Phase II study of tirapazamine plus cisplatin in patients with advanced or recurrent cervical cancer. *International Journal of Gynecological Cancer* **16**: 1165-1171.

Marchal, J.A., Boulaiz, H., Suarez, I., Saniger, E., Campos, J., Carrillo, E., Prados, J., Gallo, M.A., Espinosa, A. and Aranega, A. (2004) Growth inhibition, G1-arrest, and apoptosis in MCF-7 human breast cancer cells by novel highly lipophilic 5-fluorouracil derivatives. *Investigational New Drugs* **22**:379-389.

Masi, G., Cupini, S., Marcuci, L., Cerri, E., Loupakis, F., Allegrini, G., Brunetti, A.M., Pfanner, E., Viti, M., Goletti, O., Filiponni, F. and Falcone, A. (2006) Treatment with 5-Fluorouracil/Folinic acid, oxaliplatin and irinotecan enables surgical resection of metastases in patients with initially unresectable metastatic colorectal cancer. *Annals of Surgical Oncology* **13**: 58-65.

Masso-Welch, P.A., Zangani, D., Ip, C., Vaughan, M.M., Shoemaker, S., Ramirez., R.A. and Ip., M.M. (2002) Inhibition of angiogenesis by the cancer chemopreventive agent conjugated linoleic acid. *Cancer Research* **62**: 4383-4389.

Matthews, C.K. and van Holde, K.E. (1990) Chapter 10: Enzymes: Biological Catalysts. *Biochemistry* Benjamin/Cummings Publishing Company.

McCann, S.E., Ip, C., Ip, M.M., McGuire, M.K., Muti, P., Edge, S.B., Trevisan, M. and Freudenheim, J.L. (2004) Dietary intake of conjugated linoleic acids and risk of premenopausal and postmenopausal breast cancer, Western New York Exposures and Breast Cancer Study (WEB Study). *Cancer Epidemiology, Biomarkers and Prevention* **13**: 1480-1484.

McDonnell, S., Murray, D., Hughes, L. and Redmond, A. (2006) Chapter 3: Molecular aspects of cancer invasion. *The Molecular and Cellular Pathology of Cancer Progression and Prognosis*. Edited by GV Sherbet. Research Signpost.

McLeod, H.L., McKay, J.A., Collie-Duguid, E.S.R. and Cassidy, J. (2000) Therapeutic opportunities from tumour biology in metastatic colon cancer. *European Journal of Cancer* **36**: 1706-1712.

McWilliams, R.R. and Erlichman C. (2005) Novel therapeutics in colorectal cancer. *Diseases of the Colon & Rectum* **48**: 1632-1650.

Menendez, J.A., Ropero, S., del Mar Barbacid, M., Montero, S., Solanos, M., Escrich, E., Cortes-Funes, H. and Colomer, R. (2002) Synergistic interaction between vinorelbine and gamma-linolenic acid in breast cancer cells. *Breast Cancer Research and Treatment* **72**: 203-219.

Menendez, J.A., Lupu, R. and Colomer, R. (2005) Exogenous supplementation with ω-3 polyunsaturated fatty acid docosahexanoic acid (DHA; 22:6*n*-3) synergistically enhances taxane cytotoxicity and downregulates Her-2/*neu* (c-*erb*B-2) oncogene expression in human breast cancer cells. *European Journal of Cancer Prevention* **14**: 263-270.

Michor, F., Iwasa, Y., Lengauer, C. and Nowak, M.A. (2005) Dynamics of colorectal cancer. *Seminars in Cancer Biology* **15**: 484-493.

Miglietta, A., Bozzo, F., Bocca, C., Gabriel, L., Trombetta, A., Belotti, S. and Canuto, R.A. (2006a) Conjugated linoleic acid induces apoptosis in MDA-MB-

231 breast cancer cells through ERK/MAPK signalling and mitochondrial pathway. *Cancer Letters* **234**: 149-157.

Miglietta, A., Bozzo, F., Gabriel, L., Bocca, C. and Canuto, R.A. (2006b) Extracellular signal-regulated kinase 1/2 and protein phosphatase 2A are involved in the antiproliferative activity of conjugated linoleic acid in MCF-7 cells. *British Journal of Nutrition* **96**: 22-27.

Miller, Á., Stanton, C. and Devery, R. (2001) Modulation of arachadonic acid distribution by conjugated linoleic acid isomers and linoleic acid in MCF-7 and SW480 cancer cells. *Lipids* **36**: 1161-1168.

Miller, Á., Stanton, C., Murphy, J. and Devery, R. (2003) Conjugated linoleic acid (CLA)-enriched milk fat inhibits growth and modulates CLA-responsive biomarkers in MCF-7 and SW480 human cancer cell lines. *British Journal of Nutrition* **90**: 877-885.

Minotti, G., Menna, P., Salvatorelli, E., Cairo, G. and Gianni, L. (2004) Anthracyclines: Molecular advances and pharmacologic developments in antitumour activity and cardiotoxicity. *Pharmacological Reviews* **56**: 185-229.

Moya-Camarena, S.Y., Vanden Heuvel, J.P. and Belury, M.A. (1999) Conjugated linoleic acid activates peroxisome proliferator-activated receptor α and β subtypes but does not induce hepatic peroxisome proliferation in Sprague-Dawley rats. *Biochimica et Biophysica Acta* **1436**: 331-342.

Murphy, G. (1998) Gelatinase A. *Handbook of Proteolytic Enzymes* 1199-1205. Academic Press. Edited by Alan J. Barrett, Neil D. Rawlings and J. Fred Woessner.

Murray, D., Morrin, M. and McDonnell, S. (2004) Increased invasion and expression of MMP-9 in human colorectal cell lines by a CD-44 dependent mechanism. *Anticancer Research* **24**: 489-494.

National Cancer Forum. (2006) A strategy for cancer control in Ireland. Chairperson: Prof. Paul Redmond.

National Cancer Registry. (2006) Trends in Irish cancer incidence 1994-2002, with projections to 2020. (http://www.ncri.ie/pubs/pubfiles/proj_2020.pdf)

O'Shea, M., Lawless, F., Stanton, C. and Devery, R. (1998) Conjugated linoleic acid in bovine milk fat: a food-based approach to cancer chemoprevention. *Trends in Food Science and Technology* **9**: 192-196.

Palmer, D.H., Mautner, V., Mirza, D., Oliff, S., Gerritsen, W., van der Sijp, J.R.M., Hubscher, S., Reynolds, G., Bonney, S., Rajaratnam, R., Hull, D., Horne, M., Ellis, J., Mountain, A., Hill, S., Harris, P.A., Searle, P.F., Young, L.W., James, N.D. and Kerr, D.J. (2004) Virus-directed enzyme prodrug therapy: Intratumoral administration of a replication-deficient adenovirus encoding nitroreductase to patients with respectable liver cancer. *Journal of Clinical Oncology* **22**: 1546-1552.

Palombo, J.D., Ganguly, A., Bistrian, B.R. and Menard, M.P. (2002) The antiproliferative effects of biologically active isomers of conjugated linoleic acid on colorectal and prostatic cancer cells. *Cancer Letters* **177**: 163-172.

Parkinson, G.N., Skelly, J.V. and Neidle, S. (2000) Crystal structure of FMN-dependent nitroreductase from *Escherichia coli* B: A prodrug activating enzyme. *Journal of Medicinal Chemistry* **43**: 3624-3631.

Pariza, M.W., Park, Y. and Cook, M.E. (2000) Mechanisms of action of conjugated linoleic acid: Evidence and speculation. *Proceedings of the Society for Experimental Biology and Medicine* **223**: 8-13.

Pariza, M.W., Park, Y. and Cook, M.E. (2001) The biologically active isomers of conjugated linoleic acid. *Progress in Lipid Research* **40**: 283-298.

Patterson, L.H. and McKeown, S.R. (2000) AQ4N: a new approach to hypoxia-activated cancer chemotherapy. *British Journal of Cancer* **83**: 1589-1593.

Patterson, L.H., McKeown, S.R., Ruparelia, K., Double, J.A., Bibby, M.C., Cole, S. and Startford, I.J. (2000) Enhancement of chemotherapy and radiotherapy of murine tumours by AQ4N, a bioreductively activated anti-tumour agent. *British Journal of Cancer* **82**: 1984-1990.

Patterson, L.H. (2002) Bioreductively activated antitumour *N*-oxides: The case of AQ4N, a unique approach to hypoxia-activated cancer chemotherapy. *Drug Metabolism Reviews* **34**: 581-592.

Polyak, K. (2001) On the birth of breast cancer. *Biochimica et Biophysica Acta* **1552**: 1-13.

Ponti, D., Costa, A., Zaffaroni, N., Pratesi, G., Petragolini, G., Coradini, D., Pilotti, S., Pierotti, M.A. and Daidone, M.G. (2005) Isolation and *in vitro* propagation of tumorigenic breast cancer cells with stem/progenitor cell properties. *Cancer Research* **65**: 5506-5511.

Price, J.E. (1986) Clonogenicity and experimental metastatic potential of spontaneous mouse mammary neoplasms. *Journal of National Cancer Institute* **2**: 529-535.

Relling, M.V. and Dervieux, T. (2001) Pharmacogenetics and cancer therapy. *Nature Reviews Cancer* **1**: 99-108.

Reya, T., Morrison, S.J., Clarke, M.F. and Weissman, I.L. (2001) Stem cells, cancer, and cancer stem cells. *Nature* **414**: 105-111.

Reyes, N., Reyes, I., Tiwara, R. and Geliebter, J. (2004) Effect of linoleic acid on proliferation and gene expression in the breast cancer cell line T47D. *Cancer Letters* **209**: 25-35.

Richert, M.M., Schwertfeger, K.L., Ryder, J.W. and Anderson, S.M. (2000) An atlas of mouse mammary gland development. *Journal of Mammary Gland Biology and Neoplasia* **5**: 227-241.

Riezzo, G., Chiloiro, M. and Russo, F. (2005) Functional foods: Salient features and clinical applications. *Current Drug Targets – Immune, Endocrine and Metabolic Disorders* **5**: 331-337.

Roche, H.M., Noone, E., Nugent, A. and Gibney, M.J. (2001) Conjugated linoleic acid: a novel therapeutic nutrient? *Nutrition Research Reviews* **14**: 173-187.

Rooseboom, M., Commandeur, J.N.M. and Vermeulen, N.P.E. (2004) Enzyme-catalyzed activation of anticancer prodrugs. *Pharmacological Reviews* **56**: 53-102.

Rose, D.P. and Connolly, J.M. (1999) Omega-3 fatty acids as cancer chemoprevention agents. *Pharmacology and Therapeutics* **83**: 217-244.

Saeb-Parsy, K, Assomull, R.G., Khan, F.Z., Saeb-Parsy, K. and Kelly, E. (1999) Instant Pharmacology. John Wiley & Sons.

Sampath, D. and Plunkett, W. (2001) Design of new anticancer therapies targeting cell cycle checkpoint pathways. *Current Opinions in Oncology* **13**: 484-490.

Searle, P.F., Chen, M.J., Hu, L., Race, P.R., Lovering, A.L., Grove, J.I., Guise, C., Jaberipour, M., James, N.D., Mautner, V., Young, L.S., Kerr, D.J., Mountain, A., White, S.A. and Hyde, E.I. (2004) Nitroreductase: A prodrug-activating enzyme for cancer gene therapy. *Clinical and Experimental Pharmacology and Physiology* **31**: 811-816.

Silverman, R.B. (1992) The organic chemistry of drug design and drug action. Academic Press.

Sinhababu, A.K. and Thakker, D.R. (1996) Prodrugs of anticancer agents. *Advanced Drug Delivery Reviews* **19**: 241-273.

Smalley, M. and Ashworth, A. (2003) Stem cells and breast cancer: A field in transit. *Nature Reviews Cancer* **3**: 832-844.

Smyth, G.E. and Orsi, B.A. (1989) Nitroreductase activity of NADH dehydrogenase of the respiratory redox chain. *Biochemical Journal* **257**: 859-863.

Soel, S.M., Choi, O.S., Bang, M.H., Park, J.H.Y. and Kim, W.K. (2007) Influence of conjugated linoleic acid isomers on the metastasis of colon cancer cells in vitro and in vivo. *Journal of Nutritional Biochemistry*, Epub ahead of print.

Sternlicht, M.D. and Werb, Z. (2001) How matrix metalloproteinases regulate cell behaviour. *Annual Review of Cell and Developmental Biology* **17**: 463-516.

Stoll, B.A. (1998) Breast cancer and the western diet: Role of fatty acids and antioxidant vitamins. *European Journal of Cancer* **34**: 1852-1856.

Tanmahasamut, P., Liu, J., Hendry, L.B. and Sidell, N. (2004) Conjuated linoleic acid blocks estrogen signaling in human breast cancer cells. *Journal of Nutrition* **134**: 674-680.

Thomas, G. (2000) Medicinal Chemistry: An Introduction. John Wiley & Sons, Ltd, Chichester, UK.

Thompson, H., Zhu, Z., Banni, S., Darcy, K., Loftus, T. and Ip, C. (1997) Morphological and biochemical status of the mammary gland as influenced by conjugated linoleic acid: Implications for the reduction in mammary cancer risk. *Cancer Research* **57**: 5067-5072.

Tokunaga, E., Oda, S., Fukushima, M., Maehara, Y. and Sugimachi, K. (2000) Differential growth inhibition by 5-fluorouracil in human colorectal carcinoma cell lines. *European Journal of Cancer* **36**: 1998-2006.

Venook, A. (2005) Critical evaluation of current treatments in metastatic colorectal cancer. *The Oncologist* **10**: 250-261.

Voorrips, L.E., Brants, H.A.M., Kardinaal, A.F.M., Hiddink, G.J., van den Brandt, P.A. and Goldbohm, R.A. (2002) Intake of conjugated linoleic acid, fat, and other fatty acids in relation to postmenopausal breast cancer: the Netherlands Cohort Study on Diet and Cancer. *American Journal of Clinical Nutrition* **76**: 873-882.

Wahle, K.W.J., Heys, S.D. and Rotondo, D. (2004) Conjugated linoleic acids: are they beneficial or detrimental to health? *Progress in Lipid Research* **43**: 553-587.

Wang, P., Song, Y., Zhang, L., He, H. and Zhou, X. (2005) Quinone methide derivatives: Important intermediates to DNA alkylating and DNA cross-linking actions. *Current Medicinal Chemistry* **12**: 2893-2913.

Warusavitarne, J., Ramanathan, P., Kaufman, A., Robinson, B.G. and Schnitzler, M. (2006) 5-Fluorouracil (5FU) treatment does not influence invasion and metastasis in microsatellite unstable (MSI-H) colorectal cancer. *International Journal of Colorectal Disease* **21**: 625-631.

Weedon, S.J., Green, N.K., McNeish, I.A., Gilligan, M.G., Mautner, V., Wrighton, C.J., Mountain, A., Young, L.S., Kerr, D.J. and Searle, P.F. (2000) Sensitisation of human colorectal carcinoma cells to the prodrug CB1954 by adenovirus vector-mediated expression of *E. coli* Nitroreductase. *International Journal of Cancer* **86**: 848-854.

Whelan, J. and McEntee, M.F. (2004) Dietary (n-6) PUFA and intestinal tumorigenesis. *Journal of Nutrition* **134**: 3421S-3426S.

Williams, K.J., Cowen, R.L. and Stratford, I.J. (2001) Hypoxia and oxidative stress in breast cancer tumour hypoxia – therapeutic considerations. *Breast Cancer Research* **3**: 328-331.

Wolff, A.C., Donehower, R.C., Carducci, M.K., Brahmer, J.R., Zabelina, Y., Bradley, M.O., Anthony, F.H., Swindell, C.S., Witman, P.A., Webb, N.L. and Baker, S.D. (2003) Phase I study of docosahexanoic acid-paclitaxel: a taxane-fatty acid conjugate with a unique pharmacology and toxicity profile. *Clinical Cancer Research* **9**: 3589-3597.

Wurm, F. and Bernard, A. (1999) Large-scale transient expression in mammalian cells for recombinant protein production. *Current Opinion in Biotechnology* **10**: 156-159.

Xiong, H.Q. and Ajani, J.A. (2004) Treatment of colorectal cancer metastasis: The role of chemotherapy. *Cancer and Metastasis Reviews* **23**: 145-163.

Xu, G. and McLeod, H. (2001) Strategies for enzyme/prodrug cancer therapy. *Clinical Cancer Research* **7**: 3314-3324.

Yang, T.T., Sinai, P. and Kain, S.R. (1996) An acid phosphatase assay for quantifying the growth of adherent and nonadherent cells. *Analytical Biochemistry* **241**: 103-108.

Appendix A

Plasmid map for F179

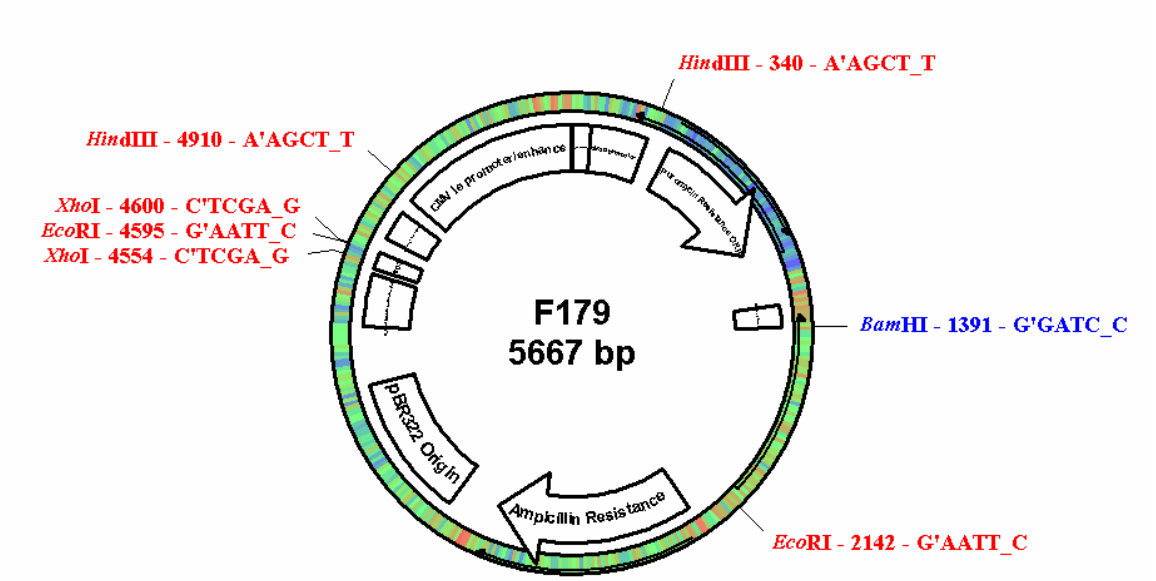

Plasmid map for F184

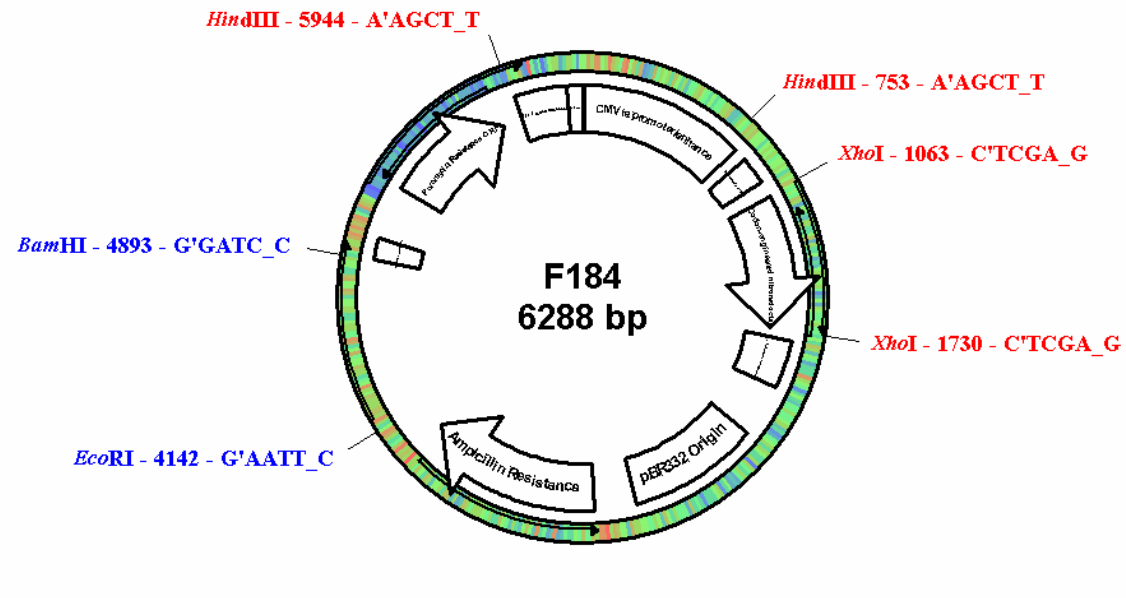

Plasmid maps were drawn using pDRAW from Acaclone Software.

Plasmid map for pCH110

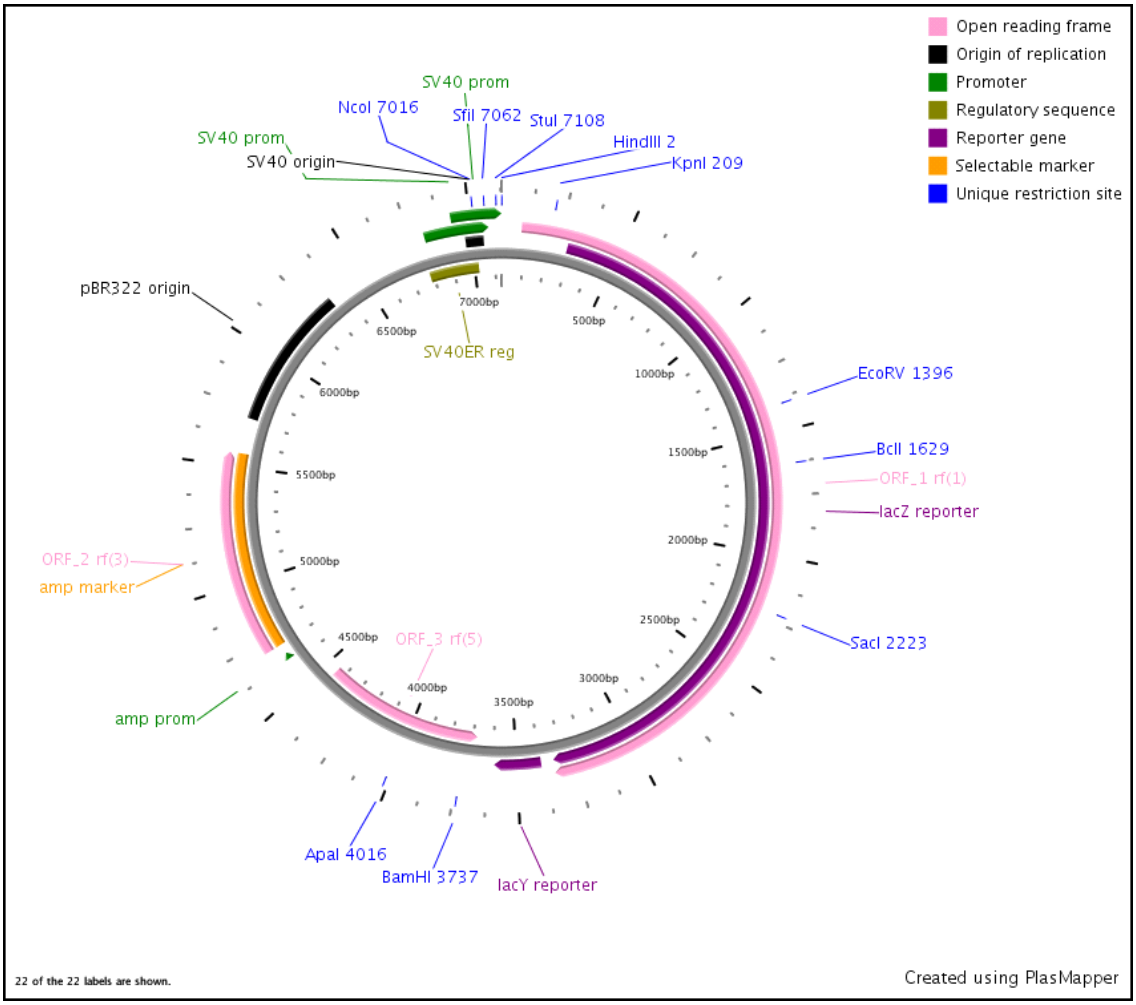

Plasmid map was drawn using PlasMapper
(http://wishart.biology.ualberta.ca/PlasMapper/).
Xiaoli Dong, Paul Stothard, Ian J. Forsythe, and David S. Wishart "PlasMapper: a web server for drawing and auto-annotating plasmid maps" Nucleic Acids Res. 2004 Jul 1;32(Web Server issue):W660-4.